"Reifung und Assemblierung der [NiFe]-Hydrogenasen aus
Escherichia coli: Eisen und Regulation "

D i s s e r t a t i o n

zur Erlangung des akademischen Grades

doctor rerum naturalium (Dr. rer. nat.)

vorgelegt der

Naturwissenschaftlichen Fakultät I
Biowissenschaften

der Martin-Luther-Universität Halle-Wittenberg

von

Frau Constanze Pinske

geb. am 24.12.1983 in Berlin

Gutachter /in

1. Prof. Dr. R. Gary Sawers

2. Prof. Dr. Milton T. Stubbs

3. Prof. Dr. Thomas Happe

Halle (Saale), den 27.06.2012

"Whatever it is you're seeking won't come in the form you're expecting."
— Haruki Murakami 'Kafka on the Shore' —

Inhaltsverzeichnis

Abkürzungsverzeichnis

ABC	A̲TP b̲inding c̲assette
ATC	A-typ Träger (A̲-t̲ype c̲arrier) Protein
ATP	Adenosin-5'-triphosphat
BV	Benzylviologen (1,1'-Dibenzyl-4,4'-bipyridinium dichlorid)
Da	Dalton (Masseneinheit – 1 Da = 1 g mol^{-1})
DMSO	Dimethylsulfoxid
DNA	Desoxyribonukleinsäure
e^-	Elektron
$E^{0'}$	Redoxpotential unter Standardbedingungen (25 °C, pH 7,0, 1 atm)
EPR	Elektronenspinresonanz (e̲lectron p̲aramagnetic r̲esonance)
et al.	et alii – und andere
FAD	Flavin-Adenin-Dinukleotid
Fdh-H/-O/-N	Formiatdehydrogenase-H (hydrogen) /-O (oxygen)/-N (nitrate)
[FeS]-Cluster	Eisen-Schwefel-Cluster
FHL	Formiat Hydrogenlyase
Fnr	Transkriptionsregulator für Sauerstoff (f̲umarate n̲itrate r̲egulator)
Fur	Transkriptionsregulator für Eisenaufnahme (f̲erric u̲ptake r̲egulation)
H$_4$MPT	N^5,N^{10}- (Methenyl/Methylen)-tetrahydromethanopterin
Hyd	Hydrogenase
Isc	Eisen-Schwefel Cluster Insertion (i̲ron s̲ulfur c̲luster)
K_M	Michaelis-Menten Konstante
MS	Massenspektrometrie
Mo-bis-MGD	Molybdopterin-Guanin Dinukleotid Kofaktor
NAD/NADH	Nicotinamid-Adenin-Dinucleotide oxidiert/reduziert
Nar	Nitratreduktase
Page	Polyacrylamid-Gelelektrophorese
PDB	Proteindatenbank für Kristallstrukturen
pKd	negativer dekadischer Logarithmus der Dissoziationskonstante
pKa	negativer dekadischer Logarithmus der Säurekonstante
RNA	Ribonukleinsäure (mRNA – messenger; tRNA - transfer)
SDS	Natriumdodecylsulfat
Suf	Eisen-Schwefel Cluster Insertion (s̲ulfur a̲ssimilation)
Tat	Proteintransportsystem (T̲win a̲rginine t̲ranslocation)
U	Unit (Umsatz von 1 µmol Substrat je Minute)

Abbildungsverzeichnis

1. Einleitung

Die Zusammensetzung des uns zugänglichen Teils des Weltalls wird auf 63 % Wasserstoff (H), 36 % Helium und 1 % übriger Elemente geschätzt und damit kann Wasserstoff als das häufigste Element des Weltalls bezeichnet werden. Auf der Erde kommt Wasserstoff fast nur chemisch gebunden vor und macht dabei 88 % der Gesamtmasse der Erdkruste aus (Römpp *et al.*, 1992). Freier molekularer Wasserstoff tritt dagegen nur in Spuren auf und hat einen Volumenanteil von 500 ppm an der Lufthülle der Erde. Dieses Gas wurde 1766 von Henry Cavendish bei der Auflösung von Metallen in Säuren entdeckt und als leicht entflammbare Luft, die zu Wasser verbrennt, beschrieben (Gaffney & Marley, 2005; Tomory, 2009). Physiologisch sind Wasserstoff-Transfer Reaktionen, katalysiert durch Dehydrogenasen, Hydrogenasen und Oxidoreduktasen oftmals unter Beteiligung von Kofaktoren wie NAD und FAD, wichtig und liefern durch den Aufbau von Protonengradienten an Membranen weit mehr Energie als z.B. die Oxidation von Kohlenstoff zu CO_2. Eine besondere Rolle spielen Hydrogenasen (Hyd), welche erstmals von Stephenson und Stickland beschrieben wurden und welche die reversible Oxidation von molekularem Wasserstoff zu Protonen und Elektronen katalysieren (Stephenson & Stickland, 1931). Sie werden in der Enzymklasse EC 1.12.1.2 den Oxidoreduktasen zugeordnet. Der von diesen Enzymen verwendete H_2 ist aus technologischer Sicht unentbehrlich, denn es entstehen bei der Verbrennung von H_2 mit Sauerstoff nur Verbrennungswärme (120 MJ kg^{-1}) und Wasser, weshalb Wasserstoff für die sauberste Alternative zu fossilen Brennstoffen gehalten wird (Thauer *et al.*, 2010).

Hydrogenasen kommen ubiquitär in den drei Domänen des Lebens vor (Vignais *et al.*, 2001). Phylogenetische Analysen basierend auf den Aminosäuresequenzen der katalytischen Untereinheiten erlauben hierbei eine Klassifizierung in drei distinkte Arten (Wu & Mandrand-Berthelot, 1993), die evolutiv unabhängig voneinander entstanden sind (Abb. 1). Man unterscheidet dabei die bei den Bacteria und Archaea vertretenen Nickel-Eisen Hydrogenasen [NiFe], die bei den Eukarya und Bacteria vorkommenden Eisen-Eisen-Hydrogenasen [FeFe] und die bisher nur bei den methanogenen Euryarchaeota identifizierten Eisen-Hydrogenasen [Fe] (Vignais & Billoud, 2007). Alle drei Arten nutzen verschiedene Kombinationen von Metallionen und Kofaktoren um Wasserstoff zu aktivieren. So zeigte Thauer 1981 erstmals, dass die gereinigte Hydrogenase aus einem Methanogenen Archaeon Nickel enthält (Graf & Thauer, 1981). Das metallene aktive Zentrum liegt tief in der katalytischen Untereinheit, zu welchem molekularer Wasserstoff durch Gaskanäle diffundiert (Cammack, 1995; Fontecilla-Camps *et al.*, 2007; Liebgott *et al.*, 2010). Am Metallzentrum erfolgt die heterolytische

Bindungsspaltung endergon mit 200 kJ mol^{-1} (20 °C) in ein Proton und ein Hydridion. Die Elektronen werden über eine Reihe von Elektronenüberträgern auf spezifische Elektronenakzeptoren übertragen, während zwei Protonen entlassen werden (Cammack, 1995; Thauer *et al.*, 2010). Bei den [Fe]-Hydrogenasen dient ein spezieller Eisen-Guanylylpyridinol Kofaktor (FeGP) als Hydridakzeptor um das Kosubstrat Methenyl-tetrahydromethanopterin (Methenyl-H$_4$MPT) zu Methylen-H$_4$MPT zu reduzieren (Thauer *et al.*, 2010). Diese [Fe]-Hydrogenase der Methanogenen ohne Cytochrome wird als alternative Hydrogenase unter Nickel Limitierung synthetisiert (Corr & Murphy, 2011). Das Enzym unterläuft mit jedem Katalysezyklus eine für andere Hydrogenasen untypische Konformationsänderung, um Substrat und Kosubstrat zu entlassen. Untersuchungen zur metabolischen Herkunft der Atome des Kosubstrates identifizierten Acetat, Methionin, Pyruvat und CO$_2$ jedoch konnten deren weitere Biosynthesewege noch nicht aufgeklärt werden (Thauer *et al.*, 2010).
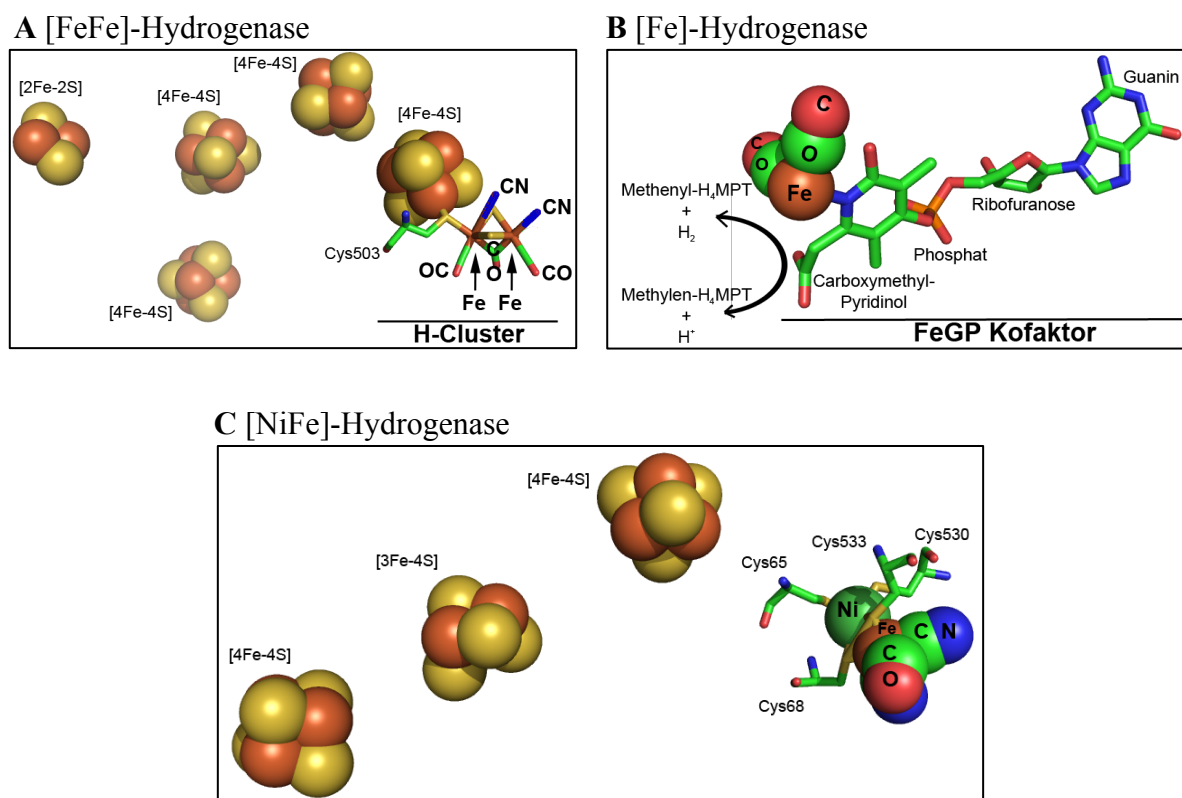
Abbildung 1 Darstellung der aktiven Zentren und prosthetischen Gruppen der [FeFe]-, [Fe]- und [NiFe]-Hydrogenasen. A: Die [FeFe]-Hydrogenase aus *Clostridium pasteurianum* wurde mit Pymol von PDB-Datei 1FEH modelliert (Peters *et al.*, 1998). Das H-Cluster mit seinem über einen Cystein-Liganden verbrückten [4Fe-4S]-Cluster sowie die weiteren [FeS]-Cluster befinden sich in einem Protein. Die diatomaren Liganden an den Fe Atomen wurden nach (Thauer *et al.*, 2010) modifiziert. **B:** Für die Abbildung des aktiven Zentrums der [Fe]-Hydrogenase wurde die PDB-Datei 3DAG mit der Struktur aus *Methanocaldococcus jannaschii* genutzt (Shima *et al.*, 2008). **C:** Als Grundlage für die Abbildung der löslichen [NiFe]-Hydrogenasen aus *Desulfovibrio gigas* (Volbeda *et al.*, 1996) wurde PDB-Datei 2FRV verwendet. Die [FeS]-Cluster befinden sich in der kleinen Untereinheit in einem Winkel von 112° zum aktiven Zentrum der großen Untereinheit. Die Farben entsprechen: Gelb-Schwefel; Braun-Eisen; Rot-Sauerstoff; Blau-Stickstoff; Hellgrün-Kohlenstoff; Dunkelgrün-Nickel.

Alle Hydrogenasen entsprechen einem gemeinsamen Aufbau und sind essentiell auf Eisen im katalytischen Zentrum angewiesen. Dieses Eisen ist mit den diatomaren Liganden CO und bei einigen zusätzlich mit CN⁻ komplexiert. Die Anordnung der an der Katalyse beteiligten Metalle der aktiven Zentren aller drei Arten ist in Abb. 1 gezeigt und wird im Folgenden anhand von Beispielen erläutert.

1.1 [FeFe]-Hydrogenase von *Chlamydomonas reinhardtii*

Die Klasse der [FeFe]-Hydrogenasen besitzt ein als H-Cluster bezeichnetes aktives Zentrum in der katalytischen Untereinheit. Dieses besteht aus einem klassischen [4Fe-4S]-Cluster, welches über ein Cystein mit einem binuklearem Eisen Zentrum verbunden ist (vgl. Abb. 1). An jedem dieser beiden Eisenatome sind jeweils ein Kohlenstoffmonoxid- (CO) und ein Cyanid- (CN⁻) Ligand gebunden, zusätzlich sind die Fe-Atome über einen CO Liganden verbrückt (Abb. 1). Diese Hydrogenasen sind vergleichsweise O_2 sensitiv, katalysieren jedoch *in vivo* die biotechnologisch interessante H_2-Produktion mit höheren Umsatzraten im Vergleich zu [NiFe]-Hydrogenasen (Adams, 1990; Frey, 2002; Goldet *et al*., 2009; Lambertz *et al*., 2011; Stripp *et al*., 2009). So beträgt die spezifische Aktivität der [FeFe]-Hydrogenase aus der eukaryotische Grünalge *Chlamydomonas reinhardtii* 1800 U mg^{-1} (Ferredoxin:H_2) (Roessler & Lien, 1984) im Vergleich zur [NiFe]-Hydrogenase 2 aus *E. coli* mit 320 U mg^{-1} (H_2:Benzylviologen) (Ballantine & Boxer, 1986). Neben *Chlamydomonas* sind weitere bekannte Organismen mit gut untersuchten [FeFe]-Hydrogenasen das sulfatreduzierende Bakterium *Desulfovibrio gigas* und der anaerobe Stickstofffixierer *Clostridium pasteurianum* (Adams *et al*., 1981).

Die Aufklärung des Mechanismus der H-Cluster Biosynthese der [FeFe]-Hydrogenasen hat durch die Arbeiten der Gruppen um Swartz, Peters, Broderick, Roach und Happe in den letzten Jahren große Fortschritte gemacht (Czech *et al*., 2010; Driesener *et al*., 2010; Kuchenreuther *et al*., 2009; 2011; McGlynn *et al*., 2007; 2008; Shepard *et al*., 2010a; 2010b). Bei der heterologen Produktion in *E. coli* und anschließender kristallographischer Strukturanalyse von HydA1 aus *C. reinhardtii* konnte das zum H-Cluster gehörende [4Fe-4S]-Cluster bereits als vom Wirtsorganismus inseriert identifiziert werden, während das [2Fe-2S]-Cluster nicht nachgewiesen werden konnte (Mulder *et al*., 2010). Dies wird darauf zurückgeführt, dass die drei für die vollständige Biosynthese des H-Clusters der [FeFe]-Hydrogenasen essentiellen Proteine HydE, F und G im Genom von *E. coli* nicht kodiert werden (Böck *et al*., 2006). Die Reifungsproteine HydE und HydG besitzen Radikal-*S*-

Adenosylmethionin-Protein Motive und ein [4Fe-4S]-Cluster. *In vitro* Versuche zur Reifung von HydA1 zeigten, dass separat gereinigte HydE, F und G Proteine in der Lage sind, das aktive Zentrum von HydA1 zu vervollständigen (McGlynn *et al.*, 2007). HydG katalysiert dabei über einen Radikalmechanismus die Spaltung von Tyrosin für die Synthese sowohl der CO als auch der CN$^-$ Liganden (Nicolet *et al.*, 2010; Shepard *et al.*, 2010b), während HydE die Synthese des unbekannten Dithiolat verbrückenden Liganden ermöglicht (Mulder *et al.*, 2011). Wird HydF gemeinsam mit HydE und G exprimiert und von diesen anschließend separiert, ist es in Abwesenheit von HydE und HydG in der Lage, das gesamte H-Cluster oder möglicherweise auch nur das [2Fe-2S]-Cluster von HydA1 zu assemblieren. Es dient somit als *Scaffold* Protein mit GTPase Aktivität (McGlynn *et al.*, 2008).

1.2 Verschiedene Lebensweisen bedingen verschiedene Reaktionsrichtungen

Anhand ihrer Lebensweise werden Mikroorganismen und deren Einsatz von Hydrogenasen unterschieden (Vignais & Billoud, 2007). So dient die H_2-Produktion bei der Fermentation der „Entsorgung" von Elektronen indem Protonen als finale Elektronenakzeptoren genutzt werden. Weiterhin wird H_2 von vielen Mikroorganismen als Energiequelle genutzt indem durch Elektronen-Transportphosphorylierung ATP konserviert wird, während Sulfat (*Desulfovibrio gigas*), Nitrat (*Paracoccus denitrificans*), CO_2 (Methanogene Archaea) oder Fumarat (*Wolinella succinogenes*, *Clostridium formicaceticum*) als Elektronenakzeptor dienen (Andreesen *et al.*, 1970; Friedrich *et al.*, 1986; Kröger *et al.*, 2002; Niederman & Wolin, 1972; Thauer *et al.*, 1977; 2010).

Während der Methanogenese, der anaeroben Bildung von Methan durch methanogene Archaea, stellt Wasserstoff die Haupt-Reduktionskraft zur Konvertierung variabler Kohlenstoff-Substrate dar. Man kann bei der Verwendung von H_2 innerhalb der Archaea zwischen vier verschiedenen Arten der [NiFe]-Hydrogenasen unterscheiden, von denen z.B. die membrangebundene, Energie-konvertierende [NiFe]-Hydrogenase (Ech) die Energie für die Re-Reduktion eines Ferredoxins mit H_2 aus einem Protonen- oder Natriumgradienten konserviert (Kurkin *et al.*, 2002).

Als weitere Quelle für Wasserstoff, der als Nebenprodukt in stöchiometrischen Mengen entsteht, ist die Nitrogenase-katalysierte Reduktion von molekularem Stickstoff zu Ammoniak in Stickstofffixierenden Mikroorganismen. Der erste Teilschritt dabei, die Reduktion von Protonen, ist ATP abhängig und findet in Abwesenheit von anderen Substraten

wie N_2 statt. Dies führte zum Rückschluss, dass es sich um eine Aktivierung der Nitrogenase handelt (Bothe *et al.*, 2010). An der Reaktion ist ein FeMo-Kofaktors in der Alpha Untereinheit (MoFe Protein oder Dinitrogenase) beteiligt, für dessen Assemblierung ein Minimum von 12 *nif* Genprodukten identifiziert werden konnten (Einsle *et al.*, 2002; Jacobson *et al.*, 1989). Dieser FeMo-Kofaktor besteht aus Mo-[7Fe-9S], *R*-Homocitrat und, ähnlich den diatomaren Liganden der Hydrogenasen, einem zentralen, die Fe Atome verbindenden, C-Atom (Ramaswamy, 2011; Spatzal *et al.*, 2011). Zusätzlich ist ein weiteres aus [8Fe-7S] bestehendes P-Cluster vorhanden. Die Beta Untereinheit der Nitrogenase (Fe Protein oder Dinitrogenase Reduktase) transferiert vermutlich die Elektronen von Ferredoxin zum aktiven Zentrum (Bothe *et al.*, 2010). Analog zu [FeFe]-Hydrogenasen erfolgt die Assemblierung des FeMo-Kofaktors separat vom Apo-Protein auf NifEN, um dann inseriert zu werden (Hu & Ribbe, 2011; Rubio & Ludden, 2008; Shepard *et al.*, 2011). Als erster Schritt erfolgt die P-Cluster Synthese direkt im MoFe Protein durch Schwefel Bereitstellung der Cystein-Desulfurase NifS und Assemblierung als [FeS]-Cluster auf NifU. *In vitro* wird Eisen(II) direkt eingebaut, es ist jedoch unwahrscheinlich, dass es physiologisch frei vorliegt. Die Proteine NifSU stellen Homologe der generellen [FeS]-Cluster Assemblierungsproteine IscS und IscU dar, die in vielen Organismen verbreitet sind (Abb. 7) (Shepard *et al.*, 2011).

Auch einige Cyanobakterien wie *Synechocystis*, *Nostoc punctiforme* und *Anabena* können Stickstoff fixieren und besitzen damit assoziiert und ko-reguliert eine Aufnahme [NiFe]-Hydrogenase (Hup) (Tamagnini *et al.*, 2002). Dadurch wird die Bildung von H_2 gering gehalten, wobei die Oxidation entweder dazu dient den für die Nitrogenase schädlichen O_2 zu entfernen, Ansammlung größerer Mengen Nitrogenase hemmenden H_2 zu verhindern oder Reduktionsäquivalente der Nitrogenase-Reaktion zurückzugewinnen (Bothe *et al.*, 2010). Diese enge Assoziation einer Hydrogenase mit einer anderen Enzymaktivität zeigt einmal mehr wie essentiell die Oxidation von H_2 bzw. die Reduktion von Protonen sind.

1.3 Wasserstoffoxidation und Reduktion sind in *E. coli* möglich

Das *Escherichia coli* Genom kodiert für 4 distinkte [NiFe]-Hydrogenasen (Hyd), von denen jedoch nur drei bisher biochemisch charakterisiert werden konnten (Andrews *et al.*, 1997; Forzi & Sawers, 2007). Diese werden unter fermentativen Bedingungen, das heißt in Abwesenheit externer Elektronenakzeptoren wie Nitrat und Sauerstoff, exprimiert (Richard *et al.*, 1999). Die Hyd-1 und Hyd-2 werden ins Periplasma transloziert und katalysieren dort bevorzugt die Oxidation von molekularem H_2 zu Protonen und Elektronen (Abb. 2)

(Ballantine & Boxer, 1985). Hyd-3 ist Teil des auf der cytoplasmatischen Seite membranassoziierten Formiat-Hydrogenlyase (FHL)-Enzymkomplexes, der gemeinsam mit der Formiatdehydrogenase H (Fdh-H) die Spaltung von Formiat zu CO_2 und H_2 katalysiert (Abb. 2) (Böhm *et al.*, 1990; Sauter *et al.*, 1992; Sawers *et al.*, 1985). Generell befinden sich die H_2-Aufnahme Hydrogenasen membranassoziiert im Periplasma, während im Cytoplasma befindliche Hydrogenasen die H_2-Produktion katalysieren (Vignais *et al.*, 2001). Viele der wasserstoffoxidierenden Hydrogenasen zeichnen sich durch ein charakteristisches *N*-terminales Signalpeptid an der kleinen Untereinheit aus, welches aus einem konservierten RRXFLK Aminosäuremotiv besteht und vom Tat (*Twin arginine translocation*)-Protein Transport System erkannt wird (Palmer *et al.*, 2005). Dabei wird das Heterodimer aus großer und kleiner Untereinheit im gefalteten Zustand mit insertiertem Kofaktoren transloziert. Entdeckt wurde das Tat-System durch Analyse der *N*-terminalen Proteinsequenzen periplasmatischer Proteine u.a. der kleinen Untereinheit der [NiFe]-Hydrogenase 2 aus *E. coli* (Berks, 1996; Wu & Mandrand, 1993).
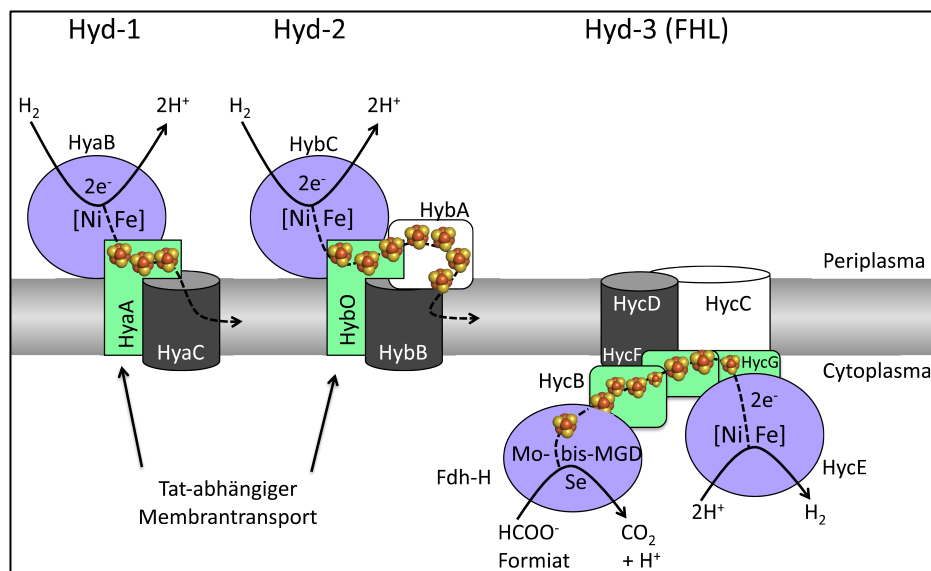
Abbildung 2 Anordnung der *E. coli* Hydrogenasen in der Cytoplasmamembran nach (Forzi & Sawers, 2007). Die beiden H_2-oxidierenden Enzyme sind im Periplasma lokalisiert, während Hyd-3 als Teil des Formiat Hydrogenlyase Komplexes (FHL) ins Cytoplasma gerichtet ist und die H_2-Produktion katalysiert. Die großen Untereinheiten besitzen das katalytische [NiFe]-Zentrum und sind in Lila dargestellt. Die Formiatdehydrogenase H (Fdh-H) besitzt im aktiven Zentrum ein Selenocystein (Se) und einen Molybdopterin-guanin Dinukleotid (Mo-bis-MGD) Kofaktor. Die kleinen, Elektronen transferierenden Untereinheiten sind in Grün und die Membranuntereinheiten in Schwarz dargestellt. Für Hyd-2 existiert eine zusätzliche Elektronen transferierende Untereinheit, HybA. [FeS]-Cluster sind unabhängig von ihrer Beschaffenheit als [4Fe-4S] oder [3Fe-4S]-Cluster als braune (Fe) und gelbe (S) Kugeln dargestellt.

Hyd-1 wird vom *hyaABCDEF*-Operon kodiert, bei dem *hyaA* für die kleine [FeS]-Cluster enthaltende Untereinheit kodiert, während *hyaB* die katalytische Untereinheit mit dem aktiven [NiFe]-Zentrum kodiert (Menon *et al.*, 1991). In ähnlicher Weise wird Hyd-2 durch das

Operon *hybOABCDEFG*-Operon kodiert, in welchem *hybO* die kleine und *hybC* die große Untereinheit kodieren (Menon *et al.*, 1994; Sargent *et al.*, 1998). Beide kleinen Untereinheiten sind je über eine hydrophobe *C*-terminale α-Helix in der Membran verankert, transferieren jedoch Elektronen über weitere membranintegrale Cytochrom *b* ähnliche (HyaC) oder Kofaktorfreie (HybB) Untereinheiten in den Chinonpool (Dubini *et al.*, 2002; Vignais *et al.*, 2001).

Die Expression der Gene für die abundantere Hyd-1 erfolgt bevorzugt in der stationären Phase (Brøndsted & Atlung, 1994), während die Gene für Hyd-2 schon während der exponentiellen Phase exprimiert werden und die Expression beider Operons durch die Anwesenheit von Nitrat oder Sauerstoff gehemmt wird (Abb. 5) (Richard *et al.*, 1999). Durch die erhöhte Proteinmenge von Hyd-2 in Anwesenheit von Fumarat wurde eine Involvierung in den Elektronentransfer von H_2 auf Fumarat vorgeschlagen, während für Hyd-1 eine Reoxidation des H_2 vom FHL Komplex vermutet wurde (Sawers *et al.*, 1985). Jedoch zeigten Metabolitanalysen von Hyd-1⁻ Mutanten, dass Hyd-1 in *E. coli* keinen signifikanten Beitrag zur H_2-Oxidation hat, während es bei *Salmonella enterica* so effizient funktioniert, dass keine netto H_2-Produktion messbar ist (Redwood *et al.*, 2007; Zbell & Maier, 2009). Auch die physiologische Rückreaktion, Bildung von H_2, kann *in vitro* durch Hyd-1 aus reduziertem Methylviologen erfolgen (Sawers & Boxer, 1986), ist jedoch nach der Adsorption auf eine Graphitelektrode nicht messbar. Diese widersprüchliche Eigenschaft lässt sich eventuell durch unterschiedliche Reinigungen erklären, bei denen es schnell zu proteolytischem Abbau der kleinen Untereinheit (HyaA) kommt, resultierend in unterschiedliche katalytische Eigenschaften (Sawers & Boxer, 1986).

Durch Zyklovoltammetrische Analysen (Abb. 3) lassen sich eine Reihe von Unterschieden zwischen Hyd-1 und Hyd-2 in der Katalyse feststellen (Lukey *et al.*, 2010). Zum einen ist der K_M unter diesen Bedingungen für Hyd-1 mit 9 µM niedriger als für Hyd-2 mit 17 µM womit, vereinfacht gesagt, Hyd-1 eine höhere Affinität zum Substrat hat. Zum anderen ist das Mittelpunkt Potential (Stern/* in Abb. 3) für Hyd-1 höher welches angibt bei welchem Redoxpotential das Enzym nach Inaktivierung reaktiviert wird und damit ist Hyd-1 noch bei höherem Redoxpotential aktiv als Hyd-2. Bei Anwesenheit von 10 % H_2 wird Oxidation nur bei Überpotential katalysiert, was bedeutet, dass für den Elektronentransfer mehr Energie aufgebracht werden muss als das theoretische Redoxpotential des Substrates erfordert (Lukey *et al.*, 2010). Dieses Überpotential sinkt mit abnehmender H_2-Konzentration, was bedeutet,

dass die Oxidation bei geringen H_2-Konzentrationen thermodynamisch günstiger ist. Letztendlich erschließt sich durch ausschließlichen Stromfluss im positiven Bereich, dass Hyd-1 so gut wie nicht reversibel ist, während Hyd-2 die Rückreaktion katalysieren kann. Zusammenfassend könnte Hyd-1 *in vivo* dann zur Oxidation von H_2 dienen, wenn dieses in geringen Spuren bei höheren Redoxpotentialen vorhanden ist weil das Enzym nicht sofort inaktiviert wird, während Hyd-2 durch höhere Umsatzraten in der Lage ist bei hohen H_2-Konzentrationen dieses effizient zu oxidieren.
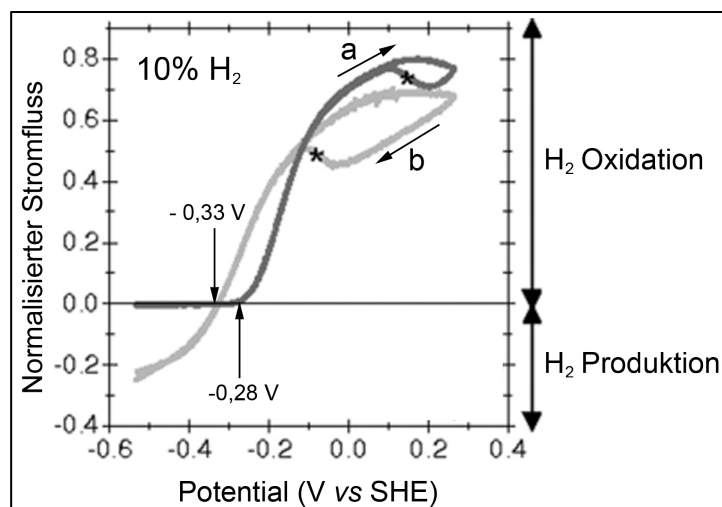
Abbildung 3 Zyklovoltammetrische Analyse der Hyd-1 (Dunkelgrau) und Hyd-2 (Hellgrau) Aktivitäten aus *E. coli* (entnommen und modifiziert nach (Lukey *et al.*, 2010)). Die gereinigten Enzyme werden dabei auf einer Graphitelektrode adsorbiert und die Spannung (Potential) entsprechend der Pfeile (a und b) verändert. Der bei Substratanwesenheit (10 % H_2) resultierende Stromfluss wird gegen eine Referenzelektrode (SHE - Standard Wasserstoff Elektrode) gemessen während die Enzymelektrode rasch rotiert, um Diffusionskontrolle auszuschließen. Der Stern (*) gibt das Mittelpunkt Potential für die Reaktivierung des Enzyms an, welches bei + 0,150 V für Hyd-1 und - 0,085 V für Hyd-2 liegt. Stromfluss im oberen Bereich des Diagramms steht für die Oxidation von H_2, während im unteren Bereich Produktion aus Protonen bestimmt wird. Die Kurve für Hyd-1 kreuzt diese Linie im Gegensatz zur Hyd-2 Kurve nicht. Dieser Punkt in der Hyd-2 Kurve ist bei -0,33 V mit einem Pfeil gekennzeichnet und entspricht dem unter diesen Bedingungen aus der Nernst-Gleichung berechnetem Redoxpotential für 2 H^+/H_2. Die Hyd-1 Kurve beginnt erst bei -0,28 V anzusteigen und benötigt damit ein Überpotential um H_2-Oxidation unter diesen Bedingungen zu katalysieren. Dieses Überpotential wird jedoch mit abnehmender H_2-Konzentration geringer.

1.4 Formiatmetabolismus

Während der gemischten Säuregärung wird ein Drittel der Kohlenstoffatome aus Glukose zu Formiat umgewandelt (Sawers, 2005a). Diese Reaktion wird anaerob hauptsächlich nicht-oxidativ durch die PFL (Pyruvat-Formiat Lyase), ein Glycyl-Radikalenzym, katalysiert (Gl. 1a), wird unter aeroben Bedingungen jedoch oxidativ vom Pyruvat-Dehydrogenase Komplex (PDH) durchgeführt (Gl. 1b) (Knappe & Sawers, 1990). Unter mikroaeroben Bedingungen und bei Nitratatmung sind beide Enzyme aktiv und neueste Erkenntnisse zeigten, dass PDH das anaerobe Wachstum auf Glukose durch CO_2 Generation ebenfalls deutlich unterstützt (Murarka *et al.*, 2010). Die Regulation des *focA-pflB* Operons unterliegt transkriptioneller

Kontrolle u.a. durch ArcA (*anoxic redox control*), Fnr (*fumarate nitrate regulator*), IHF (*integration host factor*) und Crp (*catabolite repressor protein*) sowie weiterer post-translationeller Kontrolle und reagiert auf den intrazellulären Redoxstatus (Sawers, 2005b; 2006).

$$\text{Pyruvat} + \text{Coenzym-A} \rightleftharpoons \text{Formiat} + \text{Acetyl-CoA} \qquad \text{Gleichung 1a}$$
$$\text{Pyruvat} + \text{NAD}^+ + \text{Coenzym-A} \rightleftharpoons \text{Acetyl-CoA} + \text{CO}_2 + \text{NADH} \qquad \text{Gleichung 1b}$$
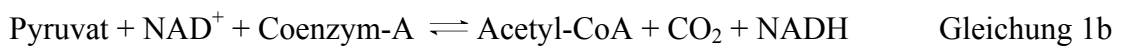
Da eine Anhäufung von Formiat toxisch für die Zelle ist, wird dieses Metabolit entweder verstoffwechselt oder über einen Formiattransporter (FocA) aus der Zelle entfernt (Sawers, 2005a; Sawers & Clark, 2004; Suppmann & Sawers, 1994). Hierfür sind im *E. coli* Genom drei Formiatdehydrogenase (Fdh) Enzyme kodiert, die unter verschiedenen Bedingungen synthetisiert werden (Sawers, 1994) und die Umwandlung von Formiat in CO_2, Protonen und Elektronen katalysieren (Gl. 2a). Alle drei Enzyme haben ein Selenocystein gemeinsam, welches in der RNA durch ein *amber*-Stopp Codon (UGA) kodiert wird, sowie einen Molybdopterin-Guanin Dinukleotid Kofaktor (Mo-bis-MGD) (Sawers, 1994; Zinoni *et al.*, 1986). Der Einbau des Selenocysteins erfolgt ko-translationell mit Hilfe der *sel*-Genprodukte und einer spezifischen tRNA (*selC*). Die Synthese des Mo-bis-MGD erfolgt ausgehend von einem zyklischen Pyranopterin (Böck *et al.*, 1991; Leimkühler *et al.*, 2011).

Die für Fdh-N und Fdh-O kodierenden Gene werden in Anwesenheit von Nitrat bzw. Sauerstoff exprimiert. Die korrespondierenden Enzyme übertragen, nach Tat-Transport auf die periplasmatische Seite der Cytoplasmamembran, Elektronen von Formiat über die Atmungskette auf einen externen terminalen Elektronenakzeptor (Sawers, 1994; Unden & Bongaerts, 1997). Beide Enzyme haben eine Membrananordnung in der das Heterotrimer aus katalytischer, kleiner und membrangebundener Untereinheit nochmals trimerisiert (Jormakka, 2002). Die Fdh-N formt mit der diametral membranassoziierten Nitratreduktase (Nar) eine Redoxschleife und generiert dabei Protonenmotorische Kraft zur Energiekonservierung (Richardson & Sawers, 2002; Unden & Bongaerts, 1997). Die formell ablaufenden Teilreaktionen der Fdh-N (Gl. 2a) und der Nar (Gl. 2b), bei denen zusätzlich durch Chinon vermittelten Elektronentransfer Protonen über die Membran transloziert werden, sind (Boyington *et al.*, 1997, Unden & Bongaerts, 1997):

$$\text{HCO}_2^- \rightleftharpoons \text{CO}_2 + \text{H}^+ + 2e^- \qquad (E^{0'} \ \text{-430 mV}) \qquad \text{Gleichung 2a}$$
$$\text{NO}_3^- + 2e^- + 2\text{H}^+ \rightleftharpoons \text{NO}_2^- + \text{H}_2\text{O} \qquad (E^{0'} \ \text{+420 mV}) \qquad \text{Gleichung 2b}$$
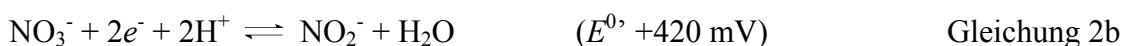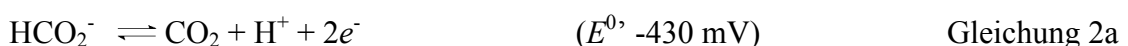
Bei der Nar handelt es sich ebenfalls um ein Molybdoenzym, dessen große und kleine Untereinheiten [FeS]-Cluster zum Elektronentransport beherbergen, deren katalytisches Zentrum jedoch im Cytoplasma lokalisiert ist (Bertero *et al*., 2003; Jormakka *et al*., 2004). Zellen, denen entweder die Fdh-N oder die Nar Enzymaktivitäten fehlen, können keine Nitratatmung durchführen (Berg & Stewart, 1990; Enoch & Lester, 1975; Ruiz-Herrera & DeMoss, 1969; Stewart, 1988).

Die dritte Formiatdehydrogenase (Fdh-H) ist Teil des FHL-Komplexes und mit diesem im Cytoplasma lokalisiert. Die strukturellen Komponenten werden im *hyc*-Operon von *hycBCDEFG* und von *fdhF* kodiert, wobei HycC und HycD Membranuntereinheiten sind, HycE und HycG die große und kleine Untereinheit der Hyd-3 bilden und HycB und HycF als Elektronentransportproteine dienen (Abb. 2 und 4) (Sauter *et al*., 1992). HycA ist ein negativer Regulator, HycI eine für die Reifung von HycE nötige und HycE-spezifische Endopeptidase, während die Funktion von HycH ungeklärt ist (Rossmann *et al*., 1995; Sauter *et al*., 1992). Die Expression der Komponenten des FHL Komplexes ist abhängig von der Sigma-54 RNA Polymerase Untereinheit, einem niedrigen pH, von ModE sensiertem Molybdat und von FhlA sensiertem Formiat (Abb. 5) (Birkmann & Böck, 1989; Hasona *et al*., 1998; Rossmann *et al*., 1991). Der Aufbau des FHL-Komplexes hat große Ähnlichkeit mit dem Komplex I der Atmungskette (NADH:Ubichinon Oxidoreduktase) und außerdem Ähnlichkeit zu vom kryptischen *hyf*-Operon kodierten putativen Genprodukten der vierten Hydrogenase sowie zur Ech Hydrogenase, jedoch konnte im Gegensatz zur Ech Hydrogenase für den FHL Komplex keine Energiekonservierung nachgewiesen werden (Andrews *et al*., 1997; Böhm *et al*., 1990; Hedderich & Forzi, 2005). Dennoch wurde in *Salmonella typhimurium* ATPase Mutanten ein Fehlen der H_2-Produktion beobachtet (Sasahara *et al*., 1997) oder in *E. coli* eine Inhibition des FHL Komplexes durch den ATPase Inhibitor *N,N'*-dicyclohexylcarbodiimide (Bagramyan & Martirosov, 1989; Bagramyan *et al*., 2002), aber pleiotrope Effekte auf alle Enzymsysteme unter diesen Bedingungen können nicht ausgeschlossen werden. Weiterhin konnte für das Archaeon *Thermococcus onnurineus* nachgewiesen werden, dass es durch die Disproportionierung von Formiat im FHL Komplex einen Protonengradienten aufbauen kann, um dadurch Energie zu konservieren (Kim *et al*., 2010). Tatsächlich erhält man bei bioinformatischen Strukturvorhersagen für HycE eine Faltungsvorhersage basierend auf der NADH:Ubichinon Oxidoreduktase Untereinheit 4 (Efremov *et al*., 2010) und nicht einer der zahlreichen löslichen [NiFe]-Hydrogenasen der

PDB-Datenbank (Kelley & Sternberg, 2009; Maeda *et al.*, 2008; Volbeda *et al.*, 1995), was ausreichend Potential für zukünftige Untersuchungen birgt.

1.5 Reifung und Ni-Fe(CN)$_2$CO Insertion

Die Eigenschaft der großen Hyd-3 Untereinheit HycE sich löslich in Abwesenheit weiterer FHL Komponenten reinigen zu lassen, erleichtere die Erstellung eines Reifungsmodells der [NiFe]-Hydrogenasen durch die Gruppe von August Böck (Böck *et al.*, 2006; Forzi & Sawers, 2007). Als Reifung wird hierbei die Assemblierung und Insertion des [NiFe]-Zentrums bezeichnet, für die spezielle Reifungsproteine (Hyp) benötigt werden (Böck *et al.*, 2006; Forzi & Sawers, 2007). Ein Teil, der für die Hyp Proteine kodierenden Gene, die *hypA-E*-Gene (*hydrogen pleiotropic*), wird divergent vom *hyc*-Operon transkribiert und die Expression erfolgt unter Anaerobiose und ist Fnr abhängig (Abb. 4 und 5) (Lutz *et al.*, 1991; Messenger & Green, 2003). Während sich Mutationen in den Genen *hypB*, *hypD*, *hypE* und *hypF* auf alle Hyd auswirken, sind Effekte von Mutationen in den Genen *hypC* und *hypA* hauptsächlich auf die Aktivität der Hyd-3 begrenzt, weil homologe Proteine für die Reifung von Hyd-1 und Hyd-2 von den Genen *hybF* und *hybG* kodiert werden (Hube *et al.*, 2002; Jacobi *et al.*, 1992).
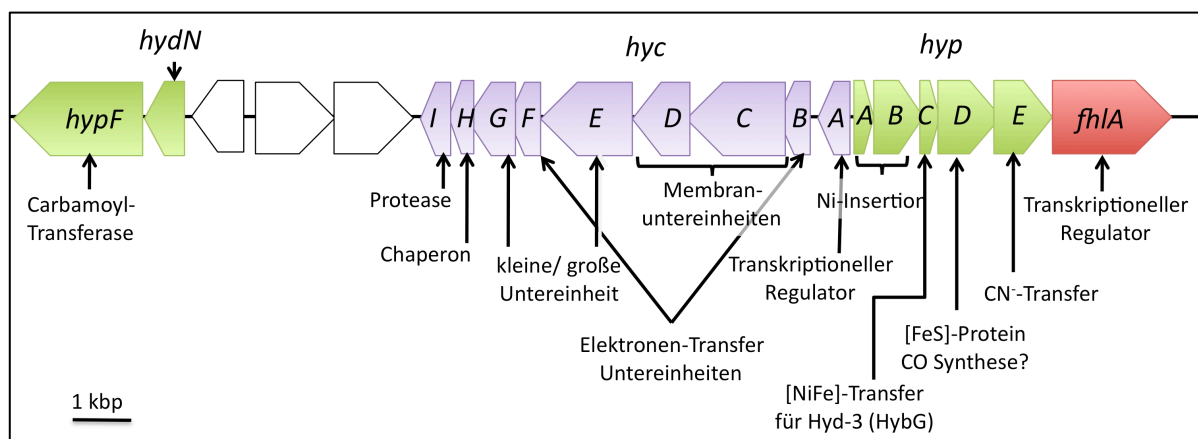
Abbildung 4 Anordnung der Gene *hypF*, *hycA-I*, *hypA-E* und *fhlA* auf dem *E. coli* Genom. Die Gene des *hyc*-Operons (Blau) kodieren für die strukturellen und akzessorischen Komponenten des FHL Komplexes, mit Ausnahme des Gens *fdhF*, welches für die Fdh-H kodiert und in einem anderen Teil des Genoms kodiert ist (Sauter *et al.*, 1992). Das *fhlA* Gen (Rot) kodiert für den transkriptionellen Regulator FhlA (Formiat-Hydrogenlyase Aktivator), der die Expression der *hyp* Gene, *hyc* Gene, des *fdhF* Gens sowie des *fhlA* Gens in Anwesenheit von Formiat aktiviert (Rossmann *et al.*, 1991). Dieser positiven Autoregulation wird durch die Expression von *hycA* entgegengewirkt (Sauter *et al.*, 1992). Die *hyp*-Gene (Grün), mit Ausnahme der Hyd-3 spezifischen Genprodukte von *hypA* und *hypC*, kodieren für universelle Reifungsproteine der [NiFe]-Hydrogenasen. Die Genprodukte von *hypF*, *hypE*, *hypD* und *hypC* bzw. *hybG* formen dabei einen Komplex der den Fe(CN)$_2$CO Teil des aktiven Zentrums auf die großen Untereinheiten überträgt während die *hypB* und *hypA* bzw. *hybF* Genprodukte die anschließende Nickelinsertion katalysieren (Blokesch *et al.*, 2004a; Böck *et al.*, 2006; Forzi & Sawers, 2007).

Für die Insertion des Eisens mit den diatomaren CN^- und CO Liganden assemblieren die Reifungsproteine HypC, D, E und F zu einem Komplex (Blokesch et al., 2004a), in welchem HypF Carbamoylphosphat durch Transfer auf ATP aktiviert und unter ATP Verbrauch als Carbamoyl-Gruppe auf das C-terminale Cystein (Cys322) von HypE überträgt (Blokesch et al., 2004b; Paschos et al., 2002; Reissmann et al., 2003). Mit Hilfe der Kristallstruktur konnten die an der ATP Bindung und Transcarbamoylierung beteiligten Aminosäurereste identifiziert und ein Übergangszustand bestätigt werden (Petkun et al., 2011). Unter weiterer ATP Spaltung wird die Carboxamidgruppe an HypE zu einem Thiocyanat umgewandelt und kann damit auf Eisen übertragen werden (Blokesch et al., 2004b; Paschos et al., 2002; Reissmann et al., 2003). Die Herkunft des Eisens für das aktive Zentrum ist noch unbekannt, durch die Kristallstruktur von HypD kann dessen [4Fe-4S]-Cluster als Donor jedoch ausgeschlossen werden (Blokesch & Böck, 2006; Watanabe et al., 2007). Somit wird Eisen entweder direkt in der großen Untereinheit gebunden und mit seinen Liganden assembliert oder durch Interaktion verschiedener Reifungsproteine miteinander, z.B. HypC mit HypD oder HypE mit HypD, vorgefertigt. HypE tritt in vitro als Homodimer auf während HypD nur als Monomer gefunden wurde (Blokesch et al., 2004a; 2004b), was möglicherweise eine Erklärung für die Anzahl der Liganden am Eisenatom liefert. Durch ^{13}C-Markierung von Citrullin, aus welchem intrazellulär Carbamoylphosphat entsteht, konnte bewiesen werden, dass dieses alleiniger Donor für die Cyanidliganden ist, jedoch nicht als CO Ligand eingebaut werden kann (Forzi et al., 2007; Lenz et al., 2007). Externes CO-Gas kann bei der Reifung zwar als CO-Ligand verwendet werden, ist jedoch in dieser Form physiologisch nicht in genügend hohen Konzentrationen vorhanden (Bürstel et al., 2011; Forzi et al., 2007; Lenz et al., 2007). Deshalb muss die Quelle des CO Liganden metabolischen Ursprungs sein, wobei für heterotroph wachsende R. eutropha die Abhängigkeit von 1,3-^{13}C$_2$-Glycerol gezeigt werden konnte, welches jedoch in einer Vielzahl von Reaktionen metabolisiert wird und damit das unmittelbare CO-Substrat unbekannt bleibt (Bürstel et al., 2011).

Eindeutig konnte gezeigt werden, dass der Einbau des Fe(CN)$_2$CO dem Einbau des Nickelions in der großen Untereinheit vorausgeht (Maier & Böck, 1996; Menon & Robson, 1994; Rossmann et al., 1994). Für die Ni-Insertion in Hyd-3 interagieren HypA, HypB und SlyD miteinander, wobei HypB eine GTPase Aktivität besitzt, GTP abhängig dimerisieren kann und das Nickel Ion überträgt, während HypA als Gerüstprotein fungiert (Chan Chung & Zamble, 2011a; Gasper et al., 2006; Leach et al., 2005). SlyD, eine Peptidyl-Prolyl cis/trans Isomerase, ist nicht essentiell für Hydrogenase Aktivität, erleichtert jedoch die Freigabe des

Ions und vermittelt die Interaktion von HypB mit HycE (Chan Chung & Zamble, 2011b; Zhang *et al.*, 2005). Eine *hypB* Mutante kann phänotypisch durch die Zugabe hoher Nickelmengen im Medium komplementiert werden (Lutz *et al.*, 1991). Neben dem Einbau des Nickels ins aktive Zentrum der Hydrogenasen, konnte ebenfalls gezeigt werden, dass HypA und HypB das Nickel-Zentrum der Urease aus *Helicobacter pylori* bereitstellen und die *hypAB* Deletion in diesem Organismus in verminderte Pathogenität resultiert (Kaluarachchi *et al.*, 2010; Sydor *et al.*, 2011).

Die abschließende *C*-terminale proteolytische Prozessierung der großen Untereinheit durch HycI führt wahrscheinlich zu einer Konformationsänderung, durch welche das von HypC gelieferte aktive Zentrum im Protein eingeschlossen wird (Drapal & Böck, 1998). Da die Sequenz des *C*-terminalen Peptides nicht hoch-konserviert ist, dessen Anwesenheit jedoch für die Insertion des aktiven Zentrums benötigt wird und Proteolyse ohne Nickel nicht stattfindet, kann von einer spezifischen das Nickel in den Mechanismus einbeziehenden Proteolyse von HycI ausgegangen werden (Kumarevel *et al.*, 2009; Rossmann *et al.*, 1995; Theodoratou *et al.*, 2000; 2005). Für Hyd-1 und Hyd-2 existieren die ebenfalls spezifischen Endopeptidasen HyaD und HybD (Fritsche *et al.*, 1999). Über die Assemblierung der weiteren Komponenten des FHL Komplexes sowie deren Stöchiometrie ist nicht viel bekannt, jedoch besitzt keine Untereinheit eine für den Membrantransport wichtige Signalsequenz. Für Hyd-1 und Hyd-2 muss die Interaktion der großen mit der kleinen Untereinheit erfolgen, um mit Hilfe deren *N*-terminalen Tat-Signals über die Membran transloziert zu werden (Dubini & Sargent, 2003).

1.6 Aufnahme von Metallen und Regulation

In Mikroorganismen erfolgt die Aufnahme von Metallen aus dem Medium hochspezifisch und unabhängig von der Konzentration anderer Metalle im Medium (Cvetkovic *et al.*, 2010). Die häufigsten Metalle der 343 cytoplasmatischen Metalloproteine in z.B. *Pyrococcus furiosus* sind Eisen und Zink (97 %), gefolgt von Wolfram und Nickel (< 2,5 %) mit einem Anteil der restlichen Metalle von weniger als 0,5 % (Cvetkovic *et al.*, 2010). Der Transport und Einbau des Nickel-Ions ins aktive Zentrum von Hydrogenasen ist bereits gut untersucht. Durch Mutagenese konnte ein spezifischer Nickel ABC (*A*TP-*b*inding *c*assette)-Transporter entdeckt werden, dessen Deletion die Ausbildung aktiver [NiFe]-Hydrogenasen verhindert und sich phänotypisch nur durch Zugabe hoher Nickelmengen im Medium supprimieren lässt (Wu & Mandrand-Berthelot, 1986; Wu *et al.*, 1989; 1991). Die Bindung von Nickel an NikA, dem periplasmatischen Bindeprotein, erfolgt mit einem K_d von < 0,1 µM (De Pina *et al.*,

1995; Mulrooney & Hausinger, 2003). Der Transport erfolgt durch die Membrankomponenten NikB und NikC, wobei die Energie von den ATP-bindenden Komponenten NikD und NikE bereitgestellt wird (Navarro *et al.*, 1993). Die Expression der Gene für den Nickel-ABC Transporter ist abhängig von Fnr und wird in Anwesenheit hoher Nickelkonzentrationen durch NikR reprimiert (Abb. 5) (Rowe *et al.*, 2005; Wu *et al.*, 1989; 1991).
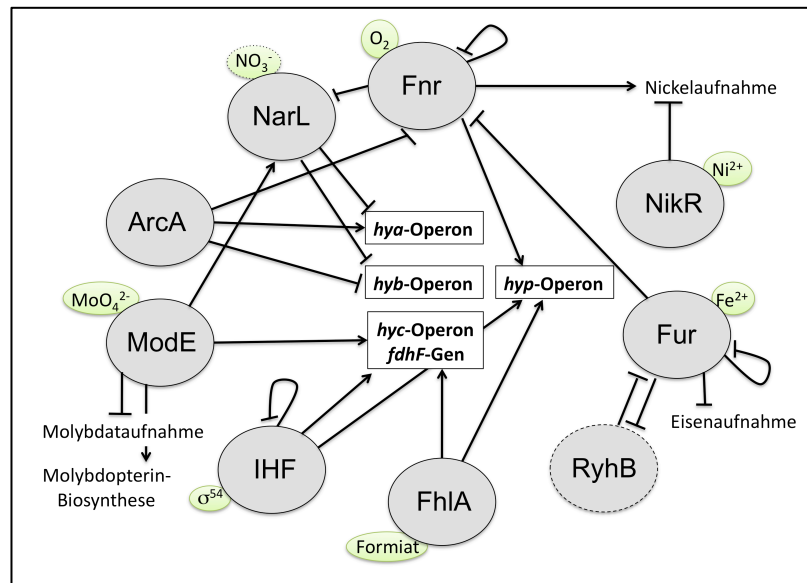
Abbildung 5 Regulatorisches Netzwerk der strukturellen und akzessorischen Hydrogenasegene. Die transkriptionellen Regulatorproteine und die sRNA RyhB und ihre aktivierende (→) oder hemmende (⊣) Wirkung auf die Expression der Hydrogenase-spezifischen Gene sowie die Regulation der Transkriptionsfaktoren untereinander. Die Effektormoleküle für die Aktivierung sind in Grün gezeigt und binden entweder direkt oder lösen eine Phosphorylierung des Regulators z.B. NarX für NarL aus.

Die Aufnahme von Nickel in *E. coli* erfolgt ausschließlich über den NikABC-Transporter, während in *H. pylori* ein weiteres homologes Nickel-Aufnahme System existiert (Mulrooney & Hausinger, 2003). Im Gegensatz dazu ist die Eisen-Aufnahme in *E. coli* weit differenzierter. Es existieren hoch-affine Aufnahmesysteme (FeoABC) sowie diverse Siderophor-vermittelte Aufnahmesysteme (FecA-E, FepA-G, FhuA-D) und weitere Transporter, welche unspezifisch Eisen translozieren können (vgl. Abb. 9) (Andrews *et al.*, 2003; Cartron *et al.*, 2006; Hantke, 2003). Die Kontrolle der Expression der Gene für die Eisenhomöostase erfolgt durch den Fur Regulator (*ferric uptake regulation*) (Hantke, 1981). Dieser bindet Eisen und ist damit in der Lage an eine Konsensussequenz der DNA im Promotorbereich des zu regulierenden Genes zu binden und die Transkription zu verhindern (Hantke, 2002). Genau wie die Nickel- und Eisenaufnahme wird auch die Transkription der Gene für Molybdataufnahme durch den Regulator ModE kontrolliert, wobei dieser ebenfalls

die Expression der Gene, deren Produkte Molybdat verwenden, reguliert (Abb. 5) (Anderson *et al.*, 2000; Hasona *et al.*, 1998; Self *et al.*, 1999).

1.7 Fnr Regulator und [FeS]-Cluster Biosynthese

Als anorganische Verbindung von Eisen mit Schwefel ist Pyrit, ein als Katzengold bezeichnetes Erz der Formel FeS_2, bekannt. Einer Theorie zufolge könnten Reaktionen an der Oberfläche solcher Übergangsmetall-Schwefel Verbindungen zur Entstehung des Lebens beigetragen haben, indem durch die Reduktionskraft vulkanischer Ausströmungen wie Ammoniak, Kohlenstoffmonoxid und Schwefelwasserstoff Pyruvat, Aminosäuren und Peptide entstanden sind (Cody *et al.*, 2000; Huber & Wächtershäuser, 1998; Wächtershäuser, 2000; 2007). Auf diese Weise basiert die Entstehung von organischen Molekülen auf initialer CO_2-Fixierung (Martin & Russell, 2007). Dank der Vielfalt möglicher Reaktionen an [FeS]-Verbindungen erfüllen diese ein breites Funktionsspektrum in biologischen Systemen.
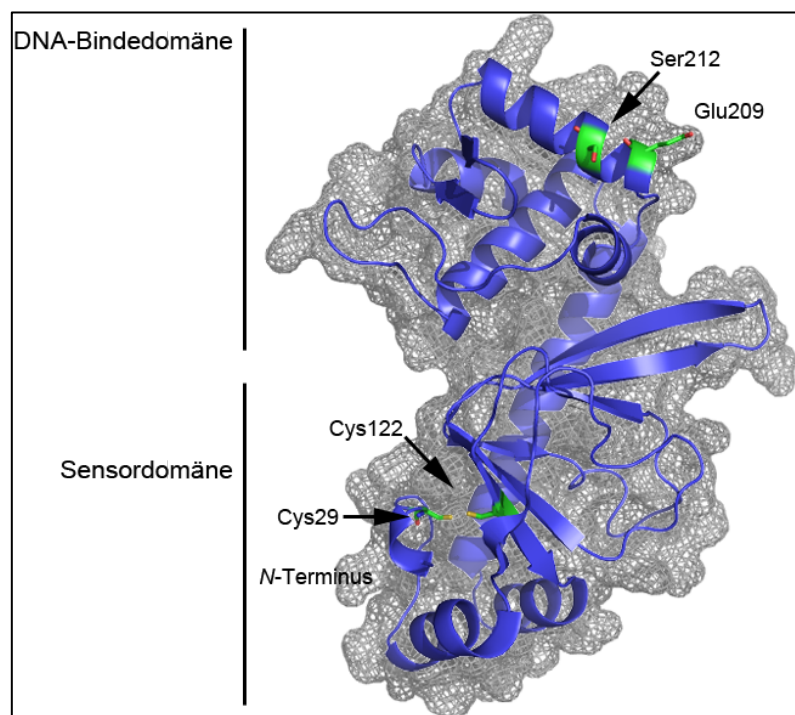
Abbildung 6 Sekundärstruktur- und Oberflächen-Darstellung einer PHYRE Vorhersage der Fnr Struktur (Kelley & Sternberg, 2009). Basierend auf der von der Aminosäuresequenz abgeleiteten Sekundärstrukturelemente wird vom Algorithmus mit Hilfe bekannter Strukturen homologer Proteine die Tertiärstruktur modelliert. Dieses Modell basiert u.a. auf der Struktur des Transkriptionsregulators CRP (*catabolite repressor protein*) PDB-Datei 2GAU und 2FMY. In der DNA-Bindedomäne des *C*-Terminus sind die Aminosäuren Glu209 und Ser212, die für die DNA Bindung essentiell sind, hervorgehoben. In der *N*-terminalen Sensordomäne sind die ersten 24 Aminosäuren, die zwei Cysteine die das für die O_2 Sensierung wichtige [FeS]-Cluster binden, nicht modelliert worden. Die weitern zwei Cysteine sind gekennzeichnet (Yan & Kiley, 2008).

Der globale Regulator Fnr sensiert die Anwesenheit von O_2 und aktiviert neben den oben genannten Genen hauptsächlich Gene des anaeroben Stoffwechsels wie für die Nitratatmung

oder die Pyruvat-Formiat-Lyase (Spiro & Guest, 1990; 1991). Das Fnr Bindemotiv in den regulierten Promotorregionen hat die Konsensussequenz TTGAT-N_4-ATCAA wobei das Regulon bis zu 115 Operons umfasst (Constantinidou *et al.*, 2006; Spiro & Guest, 1991). Fnr wird konstitutiv exprimiert, jedoch sind die Expressionslevel verschiedener *E. coli* Stämme von einem stromaufwärts gelegenen Transposon abhängig (Ferenci *et al.*, 2009; Sawers, 2005c). In seiner aktiven Form dimerisiert Fnr mit jeweils einem [4Fe-4S]-Cluster pro Monomer, welches bei Anwesenheit von 1 µM O_2 oxidiert und das Protein zum Monomer zerfallen lässt (Crack *et al.*, 2008; Kiley & Beinert, 1998). Dieses [FeS]-Cluster wird in der *N*-terminalen Domäne über 4 Cysteine gebunden, eine Region die im strukturell verwandten CRP nicht konserviert ist (Abb. 6) (Green *et al.*, 1993; Yan & Kiley, 2008). Die Aktivierung und Rekonstitution des [4Fe-4S]-Clusters erfolgt bei Abwesenheit von O_2 durch die allgemeine [FeS]-Biosynthese Maschinerie (Mettert *et al.*, 2008).

Neben dieser regulatorischen Funktion haben [FeS]-Cluster auch strukturelle und Elektronen-transferierende Funktionen. So besitzen die modular aufgebauten Oxidoreduktasen eine Aneinanderreihung von [FeS]-Clustern im Abstand von ≈14 Å in ihren kleinen Untereinheiten und gelegentlich, um Elektronentransfer zu gewährleisten, auch in den großen Untereinheiten (Page *et al.*, 2003). Die Assemblierung der Elektronen-transferierenden [FeS]-Cluster erfolgt nicht spontan und es gibt nicht für jedes [FeS]-Cluster spezifische Proteine. Stattdessen haben Mikroorganismen drei allgemeine und unabhängige Systeme für die Biosynthese von [FeS]-Clustern evolviert (Py & Barras, 2010; Takahashi & Tokumoto, 2002). Für die Nitrogenase wurden zunächst die Proteine NifU und NifS entdeckt, welche nicht nur die Biosynthese des FeMo-Kofaktors katalysieren (Hu & Ribbe, 2011). Orthologe Proteine des sogenannten Isc (*iron sulfur cluster*) und des Suf (*sulfur assimilation*) Systems konnten in *E. coli* identifiziert werden (Abb. 7). Das Suf System setzt sich mindestens aus den 6 Genprodukten des Operons *sufABCDSE* zusammen, dass hauptsächlich unter oxidativem Stress exprimiert wird (Fontecave *et al.*, 2005). Das *isc* Operon wird dagegen durch IscR negativ reguliert und umfasst die Genprodukte *iscRSUA-hscBA-fdx* (Schwartz *et al.*, 2001; Tokumoto & Takahashi, 2001). Beide Systeme haben homologe Komponenten. Der Schwefel wird von einer Desulfurase, IscS oder SufS, aus Cystein rekrutiert und in einem instabilen [2Fe-2S]-Cluster auf IscU bzw. SufBCD assembliert (Py & Barras, 2010; Shepard *et al.*, 2011). Die physiologische Eisenquelle ist unbekannt, *in vitro* kann jedoch Fe^{2+} oder CyaY als Donor dienen, *in vivo* ist bisher lediglich eine Interaktion von CyaY mit IscS und eine regulatorische Funktion nachgewiesen worden (Adinolfi *et al.*, 2009; Ding *et al.*, 2007; Layer

et al., 2006). Der Transfer des [FeS]-Clusters auf das Apo-Protein erfolgt wahrscheinlich mittels *A-type carrier* (ATC)-Proteinen wie IscA, SufA und ErpA, deren Transportwege durch Kombination von Mutagenese, Interaktions- und *in vitro* [FeS]-Transfer Studien untersucht wurden (Vinella *et al.*, 2009). Allerdings ist über die Spezifität des Einbaus von [FeS]-Clustern in die modularen Oxidoreduktasen nicht viel bekannt.
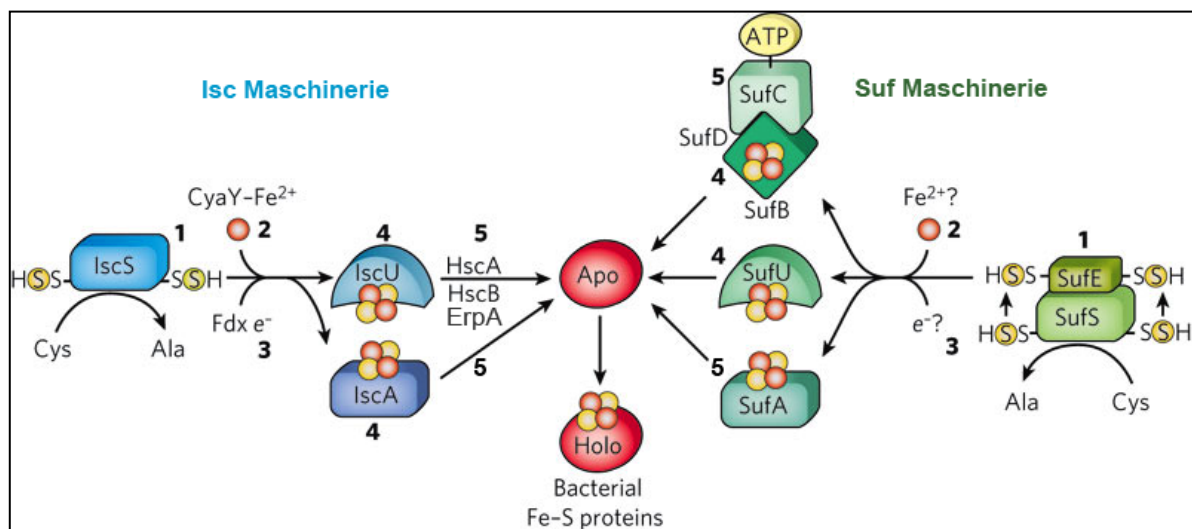
Abbildung 7 Mechanismus der bakteriellen [FeS]-Biosynthese mittels des Isc und des Suf-Systems (modifiziert nach Lill, 2009). Das Suf System liefert unter oxidativem Stress [FeS]-Cluster, während das Isc System unter normalen Wachstumsbedingungen aktiv ist. Es stellen dabei SufA und IscS Cystein Desulfurasen dar, SufU und IscU Gerüstproteine, SufA, IscA und ErpA Transportproteine. Das Apoprotein ist ein Protein, welchem durch eines der beiden Systeme [FeS]-Cluster geliefert bekommt, um zum Holoprotein zu werden. Die Schritte sind 1: Cystein Bereitstellung, 2: Eisen Bereitstellung, 3: Elektronentransfer, 4: Gerüstproteine, 5: Cluster Transfer und die Pfeile geben mögliche [FeS]-Transfer Wege an.

1.9 Ziel der vorliegenden Arbeit war es, durch gezielte Gendeletionen Einflüsse der Eisenhomöostase und Metabolitreduktion auf die Expression und Aktivität der anaeroben Atmungsenzyme in *E. coli* wie Fdh-N und Nar im Allgemeinen sowie der Enzyme der gemischten Säuregärung wie [NiFe]-Hydrogenasen im Speziellen, aufzudecken. Dabei sollte insbesondere auf den Aspekt der unterschiedlichen Anteile der einzelnen Hydrogenasen an der Gesamtaktivität unter verschiedenen Bedingungen eingegangen werden und die Rolle der kleinen Untereinheiten und die Spezifität der [FeS]-Maschinerie auf diese untersucht werden.

2. Ergebnisse

2.1 Übersicht über Publikationen und Manuskripte

Pinske C & Sawers RG (2010). The role of the ferric-uptake regulator Fur and iron homeostasis in controlling levels of the [NiFe]-hydrogenases in *Escherichia coli*. *International Journal of Hydrogen Energy* 35, 8938–8944.

> Eigenanteil: Planung, Durchführung und Auswertung aller Experimente. Anfertigung der Abbildungen 2 und 3, Entwurf des Material und Methodenteils.

Pinske C & Sawers RG (2011). Iron restriction induces preferential down-regulation of H_2-consuming over H_2-evolving reactions during fermentative growth of *Escherichia coli*. *BMC Microbiol* 11, 196.

> Eigenanteil: Planung, Durchführung und Auswertung aller Experimente. Anfertigung der Abbildung und von Teilen (ca. 40 %) des Manuskriptes.

Pinske C, Krüger S, Soboh B, Ihling C, Kuhns M, Braussemann M, Jaroschinsky M, Sauer C, Sargent F, Sinz A & Sawers RG (2011). Efficient electron transfer from hydrogen to benzyl viologen by the [NiFe]-hydrogenases of *Escherichia coli* is dependent on the coexpression of the iron-sulfur cluster-containing small subunit. *Arch Microbiol* 193, 893-903.

> Eigenanteil: Planung, Durchführung und Auswertung der *in vivo* Experimente, Planung der Klonierungen sowie Anfertigung der Abbildungen 3, 4 und 5a und des Material und Methodenteils, Entwurf der Einleitung.

Pinske C, Bönn M, Krüger S, Lindenstrauß U & Sawers RG (2011). Metabolic deficiences revealed in the biotechnologically important model bacterium *Escherichia coli* BL21(DE3). *PLoS ONE* 6 (8), e22830.

> Eigenanteil: Planung, Durchführung und Auswertung aller Experimente, Anfertigung des Manuskriptes.

Soboh B*, **Pinske C***, Kuhns M, Waclawek M, Ihling C, Trchounian K, Trchounian A, Sinz A & Sawers RG (2011). The respiratory molybdo-selenoprotein formate dehydrogenases of *Escherichia coli* have hydrogen: benzyl viologen oxidoreductase activity. *BMC Microbiol* 11, 173

> * Gemeinsame Erstautorenschaft.
>
> Eigenanteil: Planung, Durchführung und Auswertung der Experimente zur physiologischen Verifikation und für Abbildung 4 sowie Anfertigung der Abb. 4.

Pinske C & Sawers RG (2011). The A-type carrier protein ErpA is essential for formation of an active formate-nitrate respiratory pathway in *Escherichia coli* K-12. *J Bacteriol*, im Druck.

> Eigenanteil: Planung, Durchführung und Auswertung aller Experimente. Anfertigung der Abbildung und Entwurf des Manuskriptes.

Pinske C & Sawers RG (2011). Delivery of iron-sulfur clusters to [NiFe]-hydrogenases in *Escherichia coli* requires the A-type carrier proteins ErpA and IscA. *PLoS ONE*, eingereicht.

> Eigenanteil: Planung, Durchführung und Auswertung aller Experimente. Anfertigung der Abbildung und Entwurf des Manuskriptes.

Darlegung des Eigenanteils und Bestätigung durch einen Koautor:

Constanze Pinske   Prof. R. Gary Sawers

2.2 Die Rolle des Eisen-Aufnahme Regulators Fur und der Eisen-Homöostase bei der Kontrolle der [NiFe]-Hydrogenase Mengen in *Escherichia coli.*

2.2.1 Zusammenfassung

Das Fur Protein (*ferric uptake regulation* – Eisenaufnahmeregulation) ist ein negativer Regulator z.B. der Gene des Enterobactin und des Feo-Operons sowie weiterer Siderophor vermittelter Eisenaufnahmesysteme, um die Eisenhomöostase innerhalb der Zelle zu gewährleisten (Bagg & Neilands, 1987; Hantke, 2002). Es sensiert dabei die Konzentration intrazellulären Eisens und kann in dessen Anwesenheit an die -35 Box in der Promotorregionen des zu regulierenden Gens binden und die Transkription reprimieren.

Um Indizien zu gewinnen wie [NiFe]-Hydrogenasen auf veränderte Eisenkonzentrationen reagieren, wurde das für Fur kodierende Gen deletiert und die Mengen und Aktivitäten aller drei unter fermentativen Bedingungen aktiven Hydrogenasen untersucht. Dabei wurde ein Verlust der Gesamtaktivität um 80-90 % festgestellt. Unter den gewählten Bedingungen wurden die bei der Messung der Gesamthydrogenaseaktivität bestimmte Aktivität des Wildtyps bis zu 90 % vom FHL Komplex beigesteuert. Die Aktivität der darin befindlichen Hyd-3 kann unabhängig von Hyd-1 und Hyd-2 als H_2-Produktion gemessen werden und diese zeigte sich in einem Fur Deletionsstamm um 82 % reduziert. Als Grund für diese Reduktion konnte durch *lacZ* Genfusionen verringerte Transkription der *fdhF* und *hyc* Gene, die für strukturelle Komponenten des FHL Komplexes kodieren, festgestellt und auf Translationsebene durch verringerte Mengen des HycE Proteins bestätigt werden.

Gleichzeitig sind die Proteinmengen und Aktivitäten der Wasserstoffoxidierenden Hyd-1 und Hyd-2 deutlich reduziert obwohl die Transkription der Gene von Hyd-2 unverändert und von Hyd-1 nur um 30 % verringert ist. Dies lässt auf post-transkriptionelle Regulation der beiden Enzyme schließen. Ein Unterschied in der Regulation zu den FHL Komponenten besteht in deren Abhängigkeit von Formiat und Molybdat. Nichtsdestotrotz konnte Zugabe von Formiat zum Medium die Transkription von *fdhF* nur von 10 % auf 26 % des Wildtypniveaus unter den jeweils gleichen Bedingungen anheben, was auf einen nicht durch Formiatmangel hervorgerufenen Effekt deutet. Ein Vergleich der Hyd Proteinmengen mit einer multiplen Eisentransportmutante (Δ*fecA-E zupT mntH feoB entC*) zeigte jedoch, dass in dieser alle Hydrogenasen großen Untereinheiten gleichartig reduziert waren, was im Umkehrschluss bedeutet, dass durch Fur Deletion kein durch Eisenmangel hervorgerufener Phänotyp sichtbar

wurde. Intrazellulärer Eisenmangel kann zudem durch das bereits bekannte Regulationsmuster des Fur Proteins ausgeschlossen werden (Hantke, 1981). Weiterhin konnte ausgeschlossen werden, dass die Reifung der großen Hydrogenase Untereinheiten durch die *fur* Deletion beeinflusst wurde, da die Transkription der für die benötigten Reifungsproteine kodierenden Gene unbeeinflusst blieb. Die gesammelten Ergebnisse deuten auf eine indirekte Fur abhängige Regulation des FHL Komplexes hin. Als sich aus den Daten ableitendes Modell bietet sich die durch RhyB vermittelte Repression des *iscSUA* Operons an. In Abwesenheit von Fur wird die regulatorische RNA RyhB dereprimiert, die normalerweise die Funktion von Fur unterstützt und Translation von mRNAs verhindert. Gleichzeitig wird IscR stabilisiert und die Expression der *hya*- (Abb. 8) und *hyb*-Operons (Giel *et al.*, 2006) gehemmt. Allgemein konnte mit diesen Experimenten erstmals ein Zusammenhang zwischen der Eisen-Homöostase und dem H_2-Stoffwechsel gezeigt werden.
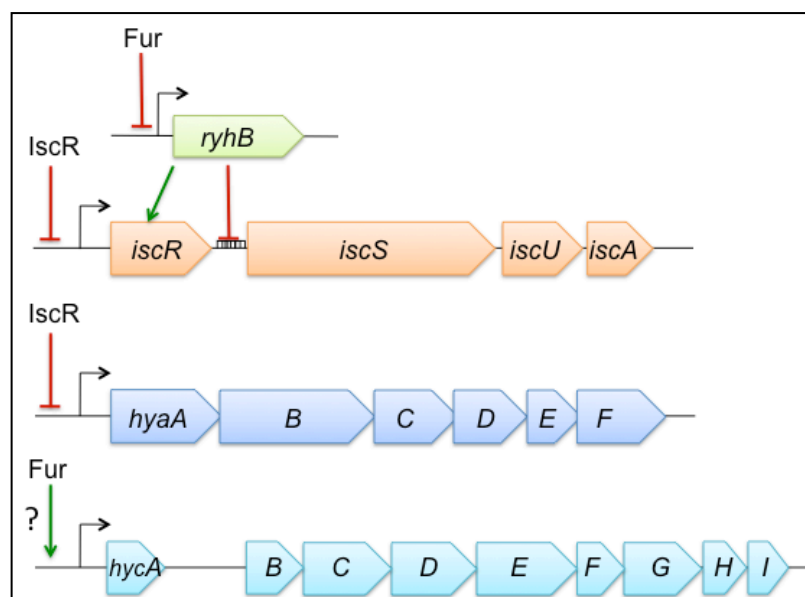
Abbildung 8 Mögliche durch Fur-vermittelte Regulation der Hydrogenasen. Die Gene *ryhB*, *iscRSUA*, *hyaA-F* und *hycA-I* und deren Hemmung (rote Balken) oder Aktivierung (grüne Pfeile) durch Fur und IscR sowie der regulatorischen RNA RyhB sind dargestellt. Die Gene sind nicht maßstabsgetreu und die Art der Fur vermittelten Regulation des *hyc*-Operons ist unbekannt, da im Promotorbereich keine Fur Bindestelle identifiziert wurde.

2.2.2 Artikelkopie

The Role of the Ferric-Uptake Regulator Fur and Iron Homeostasis in Controlling Levels of the [NiFe]-Hydrogenases in *Escherichia coli*

Constanze Pinske and R. Gary Sawers[*]

Institute for Biology/ Microbiology, Martin-Luther University Halle-Wittenberg, Kurt-Mothes-Str. 3, 06120 Halle (Saale), Germany

[*] For correspondence: R.G. Sawers, Institute for Biology/ Microbiology, Martin-Luther University Halle-Wittenberg, Kurt-Mothes-Str. 3, 06120 Halle (Saale) Germany
Tel., +49 345 5526350; Fax., +49 345 5527010; Email, gary.sawers@mikrobiologie.uni-halle.de

Abstract
Escherichia coli when growing anaerobically synthesizes three [NiFe]-hydrogenases. We investigated the consequences on hydrogenase levels, enzyme activity and gene expression of deleting the *f*erric iron-*u*ptake *r*egulator Fur, which is required to coordinate intracellular iron levels. Total hydrogenase activity was reduced between 80-90% in the *fur* mutant. Hydrogen production by the formate hydrogenlyase pathway was strongly reduced. Analysis of *lacZ* fusions to the various hydrogenase structural operons demonstrated that regulation of *hya* and *hyb* was not transcriptional, while the effect of the *fur* mutation on *hyc* was partly due to reduced intracellular formate. Immunological analysis of the hydrogenase large subunits revealed that the absolute levels of the enzymes were reduced suggesting that either post-transcriptional or post-translational control, possibly through enhanced enzyme turnover, was a major cause of reduced activity. A mutant defective in multiple iron transport systems also essentially lacked hydrogenase activity highlighting the importance of intracellular iron availability in regulating hydrogenase synthesis.

Keywords: Fe^{3+}-uptake regulator, Fur; iron transport; dihydrogen evolution; dihydrogen oxidation; [NiFe]-hydrogenase

1. Introduction
The study of biohydrogen production through the action of microbial hydrogenases is a rapidly expanding area of scientific research [1, 2]. In order to make significant headway in improving microbial systems for biohydrogen production we must first attempt to understand hydrogen metabolism completely and this can be achieved most usefully using well-characterized model systems such as *Escherichia coli*. Although *E. coli* has the coding capacity to synthesize four [NiFe]-hydrogenases, so far only three hydrogenases have been identified and characterized [3]. All three [NiFe]-hydrogenases are synthesized anaerobically and a complex machinery of enzymes for the biosynthesis of their active sites and insertion of the fully formed enzymes into the cytoplasmic membrane is required [4, 5]. Hydrogenases 1 (Hyd-1) and Hyd-2 are membrane-associated and have their active sites located on the periplasmic side of the cytoplasmic membrane. Hyd-1 and Hyd-2 oxidize dihydrogen and are encoded by the *hya* and *hyb* operons, respectively. Hyd-3, on the other hand, forms part of the dihydrogen-evolving formate hydrogenlyase (FHL) complex, which is also a membrane-bound protein complex but has its active centres oriented toward the cytoplasm [3]. The FHL complex comprises 6 Hyc proteins, encoded by the *hyc* operon, along with a formate dehydrogenase H component encoded by the *fdhF* gene. Synthesis of the FHL complex is absolutely dependent upon formate [6]. These large enzyme complexes have a significant demand for iron not only from the perspective of their complex active sites but also through numerous iron-sulphur clusters in their electron-transferring subunits.

While we understand a considerable amount, but by no means all, concerning the biosynthesis of the active site of [NiFe]-hydrogenases [5], as well as much of the detail of nickel uptake and delivery to the active site machinery [5], next to nothing is known regarding the uptake and delivery of iron for active site biosynthesis. Iron is also required for the iron-sulfur (Fe-S) clusters in the small subunits and electron-transfer components of the hydrogenases; however, the route of iron delivery

and which of the Fe-S cluster biosynthetic machineries [7,8,9] are involved in Fe-S synthesis is unresolved.

A key regulator of intracellular iron homeostasis is the ferric uptake regulator Fur [10]. Fur was originally identified as a negative regulator of many iron transport systems [10], but more recently it has been shown to regulate expression of some genes positively [11,12]. Fur achieves this on the one hand by controlling cellular iron-protein levels in response to iron availability, particularly large enzyme complexes with a high demand for iron [12] and on the other it represses transcription of a small 90 base regulatory RNA RyhB that binds to several mRNAs encoding gene products involved in iron metabolism. RyhB functions by enhancing degradation of particular mRNAs [11]. In this study we examined the impact of deleting the gene encoding Fur on hydrogenase biosynthesis and discovered that the levels and activities of all three [NiFe]-hydrogenases in *E. coli* were compromised.

2. Materials and methods

1.1 Strains and growth conditions

The bacterial strains used in this study are listed in Table 1. Introduction of the *fur*::Cm^R mutation from GG190 into MC4100 by P1*kc* phage transduction to create CP500 was performed according to Miller [20].

E. coli strains were grown routinely at 37 °C on LB-agar plates [20] and those with either a *fur*::Cm^R mutation or carrying a single copy *lacZ* fusion included 12.5 μg per ml of chloramphenicol or 50 μg per ml of kanamycin, respectively, in the plates. Anaerobic growths were performed at 37 °C in sealed bottles filled with anaerobic media and under a nitrogen gas atmosphere. Cultures for determination of hydrogenase enzyme activity and processing of the respective hydrogenase large subunits were grown in TYEP media pH 6,5 [21] supplemented with 0.8% (w/v) of glucose (TGYEP), 7.5 μM FeCl$_3$ and 0.1 μM NiCl$_2$. Where indicated formate was added to a final concentration of 15 mM.

When required kanamycin (50 μg ml^{-1}), ampicillin (100 μg ml^{-1}) or chloramphenicol (12.5 μg ml^{-1}) were added to the growth media.

2.2. Construction of single copy *lacZ* fusions

Recombinant DNA work was carried out according to published methods [22]. To construct the *hypA*::*lacZ* fusion a 541 bp (IR1) DNA fragment including the *hyp* promoter and regulatory region was amplified from the chromosome of MC4100 by PCR using Phusion DNA polymerase (Finnzymes, Germany) and the oligonucleotides IR1 (5'-CTC*GGATCC* TGTCACCATGACACTGTGGA-3' and 5'-CTC*GGATCC* GCGATGTAATCGGCTTTCTC-3') (Metabion, Germany). The DNA fragment was ligated into pRS551 [23], which had been digested with BamHI and dephosphorylated with shrimp alkaline phosphatase (Roche, Germany). This procedure delivered pRS-IR1. The complete

DNA sequence of the fragment was verified by sequencing (Seqlab, Germany) and the insert was transferred to λRS45 [23]. The resulting λ(*hypA*::*lacZ*) operon fusion was introduced in single copy into the λ attachment site of wild-type strain MC4100, delivering strain CP543. Construction of the M17s (single copy *hycB*::*lacZ*) [18] λ*fdhF*::*lacZ* fusion [17] and strains DJR10 λ(*hyaA–lacZ*) and DJR100 λ(*hybO–lacZ*) [19] has been described. Similarly, the *fur* derivatives CP744 (*hyaA*::*lacZ*), CP746 (*hybO*::*lacZ*), CP763 (*hycB*::*lacZ*), CP747 (*hypA*::*lacZ*) and CP749 (*fdhF*::*lacZ*) were constructed using CP500 (MC4100 *fur*::Cm^R) as a host.

2.3. Preparation of cell extracts and determination of hydrogenase-dependent enzyme activities

Anaerobic cultures were harvested at an OD$_{600nm}$ of approximately 0.8. Cells from cultures were harvested by centrifugation at 4000 x g for 10 min at 4°C, resuspended in 1% (v/v) of the culture volume of 50 mM MOPS buffer pH 7.0 and lysed on ice by sonification (30 W power for 5 minutes with 0.5 sec pulses). Unbroken cells and cell debris were removed by centrifugation for 15 min at 10, 000 x g and 4°C and the supernatant was used as the crude cell extract. Total hydrogenase enzyme activity was measured according to [24] except that the buffer used was 50 mM MOPS buffer, pH 7.0. The detection wavelength used was 578 nm and an E$_M$ value of 8,600 M^{-1} cm^{-1} was assumed for reduced benzyl viologen. One unit of activity was defined as the oxidation of 1 μmol of hydrogen per min.

Dihydrogen production by the FHL pathway was determined by gas chromatography. Cultures were grown anaerobically in TGYEP pH 6.5 with 15 mM formate and cells from a 100 ml culture were harvested and resuspended to an OD$_{600}$ = 1.0 per ml in 40 mM MOPS buffer pH 7.0, including 20 % (v/v) glycerol. Small anaerobic reaction tubes (mini-Hungate tubes 5 ml, Ochs Boveden-Lenglern) were filled in an anaerobic chamber (Coy, Michigan, USA) with 0.73 ml MOPS/ glycerol buffer and the residual hydrogen gas was removed under vacuum and replaced with nitrogen gas. A 100 μl aliquot of the cell suspension was added to the Hungate tubes and the mixture was reduced with sodium dithionite and equilibrated at 37 °C for 5 min. The reaction was started by the addition of 20 μl of 3 M sodium formate and 200 μl of the gas phase were analysed at 6 time points between 3 and 18 minutes by gas chromatography (GC4000 Fisosna Instruments, Mainz-Kastel Germany) with a molecular sieve column 5A, 80/ 100 mesh. Pure nitrogen was used as the carrier gas. The amount of dihydrogen gas produced per unit time was calculated based on a standard curve using defined concentrations of dihydrogen gas. From the initial velocities the specific activities were calculated and are given either in mU per mg protein or U per ml of equivalent cell number. Each experiment was repeated minimally three times and the standard deviation is shown.

Protein concentration of crude extracts was determined [25] with bovine serum albumin as standard.

2.4. Polyacrylamide gel electrophoresis and immunoblotting

For Western blot analysis, aliquots of 25 μg of protein from crude extracts were separated in 10% (w/v) SDS-polyacrylamide gel electrophoresis (SDS-PAGE) [26] and transferred to nitrocellulose membranes as described [27]. Antibodies raised against Hyd-1 (1: 10,000; [24]), Hyc-3 (1:3,000; [25]), Hyd-2 (1:20,000; a kind gift from F. Sargent)

and AdhE (1:20,000) were used. Secondary antibody conjugated to horseradish peroxidase was obtained from Bio-Rad. Visualisation was done by the enhanced chemiluminescent reaction (Stratagene).

Non-denaturing PAGE was performed using 7.5% (w/v) polyacrylamide gels pH 8.5 and included 0.1% (w/v) Triton-X100 in the gels exactly as described [20]. Samples of crude extract (15 – 20 μg of protein) were incubated with 5% (w/v) Triton X-100 prior to application to the gels. Gels were stained with either Coomassie Brilliant Blue or by in-gel staining for hydrogenase activity as described [24] except that the buffer used was 50 mM MOPS pH 7.0.

β-Galactosidase enzyme activity was determined as described by Miller [20] and performed at room temperature. All assays were performed in triplicate and repeated at least three times with results varying by no more than 15%.

3. Results and discussion

3.1. Fur is required for hydrogenase activity

Total hydrogenase activity was determined in cell extracts of *E. coli* wild type MC4100, its isogenic *fur* mutant CP500 and, as a control, a *hypF* mutant, which is unable to synthesize active [NiFe]-hydrogenases [14]. The results in Table 2 show that, as expected, the *hypF* mutant lacks hydrogenase activity, while the activity in a *fur* mutant was reduced approximately 80% compared with activity levels in the wild type. This result was surprising because mutants unable to synthesize the Fur repressor generally exhibit enhanced iron uptake [10]. This finding indicates that Fur is important for maximal hydrogenase activity in anaerobically growing *E. coli*.

To demonstrate that this effect was not strain-specific, the total hydrogenase activity of a different *E. coli* wild type strain W3110 [15] and its isogenic *fur* mutant were determined (Table 2). Extracts of W3110 had an activity similar to that of MC4100 and introduction of the *fur* deletion resulted in a corresponding 80% reduction in activity. As a control we analyzed hydrogenase activity in mutant ECA458, which lacks five iron transport systems (deletions in *entC, fecA-E, feoAB, mntH* and *zupT*). Extracts derived from anaerobically grown ECA458 were almost completely devoid of hydrogenase activity, which indicates the importance of both Fe^{2+} and Fe^{3+} acquisition systems for the synthesis of all three [NiFe]-hydrogenases in *E. coli*. It should be noted that none of the characterized mutants was significantly impaired in anaerobic growth in the rich medium used and growth media were supplmented with 7.5 μM iron and 0.1 μM nickel.

3.2. Lower levels of hydrogenases 1 and 2 are present in *fur* mutants

In order to examine the effect of the *fur* mutation on the levels of the individual hydrogenase enzymes more specifically we analyzed first of all the activities of Hyd-1 and Hyd-2 by staining for activity after native polyacrylamide gel electrophoresis (PAGE) [24]; due to its extreme lability under these conditions the Hyd-3 component of the FHL complex cannot be analyzed by this method [24]. It is clear from the data presented in Fig. 1A that particularly Hyd-1 levels are significantly lower in extracts of the *fur* mutant compared with the corresponding wild type strain MC4100. It is important to note that Hyd-1 contributes approximately only 1-2% of the total hydrogenase activity under the growth conditions used [28]. Hyd-2 also shows an approximate 2-fold lower activity. As a loading control a gel with the same samples was stained with Coomassie Brilliant Blue (right panel in Fig. 1A). The activity-stained Hyd-2 complexes were signficantly larger than the Hyd-1 active complex (Fig. 1A, compare left and right panels). In the W3110 background the *fur* mutation had a less pronounced effect on Hyd-1 and Hyd-2 (Fig. 1B).

In accord with the lack of hydrogenase activity (see 3.1.) no activity bands corresponding to Hyd-1 or Hyd-2 could been seen in extracts of DHP-F2 (Δ*hypF*) (Fig. 1A) and only extremely low levels of activity were observed in extracts from ECA458 (the iron transport-defective mutant) (Fig. 1B).

Active hydrogenases have a faster migrating form of their large subunit due to processing of the C-terminus subsequent to insertion of the NiFe-center into the active site [5]. The unprocessed, more slowly migrating species of the subunit is inactive and is frequently observed in extracts of the wild type, which provides a ,snap-shot' of both processed and newly synthesized, unprocessed enzyme species [5]. These species can be distinguished using denaturing SDS-PAGE and hydrogenase-specific antiserum. The Western blots in Fig. 1C demonstrate that antibodies raised against Hyd-1, Hyd-2 and Hyd-3 identify uprocessed and processed enzyme species that migrate with molecular masses varying between 60-65 kDa. The antibodies raised against Hyd-2 and Hyd-3 also show signals with some unidentified cross-reacting polypeptides. Focussing on the region of the gels migrating between 50 and

70 kDa it can be seen in Fig. 1D that the amounts of both unprocessed and processed forms of the large subunits of Hyd-1 and Hyd-2 were lower in the *fur* mutant. The most profound effect, however, was observed for the Hyd-3 large subunit where only barely detectable amounts of the processed species were observed (Fig. 1D). This finding indicates that active Fur is required for synthesis or stabililty and processing of Hyd-3. None of the processed species of the large subunits could be detected in extracts of ECA458 (the iron transport-defective mutant) indicating that without the key iron transport systems no processing of the hydrogenase large subunits occurs.

To demonstrate the specificity of the Fur protein for [NiFe]-hydrogenases, we could demonstrate that the level of iron-dependent alcohol dehydrogense, AdhE [29], which has a subunit molecular mass of 110 kDa was unaffected in the *fur* mutant (see lower panel in Fig. 1D). This panel also served as an internal loading control for the experiment. Moreover, the amount of AdhE was only marginally decreased in ECA458, indicating that not all iron-dependent enzymes were affected to the same extent by the mutations in iron transport systems.

3.3. Dihydrogen production is reduced 80% in a *fur* mutant

Hyd-3 is the active component of the FHL pathway and is required for dihydrogen evolution by fermenting *E. coli* cultures [3]. Dihydrogen production by cells of the *fur* mutant CP500 was only 20% of that observed for the wild type MC4100 (Fig. 2), which is in good agreement with the reduced levels of Hyd-3 polypeptides present in the mutant (see Fig. 1D in 3.2.). Under the fermenting growth conditions used for these studies Hyd-3 comprises 70-95% of the total hydrogenase enzyme activity (compare with Table 2, section 3.1.) [30,31]. The findings presented here suggest, therefore, that the Fur protein is important for optimal synthesis and activity of the FHL complex.

3.4. The absence of Fur does not negatively affect transcriptional regulation of the operons encoding the Hyd-1 or Hyd-2 structural components

The expression of the operons encoding Hyd-1 (*hya*) and Hyd-2, (*hyb*) was determined after anaerobic growth of the wild type, MC4100, and its isogenic *fur* deletion mutant CP500 using transcriptional *lacZ* fusions (Fig. 3). The results show that the *fur* mutation had no effect on the expression of either the *hybO::lacZ* gene fusion, while the expression of the *hyaA::lacZ* fusion was decreased by approximately 30% relative to the level in the wild type. These results indicate that the regulation imposed by Fur is not directly at the transcriptional level of these two operons. Rather regulation occurs at the post-transcriptional or post-translational level, possibly through increased turnover of the unprocessed large subunits of the enzymes because of the reduced levels of the the [NiFe]-cofactor in the active site [5] or through decreased mRNA stablility or translation [11]. Moreover, the small subunits of these enzymes are electron-transferring, iron-sulfur proteins and iron limitation will also result in production of apo-proteins lacking a complete FeS-cluster complement [3,5].

The *hyp* operon encodes components required for maturation of all three hydrogenases in *E. coli* [5]. Analysis of a *hyp*::*lacZ* transcriptional fusion revealed that the *fur* mutation had no effect on the expression of the operon encoding the hydrogenase maturation machinery (Fig. 3).

3.5. A *fur* mutant has reduced *fdhF* and *hyc* operon expression

In contrast to the lack of regulation of the hydrogenase structural operons, however, expression of the *fdhF* gene and *hyc* operon, both encoding structural components of the FHL complex was reduced 10-fold in the *fur* mutant (Fig. 3). Addition of formate to the culture medium elevated expression levels of the *fdhF*::*lacZ* fusion to 820 ± 100 in the *fur* mutant and to 3150 ± 490 in the wild type, indicating that formate restored expression to 25% of the levels observed for the wild type. These findings are in accord with the observed reduction in dihydrogen production via the FHL complex observed in Fig. 2 (see section 3.3.). Moreover, the results also suggest that part of the reason for the reduced *fdhF* and *hyc* expression is a lower intracellular formate concentration [6]. A recent survey of RyhB-regulated genes identified the *pflA* gene as a target [11]. PflA is a radical-SAM enzyme possessing a [4Fe-4S]-cluster and it is also the post-translational activator of pyruvate formate-lyase, which generates formate intracellularly from pyruvate [32]. Reduced levels of PflA result in a reduced intracellular formate pool. Clearly, however, reduced formate levels are

not the sole reason for reduced FHL activity in the *fur* mutant.

3.6. Iron homeostasis and hydrogenase activity - a physiological rationale for the role of Fur in hydrogen metabolism

RyhB controls the degradation of a number of mRNAs including the *iscSUA* portion of the *iscRSUA* operon [33], which encodes the machinery for biosynthesis of Fe-S clusters in anaerobically growing *E. coli*. Under iron-limiting conditions, or in mutants devoid of Fur, RyhB synthesis is increased and it binds to the *iscS* portion of the *iscRSUA* transcript promoting degradation of the *iscSUA* but concomitantly stabilizing the *iscR* portion of the transcript; IscR is a negative regulator of *hya* and *hyb* operon expression during aerobiosis [34]. The consequence is that Fe-S-cluster biogenesis is compromised and Fe-S cluster-containing proteins such as hydrogenases are no longer synthesized in an active form. Indeed, the total hydrogenase activity in an *iscA* mutant was approximately 5% (0.13 units mg protein^{-1}) that of the wild type, which would be consistent with a reduction in the levels of Fe-S cluster-containing enzymes. This mechanism could at least partially explain the negative effect of a *fur* mutation on hydrogenase enzyme activity, thus circumventing the requirement for direct transcriptional regulation and provides an elegant means of controlling hydrogenase biosynthesis in response to iron homeostasis. Moreover, the fact that the *hyb* operon was recently identified as a RyhB target [11] suggests that the steady-state levels of *hyb* operon mRNA should be reduced in a *fur* mutant and this could also contribute to the reduced levels of Hyd-2 in the *fur* mutant. Future studies will aim to determine the role of the Fe-S cluster biogenesis systems in hydrogenase biosynthesis.

4. Conclusions

The Fe^{2+}-responsive regulator Fur plays a central role in iron homeostasis. The initially surprising finding that a *fur* deletion mutant has an approximate 80-90% reduction in hydrogenase activity is possibly a direct consequence of a reduction in the levels of the Fe-S cluster biosynthetic machineries. Notably the hydrogenase 3 component of the dihydrogen-evolving FHL complex is strongly reduced in both amount and, as a consequence, activity in a *fur* mutant. The two hydrogen-oxidizing [NiFe]-hydrogenases synthesized under anaerobic conditions, Hyd-1 and Hyd-2, also exhibit somewhat reduced levels and activity in a mutant devoid of Fur. Not only is iron supply crucial for the optimal synthesis of [NiFe]-hydrogenases as evidenced by the absence of active hydrogenases in a mutant devoid of multiple transport systems but also the coordination of hydrogenase enzyme synthesis with intracellular iron metabolism is important for hydrogen metabolism in general. The key coordinator is Fur.

Abbreviations

Ferric-uptake regulator (Fur); Formate hydrogenlyase (FHL); Hydrogenase (Hyd); iron-sulfur (Fe-S); pyruvate formate-lyase-activating enzyme (PflA); radical-SAM (radical-S-adenosyl methionine)

References

[1] Chong M-L, Rahman NA, Yee PL, Aziz SA, Rahim RA, Shirai Y, Hassan MA.Effects of pH, glucose and iron sulfate concentration on the yield of biohydrogen by *Clostridium butyricum* EB6. Int J Hyd Energy 2009;34: 8859-8865.

[2] Ghosh D, Hallenbeck PC. Fermentative hydrogen yields from different sugars by batch cultures of metabolically engineered *Escherichia coli* DJT135. Int J Hyd Energy 2009;34: 7979-7982.

[3] Forzi L, Sawers RG. Maturation of [NiFe]-hydrogenases in *Escherichia coli*. BioMetals 2007;20:567-78.

[4] Sawers RG, Blokesch M, Böck A. Anaerobic formate and hydrogen metabolism. September 2004, posting date. Chapter 3.5.4. *In* R. Curtiss III (Editor in Chief), *EcoSal--Escherichia coli and Salmonella: Cellular and Molecular Biology.* [Online.] http://www.ecosal.org. ASM Press, Washington, D.C.

[5] Böck A, King PW, Blokesch M, Posewitz MC. Maturation of hydrogenases. Adv Microbiol Physiol 2006;51:1-71.

[6] Rossmann R, Sawers G, Böck A. Mechanism of regulation of the formate-hydrogenlyase pathway by oxygen, nitrate, and pH: definition of the formate regulon. Mol Microbiol 1991;5:2807–14.

[7] Schwartz CJ, Djaman O, Imlay JA, Kiley PJ. The cysteine desulfurase, IscS, has a major role in in vivo Fe-S cluster formation in Escherichia coli. Proc Natl Acad Sci USA 2000;97:9009–14.

[8] Takahashi Y, Tokumoto U. A third bacterial system for the assembly of iron-sulfur clusters with homologs in archaea and plastids. J Biol Chem 2002;277:28380-83.

[9] Vinella D, Brochier-Armanet C, Loiseau L, Talla E, Barras F. Iron-sulfur (Fe/S) protein biogenesis: phylogenomic and genetic studies of A-type carriers. PLoS Genet 2009;5:1-16.

[10] Hantke K. Regulation of ferric iron transport in *Escherichia coli* K12: isolation of a constitutive mutants. Mol Gen Genet 1981; 182:288-92.

[11] Massé E, Vanderpool CK, Gottesman S. Effect of RyhB small RNA on global iron use in *Escherichia coli*. J Bacteriol 2005;187:6962–71.

[12] McHugh JP, Francisco Rodrıguez-Quinones F, Abdul-Tehrani H, Svistunenko_DA, Poole RK, Cooper CE,_ Andrews SC. Global iron-dependent gene regulation in *Escherichia* coli: a new mechanism for iron homeostasis. J Biol Chem 2003; 278:29478–29486.

[13] Casadaban M, Cohen SN. Lactose genes fused to exogenous promoters in one step using Mu-*lac* bacteriophage: *in vivo* probe for transcriptional control sequences. Proc Natl Acad Sci USA 1979;76:4530-33.

[14] Paschos A, Bauer A, Zimmermann A, Zehelein E, Böck A. 2002. HypF, a carbamoyl phosphate-converting enzyme involved in [NiFe] hydrogenase maturation. J Biol Chem 2002;277:49945–51.

[15] Bachmann BJ. Pedigrees of some mutant strains of *Escherichia coli* K-12. Bacteriol Rev 1972;36:525–57.

[16] Grosse C, Scherer J, Koch D, Otto M, Taudte N, Grass G. A new ferrous-uptake transporter, EfeU (YcdN), from *Escherichia coli*. Mol Microbiol 2006;62:120-31.

[17] Falke D, Schulz K, Doberenz C, Beyer L, Lilie H, Thiemer B, Sawers RG. Unexpected oligomeric structure of the FocA formate channel of *Escherichia coli*: a paradigm for the formate-nitrite transporter family of integral membrane proteins. FEMS Microbiol Lett 2009; PMID: 20041954.

[18] Pecher A, Zinoni F, Jatisatienr C, Wirth R, Hennecke H, Böck A. On the redox control of synthesis of anaerobically induced enzymes in enterobacteriaceae. Arch Microbiol 1983;136:131-136.

[19] Richard DJ, Sawers G, Sargent F, McWalter L, Boxer DH. Transcriptional regulation in response to oxygen and nitrate of the operons encoding the [NiFe]-hydrogenases 1 and 2 of *Escherichia coli*. Microbiology 1999;145:2903-12.

[20] Miller JH. Experiments in molecular genetics. 1972 Cold Spring Harbor Laboratory, Cold Spring Harbor, N.Y.

[21] Begg YA, Whyte JN, Haddock BA. The identification of mutants of *Escherichia coli* deficient in formate dehydrogenase and nitrate reductase activities using dye indicator plates. FEMS Microbiol Lett 1977;2:47-50.

[22] Sambrook J, Fritsch EF, Maniatis T. Molecular cloning: a Laboratory Manual, 2nd ed. 1989 Cold Spring Harbor Laboratory Press, Cold Spring Harbor, N.Y.

[23] Simons RW, Houman F, Kleckner N. Improved single and multicopy *lac*-based protein and operon fusion cloning tools. Gene 1987;53:85-96.

[24] Ballantine SP, Boxer DH. Nickel-containing hydrogenase isoenzymes from anaerobically grown *Escherichia coli* K-12. J Bacteriol 1985;163:454–59.

[25] Lowry OH, Rosebrough NJ, Farr AL, Randall RJ. 1951. Protein measurement with the Folin phenol reagent. J Biol Chem 1951;193:265-275.

[26] Laemmli UK. Cleavage of structural proteins during the assembly of the head of bacteriophage T4. Nature 1970;227:680-685.

[27] Towbin H, Staehelin T, Gordon J. Electrophoretic transfer of proteins from polyacrylamide gels to nitrocellulose sheets: procedure and some applications. Proc Natl Acad Sci USA 1979;76:4350-4354.

[28] Sawers RG, Boxer DH. Purification and properties of membrane-bound hydrogenase isoenzyme 1 from anaerobically grown *Escherichia coli* K12. Eur J Biochem 1986;156:265–75.

[29] Kessler D, Leibrecht I, Knappe J. Pyruvate-formate-lyase-deactivase and acetyl-CoA reductase activities of *Escherichia coli* reside on a polymeric protein particle encoded by *adhE*. FEBS Lett 1991;281:59–63.

[30] Sauter M, Böhm R, Böck A. Mutational analysis of the operon (*hyc*) determining hydrogenase 3 formation in *Escherichia coli*. Mol Microbiol 1992;6:1523–32.

[31] Sawers RG, Ballantine SP, Boxer DH. Differential expression of hydrogenase isoenzymes in *Escherichia coli* K-12: evidence for a third isoenzyme. J Bacteriol 1985;164:1324–1331.

[32] Sawers RG, Clark DP. Fermentative pyruvate and acetyl CoA metabolism. July 2004, posting date. Chapter 3.5.3. *In* R. Curtiss III (Editor in Chief), *EcoSal--Escherichia coli and Salmonella: Cellular and Molecular Biology.* [Online.] http://www.ecosal.org. ASM Press, Washington, D.C.

[33] Desnoyers G, Morissette A, Prévost K, Massé E. Small RNA-induced differential degradation of the polycistronic mRNA *iscRSUA*. EMBO J 2009;28:1551-61.

[34] Giel JL, Rodionov D, Liu M, Blattner FR, Kiley PJ. IscR-dependent gene expression links iron-sulphur cluster assembly to the control of O_2-regulated genes in *Escherichia coli*. Mol Microbiol 2006;60:1058-75.

Figure legends
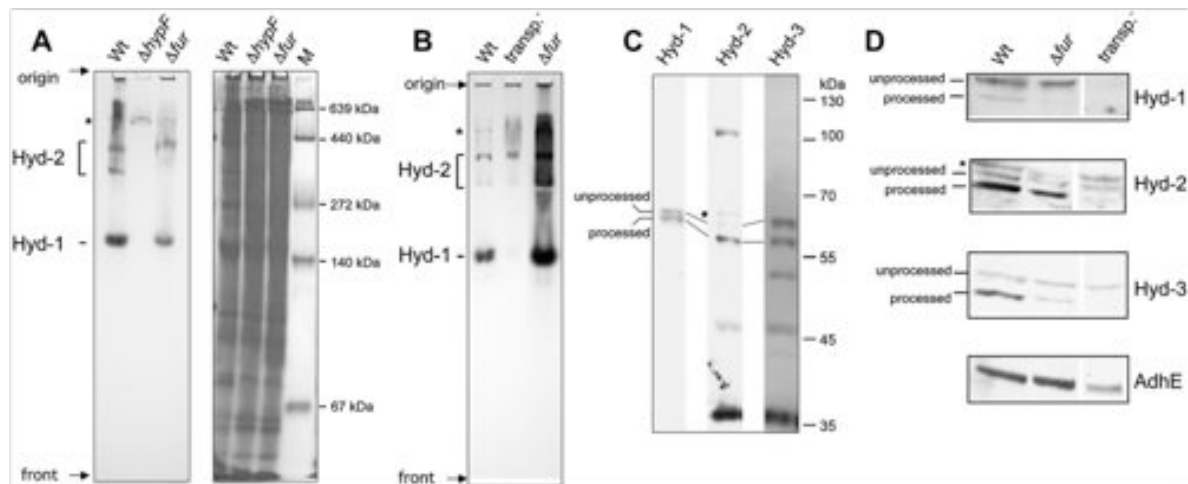
Figure 1. The [NiFe]-hydrogenases show reduced enzyme activity and protein levels in a *fur* mutant. Polypeptides in crude extracts (25 μg of protein) derived from (A) MC4100 (Wt), DHP-F2 (Δ*hypF*) and CP500 (Δ*fur*) and (B) W3100 (Wt), ECA458 (transport⁻) and GG209 (Δ*fur*) were separated by non-denaturing PAGE and subsequently stained for either hydrogenase enzyme activity as described in 2.4 or protein (right panel in part A). The locations of Hyd-1 and Hyd-2 are shown. The asterisk respresents a weak, hydrogenase-independent activity. Molecular mass markers (lane M) shown in the Coomassie-Blue-stained native PAGE were thyroglobulin (639 kDa), ferritin (440 kDa), catalase (272 kDa), lactate dehydrogenase (140 kDa) and BSA (67 kDa). C. Polypeptides in crude extracts (50 μg of protein) derived from MC4100 were separated under denaturing conditions by SDS-PAGE and after transfer to nitrocellulose membranes the samples were treated with antiserum raised against Hyd-1, Hyd-2 or Hyd-3. The locations of the unprocessed and processed forms of the respective hydrogenase large subunits are shown. The location of molecular mass size markers (Fermentas, Germany) is shown on the right of the panel. D. Polypeptides in crude extracts (50 μg of protein) derived from W3110 (Wt), ECA458 (transport ⁻) and GG209 (Δ*fur*) were separated under denaturing conditions by SDS-PAGE and hydrogenase and AdhE antigens were detected using specific antiserum raised against Hyd-1, Hyd-2, Hyd-3 and AdhE. In the interest of clarity only the portion of the gel between 50 and 70 kDa is shown. The bands labelled unprocessed and processed represent precursor and mature forms of the respective hydrogenase large subunits [5]. The asterisk next to the Western blot of Hyd-2 in panels C and D signifies an unidentified polypeptide that cross-reacts with the antiserum.
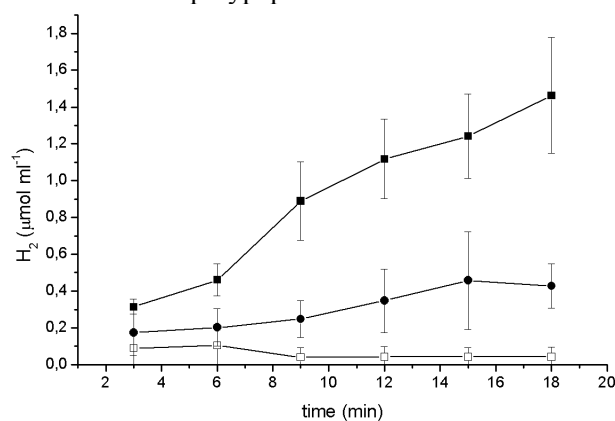
Figure 2. Activity of the dihydrogen-producing FHL complex is reduced in a *fur* mutant. Dihydrogen gas-producing activity from a representative series of measurements is shown. The experiment was performed several times always with a similar result. Samples were withdrawn at the indicated time points and the amount of hydrogen gas determined. Shown are the wild type MC4100 (filled squares), the negative control DHP-F2 (open squares) and CP500 (Δ*fur*) (filled circles). The specific hydrogen production activity for each strain was calculated to be 17.8 mU mg protein⁻¹ for MC4100, 0 mU mg protein⁻¹ for DHP-F2 and 3.2 mU mg protein⁻¹ for CP500.
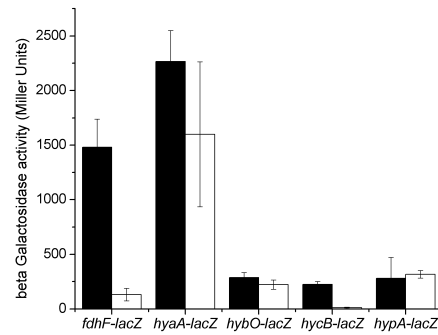
Figure 3. Expression of the *fdhF* gene and *hyc* operon, but not the Hyd-1 and Hyd-2 structural genes, is reduced in a *fur* mutant. β−Galactosidase activities in Miller units from cells grown in TGYEP, pH 6.5. Black bars represent *lacZ* fusions in MC4100 and white bars in CP500 (Δ*fur*).

Table 1. Strains used in this study.

Strains	Genotype	Reference or source
MC4100	F⁻ *araD139* Δ(*argF-lac*)*U169 ptsF25 deoC1 relA1 flbB5301 rspL150* ⁻	[13]
DHP-F2	Like MC4100 but Δ*hypF*	[14]
W3110	Wild type K12 derivative	[15]
GG209	W3110 Δ*fur*::FRT	G. Grass
GG190	BW25113 Δ*fur*::CmR	G. Grass
ECA373	Like W3110 but Δ*fur*	[16]
ECA458	Like W3110 but Δ*fecA-E,* Δ*zupT,* Δ*mntH,* Δ*feoB,* Δ*entC*	N. Taudte
CP266	Like MC4100 but λ*fdhF::lacZ*	[17]
M17s	Like MC4100 but *hyd-17*::MudI (ApR *lac*)	[18]
CP500	Like MC4100 but Δ*fur*:: CmR introduced from GG190	This work
CP543	Like MC4100 but λ*hycA::lacZ*	This work
DJR10	Like MC4100 but λ(*hyaA–lacZ*)	[19]
DJR100	Like MC4100 but λ(*hybO–lacZ*)	[19]
CP744	Like CP500 but λ*hyaA::lacZ*	This work
CP746	Like CP500 but λ*hybO::lacZ*	This work
CP747	Like CP500 but λ*hycA::lacZ*	This work
CP749	Like CP500 but λ*fdhF::lacZ*	This work
CP763	Like CP500 but *hyd-17*::MudI (ApR *lac*)	This work

Table 2. Total hydrogenase enzyme activity in *fur* mutants.

Strain[a]	Hydrogenase Sp. Activity (μmol H₂ oxidized min⁻¹ mg protein⁻¹)
MC4100 (wild type)	2.70 ± 0.8
DHP-F2 (Δ*hypF*)	0.02 ± 0.001
CP500 (Δ*fur*)	0.25 ± 0.13
W3110 (wild type)	2.34 ± 0.7
ECA458 (Δ*fecA-E,* Δ*zupT,* Δ*mntH,* Δ*feoB,* Δ*entC*)	0.05 ± 0.01
ECA373 (Δ*fur*)	0.64 ± 0.35

[a] Strains were grown anaerobically in TGYEP with 15 mM formate and total hydrogenase activity was determined in crude extracts.

2.3 Eisen Limitierung induziert die präferentielle Herabregulation der H₂-verbrauchenden vor der H₂-produzierenden Reaktion während des fermentativen Wachstums von *Escherichia coli*.

2.3.1 Zusammenfassung

Bereits historisch ist die Generierung von Mutanten für die Identifikation der Proteine, Aufklärung der Reifung und metabolische Einflüsse auf die Aktivität der [NiFe]-Hydrogenasen genutzt worden (Chippaux *et al*., 1972; Graham *et al*., 1980; Krasna, 1984; Lee *et al*., 1985; Pascal *et al*., 1975). In dieser Arbeit wurde durch ungerichtete Transposoninsertion und anschließendem Aktivitätsscreen *feoB* als Gen identifiziert, bei dessen Deletion die Gesamthydrogenaseaktivität um bis zu 76 % reduziert war, wenn kein externes Eisen zugegeben wurde. Das *feo*-Operon kodiert für ein Eisen(II)-Aufnahmesystem, welches unter den gewählten anaeroben Anzuchtbedingungen die vorherrschende Redoxstufe ist und dessen Löslichkeit höher als für Eisen(III)-Verbindungen ist (Abb. 9). Dass dieser Effekt nicht auf externen Eisenmangel zurückzuführen ist, beweist die im Vollmedium um 54 % reduzierte Gesamthydrogenaseaktivität einer *feoB* Mutante. Unter diesen Bedingungen ist die Aktivität des Wasserstoff produzierenden FHL Komplexes ebenfalls um 50 % reduziert. Auffallend ist außerdem die dramatische Abnahme der Proteinmenge der großen Hyd-1 (um 90 %) und Hyd-2 (nicht nachweisbar) Untereinheiten in einer *feoB* Mutante, bei gleichzeitig nur um 50 % verringerter Hyd-3 Proteinmenge. Diese Werte korrelieren mit den gemessenen Gesamt-Aktivitäten. Zusätzliche Kombination der *feoB* Mutation mit Deletionen in weiteren wichtigen Eisenaufnahmesystemen, wie der Enterochelin-Biosynthese *entC* und/oder dem Eisencitrat-Transporter *fecA-E* (Abb. 9), zeigten vollständigen Verlust der Hyd-1 und Hyd-2 Aktivitäten in der Aktivitätsfärbung, der sich durch die Abwesenheit beider großer Untereinheiten begründet. Erst die Kombination der drei Mutationen führte letztendlich zur Reduktion der FHL Aktivität auf 30 % und der Gesamt-Aktivität auf 7 %.

Um die Ebene der Regulation zu bestimmen, wurde die Transkription der für Hyd 1, 2 und 3 kodierenden Operons gemessen. Dabei zeigte sich, dass trotz der Deletionen von *feoB*, *entC*, *fecA-E* oder Kombinationen dieser Mutationen Transkription nur zu maximal 50 % reduziert war. Durch Deletion der Gene von Eisenaufnahmesystemen verursachter Eisenmangel bedingt also bei relativ konstanter Transkription verringerte Hydrogenase Proteinmengen und lässt auf post-transkriptionelle Effekte schließen.

Zur Kontrolle erfolgte die Komplementation der Hydrogenaseaktivität einer *feoB* Mutante durch Zugabe des kompletten *feoABC* Operons oder durch *feoB* allein auf Plasmid. Da letzteres nicht erfolgreich war kann bei der isolierten *feoB* Mutante von polaren transkriptionellen Effekten auf das stromabwärts befindliche *feoC* Gen ausgegangen werden.

Offensichtlich ist die Verfügbarkeit von Eisen essentiell für die Funktion und die Stabilität sowohl der großen als auch der kleinen Hydrogenase Untereinheiten. Dennoch muss es innerhalb der Zelle ein System geben, welches für den Eisen-Einbau zwischen verschiedenen Apoproteinen diskriminieren kann.
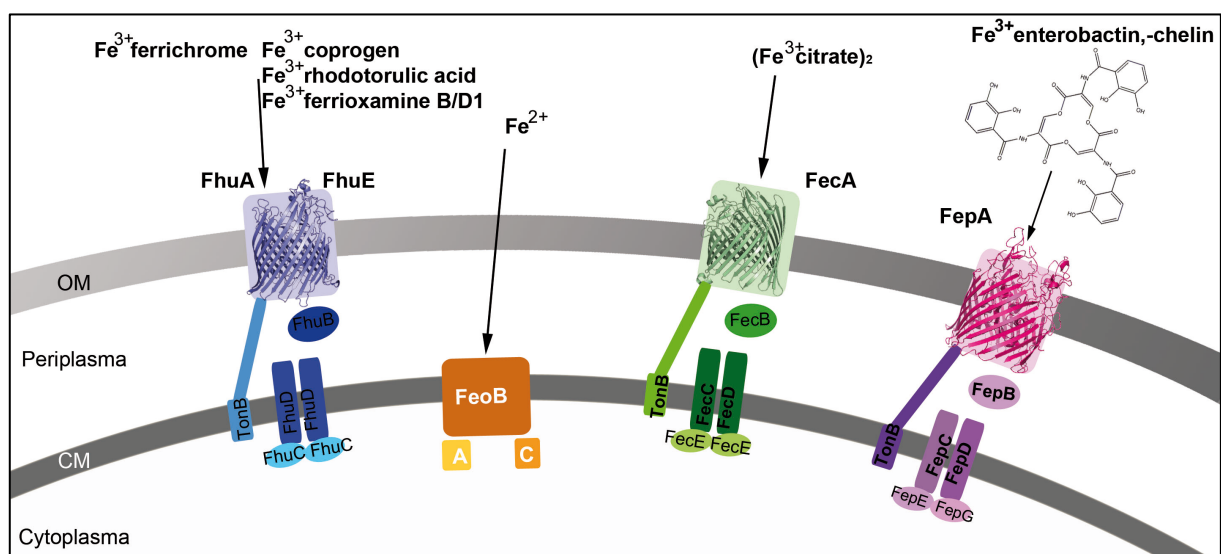
Abbildung 9 Schema der Eisen-Transportsysteme von *E. coli* (nach (Andrews *et al.*, 2003)). Die Rezeptorproteine der äußeren Membran (OM) können spezifisch Siderophore vom Hydroxamat-Typ (FhuA PDB:1QJQ, FhuE), vom Catechol-Typ (Enterobactin bei FepA PDB:1FEP) und Eisen-Citrat (FecA PDB:1KMO) aufnehmen und ins Periplasma transportieren. Die Energie für diesen Vorgang wird über den TonB-ExbB-ExbD Komplex vermittelt. Der Transport durch die Cytoplasmamembran (CM) erfolgt unter ATP Hydrolyse durch spezifische ABC-Transporter (<u>A</u>TP *<u>b</u>inding <u>c</u>assette*). Eisen(II)-Aufnahme erfolgt durch das GTP abhängige FeoABC System in der Cytoplasmamembran.

2.3.2 Artikelkopie

(Zusätzliche Online Ergebnisse befinden sich im Anhang 1)

**BMC
Microbiology**

RESEARCH ARTICLE

Open Access

Iron restriction induces preferential down-regulation of H_2-consuming over H_2-evolving reactions during fermentative growth of *Escherichia coli*

Constanze Pinske and Gary Sawers[*]

Abstract

Background: *Escherichia coli* synthesizes three anaerobically inducible [NiFe]-hydrogenases (Hyd). All three enzymes have a [NiFe]-cofactor in the large subunit and each enzyme also has an iron-sulfur-containing small subunit that is required for electron transfer. In order to synthesize functionally active Hyd enzymes iron must be supplied to the maturation pathways for both the large and small subunits. The focus of this study was the analysis of the iron uptake systems required for synthesis of active Hyd-1, Hyd-2 and Hyd-3 during fermentative growth.

Results: A transposon-insertion mutant impaired in hydrogenase enzyme activity was isolated. The mutation was in the *feoB* gene encoding the ferrous iron transport system. The levels of both hydrogen-oxidizing enzymes Hyd-1 and Hyd-2 as determined by specific in-gel activity staining were reduced at least 10-fold in the mutant after anaerobic fermentative growth in minimal medium, while the hydrogen-evolving Hyd-3 activity was less severely affected. Supplementation of the growth medium with ferric iron, which is taken up by e.g. the siderophore enterobactin, resulted in phenotypic complementation of the *feoB* mutant. Growth in rich medium demonstrated that a mutant lacking both the ferrous iron transport system and enterobactin biosynthesis (*entC*) was devoid of Hyd-1 and Hyd-2 activity but retained some hydrogen-evolving Hyd-3 activity. Analysis of crude extracts derived from the *feoB entC* double null mutant revealed that the large subunits of the hydrogen-oxidizing enzymes Hyd-1 and Hyd-2 were absent. Analysis of *lacZ* fusions demonstrated, however, that expression of the *hya*, *hyb* and *hyc* operons was reduced only by maximally 50% in the mutants compared with the wild type.

Conclusions: Our findings demonstrate that the ferrous iron transport system is the principal route of iron uptake for anaerobic hydrogenase biosynthesis, with a contribution from the ferric-enterobactin system. Hydrogen-oxidizing enzyme function was abolished in a *feoB entC* double mutant and this appears to be due to post-translational effects. The retention of residual hydrogen-evolving activity, even in the *feoB entC* double null mutant suggests that sufficient iron can be scavenged to synthesize this key fermentative enzyme complex in preference to the hydrogen-uptake enzymes.

Background

[NiFe]-hydrogenases catalyze the reversible activation of molecular hydrogen [1]. The genome of *Escherichia coli* encodes four membrane-associated [NiFe]-hydrogenases, only three of which are synthesized under standard anaerobic growth conditions. Two of these enzymes, hydrogenase 1 (Hyd-1) and Hyd-2, oxidize hydrogen while the third, Hyd-3, is part of the hydrogen-evolving formate hydrogenlyase (FHL) complex [2], which disproportionates formic acid into CO_2 and H_2 and is an important means of preventing acidification of the cytoplasm during mixed-acid fermentation. While all three Hyd enzymes are synthesized during fermentation Hyd-3 appears to contribute the bulk (80-90%) of the measureable hydrogenase activity (measured as H_2: benzyl viologen oxidoreductase activity) under these conditions,

* Correspondence: gary.sawers@mikrobiologie.uni-halle.de
Institute for Microbiology, Martin-Luther University Halle-Wittenberg, Kurt-Mothes-Str. 3, 06120 Halle (Saale), Germany

with Hyd-2 and Hyd-1 contributing the remainder [3]. Moreover, it has been recently demonstrated that Hyd-2 is functional in hydrogen oxidation at more reducing redox potentials while Hyd-1 is optimally active at more oxidizing potentials and is less oxygen-sensitive than Hyd-2 [4]. This presumably provides the bacterium with the capability of oxidizing hydrogen over a broad range of redox potentials.

The active site of the [NiFe]-hydrogenases comprises a Ni atom and a Fe atom to which the diatomic ligands CO and CN^- are attached [5]. The Hyp proteins synthesize this hetero-bimetallic centre and mutations in the genes encoding these Hyp maturases result in a hydrogenase-negative phenotype [2,5]. Iron is also required as a key component of the [Fe-S] clusters in the respective electron-transferring small subunits of the hydrogenases [5,6]. In addition, iron is required for the function of at least one of the Hyp maturases, HypD [7,8].

While the route of nickel transport for hydrogenase biosynthesis in *E. coli* has been well characterized [5,9], it has not been determined which of the characterized iron uptake systems is important for delivering iron to the hydrogenase maturation pathway. *E. coli* has a number of iron transport systems for the uptake of both ferric and ferrous iron [10]. Under anaerobic, reducing conditions Fe^{2+} is the predominant form of iron and it is transported by the specific ferrous-iron FeoABC transport system [11,12]. Under oxidizing conditions, where the highly insoluble Fe^{3+} is the form that is available, *E. coli* synthesizes Fe^{3+}-specific siderophores to facilitate iron acquisition [13]. These Fe^{3+}-siderophore complexes are transported into the cell by specific transport systems, e.g. Fe^{3+}-citrate is transported by the Fec system, Fe^{3+}-hydroxamate by the Fhu system and Fe^{3+}-enterobactin by the Fep system. In this study we examined the biosynthesis and activities of the [NiFe]-hydrogenases during fermentative growth in null mutants lacking defined iron transport systems.

Results

A *feoB* mutant has reduced hydrogenase activity in both minimal and rich medium

All three [NiFe]-hydrogenases in *E. coli* catalyze the hydrogen-dependent reduction of the artificial redox dye benzyl viologen (BV) [3,14]. This activity can be visualized in colonies on agar plates after anaerobic fermentative growth. The colonies of wild type cells develop a dark violet colour in the presence of hydrogen and BV, while mutants unable to synthesize hydrogenase remain colourless [15]. Approximately 4000 kanamycin-resistant Tn5-insertion mutants were screened for an impaired ability to catalyze the hydrogen-dependent reduction of BV after anaerobic fermentative growth on M9 minimal medium plates with glucose as carbon source (see

Methods for details). One of eight putative mutants isolated had a pale violet colony colour after BV-overlay in the presence of hydrogen; the characterization of the remaining seven putative mutants will be described elsewhere. Transduction of the mutation in the pale-violet mutant into a 'clean' MC4100 genetic background resulted in the mutant PM06, which retained the phenotype of the originally isolated mutant. Sequence analysis of the site of Tn5 insertion in the mutant revealed that it had inserted in the *feoB* gene, which encodes the GTPase component of the ferrous iron transporter [12].

The hydrogen-dependent reduction of BV was determined in extracts derived from MC4100 (wild type) and PM06 (*feoB*::Tn5) grown anaerobically in M9 minimal medium with glucose as carbon source and with different iron sources (Table 1). The wild type MC4100 grown without addition of iron compounds had a total hydrogenase activity of 2.0 U mg of protein^{-1} (Table 1). Growth of MC4100 in the presence of iron citrate and potassium ferricyanide had essentially no effect on enzyme activity, while ferric chloride resulted in an 80% increase and ferric ammonium sulfate a 1.6-fold increase in total hydrogenase activity (Table 1). Growth of MC4100 in the presence of potassium ferrocyanide (Fe^{2+}) resulted in extracts with a reduced but still significant hydrogen-oxidizing activity of 66% compared to the wild type grown without addition. It was noted that due to the poor growth of the strains in minimal medium in the presence of ferricyanide and ferrocyanide the hydrogenase enzyme activity was highly variable with high SD values. This phenomenon was reproducibly observed, despite attempts to harvest cells under strictly comparable conditions of growth and presumably reflects variability in the labile Hyd-3 activity (see below). Therefore, it must be stressed that only general trends in enzyme activity changes caused by these iron sources can be considered.

Extracts of a *hypF* mutant, which cannot synthesize active hydrogenases [16], had essentially no hydrogenase enzyme activity and served as a negative control. Extracts of the *feoB*::Tn5 mutant PM06 grown in M9 medium in the absence of iron had a total hydrogenase activity that was 24% that of the wild type without addition of iron compounds (Table 1). Growth of PM06 in the presence of iron chloride or ferric ammonium sulfate restored hydrogenase activity to levels similar to wild type. The exception was potassium ferricyanide, which failed to restore hydrogenase enzyme activity to wild type levels; instead activity was approximately 50% of that measured in MC4100 grown without iron supplementation and only 50% of that measured after growth of the wild type with potassium ferricyanide (Table 1). In contrast, growth of PM06 in the presence of ferrocyanide did not restore hydrogenase activity.

Table 1 Hydrogen-oxidizing enzyme activity of the *feoB*::Tn*5* mutant PM06 grown in minimal medium with different iron sources

Strain and iron supplement[a]	Hydrogenase specific activity[b] (μmol H_2 oxidized min^{-1} mg $protein^{-1}$)	
	MC4100	PM06 (*feoB*::Tn*5*)
no iron addition	2.02 ± 0.64	0.49 ± 0.19
7.5 μM iron chloride ($FeCl_3$)	3.63 ± 0.73	2.49 ± 0.64
15.3 μM hemin	1.72 ± 0.92	0.25 ± 0.18
10 μM potassium ferrocyanide ($K_4[Fe(CN)_6]$) (Fe^{2+})	1.34 ± 1.30	0.38 ± 0.33
10 μM potassium ferricyanide ($K_3[Fe(CN)_6]$) (Fe^{3+})	1.80 ± 2.82	0.93 ± 0.85
10 μM ferric ammonium sulfate ($Fe(NH_4)(SO_4)_2$)	3.33 ± 2.53	2.02 ± 2.11
50 μM iron citrate ($C_6H_5FeO_7$)	2.20 ± 0.70	3.47 ± 1.17
300 μM 2,2'-dipyridyl	< 0.01	< 0.01
300 μM 2,2'-dipyridyl and 200 μM $FeCl_3$	0.04 ± 0.07	< 0.01
300 μM 2,2'-dipyridyl and 200 μM iron citrate	1.59 ± 1.16	0.04 ± 0.06

[a] Cells were cultivated in M9 minimal medium including 0.8% (w/v) glucose. Iron sources were added at the given final concentrations.
[b] The activities were determined for triplicate experiments.

Addition of hemin as a source of oxidized iron also failed to restore hydrogenase activity to PM06, presumably because hemin cannot be taken up by *E. coli* and the oxidized iron is also tightly bound to the porphyrin. Taken together, these results are consistent with the ferrous iron transport system being an important route of iron uptake for hydrogenase biosynthesis in the wild type.

Addition of 2, 2'-dipyridyl to the growth medium resulted in total loss of hydrogenase activity of the wild type MC4100 and PM06 (Table 1). Supplementation of 200 μM iron chloride or iron citrate together with 300 μM dipyridyl showed that iron citrate restored 66% of the wild type activity while iron chloride failed to restore activity. None of these additions restored hydrogenase activity to PM06.

The activities of Hyd-1 and Hyd-2 can be visualized after non-denaturing PAGE followed by specific activity staining [14]; Hyd-3 is labile and cannot be visualized under these conditions. This method allows a specific analysis of the effect of mutations or medium supplements on Hyd-1 and Hyd-2 activity and it should be noted that this method is only semi-quantitative. Analysis of the extracts of MC4100 grown in minimal medium under all of the conditions tested identified both Hyd-1 and Hyd-2 as characteristic hydrogen-oxidizing activity-staining bands (Figure 1A). The relative intensity of the activity-staining bands was quantified by densitometric analysis (Figure 1B) as described in the Methods section. The intensity of the Hyd-1 and Hyd-2 activity-staining bands was similar when cells were grown fermentatively in the presence of iron citrate, ferric ammonium sulfate, ferricyanide or ferrocyanide. In cell-free extracts derived from PM06 grown with the three Fe^{3+} sources ferricyanide, ferric ammonium sulfate and ferric citrate the Hyd-1 activity-staining profile was similar to that of the wild type, however, the intensity was reduced

by approximately 50% (Figure 1). On the other hand, Hyd-2 attained a level that was only between 10 and 20% the intensity of the wild type grown with iron citrate, suggesting that the activity of this enzyme is less readily complemented by addition of oxidized iron. Somewhat surprising, however, was the observation that although some activity of Hyd-2 could be observed after growth of the mutant in the presence of $FeCl_3$, Hyd-1 activity was strongly reduced (Figure 1). Total hydrogenase enzyme activity measured in these extracts of PM06 was nevertheless near wild type (Table 1). It must be noted, however, that under these growth conditions the contributions of Hyd-1 and Hyd-2 to the total activity are low (around 1% for Hyd-1 and 5-10% for Hyd-2), as can be deduced from a strain lacking Hyd-3 (CP971) that retained 4% of the wild type activity with iron chloride [3,17]. This means that although Hyd-1 or Hyd-2 activities could barely be observed by in-gel staining, the increase in total hydrogenase activity by addition of $FeCl_3$ was due to Hyd-3 activity.

An extract derived from PM06 grown in the presence of ferrocyanide showed essentially no detectable activity due to either Hyd-1 or Hyd-2 (Figure 1), indicating that probably the level of iron in the mutant was insufficient to allow synthesis of wild type levels of these enzymes. This correlated with the low total hydrogenase activity measured in extracts of PM06 after fermentative growth with ferrocyanide, and indicates that the residual activity was due to Hyd-3 (Table 1). After growth of PM06 in the presence of hemin no Hyd-1 activity was detected in the gel (Figure 1), and only a very low Hyd-2 activity was detected. Total hydrogenase activity was only 10% of the total compared to wild type without addition of iron compounds, indicating that Hyd-3 activity was not recovered in PM06 by addition of hemin to the growth medium.
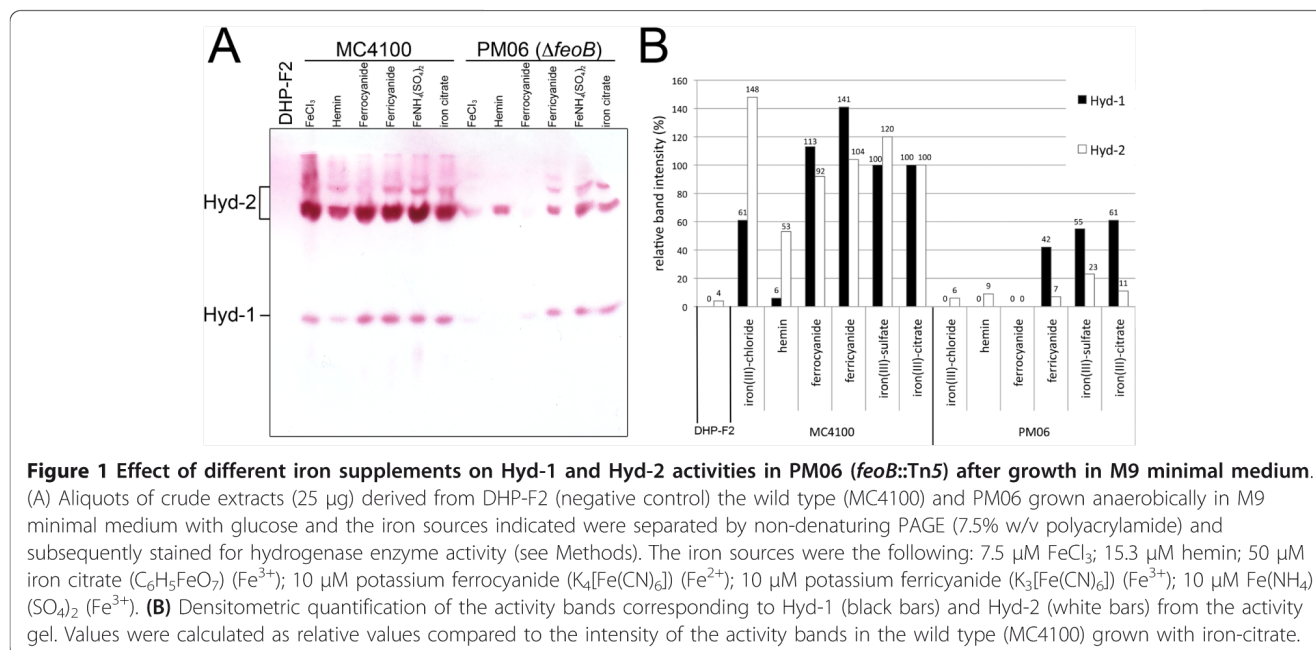
Figure 1 Effect of different iron supplements on Hyd-1 and Hyd-2 activities in PM06 (*feoB*::Tn*5*) after growth in M9 minimal medium. (A) Aliquots of crude extracts (25 μg) derived from DHP-F2 (negative control) the wild type (MC4100) and PM06 grown anaerobically in M9 minimal medium with glucose and the iron sources indicated were separated by non-denaturing PAGE (7.5% w/v polyacrylamide) and subsequently stained for hydrogenase enzyme activity (see Methods). The iron sources were the following: 7.5 μM FeCl$_3$; 15.3 μM hemin; 50 μM iron citrate (C$_6$H$_5$FeO$_7$) (Fe^{3+}); 10 μM potassium ferrocyanide (K$_4$[Fe(CN)$_6$]) (Fe^{2+}); 10 μM potassium ferricyanide (K$_3$[Fe(CN)$_6$]) (Fe^{3+}); 10 μM Fe(NH$_4$)(SO$_4$)$_2$ (Fe^{3+}). (B) Densitometric quantification of the activity bands corresponding to Hyd-1 (black bars) and Hyd-2 (white bars) from the activity gel. Values were calculated as relative values compared to the intensity of the activity bands in the wild type (MC4100) grown with iron-citrate.

The effect of the *feoB* mutation on hydrogenase enzyme activity could also be observed after growth in rich medium, whereby the hydrogenase enzyme activity of the *feoB* mutant PM06 was reduced by a little over 50% compared with the activity of MC4100 (Table 2).

In an attempt to complement the *feoB* mutation, initially the *feoB* gene was re-introduced into PM06 by transformation of plasmid pECD1079 (*feoB*$^+$). The plasmid failed to restore hydrogenase enzyme activity to the levels determined for the wild type; surprisingly, the presence of the plasmid reduced overall hydrogenase activity to only about 15% that of the wild type (Table 2). Western blot analysis of the Strep-tagged FeoB derivative encoded on pECD1079 confirmed that the protein was synthesized but that the level of synthesis was higher in aerobically grown cells compared with anaerobically grown cells (Additional file 1). The reason for the reduction in hydrogenase activity caused by over-produced Strep-tagged FeoB is unclear.

Introduction of the complete *feoABC* operon on the plasmid restored hydrogenase activity in PM06 to wild type levels (Table 2). This latter result suggests that the transposon insertion in the *feoB* gene caused a polar effect on the downstream *feoC* gene and only the presence of the complete operon on a plasmid could complement the mutation.

Combined knock-out of ferrous and ferric iron transport systems abolishes hydrogen-oxidizing activities

Single null mutations that prevented biosynthesis of ferric-enterobactin (strain CP416 Δ*entC*) or the uptake system for ferric-citrate (strain CP422, Δ*fecA-E*) essentially had little to no effect on total hydrogenase activity (Table 3). Introducing a mutation in the *fhuA* or *fhuE* genes also had no effect on total hydrogenase activity

Table 2 Hydrogen-oxidizing enzyme activity of the complemented PM06 (*feoB*::Tn*5*) mutant

Strain[a] and genotype	Hydrogenase specific activity[b] (μmol H$_2$ oxidized min^{-1} mg protein^{-1})
MC4100	2.96 (± 0.31)
DHP-F2 (*hypF*)	< 0.01
PM06 (*feoB*::Tn*5*)	1.28 (± 0.50)
PM06 pECD1079 (*feoB*$^+$)	0.44 (± 0.13)
PM06 pFEO (*feoABC*$^+$)	3.4 (± 1.30)

[a] Cell extracts were prepared from cells grown anaerobically in TGYEP plus formate.
[b] The mean and standard deviation of at least three independent experiments are shown.

Table 3 Hydrogen-oxidizing enzyme activity in various transport mutants

Strain[a] and genotype	Hydrogenase Specific activity[b] (μmol H$_2$ oxidized min^{-1} mg protein^{-1})
MC4100	2.70 ± 0.8
DHP-F2 (*hypF*)	0.02 ± 0.01
PM06 (*feoB*)	1.24 ± 1.0
CP422 (*fecA-E*)	2.54 ± 1.6
CP416 (*entC*)	2.05 ± 0.5
CP411 (*entC feoB*)	0.58 ± 0.4
CP415 (*fecA-E entC*)	1.11 ± 0.4
CP413 (*entC feoB fecA-E*)	0.19 ± 0.16

[a] Cell extracts were prepared from cells grown anaerobically in TGYEP plus 15 mM formate.
[b] The mean and standard deviation of at least three independent experiments are shown.

(data not shown). Combining the *entC* and *fecA-E* mutations (strain CP415) reduced hydrogenase activity by approximately 60% compared to the wild type. Introducing the *feoB*::Tn*5* mutation into this strain to deliver CP413 (*entC fecA-E feoB*::Tn*5*) reduced total hydrogenase activity even further such that only approximately 7% of the wild type level could be detected.

Analysis of cell-free extracts derived from these strains grown fermentatively in rich medium by non-denaturing PAGE, with subsequent staining for activity of Hyd-1 and Hyd-2, revealed that, as anticipated, the extracts of CP416 (*entC*) and CP422 (*fecA-E*) showed essentially wild-type Hyd-1 and Hyd-2 activity profiles (Figure 2). However, an extract from PM06 (*feoB*::Tn*5*) showed clearly reduced intensity bands for both enzymes, which is in accord with the results after growth in minimal medium (see Figure 1). Extracts from CP411 (*entC feoB*::Tn*5*) or CP413 (*entC fecA-E feoB*::Tn*5*) grown fermentatively in rich medium had neither Hyd-1 nor Hyd-2 enzyme activities. This result indicates that the residual hydrogenase enzyme activity in CP413 must result from Hyd-3 (compare Table 3). To test this, we determined the FHL enzyme activity present in whole cells of the various mutants (Table 4) and could demonstrate that while cells of CP411 (*entC feoB*::Tn*5*) had an FHL activity of approximately 50% of the wild-type, strain CP413 (*entC fecA-E feoB*::Tn*5*) still retained 30% of the wild-type FHL activity, confirming that the residual hydrogenase activity in extracts of CP413 was indeed due to Hyd-3.

Hyd-1 and Hyd-2 large subunits are absent in CP413 (*entC feoB*:: Tn*5*)

In order to determine whether the lack of Hyd-1 and Hyd-2 activity in the mutants devoid of ferrous and ferric uptake was due to lack of processing of the large subunits because of iron-limitation, the precursor and processed forms of the large subunits of Hyd-1, Hyd-2 and Hyd-3 in cell-free extracts derived from the iron transport mutants after growth in rich medium were analysed by Western blotting with enzyme-specific antisera. Extracts derived from MC4100 (wild type) revealed mainly the processed form of the catalytic subunit of all three enzymes (Figure 3A), which is indicative of successful insertion of the [NiFe]-cofactor [5]. In contrast, a mutant unable to synthesize the HypF protein (DHP-F2) is unable to generate the diatomic CN⁻ ligands and consequently fails to insert the cofactor. Extracts from a *hypF* mutant therefore only showed the unprocessed form of each catalytic subunit (Figure 3A), which indicates that the large subunit lacks a cofactor [5]. Extracts derived from CP416 (*entC*) and CP422 (*fecA-E*) both showed levels of processed large subunits for Hyd-1, Hyd-2 and Hyd-3 similar to those seen for the wild-type
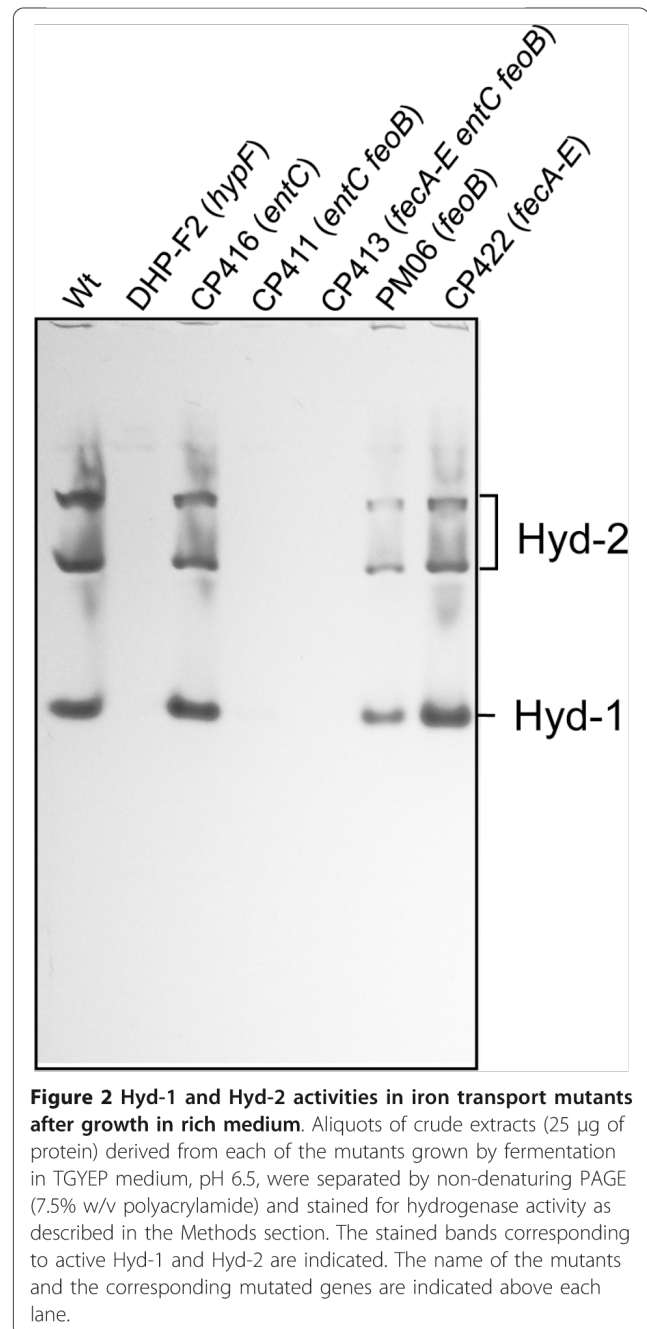
Figure 2 Hyd-1 and Hyd-2 activities in iron transport mutants after growth in rich medium. Aliquots of crude extracts (25 μg of protein) derived from each of the mutants grown by fermentation in TGYEP medium, pH 6.5, were separated by non-denaturing PAGE (7.5% w/v polyacrylamide) and stained for hydrogenase activity as described in the Methods section. The stained bands corresponding to active Hyd-1 and Hyd-2 are indicated. The name of the mutants and the corresponding mutated genes are indicated above each lane.

MC4100 (Figure 3A). Densitometric analysis of the levels of these processed polypeptides in the autoradiogram shown in Figure 3A, however, revealed that in extracts of CP416 and CP422 Hyd-1 large subunit levels were only 20% and 50%, respectively, of that observed in the wild type, while in extracts of CP416 the level of Hyd-3 large subunit HycE was almost 3-fold increased compared with the level in the wild type (Figure 3B). Extracts derived from the *fecA-E entC* double null mutant CP415 showed the similar increased level of Hyd-3 large subunit and decreased level of Hyd-1 large

Table 4 Formate hydrogenlyase activity of the transport mutants

Strain[a]	Specific hydrogen evolving activity (mU mg protein^{-1})[b]
MC4100	30 ± 7
DHP-F2 (*hypF*)	< 1
CP416 (*entC*)	20 ± 5
PM06 (*feoB*)	15 ± 3
CP411 (*entC feoB*)	15 ± 6
CP413 (*entC feoB fecA-E*)	9 ± 1

[a] Cells were grown anaerobically in TGYEP.

[b] The mean and standard deviation of at least three independent experiments are shown.

subunit as was observed with CP416; however, the difference was that Hyd-2 levels were decreased by approximately 40% compared with the wild type. These results suggest that under mild iron-limiting conditions, intracellular iron is preferentially used for hydrogen-evolving function. The *feoB* mutant PM06 showed strongly reduced levels of processed Hyd-1 large subunit and barely detectable levels of Hyd-2 processed large subunit; the amount of processed Hyd-3 large subunit was approximately 50% that of the wild-type. Cell-free extracts of CP411 (*entC feoB*::Tn5) and CP413 (*entC fecA-E feoB*::Tn5), on the other hand, essentially completely lacked either the unprocessed or processed forms of the large subunits of Hyd-1 or Hyd-2, which correlates with the lack of Hyd-1 and Hyd-2 enzyme activity observed in Figure 2. Both the processed and unprocessed forms of the Hyd-3 large subunit HycE were observed in extracts from both strains but at significantly reduced levels, which is in accord with the observed FHL activity measured in the strains (see

Table 4). Although the level of processed HycE in both strains was significantly reduced compared with the wild-type, the amounts of full-length, unprocessed polypeptide were similar to those seen in the wild-type (Figure 3A), suggesting that there was a limitation in processing capacity in the mutants.

Expression of the *hya*, *hyb* and *hyc* operons is only marginally reduced in the iron-transport mutants

The *hya*, *hyb* and *hyc* operons encode Hyd-1, Hyd-2 and Hyd-3, respectively [2,18,19]. To determine whether expression of these operons was affected in the different iron-transport-defective mutants, we constructed *lacZ* translational fusions to the first gene of each operon, which encode the respective small subunits of the enzymes Hyd-1 and Hyd-2, while the *hycA* gene encodes a transcriptional regulator (see Methods). After transfer to the lambda phage λRS45 [20], the *hyaA'-'lacZ*, *hybO'-'lacZ* and *hycA'-'lacZ* fusions were introduced in single copy onto the chromosome of the respective mutants. To demonstrate that the fusions were functional we analyzed expression levels after growth under both aerobic and anaerobic conditions. Expression of *hyaA'-'lacZ* was strongly reduced when wild type cells were grown aerobically, while expression was up-regulated approximately 70-80 fold during fermentative growth (Table 5). The *hybO'-'lacZ* expression was shown to be approximately 5 fold higher in anaerobically grown compared with aerobically grown cells. Expression of *hycA'-'lacZ* was up-regulated 3 fold in the presence of formate. All fusions showed near background β-galactosidase enzyme activity when cells were grown aerobically [21,22].

The results in Table 5 show that in *entC* or *feoB* mutants, expression of *hyaA* was reduced by
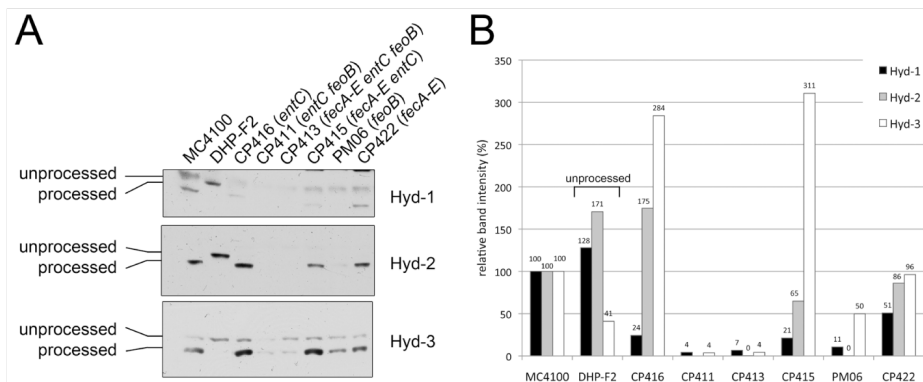
Figure 3 Analysis of hydrogenase large subunit processing. **(A)** The three panels show portions of Western blots in which the large subunits of Hyd-1, Hyd-2 and Hyd-3 (HycE) are shown. The positions of the unprocessed and processed forms of the polypeptides are indicated on the left of the Figure. Crude extracts (25 μg of protein) derived from cells grown anaerobically in TGYEP plus formate were separated in 10% (w/v) SDS-PAGE and incubated with antibodies specific for the respective enzymes. **(B)** Densitometric quantification of the processed protein bands (and for the unprocessed band from DHP-F2) corresponding to Hyd-1 (black bars), Hyd-2 (gray bars) and Hyd-3 (white bars) from the western blot. Values were calculated as relative intensities compared to the intensity of the wild type MC4100.

Table 5 Influence of iron transport mutations on expression of *hyaA*, *hybO* and *hycA lacZ* fusions

Strain/genotype[a]	β-Galactosidase specific activity in Miller Units (± standard deviation)		
	Φ(*hyaA'-'lacZ*)	Φ(*hybO'-'lacZ*)	Φ(*hycA'-'lacZ*)
MC4100 (wild type)	818 ± 232	52 ± 46	44 ± 9
MC4100 aerobically	12 ± 3	12 ± 3	13 ± 2
MC4100 + 15 mM formate	770 ± 535	87 ± 30	126 ± 57
DHP-F2 (Δ*hypF*)	620 ± 221	60 ± 27	53 ± 22
Δ*fecA-E*	633 ± 252	52 ± 17	41 ± 11
Δ*feoB*	355 ± 96	36 ± 7	65 ± 40
Δ*entC*	410 ± 110	40 ± 15	33 ± 20
Δ*fecA-E feoB*	491 ± 139	43 ± 11	28 ± 13
Δ*entC fecA-E feoB*	371 ± 94	45 ± 11	35 ± 24
Δ*entC feoB*	574 ± 155	45 ± 21	49 ± 32
Δ*entC fecA-E*	340 ± 211	47 ± 12	57 ± 19

[a] In the interest of clarity only the genotype of the strains is given. The strains used can be found in Table 6. Growth was performed under fermentative conditions in TGYEP, unless indicated otherwise.
n. d.-not determined

approximately 50% compared with the wild type MC4100. Expression of *hybO* attained levels that were only approximately 10% those of *hyaA* (Table 5), consistent with transcriptional regulation data for these operons reported earlier [21]. The expression of the *hybO'-'lacZ* fusion was reduced by approximately 40% in a *feoB* mutant background and by 35% in an *entC* mutant compared with the level of expression measured in the wild type (Table 5). Expression of the *hyc* operon remained comparatively constant among the strains, but was reduced by maximally 40% in a *fecA-E feoB* double mutant. A slight increase in *hyc* expression in the *feoB* single mutant was observed; however, it should be noted that expression levels were variable in the mutant backgrounds. Addition of dipyridyl to the growth medium had no effect on *hyc* expression (data not shown).

Discussion

In a previous study [23] it was shown that hydrogen metabolism of *E. coli* was significantly affected by introduction of a *fur* mutation. Fur is a global regulator controlling iron homeostasis [24,25]. Differential effects on hydrogen-oxidizing hydrogenase activity compared with hydrogen-evolving enzyme function were observed previously in the *fur* mutant [23]. The *fur* mutation, which has both negative and positive effects on gene expression of iron metabolism including depression of iron uptake systems, caused a strong reduction in FHL activity, suggesting Fur is required for FHL synthesis. In the current study we could show in an otherwise Fur⁺ background that causing iron limitation by removing key iron uptake systems also resulted in differential effects on hydrogen uptake and hydrogen evolution: hydrogen-oxidizing hydrogenase function was compromised first while hydrogen-evolving hydrogenase activity was partially retained. During a search for genes affecting

hydrogenase biosynthesis or activity, a mutant with a transposon insertion in *feoB* encoding the GTPase component of the postulated ferrous iron transport system [12] was isolated. The alteration in hydrogen metabolism caused by the mutation could not be phenotypically complemented by ferrous iron but could be complemented by supplementing the growth medium with oxidized iron. This result supports the important role of the Feo system in transport of iron under reducing conditions. Although this finding was perhaps not surprising considering that the hydrogenases are synthesized under anaerobic fermentative conditions when Fe^{2+} ions are available and the Feo transport system is active [10-12], it was nevertheless important to demonstrate the involvement and importance of this route of iron acquisition for enzymes that have a high demand for iron atoms.

Combining the *feoB* mutation with a mutation in *entC*, which impairs biosynthesis of the siderophore enterobactin, abrogated Hyd-1 and Hyd-2 activities. Notably, however, significant Hyd-3, and consequently FHL, activity was retained in the double null mutant, suggesting that when iron is limited during fermentative growth the synthesis of the hydrogen-evolving Hyd-3 takes precedence over the two hydrogen-oxidizing enzymes Hyd-1 and Hyd-2. The fact that Hyd-2 is maximally active under more reducing conditions, while Hyd-1 is an oxygen-tolerant enzyme and is active at more positive redox potentials [4], did not influence this preference. Even when a further mutation preventing synthesis of the iron-citrate transport system was introduced, residual Hyd-3 and FHL activities were retained. Indeed, previous studies demonstrated that only when *zupT* and *mntH* mutations were also introduced into this background was FHL activity abolished [23]. This suggests that the FHL system can scavenge residual iron entering the cell through unspecific transport systems,

but that these levels of iron either are insufficient for synthesis of Hyd-1 and Hyd-2 or that the iron is directed preferentially to Hyd-3 biosynthesis. Further studies will be required to elucidate which of these possibilities is correct.

A somewhat unexpected result of this study was the finding that under iron limitation no unprocessed species of the Hyd-1 or Hyd-2 large subunits were present and only very low amounts of the processed proteins were observed. This was unexpected because in *hyp* mutants, where active site biosynthesis cannot be completed [5], significant levels of the unprocessed form of the large subunit are always detected (for example see extracts of DHP-F2 in Figure 3). The fact that expression of translational *lacZ* fusions of the *hya* and *hyb* structural gene operons was largely unaffected by the deficiency in iron transport suggests that a different level of regulation in response to iron availability exists. This regulation might possibly be post-translational, for example through altered protein turnover due to insufficient iron.

Conclusions

Mutants unable to acquire iron through the ferrous iron transport and siderophore-based uptake systems lacked the hydrogen-oxidizing enzymes Hyd-1 and Hyd-2 under anaerobic fermentative conditions. Iron limitation did not affect transcription of the *hya*, *hyb* or *hyc* operons. The Hyd-3 component of the FHL complex was less severely affected by defects in these iron uptake systems, indicating that a greater degree of redundancy in iron acquisition for this enzyme exists. Thus, when iron becomes limiting during fermentative growth synthesis of active Hyd-3 has priority over that of the hydrogen-oxidizing enzymes Hyd-1 and Hyd-2. This probably reflects a physiological requirement to maintain an active FHL complex to offset acidification of the cytoplasm caused by formate accumulation via disproportionation of the metabolite into the freely diffusible gaseous products CO_2 and H_2.

Methods

Strains, plasmids and growth conditions

All bacterial strains, plasmids and phages used in this study are listed in Table 6.

For the purposes of chromosomal and plasmid DNA isolation, *E. coli* was grown aerobically in Erlenmeyer flasks filled to maximally 10% of their volume with LB medium on a rotary shaker (250 rpm) and incubated at 37°C. Anaerobic growths were performed at 37°C in sealed bottles filled with anaerobic medium and under a nitrogen gas atmosphere. Cultures for determination of hydrogenase processing or for enzyme activity measurements were grown either in buffered TGYEP medium

(1% w/v tryptone, 0.8% w/v glucose, 0.5% w/v yeast extract, 0.1 M potassium phosphate buffer) pH 6,5 [15] supplemented with 15 mM formate or in M9 minimal medium [26] containing 0.8% (w/v) glucose as carbon source, all standard amino acids at a final concentration of 0,04 mg/ml and 0.3 µM thiamine. When used for growth and screening for hydrogen metabolism mutants M9-glucose was supplemented with 0.29 mM citrulline, 0.89 mM uracil and was solidified with 1.5% (w/v) agar. All media were supplemented with 0.1% (v/v) SLA trace element solution [27] except when different iron sources were tested in which case $FeCl_3$ was omitted from SLA and was replaced by the appropriate iron source at the concentration indicated. Dipyridyl was added at a final concentration of 300 µM. All growth media included 0.1 µM $NiCl_2$. The antibiotics kanamycin, ampicillin, and chloramphenicol, when required, were added to the medium at the final concentrations of 50, 100, and 12.5 µg per ml, respectively. When indicated anhydrotetracycline (AHT) was added at the final concentration of 0.2 µg per ml.

Construction of *hyaA'-'lacZ*, *hybO'-'lacZ* and *hycA'-'lacZ* translational fusions

The translational fusions to *hyaA* and *hybO* were constructed by amplifying the respective promotor regions and the nucleotides coding for the first 14 or 13 amino acids, respectively, by PCR using Phusion DNA polymerase (Finnzymes, Germany) and the oligonucleotides hya_regulat_up 5'-GCG GGA TCC GCG CAG AGA TTC GAA CTC TG-3', hya_regulat_down 5'-GCG GGA TCC TGA CGC CGC ATG GCC TGG TA-3', hybO_-217 5'-CTC GGA TCC TAT GGC CGG TTA TCG CCT C-3' and hybO_+38 5'-CTC GGA TCC ATG CCG TGA GAA TGG ATG A-3'. The resulting respective 565 bp and 274 bp fragments were digested with BamHI and ligated into pRS552 [20], which had been digested with BamHI and dephosphorylated with shrimp alkaline phosphatase (Roche, Germany). This procedure delivered plasmids phyaA552 and phybO552, respectively. The DNA sequence was verified by sequencing (Seqlab, Germany) and the insert transferred to λRS45 [20]. In a similar manner the *hycA'-'lacZ* fusion was constructed using plasmid pTL101 [28]. The resulting Φ(*hyaA'-'lacZ*), Φ(*hybO'-'lacZ*) and Φ(*hycA'-'lacZ*) protein fusions were introduced in single copy into the lambda attachment site of the respective mutants as indicated in Table 6.

Isolation of mutants and identification of the transposon insertion site

XL1-Blue (Stratagene) was mutagenized using the < R6Kγori/KAN-2 > transposome (Epicentre Biotechnologies; [29]) according to the manufacturer's instructions.

Table 6 Strains and plasmids used in this study

Strains/plasmids	Genotype	Reference
MC4100	F⁻ *araD139* Δ(*argF-lac*)U169 *ptsF25 deoC1 relA1 flbB5301 rspL150* ⁻	[37]
DHP-F2	MC4100 Δ*hypF* 59-629AA	[16]
XL1-Blue	*recA*1 *endA*1 *gyrA*96 *thi*-1 *hsdR*17 *supE*44 *relA*1 *lac* [F' *proAB laclqZ*ΔM15 Tn*10* (Tet^R)]	Stratagene
PM06	Like MC4100 but *feoB*::Tn*5*	This study
PX06	Like XL1-Blue but *feoB*::Tn*5*	This study
CP411	Like MC4100 but Δ*entC*::*cat feoB*::Tn*5*	This study
CP413	Like MC4100 but Δ*fecA-E* Δ*entC*::*cat feoB*::Tn*5*	This study
CP415	Like MC4100 but Δ*fecA-E* Δ*entC*::*cat*	This study
CP416ᵃ	Like MC4100 but Δ*entC*::*cat*	This study
CP422	Like MC4100 but Δ*fecA-E* introduced from GG7	This study
GG7	W3110 Δ*fecA-E*::*kan*	G. Grass
CP971	MC4100 Δ*hycAI*::*kan*	[38]
CP612	Like MC4100 but Φ(*hyaA'-'lacZ*)	This study
CP775	Like MC4100 but Φ(*hybO'-'lacZ*)	This study
CP951	Like MC4100 but Φ(*hycA'-'lacZ*)	This study
CP1069	Like MC4100 but Δ*hypF* Φ(*hyaA'-'lacZ*)	This study
CP1084	Like MC4100 but Δ*hypF* Φ(*hybO'-'lacZ*)	This study
CP1149	Like MC4100 but Δ*hypF* Φ(*hycA'-'lacZ*)	This study
CP1073	Like MC4100 but Δ*fecA-E* Φ(*hyaA'-'lacZ*)	This study
CP1088	Like MC4100 but Δ*fecA-E* Φ(*hybO'-'lacZ*)	This study
CP1150	Like MC4100 but Δ*fecA-E* Φ(*hycA'-'lacZ*)	This study
CP1075	Like MC4100 but Δ*feoB*ᵇ Φ(*hyaA'-'lacZ*)	This study
CP1090	Like MC4100 but Δ*feoB*ᵇ Φ(*hybO'-'lacZ*)	This study
CP1151	Like MC4100 but Δ*feoB*ᵇ Φ(*hycA'-'lacZ*)	This study
CP1071	Like MC4100 but Δ*entC* Φ(*hyaA'-'lacZ*)	This study
CP1086	Like MC4100 but Δ*entC* Φ(*hybO'-'lacZ*)	This study
CP1152	Like MC4100 but Δ*entC* Φ(*hycA'-'lacZ*)	This study
CP1079	Like MC4100 but Δ*fecA-E feoB*ᵇ Φ(*hyaA'-'lacZ*)	This study
CP1094	Like MC4100 but Δ*fecA-E feoB*ᵇ Φ(*hybO'-'lacZ*)	This study
CP1153	Like MC4100 but Δ*fecA-E feoB*ᵇ Φ(*hycA'-'lacZ*)	This study
CP1081	Like MC4100 but Δ*entC feoB*ᵇ Φ(*hyaA'-'lacZ*)	This study
CP1096	Like MC4100 but Δ*entC feoB*ᵇ Φ(*hybO'-'lacZ*)	This study
CP1154	Like MC4100 but Δ*entC feoB*ᵇ Φ(*hycA'-'lacZ*)	This study
CP1077	Like MC4100 but Δ*entC fecA-E* Φ(*hyaA'-'lacZ*)	This study
CP1092	Like MC4100 but Δ*entC fecA-E* Φ(*hybO'-'lacZ*)	This study
CP1155	Like MC4100 but Δ*entC fecA-E* Φ(*hycA'-'lacZ*)	This study
CP1083	Like MC4100 but Δ*entC fecA-E feoB*ᵇ Φ(*hyaA'-'lacZ*)	This study
CP1098	Like MC4100 but Δ*entC fecA-E feoB*ᵇ Φ(*hybO'-'lacZ*)	This study
CP1163	Like MC4100 but Δ*entC fecA-E feoB*ᵇ Φ(*hycA'-'lacZ*)	This study
Plasmids		
pFEO	*feoABC*⁺ from *E. coli* in pASK-IBA7	[39]
pECD 1079	*feoB*⁺ from *E. coli* in pASK-IBA7	N. Taudte and G. Grass
pRS552	Km^R Ap^R *lacZ*⁺ *lacY*⁺ *lacA*⁺	[20]
phyaA552	like pRS552 but containing Φ(*hyaA'-'lacZ*)	This study
phybO552	like pRS552 but containing Φ(*hybO'-'lacZ*)	This study
pTL101	like pRS552 but containing Φ(*hycA'-'lacZ*), cloned from PstI within *hycA* to AvaII within *hycA*	[28]

ᵃ P1 lysate from Δ*entC*::*cat* was obtained from G. Grass and N. Taudte
ᵇ Similar to PM06, these strains were constructed using P1*kc* lysate grown on the Δ*feoB*::*kan* knockout mutant JW3372 from the Keio collection [40] with subsequent elimination of the kanamycin resistance cassette [41].

Subsequent to mutagenesis, cells were plated on M9-glucose minimal medium including the supplements described above and mutants containing transposon-insertions in the chromosome were resistant to kanamycin. Plates were incubated for 2 days at 37°C under a H_2/CO_2 (90%/10%) atmosphere (gas-generating kit, Oxoid) and kanamycin-resistant colonies were analysed via a soft-agar overlay technique with benzyl viologen (BV) at a final concentration of 0.5 mM and in a hydrogen atmosphere as described [15]. Colonies with a wild type hydrogenase phenotype developed a dark violet colour while hydrogenase-negative mutants remained creamy white. After purification of putative hydrogenase-negative colonies on LB agar the mutation was transduced into MC4100 using P1*kc* according to Miller [30] and the phenotype verified.

In order to determine the transposon insertion site, chromosomal DNA was isolated from the mutants [26], digested with KpnI, EcoRI or BamHI and religated. The ligation mixture was PCR amplified using primers KAN-2 FP-1 5'-ACC TAC AAC AAA GCT CTC ATC AAC C-3' and R6Kan-2 RP-1 5'-CTA CCC TGT GGA ACA CCT ACA-3' and the PCR product sequenced to determine the precise site of insertion.

Preparation of cell extracts and determination of enzyme activity

Anaerobic cultures were harvested at an $OD_{600\ nm}$ of approximately 0.8. Cells from cultures were harvested by centrifugation at 4,000 × g for 10 min at 4°C, resuspended in 2-3 ml of 50 mM MOPS pH 7.0 buffer and lysed on ice by sonication (30 W power for 5 minutes with 0.5 sec pulses). Unbroken cells and cell debris were removed by centrifugation for 15 min at 10, 000 × g at 4°C and the supernatant was used as the crude cell extract. Protein concentration of crude extracts was determined [31] with bovine serum albumin as standard. Hydrogenase activity was measured according to [14] except that the buffer used was 50 mM MOPS, pH 7.0. The wavelength used was 578 nm and an E_M value of 8,600 M^{-1} cm^{-1} was assumed for reduced benzyl viologen. One unit of activity corresponded to the reduction of 1 μmol of hydrogen per min. Formate hydrogenlyase (FHL) activity was measured according to [23] using gas chromatography.

Beta-galactosidase assay was performed in microtiter plates according to [32] using a BioRad microplate reader Model 3550 (BioRad, Munich).

Polyacrylamide gel electrophoresis and immunoblotting

Aliquots of 50 μg of protein from crude cell extracts were separated on 10% (w/v) SDS-polyacrylamide gel electrophoresis (PAGE) [33] and transferred to nitrocellulose membranes as described [34]. Membrane samples were treated with 2× SDS sample buffer [35] containing 10 mM DTT and incubated at room temperature for 60 min prior to loading onto the gel. Antibodies raised against Hyd-1 (1:10000), HycE (1:3000), Hyd-2 (1:20000; a kind gift from F. Sargent) or Strep-Tactin conjugated to horseradish peroxidase (IBA, Germany) were used. Secondary antibody conjugated to horseradish peroxidase was obtained from Bio-Rad. Visualisation was done by the enhanced chemiluminescent reaction (Stratagene).

Non-denaturating PAGE was performed using 7.5% (w/v) polyacrylamide gels pH 8.5 and included 0.1% (w/v) Triton-X100 in the gels [14]. Samples (25 μg of protein) were incubated with 5% (v/v) Triton X-100 prior to application to the gels.

Where indicated, the relative intensity of hydrogenase staining and protein amount from immunoblots was quantified using ImageJ from the National Institutes of Health [36].

Hydrogenase activity-staining was done as described in [14] except that the buffer used was 50 mM MOPS pH 7.0.

Additional material

Additional file 1: Plasmid-encoded FeoB synthesis in MC4100 and PM06 (*feoB*::Tn5). Extracts (25 μg protein in membrane sample buffer) from MC4100 and PM06, transformed with pECD1079 bearing *feoB* and pFEO bearing the whole *feo* operon, both cloned behind a tetracycline promotor and encoding an N-terminal *StrepII*-tag on FeoB encoded on pECD1079 were separated by SDS-PAGE (10% w/v polyacrylamide) and after transfer to nitrocellulose detected by incubation with Strep-tactin conjugated to horseradish peroxidase. Strains were grown either with or without aeration in TGYEP, pH 6.5 and gene expression was induced with 0.2 μg ml^{-1} AHT (anhydrotetracycline) as indicated. Biotin carboxyl carrier protein (BCCP) served as a loading control. The sizes of the protein standards are shown on the right side of the gel. The angled arrow indicates the position of the Strep-FeoB polypeptide. Extracts derived from MC4100 and PM06 transformed with pFEO did not synthesize Strep-tagged FeoB and therefore acted as a negative control.

Authors' contributions
CP carried out the experimental studies and helped draft the manuscript. GS conceived and coordinated the study and drafted the manuscript. Both authors read and approved the manuscript.

Competing interests
The authors declare that they have no competing interests.

References

1. Vignais P, Billoud B: **Occurrence, classification, and biological function of hydrogenases: an overview.** *Chem Rev* 2007, 4206-4272.
2. Forzi L, Sawers RG: **Maturation of [NiFe]-hydrogenases in *Escherichia coli*.** *Biometals* 2007, **20**:565-578.
3. Pinske C, Krüger S, Soboh B, Ihling C, Kuhns M, Braussemann M, Jaroschinsky M, Sauer C, Sargent F, Sinz A, Sawers RG: **Efficient electron transfer from hydrogen to benzyl viologen by the [NiFe]-hydrogenases of *Escherichia coli* is dependent on the coexpression of the iron-sulfur cluster-containing small subunit.** *Arch Microbiol* 2011.
4. Lukey MJ, Parkin A, Roessler MM, Murphy BJ, Harmer J, Palmer T, Sargent F, Armstrong FA: **How *Escherichia coli* is equipped to oxidize hydrogen under different redox conditions.** *J Biol Chem* 2010, **285**:3928-3938.
5. Böck A, King P, Blokesch M, Posewitz M: **Maturation of hydrogenases.** *Adv Microb Physiol* 2006, **51**:1-71.
6. Volbeda A, Charon M, Piras C, Hatchikian E, Frey M, Fontecilla-Camps J: **Crystal structure of the nickel-iron hydrogenase from *Desulfovibrio gigas*.** *Nature* 1995, **373**:580-587.
7. Blokesch M, Albracht SPJ, Matzanke BF, Drapal NM, Jacobi A, Böck A: **The complex between hydrogenase-maturation proteins HypC and HypD is an intermediate in the supply of cyanide to the active site iron of [NiFe]-hydrogenases.** *J Mol Biol* 2004, **344**:155-167.
8. Watanabe S, Matsumi R, Arai T, Atomi H, Imanaka T, Miki K: **Crystal structures of [NiFe] hydrogenase maturation proteins HypC, HypD, and HypE: insights into cyanation reaction by thiol redox signaling.** *Mol Cell* 2007, **27**:29-40.
9. Eitinger T, Mandrand-Berthelot MA: **Nickel transport systems in microorganisms.** *Arch Microbiol* 2000, **173**:1-9.
10. Grass G: **Iron transport in *Escherichia coli*: all has not been said and done.** *Biometals* 2006, **19**:159-172.
11. Kammler M, Schön C, Hantke K: **Characterization of the ferrous iron uptake system of *Escherichia coli*.** *J Bacteriol* 1993, **175**:6212-6219.
12. Cartron M, Maddocks S, Gillingham P, Craven C, Andrews S: **Feo-transport of ferrous iron into bacteria.** *Biometals* 2006, **19**:143-157.
13. Dahm C, Müller R, Schulte G, Schmidt K, Leistner E: **The role of isochorismate hydroxymutase genes *entC* and *menF* in enterobactin and menaquinone biosynthesis in *Escherichia coli*.** *Biochim Biophys Acta* 1998, **1425**:377-386.
14. Ballantine S, Boxer D: **Nickel-containing hydrogenase isoenzymes from anaerobically grown *Escherichia coli* K-12.** *J Bacteriol* 1985, **163**:454-459.
15. Begg Y, Whyte J, Haddock B: **The identification of mutants of *Escherichia coli* deficient in formate dehydrogenase and nitrate reductase activities using dye indicator plates.** *FEMS Microbiol Lett* 1977, **2**:47-50.
16. Paschos A, Bauer A, Zimmermann A, Zehelein E, Böck A: **HypF, a carbamoyl phosphate-converting enzyme involved in [NiFe] hydrogenase maturation.** *J Biol Chem* 2002, **277**:49945-49951.
17. Sawers RG, Ballantine S, Boxer D: **Differential expression of hydrogenase isoenzymes in *Escherichia coli* K-12: evidence for a third isoenzyme.** *J Bacteriol* 1985, **164**:1324-1331.
18. Menon NK, Robbins J, Wendt J, Shanmugam K, Przybyla A: **Mutational analysis and characterization of the *Escherichia coli hya* operon, which encodes [NiFe] hydrogenase 1.** *J Bacteriol* 1991, **173**:4851-4861.
19. Menon NK, Chatelus CY, Dervartanian M, Wendt JC, Shanmugam KT, Peck HD, Przybyla AE: **Cloning, sequencing, and mutational analysis of the *hyb* operon encoding *Escherichia coli* hydrogenase 2.** *J Bacteriol* 1994, **176**:4416-4423.
20. Simons R, Houman F, Kleckner N: **Improved single and multicopy *lac*-based cloning vectors for protein and operon fusions.** *Gene* 1987, **53**:85-96.
21. Richard D, Sawers RG, Sargent F, McWalter L, Boxer D: **Transcriptional regulation in response to oxygen and nitrate of the operons encoding the [NiFe] hydrogenases 1 and 2 of *Escherichia coli*.** *Microbiology* 1999, **145**:2903-2912.
22. Rossmann R, Sawers G, Böck A: **Mechanism of regulation of the formate-hydrogenlyase pathway by oxygen, nitrate, and pH: definition of the formate regulon.** *Mol Microbiol* 1991, **5**:2807-2814.
23. Pinske C, Sawers RG: **The role of the ferric-uptake regulator Fur and iron homeostasis in controlling levels of the [NiFe]-hydrogenases in *Escherichia coli*.** *International Journal of Hydrogen Energy* 2010, **35**:8938-8944.
24. Hantke K: **Regulation of ferric iron transport in *Escherichia coli* K12: isolation of a constitutive mutant.** *Mol Gen Genet* 1981, **182**:288-292.
25. Massé E, Vanderpool CK, Gottesman S: **Effect of RyhB small RNA on global iron use in *Escherichia coli*.** *J Bacteriol* 2005, **187**:6962-6971.
26. Sambrook J, Russell D: *Molecular Cloning: A Laboratory Manual ,* Third 2001.
27. Hormann K, Andreesen J: **Reductive cleavage of sarcosine and betaine by *Eubacterium acidaminophilum* via enzyme systems different from glycine reductase.** *Arch Microbiol* 1989, **153**:50-59.
28. Lutz S: **Der H₂-Stoffwechsel von *Escherichia coli*: Analyse der Regulation des Formiat-Hydrogen-Lyase-Systems.** *PhD thesis* Ludwig-Maximilian-Universität München, Faculty of Biology; 1990.
29. Goryshin I, Jendrisak J, Hoffman L, Meis R, Reznikoff W: **Insertional transposon mutagenesis by electroporation of released Tn5 transposition complexes.** *Nat Biotechnol* 2000, **18**:97-100.
30. Miller J: *Experiments in Molecular Genetics* 1972, 466.
31. Lowry O, Rosebrough N, Farr A, Randall R: **Protein measurement with the Folin phenol reagent.** *J Biol Chem* 1951, **193**:265-275.
32. Griffith KL, Wolf RE: **Measuring beta-galactosidase activity in bacteria: cell growth, permeabilization, and enzyme assays in 96-well arrays.** *Biochem Biophys Res Commun* 2002, **290**:397-402.
33. Laemmli U: **Cleavage of structural proteins during the assembly of the head of bacteriophage T4.** *Nature* 1970, **227**:680-685.
34. Towbin H, Staehelin T, Gordon J: **Electrophoretic transfer of proteins from polyacrylamide gels to nitrocellulose sheets: procedure and some applications.** *Proc Natl Acad Sci USA* 1979, **76**:4350-4354.
35. Gallagher SR: **One-dimensional SDS gel electrophoresis of proteins.** *Current protocols in protein science/editorial board, John E Coligan [et al]* 2001, **Chapter 10**:Unit 10.1.
36. Abràmoff M, Magalhaes P, Ram S: **Image processing with ImageJ.** *Biophotonics International* 2004, **11**:36-42.
37. Casadaban MJ: **Transposition and fusion of the *lac* genes to selected promoters in *Escherichia coli* using bacteriophage lambda and Mu.** *J Mol Biol* 1976, **104**:541-555.
38. Pinske C, Bönn M, Krüger S, Lindenstrauß U, Sawers RG: **Metabolic deficiences revealed in the biotechnologically important model bacterium *Escherichia coli* BL21(DE3).** *PLoS ONE* 2011, **6**:e22830.
39. Grass G, Franke S, Taudte N, Nies D, Kucharski L, Maguire M, Rensing C: **The metal permease ZupT from *Escherichia coli* is a transporter with a broad substrate spectrum.** *J Bacteriol* 2005, **187**:1604-1611.
40. Baba T, Ara T, Hasegawa M, Takai Y, Okumura Y, Baba M, Datsenko K, Tomita M, Wanner B, Mori H: **Construction of *Escherichia coli* K-12 in-frame, single-gene knockout mutants: the Keio collection.** *Mol Syst Biol* 2006, **2**:2006 0008.
41. Cherepanov P, Wackernagel W: **Gene disruption in *Escherichia coli*: TcR and KmR cassettes with the option of Flp-catalyzed excision of the antibiotic-resistance determinant.** *Gene* 1995, **158**:9-14.

2.3.4 Zusätzliche Ergebnisse

Weiterhin war die Frage nach der Quelle des Eisen für das aktive Zentrum der großen Untereinheit von Interesse. Deshalb wurden Eisentransportmutanten und eine Fur-Mutante in M9-Minimalmedium ohne Eisenzugabe angezogen. Außerdem wurde verbliebenes Eisen durch den Chelator 2,2'-Dipyridyl entfernt und anschließend durch eine Eisen(II)- oder Eisen(III)-Quelle ersetzt. In allen diesen Proben wurde die Reifung der großen Hyd-2 Untereinheit untersucht, welche als Indikator für den Einbau des aktiven Zentrums diente (Abb. 10). Es konnte festgestellt werden, dass bei Eisen(II)-Zugabe bevorzugt gegenüber der Zugabe von Eisen(III) die Prozessierung der großen Untereinheit stattfindet (Abb. 10, Spuren 4). Es sind dabei Restmengen von Eisen im Medium bereits ausreichend um ins aktive Zentrum integriert zu werden, lediglich bei der Einführung der *entC* Deletion ist die Zelle auf Zugabe externen Eisens(II) für die Prozessierung angewiesen. Die Entfernung verbliebenen Eisens bewirkt, dass kein Polypeptid für die große Untereinheit detektierbar ist (Abb. 10, Spuren 2). Es zeigte sich erneut deutlich, dass *feoB* und *fur* Mutanten einen ähnlichen Phänotyp mit verringerter Polypeptidmenge der großen Untereinheit aufweisen, aber die Prozessierung im gleichen Maße wie bei MC4100 stattfindet (Abb. 10). Dabei ist der Effekt einer *fur* Deletion jedoch stärker ausgeprägt. Der Chelator 2,2'-Dipyridyl komplexiert hauptsächlich zweiwertige Ionen, weshalb eine Deletion in *feoB* gut durch vorhandene Eisen(III)-Aufnahmesysteme komplementiert werden könnte, diese jedoch keinen Einfluss auf die Prozessierung zeigten. Bei Deletion von *entC* konkurriert die Eisen(II)-Aufnahme entsprechend mit dem Chelator. Dennoch ist bei gleicher Menge Eisen(II) oder (III) die Aufnahme des zweiwertigen Ions bevorzugt und die Hyd Reifung findet statt.
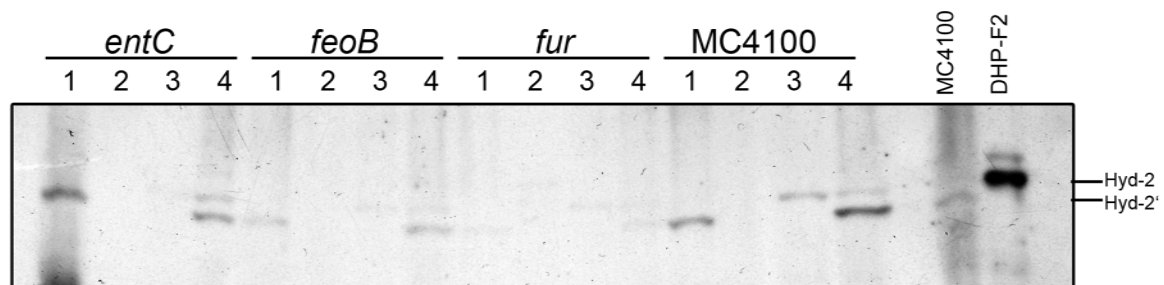
Abbildung 10 Reifung der Hyd-2 großen Untereinheit in Abhängigkeit der Eisenverfügbarkeit. Proben mit 25 µg Gesamtprotein von Kulturen der Stämme CP416 ($\Delta entC$), PM06 (*feoB*::Tn5), CP500 (Δfur), MC4100 und DHP-F2 ($\Delta hypF$) nach Wachstum in M9-Minimalmedium ohne Eisen (Spur 1), nach Zugabe von 100 µM 2,2'-Dipyridyl (Spur 2), nach Zugabe von 100 µM 2,2'-Dipyridyl und 100 µM $FeCl_3/Fe^{3+}$ (Spur 3) oder nach Zugabe von 100 µM 2,2'-Dipyridyl und 100 µM $FeSO_4/Fe^{2+}$ (Spur 4) wurden auf einem 10 % (w/v) SDS-Page aufgetrennt, auf eine Nitrocellulose Membran transferiert und mit einem Antikörper gegen Hydrogenase 2 detektiert. Die unprozessierte Form der großen Untereinheit ist als Hyd-2 und die prozessierte Form als Hyd-2' gekennzeichnet.

2.4 Effizienter Elektronentransfer von Wasserstoff zu Benzylviologen durch die [NiFe]-Hydrogenasen von *Escherichia coli* ist abhängig von der Koexpression der Eisen-Schwefel Cluster enthaltenden kleinen Untereinheit.

2.4.1 Zusammenfassung

Im Unterschied zu den [FeFe]-Hydrogenasen besitzen die [NiFe]-Hydrogenasen kein [FeS]-Cluster in der großen Untereinheit (Silakov *et al*., 2009). Das aktive Zentrum ist für den physiologischen Elektronentransfer auf das proximale [FeS]-Cluster im Abstand von weniger als 13 Å in der kleinen Untereinheit angewiesen (Volbeda *et al*., 1995). Es war lange umstritten, ob *in vitro* Elektronentransfer direkt vom aktiven Zentrum auf Redoxfarbstoffe wie Benzylviologen geschieht oder die kleine Untereinheit assoziiert sein muss. In dieser Arbeit konnte durch molekularbiologische und proteinbiochemische Methoden bewiesen werden, dass die kleinen Untereinheiten unabdingbar sind. Um die Effekte einzelner Hydrogenasen zu untersuchen, mussten jeweils die großen Untereinheiten der anderen deletiert werden. Dabei konnte der Anteil der einzelnen Hydrogenasen an der Gesamthydrogenaseaktivität unter den verwendeten Standardbedingungen bestimmt werden:

- Anzucht: TGYEP Medium, pH 6,5; 37 °C für 5-6 h,
- Messung: 4 mM BV_{ox} in MOPS-Puffer pH 7,0, 100 % H_2.

Dabei entfallen 93-94 % der Gesamthydrogenaseaktivität auf Hyd-3 und 6 % auf Hyd-2, während Hyd-1 Aktivität nur wenig über dem Hintergrund liegt. Die Komplementation der Deletion einer großen Untereinheit mit ihrem jeweiligen *Strep*-Tag Fusionstranskript zeigte, dass *N*-terminale Fusionsproteine nur marginal mit der Aktivität interferieren. Die Aktivität mit HycE, der großen Untereinheit von Hyd-3, konnte zu 43 % und mit HybC, der großen Untereinheit von Hyd-2, zu 38 % wieder hergestellt werden. Diese unvollständige Komplementation liegt vermutlich in der nicht mit den restlichen Komponenten des jeweiligen Operons koordinierten Expression begründet.

Für die Reinigung *Strep*-Tag fusionierter großer Hyd-1 und Hyd-2 Untereinheiten konnte gezeigt werden, dass die jeweiligen kleinen Untereinheiten stets ko-gereinigt werden. Für Hyd-1 konnten gemeinsam mit aktivem *Strep*-HyaB zwei distinkte Laufformen (29 und 36 kDa) für HyaA identifiziert werden, die vermutlich proteolytischem Abbau, nicht jedoch den für den Tat-Membrantransport typischen Größen entsprechen (41 kDa für Apo-Protein und 36 kDa für Tat-prozessierte Form). Bei der Reinigung von aktivem *Strep*-HybC wurden beide

kleinen Untereinheiten HybO und HybA ko-gereinigt. Eine Reinigung von Strep-HybC in einem Stamm ohne HybO zeigte keine Assoziation mit der zweiten Untereinheit HybA. Es fehlen beiden Komplexen die Membranuntereinheiten HyaC bzw. HybB, dennoch konnten im Nativen Gel Laufverhalten und bei der Quantifizierung Aktivitäten in der Größenordnung der Wildtypenzyme gemessen werden.

Weiterhin konnten in Extrakten von Mutanten, in denen die großen Untereinheiten vorhanden und die kleinen Untereinheiten deletiert waren, keine Aktivitäten nachgewiesen werden. Eine Komplementation dieser Stämme mit ihren kleinen Untereinheiten gelang und bewies, dass *in vivo* und *in vitro* die Messung der H_2:BV Aktivität die Anwesenheit der kleinen Untereinheiten benötigte. Zusätzlich konnte in diesen Stämmen die Prozessierung der großen Untereinheit mittels Western Blot nachgewiesen werden, was einen Einbau des aktiven Zentrums voraussetzt, offenbar jedoch nicht die Assoziation mit der kleinen Untereinheit.

Nichtsdestotrotz konnte die hier verwendete Art der Reinigung aktiven Hyd-2 Enzyms nicht auf Hyd-3 übertragen werden. Dies ist wahrscheinlich durch Verlust einzelner Untereinheiten erklärbar, was auch die Labilität der FHL Aktivität im Nativen Gel begründen würde.

2.4.2 Artikelkopie

Efficient Electron Transfer from Hydrogen to Benzyl Viologen by the [NiFe]-Hydrogenases of *Escherichia coli* is Dependent on the Coexpression of the Iron-Sulphur Cluster-Containing Small Subunit

Constanze Pinske[1], Sara Krüger[1], Basem Soboh[1], Christian Ihling[2], Martin Kuhns[1], Mario Braussemann[1], Monique Jaroschinsky[1], Christopher Sauer[1], Frank Sargent[3], Andrea Sinz[2] and R. Gary Sawers[1*]

[1] Institute for Microbiology, Martin-Luther University Halle-Wittenberg, Kurt-Mothes-Str. 3, 06120 Halle (Saale), Germany, [2]Institute of Pharmacy, Martin-Luther University Halle-Wittenberg, Wolfgang-Langenbeck-Str. 1, 06120 Halle (Saale), Germany, [3] Division of Molecular Microbiology, College of Life Sciences, University of Dundee, Dundee DD1 5EH, Scotland, UK,

[*] For correspondence: R.G. Sawers, Institute for Microbiology, Martin-Luther University Halle-Wittenberg, Kurt-Mothes-Str. 3, 06120 Halle (Saale) Germany
Tel., +49 345 5526350; Fax., +49 345 5527010; Email, gary.sawers@mikrobiologie.uni-halle.de

Abstract

Escherichia coli can both oxidize hydrogen and reduce protons. These activities involve three distinct [NiFe]-hydrogenases, termed Hyd-1, -2 and -3, each minimally comprising heterodimers of a large subunit, containing the [NiFe] active site, and a small subunit, bearing iron-sulphur clusters. Dihydrogen-oxidizing activity can be determined using redox dyes like benzyl viologen (BV); however, it is unclear whether electron transfer to BV occurs directly at the active site, or via an iron-sulphur center in the small subunit. Plasmids encoding Strep-tagged derivatives of the large subunits of the three *E. coli* [NiFe]-hydrogenases restored activity of the respective hydrogenase to strain FTD147, which carries in-frame deletions in the *hyaB*, *hybC* and *hycE* genes encoding the large subunits of Hyd-1, Hyd-2 and Hyd-3, respectively. Purified Strep-HyaB was associated with the Hyd-1 small subunit (HyaA) and purified Strep-HybC was associated with the Hyd-2 small subunit (HybO) and a second iron-sulphur protein, HybA. However, Strep-HybC isolated from a *hybO* mutant had no other associated subunits and lacked BV-dependent hydrogenase activity. Mutants deleted separately for *hyaA*, *hybO* or *hycG* (Hyd-3 small subunit) lacked BV-linked hydrogenase activity, despite the Hyd-1 and Hyd-2 large subunits being processed. These findings demonstrate that hydrogenase-dependent reduction of BV requires the small subunit.

Introduction

[NiFe]-hydrogenases are evolutionary ancient [Fe-S] (iron-sulphur) cluster-containing proteins that catalyze the reduction of protons to molecular hydrogen or the oxidation of hydrogen to protons and electrons (Vignais and Billoud 2007). The genome of *E. coli* encodes four membrane-associated [NiFe]-hydrogenases (Hyd-1, Hyd-2, Hyd-3 and Hyd-4), only three of which, Hyd-1, Hyd-2 and Hyd-3, are synthesized under standard anaerobic growth conditions (Forzi and Sawers 2007). Two of these enzymes, Hyd-1 (Menon et al. 1991) and Hyd-2 (Menon et al. 1994), oxidize molecular hydrogen *in vivo* on the periplasmic side of the cytoplasmic membrane and transfer the electrons to the quinone pool (Forzi and Sawers 2007; Sawers 1994). In contrast, Hyd-3 is part of the hydrogen-evolving formate hydrogenlyase (FHL) complex, which disproportionates formic acid into CO_2 and H_2.

[NiFe]-hydrogenases generally comprise a large subunit and a small subunit and often there is a further membrane-anchoring subunit associated with the complex. An exception is Hyd-2 of *E.*

coli, which has two electron-transferring subunits HybO and HybA (Sargent et al. 1998; Dubini et al. 2002). While HybO interacts directly with the large subunit HybC and therefore is regarded as the small subunit, HybA associates with the complex but does not accept electrons directly from the active site in HybC (Dubini et al. 2002). The crystal structure of soluble [NiFe]-hydrogenase (Volbeda et al. 1995) has shown that the large subunit contains the hetero-bimetallic [NiFe] active site that usually has one CO and 2 CN$^-$ ligands to the iron atom. The large subunit of the active enzyme does not have an associated [Fe-S] cluster. On the other hand, the electron-transferring small subunit typically has one [3Fe-4S] and two [4Fe-4S] clusters and these form an electron-transfer chain coupling the active site with the quinone pool via a cytochrome *b* moiety located in the membrane-anchoring subunit (Forzi and Sawers 2007; Vignais and Billoud 2007). Again, Hyd-3 presents an exception because the HycG small subunit is predicted to have a single [Fe-S] cluster and furthermore it couples electron transfer between the HycE large subunit and the other components of the FHL complex, which receive electrons from the oxidation of formate catalyzed by formate dehydrogenase H (FDH-H) (Böhm et al. 1990; Sauter et al. 1992).

As all Hyd enzymes catalyse the reversible activation of hydrogen *in vitro* their catalytic activity can be readily monitored by following the oxidation or reduction of viologen dyes, such as benzyl or methyl viologen (BV, 1,1′-dibenzyl-4,4′-bipyridylium dichloride; MV, 1,1′-dimethyl-4,4′-bipyridinium dichloride) (Akagi and Campbell, 1961; Gitlitz and Krasna, 1975). BV undergoes a colour-dependent oxidation-reduction reaction with an E^o of -350 mV (Jones and Garland 1977), which makes it suitable for accepting the electrons generated by the oxidation of H_2. It has remained unclear whether the electrons generated during the oxidation of H_2 can be transferred from the [NiFe] active site directly to BV or whether they must first reach the [Fe-S] clusters in the small subunits prior to transfer to the redox dye. However, evidence based on site-directed mutagenesis of cysteinyl residues ligating [Fe-S] clusters in the small subunit has suggested that electron transfer to redox dyes proceeds via the small subunit (Sayavedra-Soto and Arp 1993; DeLacy et al. 2000).

Construction of a series of in-frame *hyc* operon deletion mutants (Sauter et al. 1992) indicated that the small subunit of *E. coli* Hyd-3 is required for hydrogen-dependent BV reduction; however, as already mentioned, the HycG protein is unusual because it is predicted to have only one [Fe-S] center (Böhm et al. 1990). Moreover, these studies were performed in a genetic background in which the Hyd-1 and Hyd-2 enzymes were also synthesized, thus making it difficult to determine whether some BV-reducing activity was retained by the enzyme. Studies performed on the hydrogen-sensing hydrogenase from *Ralstonia eutropha* also indicated that the purified large subunit HoxC, in the absence of the small subunit, had lost the ability to activate H_2 (Winter et al. 2005).

In an earlier study on Hyd-2 of *E. coli* Dubini et al. (2002) showed that while a deletion of the *hybA* gene abolished hydrogen-dependent electron transfer to fumarate reductase the enzyme retained the ability to reduce BV, thus indicating that HybA is not the small subunit. Here we have analysed the activity of each individual hydrogenase of *E. coli* exclusively and by using a combination of deletion and complementation studies demonstrate that hydrogen-dependent reduction of BV in all three hydrogenases is dependent on the [Fe-S]-cluster-containing small subunit. Moreover, we show that in the absence of HybO, Hyd-2 cannot reduce BV, which suggests that electron transfer from the large subunit to the HybA small subunit is mediated via HybO.

Materials and Methods

Strains, plasmids and growth conditions

All *E. coli* strains and plasmids used in this study are listed in Table 1.

Strains were grown anaerobically in sealed bottles filled under a nitrogen gas atmosphere in TGYEP medium (Begg et al. 1977) and incubated at 37 °C. Where indicated cultures were supplemented with 15 mM sodium formate. When required, the growth medium was solidified with 1.5 % (w/v) agar. The growth medium was supplemented with 0.1% (v/v) SLA trace element solution (Hormann et al. 1994). The antibiotics chloramphenicol, kanamycin and ampicillin, when required, were added to the medium at the final concentrations of 12.5 µg, 50 µg and 100 µg per ml, respectively. To induce expression of recombinant genes cloned in the pASK-IBA vector, anhydrotetracycline (AHT) was typically added to the cultures at a final concentration of 0.2 µg ml^{-1}, or as indicated in the legends to the figures.

Large-scale growths for protein purification were performed anaerobically in 10 l of TGYEP medium. Gene expression was induced by the addition of 0.2 µg ml^{-1} AHT followed by incubation at 30 °C for 3 to 5 h. The cultures were harvested

after reaching an optical density at 600 nm of 0.9 and cell pellets were either used immediately or stored at -20 °C until use.

Strain construction

Strains were generally constructed by introduction of mutations from *E. coli* donor strains into recipient stains of MC4100 by P1*kc* phage transduction according to (Miller 1972) (see Table 1).

Plasmid construction

Recombinant DNA work was carried out according to published methods (Sambrook et al. 1989). The *hyaB, hybC* and *hycE* genes, encoding the large subunits of Hyd-1, -2 and -3, respectively, were amplified by PCR using genomic DNA isolated from MC4100 as template and the primers hyaB-IBA5_BsaI_FW (5'-ATGGTAGGTCTCAGCGCCATGAG CACTCAGTACGAAACTCAG-3'), hyaB-IBA5_BsaI_RW, (5'-ATGGTAGGTCTCATATCAACGCACCTGCACGGAG ATCAG-3'), hycE-IBA5_BsaI_FW, (5'-ATGGTAGG TCTCAGCGCCATGTCTGAAGAAAAATTAGGTCAACA -3') and hycE-IBA5_BsaI_RW (5'-ATGGTAGGTCTCA TATCATTTCAGCGGCGAGTTTTTACGCT-3'), as well as those published in (Soboh et al. 2010) for *hybC* (hybC-IBA5_BsaI_FW and hybC-IBA5_BsaI_RW). The resulting DNA fragments of 1794 bp (*hyaB*), 1704 bp (*hybC*) and 1710 bp (*hycE*) were digested with restriction endonuclease BsaI and ligated into pASK-IBA5$^+$ (IBA Technology, Göttingen, Germany), which had previously been digested with the same restriction endonuclease. The DNA sequence of the complete inserts in the resulting plasmids pASK-hyaB, pASK-hybC and pASK-hycE were verified. Each plasmid encoded a fusion protein with an N-terminal *Strep*-tag II.

Preparation of anaerobic cell extracts

All steps were carried out at 4 °C under anaerobic conditions in a Coy^{TM} anaerobic chamber unless specifically stated otherwise. Anaerobically grown cultures were harvested at an OD$_{600nm}$ of approximately 0.8. Harvested cells were washed in anaerobic MOPS-buffer (50 mM MOPS pH 7.5) and after centrifugation the cell pellet was resuspended typically in 3 volumes of 50 mM MOPS pH 7.5 buffer including 5 µg DNase/ml and 0.2 mM phenylmethylsulfonyl fluoride for determination of enzyme activity or in buffer A (see below) for purification of Strep-tagged proteins. Typically 15-30 g wet weight of cells were disrupted by sonication (30W power for 5 min with 0.5 sec pulses). Unbroken cells and cell debris were removed by centrifugation for 30 min at 50 000 xg and at 4 °C and the supernatant (crude extract) was either used immediately or stored anaerobically at -80 °C until used. Protein concentration of crude extracts was determined (Lowry et al. 1951) with bovine serum albumin as standard.

Purification of Strep-tagged Hyd-1 and Hyd-2

Strep-HyaB and Strep-HybC protein complexes were purified anaerobically from anaerobically prepared crude cell extracts by affinity chromatography using StrepTactin sepharose (10 ml column volume) as indicated by the manufacturer. The matrix was equilibrated with 100 mM Tris-HCl, pH 8.0 containing 150 mM NaCl (buffer A). The crude extracts were incubated with avidin (80 µg ml^{-1} of crude extract) for 45 min at 4 °C and then membrane fractions were prepared by anaerobic ultracentrifugation at 120,000 x g for 2 h as previously described (Soboh et al. 2010). The soluble fractions were decanted and stored for later use and the membranes were resuspended in buffer A and Triton X-100 was added to a final concentration of 5 % (w/v) and the

solution was gently stirred overnight at 4 °C. After a further centrifugation step to remove insoluble membrane material the supernatant was applied to column at a flow-rate of approximately 1 ml min^{-1}. Unbound proteins were removed by washing with three column volumes of buffer A. Bound *Strep*-tap II fusion proteins were eluted by applying 3 column volumes of buffer A supplemented with 2.5 mM desthiobiotin and fractions of 1 ml were collected. Purification of Strep-HyaB or Strep-HybC from the soluble fraction was performed in the same manner but with omission of the membrane solublization step. Fractions containing Strep-HyaB, -HybC or –HycE were combined and when necessary concentrated using Vivaspin 20 concentrators (Sartorius, Göttingen).

Polyacrylamide gel electrophoresis

Aliquots of 50 µg of protein from crude extracts were separated by SDS-polyacrylamide gel electrophoresis (PAGE) using 10% (w/v) polyacrylamide (Laemmli 1977). Transfer to nitrocellulose membranes and Western blot analysis using anti-*E coli* Hyd-1 and Hyd-2 antibodies was performed as described (Towbin et al. 1979).

Non-denaturing PAGE was performed using 5% (w/v) polyacrylamide gels, pH 8.5 and included 0.1% (w/v) Triton X-100 in the gels (1). Samples (14 µg of protein) were incubated with 5% (w/v) Triton X-100 prior to application to the gels. Hydrogenase activity-staining was done as described in (Ballantine and Boxer 1985) except that the buffer used was 50 mM MOPS pH 7.0.

Determination of total hydrogenase enzyme activity

Hydrogenase enzyme activity (H$_2$-dependent reduction of benzyl viologen) determines the sum of the activites of Hyd-1, Hyd.2 and Hyd-3 and was measured according to (Ballantine and Boxer 1985) except that the buffer used was 50 mM MOPS, pH 7.0. No detergent was added to extracts measured by this method. The wavelength used was 578 nm and an E$_M$ value of 8,600 M^{-1} cm^{-1} was assumed for reduced benzyl viologen (BV). One unit of activity corresponded to the reduction of 1 µmol of hydrogen per min.

Experiments were performed minimally three times and each time in triplicate. Data are presented as standard deviation of the mean.

Mass spectrometric analysis

Proteins were *in-gel* digested following standard protocols (Shevchenko et al. 2006). Briefly, protein disulfides were reduced with dithiothreitol (DTT) and cysteines were alkylated with iodoacetamide. The peptide extracts were analyzed by LC/MS on an UltiMate Nano-HPLC system (LC Packings) coupled to an LTQ-Orbitrap XL mass spectrometer (ThermoFisher Scientific) equipped with a nanoelectrospray ionization source (Proxeon). The samples were loaded onto a trapping column (Acclaim PepMap C18, 300 µm x 5 mm, 5 µm, 100Å, LC Packings, Amsterdam, NL) and washed for 15 min with 0.1 % TFA at a flow rate of 30 µl/min. Trapped peptides were eluted onto the separation column (Acclaim PepMap C18, 75 µm x 150 mm, 3 µm, 100Å, LC Packings), which had been equilibrated with 100 % A (5 % acetonitrile, 0.1 % formic acid). Peptides were separated with a linear gradient: 0-50 % B (80 % acetonitrile, 0.1 % formic acid) in 30 min, 50-100 % B in 2 min, 100 % B for 10 min. The column was kept at 30°C and the flow rate was 300 nl/min. During gradient elution, MS data were acquired in data-dependent MS/MS mode: Each high-resolution full scan (*m/z* 300 to 2000, resolution 60,000) in the orbitrap analyzer was

followed by five collision-induced dissociation (CID) product ion scans in the linear ion trap (LTQ) for the five most intense signals in the full-scan mass spectrum (isolation window 2.3 Th). Dynamic exclusion (repeat count was 3, exclusion duration 180 s) was enabled to allow detection of less abundant ions. Data analysis was performed using the Proteome Discoverer 1.0 (ThermoFisher Scientific). MS/MS data of precursor ions in the *m/z* range 600-6000 were searched against the SwissProt database (version 07/03/07, tax. *E.coli*) using Mascot (version 2.2). Mass accuracy was set to 3 ppm and 0.8 Da for precursor and fragment ions, respectively, carbamidomethylation of cysteines was set as fixed modification and oxidation of methionine as variable modification, two missed cleavages of trypsin were allowed. Proteins identified by at least two peptides with an ion score significance threshold of 0.01 were considered to be unambiguously identified.

Results and Discussion

In trans complementation of an E. coli hydrogenase-negative mutant

In the absence of the purified physiological electron acceptors for the respective [NiFe]-hydrogenases of *E. coli* the activities of Hyd-1, Hyd-2 and Hyd-3 can be facilely determined as a single activity in crude cell extracts by measuring H_2: BV oxidoreductase activity (Ballantine and Boxer 1985; Sawers et al. 1985). The activities of Hyd-1 and Hyd-2 can also be visualized after detergent solubilization and separation of the polypeptides in native PAGE, while that of Hyd-3 cannot due to apparent instabillity of the enzyme during electrophoresis (Ballantine and Boxer 1985; Sawers et al. 1985). While detergent solubilization of Hyd-1 and Hyd-2 has no deleterious effect on H_2: BV oxidoreductase activity, Hyd-3 activity is compromised by this procedure (Sawers et al. 1985).

Extracts derived from strain MC4100 (wild type positive control) were separated by non-denaturing PAGE and revealed activity bands characteristic for Hyd-1 and Hyd-2 (Fig. 1). To identify which of the activity bands was specific for Hyd-1 and which for Hyd-2, we analysed extracts derived from a mutant (HDK100) unable to synthesise Hyd-1 but retaining the genetic capacity to make Hyd-2, Hyd-3 and Hyd-4 and from a mutant (HDK200) lacking only Hyd-2 but retaining the other enzymes. Clearly, the faster-migrating, stained, active band corresponded to Hyd-1, while the two more slowly migrating activity bands resulted from the activity of Hyd-2 (Fig. 1A and B).

Strain FTD147 has in-frame deletions in the genes encoding the large subunits of Hyd-1 (Δ*hyaB*), Hyd-2 (Δ*hybC*) and Hyd-3 (Δ*hycE*) and consequently lacks the activities of all three enzymes (Redwood et al. 2008). An extract derived from FTD147 showed no activity bands corresponding to either Hyd-1 or Hyd-2 (Fig. 1) and thus acted as a negative control. The weakly staining band occasionally observed near the top of the gel, which was clearly observed in the FTD147 extract (marked with an asterisk Fig. 1B) is not hydrogenase-specific and is also observed in an extract from strain DHP-F2 (Δ*hypF*). A mutant lacking HypF is unable to mature any of the hydrogenase large subunits and has an activity pattern indistinguishable from that of FTD147 (Paschos et al. 2002; and data not shown).

In order to examine whether the activities of Hyd-1 and Hyd-2 could be restored by supplying the respective large-subunit gene on a plasmid and at the same time to determine whether a N-terminally fused *Strep*-tag II affected enzyme activity, we introduced the plasmids pASK-hyaB and pASK-hybC (see Table 2) individually into FTD147 by transformation. Introduction of a plasmid encoding a N-terminally Strep-tagged derivative of HyaB into FTD147 restored the fast-migrating activity band corresponding to Hyd-1. Notably, even without addition of exogenous AHT, which induces *hyaB* expression in plasmid pASK-hyaB, a Hyd-1-specific activity band could be observed, indicating that low-level expression of the *hyaB* gene occurred from the plasmid without induction of gene expression (Fig. 1A). Increasing concentrations of AHT resulted in a moderate increase in intensity of the Hyd-1 activity band. Notably, the introduction of the Strep-tag onto HyaB caused the activity band corresponding to Hyd-1 to migrate marginally more slowly in the gel (Fig. 1A).

A similar experiment performed with a plasmid encoding Strep-tagged HybC resulted in restoration of the activity bands corresponding to Hyd-2 (Fig. 1B). Addition of AHT concentrations up to 0.2 µg ml^{-1} caused a corresponding increase in the intensity of the Hyd-2 activity bands while AHT concentrations above this level, e.g. 0.4 µg ml^{-1}, resulted in marginally weaker activity bands (Fig. 1B).

Hydrogen-dependent reduction of the artificial electron acceptor BV provides a direct means of quantifying hydrogenase enzyme activity (Ballantine and Boxer 1985). In order to determine the contribution made by each enzyme under the

growth conditions tested, we first analyzed hydrogenase activity in double-deletion mutants in which different combinations of two hydrogenases were missing (Table 1). The results reveal that Hyd-3 (strain CP734 Δ*hyaB* Δ*hybC*) contributes more than 93-94% to the total hydrogenase activity, while Hyd-2 in extracts of strain HDK103 (Δ*hya* Δ*hycA-H*) has a specific activity of 0.21 U mg protein^{-1}, contributing 6% of the activity under these conditions. Hyd-1 has a very low specific hydrogenase activity close to background of 0.01 U mg protein^{-1} in the crude extract of HDK203 (Δ*hyb* Δ*hycA-H*), despite being the most abundant hydrogenase based on the level of protein (Jacobi et al. 1992; Sawers and Boxer 1986). It is important to consider that although all three enzymes reduce BV, the efficiency with which they do so may differ from enzyme to enzyme (Ballantine and Boxer 1986; Sawers and Boxer 1986; Laurinavichene et al. 2002). Thus, the contributions of each enzyme given in percentages is with respect to BV oxidoreductase activity only; the activity of each enzyme with its natural electron acceptor might be different. Furthermore, the hydrogenase activity observed after native PAGE is based on a cumulative assay and therefore is qualitative.

Introduction of plasmid pASK-hyaB encoding Strep-tagged HyaB into FTD147 resulted in a specific hydrogenase activity in the range of 0.01 U mg protein^{-1} (Table 2), which is in the range of that observed for the Hyd-2$^-$ Hyd-3$^-$ mutant HDK203. Note that no AHT was added to these cultures. Similarly, introduction of pASK-hybC encoding the Strep-tagged variant of the Hyd-2 large subunit HybC restored Hyd-2 hydrogenase activity to approximately 40% the level of that observed in extracts of strain HDK103. Finally, the modified *hycE* gene encoding Strep-tagged HycE was introduced into FTD147 (Δ*hyaB* Δ*hybC* Δ*hycE*) on plasmid pASK-hycE and yielded a specific activity of 1.42 U mg protein^{-1}, which corresponds to approximately 43% of the activity detected in the Hyd-1$^-$ Hyd-2$^-$ mutant CP734. Notably, introduction of pASK-hycE into FTD147 restored hydrogen gas production (data not shown). Taken together, the results of these experiments reveal that plasmid-encoded Strep-tagged derivatives of the large subunits of Hyd-1, Hyd-2 and Hyd-3 restored activity of the respective hydrogenase; however, activity was not restored to wild type levels, possibly reflecting that the genes were introduced *in trans* and consequently not in the correct chromosomal context.

Strep-HyaB and Strep-HybC from FTD147 associate with their respective electron-transferring small subunits

Isolation of cytoplasmic and membrane fractions from FTD147/ pASK-hyaB revealed that Strep-HyaB had an activity distribution of 38:62 in favour of the membrane fraction. Strep-HyaB could be purified reproducibly in a single step from both the cytoplasmic fraction and from solubilized membranes as described in the Materials and Methods. Strep-HyaB purified from the cytoplasmic fraction had a specific activity of 13 U mg protein^{-1}, while Strep-HyaB purified from the solubilized membranes had a specific activity of 21 U mg protein^{-1}. These activities are in the range observed for the native enzyme purified from solubilized membranes (Sawers and Boxer 1986), which had a specific activity of 10.6 U mg protein^{-1}. The purified enzyme migrated as a double band in activity-stained gels (Fig. 2A), which has been previously noted for purified Hyd-1 (Sawers and Boxer 1986). Analysis of the preparations by SDS-PAGE resolved three polypeptides with molecular masses ~65 kDa, ~36 kDa and ~29 kDa for the enzyme purified from membranes (Fig. 2B) and ~65 kDa and ~36 kDa for the enzyme prepared from the soluble fraction (data not shown). Mass spectrometric analysis of these polypeptides identified the ~65 kDa polypeptide as Strep-HyaB, while the smaller polypeptides both corresponded to the small subunit HyaA. No evidence for the existence of the membrane-intergral, cytochrome *b*-containing HyaC polypeptide could be found in any of our preparations. The truncated HyaA polypeptide possibly provides an explanation for the faster migrating active species of the enzyme seen in Fig. 2B. It was noted in a previous report that the small subunit of Hyd-1 was susceptible to proteolytic cleavage during purification (Sawers and Boxer 1986). The results of this analysis reveal that the Strep-HyaB polypeptide can associate with the small subunit to deliver an active enzyme.

Strep-HybC was found essentially exclusively associated with the cytoplasmic membrane. Solubilization of the membrane fraction and affinity purification on StrepTactin sepharose yielded active enzyme that migrated in a similar manner to the native enzyme in native PAGE (Fig. 2C). The specific activity of Hyd-2 ranged from

250-290 U mg protein^{-1} depending on the preparation, which is in good agreement with the activity of native Hyd-2 enzyme of 320 U mg protein^{-1} (Ballantine and Boxer 1986). The specific activities of both Hyd-1 and Hyd-2 are roughly 10-fold higher than reported recently for His-tagged derivatives of the proteins (Lukey et al. 2010). The difference in activity might result from the tag used.

Purified Strep-HycE could be isolated by Streptactin affinity chromatography (data not shown); however, the enzyme could not be isolated in an active form even when the enzyme was isolated anaerobically. Early attempts to isolate enzymatically active Hyd-3 encountered similar problems (Sawers et al 1985) and at that time this was attributed to instability of the enzyme complex.

The iron-sulphur cluster-containing small subunits are essential for BV-reducing activity

A question that has long remained unanswered is whether BV can accept electrons directly from the active site in the large subunit of *E. coli* [NiFe]-hydrogenases. The isolation of active forms of Strep-HyaB and Strep-HybC in association with their respective iron-sulphur cluster-containing, electron-transferring small subunits suggested that the presence of the small subunit(s) might be necessary to obtain effective electron transfer to oxidized BV. In order to test this, we constructed by P1-transduction a set of strains that are derivatives of FTD147 in which the gene encoding the small subunit of the respective hydrogenases was deleted (see Table 1). The construction of each strain was designed such that upon deletion of the small subunit gene, the gene encoding the respective large subunit was re-introduced into the strain. Thus, for example, strain CP792 is deleted for the *hybC*, *hycE* and *hyaA* genes but has the originally deleted *hyaB* gene, encoding the large subunit of Hyd-1, restored.

Extracts derived from strains lacking either *hyaA*, encoding the small subunit of Hyd-1, or *hybO*, encoding the small subunit of Hyd-2, were separated on native-PAGE and analysed for hydrogenase activity (Fig. 3). An extract from MC4100 yielded the typical pattern of bands characterisitic for Hyd-1 and Hyd-2, while an extract derived from FTD147 (ΔhyaB, ΔhybC, ΔhycE) showed no hydrogenase-specific activity bands (Fig. 3). An extract from strain CP792

deleted for *hyaA* but restored for *hyaB* did not show an activity band corresponding to Hyd-1 and an extract derived from strain CP793 lacking *hybO* but restored for *hybC* also lacked activity bands characteristic of Hyd-2.

To rule out possible polarity effects caused by introduction of the kanamycin-resistance cassette in the respective mutants, the cassette was deleted from CP792 and CP793 using the flip-recombinase procedure (Datsenko and Wanner 2000) and resulted in strains CP796 and CP795, respectively. Also, in extracts derived from these strains no hydrogenase-specific activity bands were observed (Fig. 3).

Finally, transformation of CP792 or CP796 with plasmid pASK-hyaB and of CP793 or CP795 with pASK-hybC also failed to restore Hyd-1 or Hyd-2 activity, respectively, in the mutants unable to synthesize the small subunits, while transformation of the same plasmids into FTD147 did restore Hyd-1 and Hyd-2 activity (Fig. 3). Attempts made to measure the hydrogenase enzyme activity in extracts of the complemented strains confirmed the lack of hydrogen-dependent BV reductase activity.

Restoration of hydrogenase enzyme activities by supplying in trans the genes encoding the small subunits

To demonstrate that the strains deleted for the genes encoding the hydrogenase small subunits could be complemented for hydrogenase activity by supplying the corresponding genes *in trans*, we introduced the missing genes encoding the small subunits on a plasmid. Analysis of an extract of strain CP796 (ΔhyaA, ΔhybC, ΔhycE) complemented with pCAN-hyaA (encoding a His-tagged version of HyaA) revealed that Hyd-1 activity could be restored in native-PAGE (Fig. 4A). Interestingly, a slow-migrating active Hyd-1 species was also observed. This might result from interference in membrane-targetting due to the N-terminal hexa-histidine tag on the small subunit.

Analysis of extracts derived from CP795 (ΔhyaB, ΔhybO, ΔhycE) transformed with pCAN-hybO (encoding a His-tagged version of HybO) revealed that introduction of the plasmid restored Hyd activity in native-PAGE (Fig. 4B). The Hyd-2 specific enzyme activity in extracts of CP795/pCAN-hybO was shown to be 0.09 U mg protein^{-1}, which is a value similar to the activity observed in extracts of FTD147/ pASK-hybC (Table 2). The Hyd-1 specific enzyme activity was close to

background activity and therefore could not be determined with accuracy in crude extracts (Table 2).

Re-introduction of the *hycE* gene into the chromosome of FTD147 with concomitant deletion of *hycG*, encoding the small subunit of Hyd-3, resulted in a strain lacking any measureable hydrogenase activity (Table 2). Transformation of the mutant with pCAN-hycG restored a hydrogenase enzyme activity of 0.5 U mg protein^{-1} in crude extract of the strain (Table 2).

The large subunits of Hyd-1 and Hyd-2 are processed in the absence of the small subunits

The data presented above clearly indicate that for Hyd-1, Hyd-2 and Hyd-3 hydrogen-dependent BV reduction is only possible when the small subunit is present. To determine whether the reason that no enzyme activity was observed is due to lack of processing of the respective large subunits, we analysed extracts of the small subunit mutant CP792, CP793 and CP796 by Western blotting using anti-Hyd-1 and anti-Hyd-2 antiserum (Fig. 5A). The results show that in the *hyaA* mutant the chromosomally encoded HyaB large subunit is processed (upper panel in Fig. 5A, lanes 5 and 6) in a similar manner to that observed in the wild type MC4100 (upper panel in Fig. 5A, lane 2). Similarly, the large subunit of Hyd-2 is clearly processed in an extract derived from CP793 lacking the HybO small subunit (lower panel in Fig. 5A, final lane). This pattern is again similar to that observed in the wild type MC4100 (lower panel in Fig. 5A, lane 2). An extract derived from anaerobically grown strain DHP-F2 (Lane 1 in Fig. 5A) showed only the unprocessed form of both large subunits, which is characteristic of inactive hydrogenase enzymes lacking the [NiFe] active site (Paschos et al. 2002).

Finally, we affinity purified the Strep-HybC protein from a strain lacking the gene encoding the *hybO* gene encoding the Hyd-2 small subunit (Fig. 5B). Two polypeptides were visualized by SDS-PAGE with molecular masses characteristic of the unprocessed and C-terminally processed Strep-HybC polypeptides. Mass spectrometric analyses confirmed that both polypeptides were indeed HybC. No polypeptides that migrated in the region of HybO or HybA were observed.

The hydrogenase specific activity of purified Strep-HybC was 0.2 U mg protein^{-1}, which was more than three orders of magnitude lower than that observed for the Strep-HybC purified with the small subunits associated.

Taken together, these findings strongly suggest that electron transfer to BV requires the small subunits and this occurs presumably via the [Fe-S] clusters. While it could be argued that if the small subunit is absent a conformational change in the large subunit could, in principle, affect electron transfer to BV, mutagenesis studies in which only the ligation of specific [Fe-S]-clusters in the hydrogenase small subunit was altered (Sayavedra-Soto and Arp 1993) delivered similar results to those observed here. The caveat remains, however, regarding the extent to which the lack of an [Fe-S] cluster affects electron transfer or even stability of the small subunit.

Conclusions

The key findings of this study are the following:

1. In the absence of the respective electron-transferring small subunit, essentially no hydrogen-dependent reduction of the electron acceptor BV by the catalytic subunit of any of the three [NiFe]-hydrogenases of *E. coli* occurs.

2. Hyd-1 (HyaB) and Hyd-2 (HybC) large subunits showed a processing pattern indistinguishable from the large subunit in the wild type, which strongly indicates that active site insertion and large subunit-processing are completed in the absence of the small subunit and membrane-association.

3. In the absence of the small subunit HybO, HybA cannot be isolated in association with HybC. This is consistent with previous suggestions (Dubini et al. 2002) and with the isolation of only the HybCO complex lacking HybA from trypyin-treated membranes (Ballantine and Boxer 1986; Sargent et al. 1998).

4. While the small subunit of Hyd-1 and Hyd-2 remains stably associated with its respective large subunit and each enzyme retains activity after detergent solubilisation of the membrane and electrophoresis, the HycE-HycG complex apparently does not tolerate these conditions and this probably explains why Hyd-3 activity cannot be visualised after native-PAGE.

References:

Akagi JM, Campbell LL (1961) Studies on thermophilic sulfate-reducing bacteria. II. Hydrogenase activity of *Clostridium nigrificans*. J Bacteriol 82:927-932.

Ballantine SP, Boxer DH (1985) Nickel-containing hydrogenase isoenzymes from anaerobically grown *Escherichia coli* K-12. J Bacteriol 163:454–459.

Ballantine SP, Boxer DH (1986) Isolation and characterisation of a soluble active fragment of hydrogenase isoenzyme 2 from the membranes of anaerobically grown *Escherichia coli*. Eur J Biochem 156:277–284.

Begg YA, Whyte JN, Haddock BA (1977) The identification of mutants of *Escherichia coli* deficient in formate dehydrogenase and nitrate reductase activities using dye indicator plates. FEMS Microbiol Lett 2:47-50.

Blokesch M, Magalon A, Böck A (2001) Interplay between the specific chaperone-like proteins HybG and HypC in maturation of hydrogenases 1, 2, and 3 from *Escherichia coli*. J Bacteriol 183:2817–2822.

Böck A, King PW, Blokesch M, Posewitz MC (2006) Maturation of hydrogenases. Adv Microbiol Physiol 51:1-71.

Böhm R, Sauter M, Böck A (1990) Nucleotide sequence and expression of an operon in *Escherichia coli* coding for formate hydrogenlyase components. Mol Microbiol 4:231–243.

Casadaban M, Cohen SN (1979) Lactose genes fused to exogenous promoters in one step using Mu-*lac* bacteriophage: *in vivo* probe for transcriptional control sequences. Proc Natl Acad Sci USA 76:4530-4533.

Datsenko KA, Wanner BL (2000) One-step inactivation of chromosomal genes in *Escherichia coli* using PCR products. Proc Natl Acad Sci USA 97:6640-6645.

Dubini A, Pye RL, Jack RL, Palmer T, Sargent F (2002) How bacteria get energy from hydrogen: a genetic analysis of periplasmic hydrogen oxidation in *Escherichia coli*. Int J Hydr Energy 27:1413–1420.

Forzi L, Sawers RG (2007) Maturation of [NiFe]-hydrogenases in *Escherichia coli*. BioMetals 20:567-578.

Gitlitz PH, Krasna AI (1975) Structural and catalytic properties of hydrogenase from *Chromatium*. Biochemistry 14:2561-26568.

Hormann K, Andreesen JR (1994) Purification and characterization of a pyrrole-2-carboxylate oxygenase from *Arthrobacter* strain Py1. Biol Chem Hoppe Seyler 375:211–218.

Jones RW, Garland PB (1977) Sites and specificity of the reaction of bipyridylium compounds with anaerobic respiratory enzymes of *Escherichia coli*. Biochem J 164:199-211.

Kitagawa et al, (2005) Complete set of ORF clones of Escherichia coli ASKA library (a complete set of E. coli K-12 ORF archive): unique resources for biological research. DNA Res 12:291-299.

Laemmli UK (1970) Cleavage of structural proteins during the assembly of the head of bacteriophage T4. Nature 227:680-685.

Laurinavichene TV, Zorin NA, Tsygankov AA (2002) Effect of redox potential on activity of hydrogenase 1 and hydrogenase 2 in *Escherichia coli*. Arch Microbiol 178:437–442.

Lowry OH, Rosebrough NJ, Farr AL, Randall RJ (1951) Protein measurement with the Folin phenol reagent. J Biol Chem 193:265-275.

Magalon A, Böck A (2000) Dissection of the maturation reactions of the [NiFe] hydrogenase 3 from *Escherichia coli* taking place after nickel incorporation. FEBS Lett 473:254–258.

McTavish H, Sayavedra-Soto LA, Arp DJ (1995) Substitution of *Azotobacter vinelandii* hydrogenase small-subunit cysteines by serines can create insensitivity to inhibition by O_2 and preferentially damages H_2 oxidation over H_2 evolution. J Bacteriol 177:3960–3964.

Menon NK, Robbins J, Wendt JC, Shanmugam KT, Przybyla AE (1991) Mutational analysis and characterisation of the *Escherichia coli hya* operon, which encodes (NiFe) hydrogenase 1. J Bacteriol 173:4851–4861.

Menon NK, Chatelus CY, Dervartanian M, Wendt JC, Shanmugam KT, Peck Jr HD, Przybyla AE (1994) Cloning, sequencing, and mutational analysis of the *hyb* operon encoding *Escherichia coli* hydrogenase 2. J Bacteriol 176:4416–4423.

Miller JH (1972) Experiments in molecular genetics. Cold Spring Harbor Laboratory, Cold Spring Harbor, N.Y.

Paschos A, Bauer A, Zimmermann A, Zehelein E, Böck A (2002) HypF, a carbamoyl phosphate-converting enzyme involved in [NiFe] hydrogenase maturation. J Biol Chem 277:49945–49951.

Redwood MD, Mikheenko IP, Sargent F, Macaskie LE (2008) Dissecting the roles of *Escherichia coli* hydrogenases in biohydrogen production. FEMS Microbiol Lett 278:48-55.

Sambrook J, Fritsch EF, Maniatis T (1989) Molecular cloning: a Laboratory Manual, 2nd ed. Cold Spring Harbor Laboratory Press, Cold Spring Harbor, N.Y.

Sargent F, Ballantine SP, Rugman PA, Palmer T, Boxer DH (1998) Reassignment of the gene encoding the *Escherichia coli* hydrogenase 2 small subunit: Identification of a soluble precursor of the small subunit in a *hypB* mutant. Eur J Biochem 255:746-754.

Sauter M, Böhm R, Böck A (1992) Mutational analysis of the operon (*hyc*) determining hydrogenase 3 formation in *Escherichia coli*. Mol Microbiol 6:1523–1532.

Sawers G (1994) The hydrogenases and formate dehydrogenases of *Escherichia coli*. Antonie van Leeuwenhoek 66:57-88.

Sawers RG, Ballantine SP, Boxer DH (1985) Differential expression of hydrogenase isoenzymes in *Escherichia coli* K-12: Evidence for a third isoenzyme. J Bacteriol 164:1324–1331.

Sawers RG, Boxer DH (1986) Purification and properties of membrane-bound hydrogenase isoenzyme 1 from anaerobically grown *Escherichia coli* K12. Eur J Biochem 156:265–275.

Sayavedra-Soto LA, Arp DJ (1993) In *Azotobacter vinelandii* hydrogenase, substitution of serine for the cysteine residues at positions 62, 65, 289, and 292 in the small (HoxK) subunit affects H_2 oxidation. J Bacteriol 175:3414-3421.

Schubert T, Lenz O, Krause E, Volkmer R, Friedrich B (2007) Chaperones specific for the membrane-bound [NiFe]-hydrogenase interact with the Tat signal peptide of the small subunit precursor in *Ralstonia eutropha* H16. Mol Microbiol 66:453-67.

Shevchenko A, Tomas H, Havlis J, Olsen JV, Mann M (2006) In-gel digestion for mass spectrometric characterization of proteins and proteomes. Nature Protocols 1:2856-2860.

Soboh B, Krüger S, Kuhns M, Pinske C, Lehmann A, Sawers RG (2010) Development of a cell-free system reveals an oxygen-labile step in the maturation of [NiFe]-hydrogenase 2 of *Escherichia coli*. FEBS Lett 584:4109–4114.

Towbin H, Staehelin T, Gordon J (1979) Electrophoretic transfer of proteins from polyacrylamide gels to nitrocellulose sheets; procedure and some applications. Proc Natl Acad Sci USA 76:4350-4354.

Vignais PM, Billoud B (2007) Occurrence, classification, and biological function of hydrogenases: an overview. Chem Rev 107:4206–4272.

Volbeda A, Charon MH, Piras C, Hatchikian EC, Frey M, Fontecilla-Camps JC (1995) Crystal structure of the nickel-iron hydrogenase from *Desulfovibrio gigas*. Nature 373:580–587.

Winter G, Buhrke T, Lenz O, Jones AK, Forgber M, Friedrich B (2005) A model system for [NiFe] hydrogenase maturation studies: Purification of an active site-containing hydrogenase large subunit without small subunit. FEBS Lett 579: 4292–4296.

Table 1. Strains and plasmids used in this study

Strains/ plasmids	Genotype	Reference
MC4100	F$^-$ *araD139* D(*argF-lac*)*U169 ptsF25 deoC1 relA1 flbB5301 rspL150* $^-$	(Casadaban and Cohen 1979)
DHP-F2	MC4100 Δ*hypF* 59-629AA	(Paschos et al. 2002)
FTD147	Δ*hyaB*, Δ*hybC*, Δ*hycE*	(Redwood et al. 2008)
HDK100	MC4100 Δ*hya* (Kan^R)	M. Sauter (unpublished)
HDK200	MC4100 Δ*hyb* (Kan^R)	(Blokesch et al. 2001)
HDK203	MC4100 Δ*hyb* (Kan^R) Δ*hycA-H*	(Jacobi et al. 1992)
HDK103	MC4100 Δ*hya* (Kan^R) Δ*hycA-H*	(Jacobi et al. 1992)
CP734	MC4100 Δ*hyaB*, Δ*hybC*	This study
CP792	MC4100 Δ*hybC*, Δ*hycE*, Δ*hyaA*::Kan^R	This study
CP796	CP792 Δ*hyaA*	This study
CP793	MC4100 Δ*hyaB*, Δ*hycE*, Δ*hybO*::Kan^R	This study
CP795	CP793 Δ*hybO*	This study
CP1007	MC4100 Δ*hyaB*, Δ*hybC*, Δ*hycG*::Kan^R	This study
CP1005	MC4100 Δ*hyaB*, Δ*hybC*, Δ*hycE*::Kan^R	This study
Plasmids		
pASK-hyaB	*hyaB* cloned in BsaI site of pASK-IBA5+	This study
pASK-hybC	*hybC* cloned in BsaI site of pASK-IBA5+	This study
pASK-hycE	*hycE* cloned in BsaI site of pASK-IBA5+	This study
pCAN-hyaA	*hyaA* in pCA24N	Keio[a]
pCAN-hybO	*hybO* in pCA24N	Keio
pCAN-hycG	*hycG* in pCA24N	Keio

[a] Keio, see Kitagawa et al, 2005.

Table 2. Hydrogen-dependent benzyl viologen oxidoreductase enzyme activity of the complemented mutants.

Strain [a] and genotype	Specific activity [b] (μmol H_2 oxidized min^{-1} mg protein^{-1})
MC4100 (wild type)	3.38 (± 0.49)
DHP-F2 (Δ*hypF*)	<0.01
FTD147 (Δ*hyaB* Δ*hybC* Δ*hycE*)	<0.01
CP734 (Δ*hyaB* Δ*hybC*)	3.61 (± 0.18)
HDK203 (Δ*hyb* Δ*hycA-H*)	0.011 (± <0.001)
HDK103 (Δ*hya* Δ*hycA-H*)	0.21 (± 0.02)
FTD147 + pASK-hyaB	0.01 (± <0.001)
FTD147 + pASK-hybC	0.08 (± 0.02)
FTD147 + pASK-hycE	1.42 (± 0.6)
CP796 (Δ*hyaA* Δ*hybC* Δ*hycE*)	<0.01
CP796 + pCAN-hyaA	<0.01
CP795 (Δ*hyaB* Δ*hybO* Δ*hycE*)	<0.01
CP795 + pCAN-hybO	0.09 ((± 0.02)
CP1007 (Δ*hyaB* Δ*hybC* Δ*hycG*::Kan^R)	<0.01
CP1007 + pCAN-hycG	0.52 (± 0.1)

[a] Cell extracts were prepared from cells grown anaerobically in TGYEP.
[b] The mean and standard error of at least three independent experiments are shown.

Figure legends:
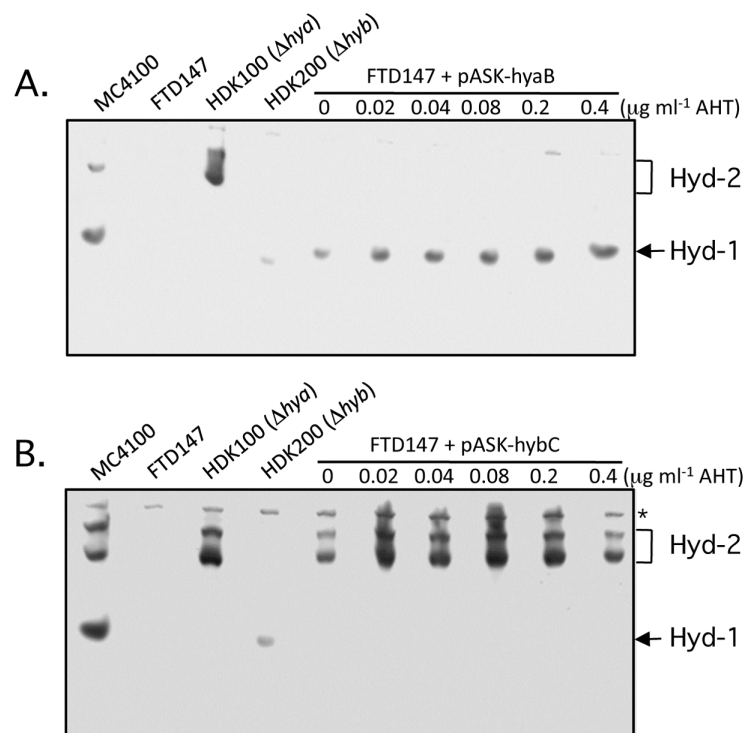
Figure 1. Strain FTD147 (Δ*hyaB* Δ*hybC* Δ*hycE*) can be complemented *in trans* by plasmid pASK-hyaB encoding Strep-tagged HyaB (A) and pASK-hybC encoding Strep-tagged HybC (B). Samples of crude extract (14 μg of protein) derived from each of the strains indicated were separated by native PAGE (7.5% (w/v) gel) under non-denaturing conditions and stained for hydrogenase activity as described in the Materials and Methods section. The stained bands corresponding to active Hyd-1 and Hyd-2 are indicated. The amount of anhydrotetracycline (AHT) used for induction of gene expression is indicated.
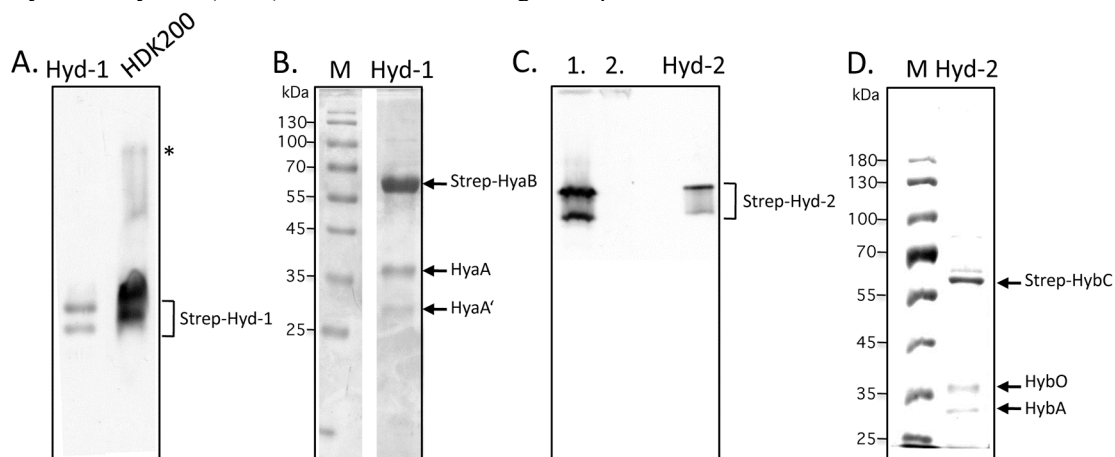
Figure 2. Strep-HyaB and Strep-HybC are isolated in complex with their respective small subunits and are enzymically active. Strep-tagged HyaB was purified from the detergent-solubilized membrane fraction of strain FTD147/ pASK-hyaB as described in the Materials and Methods and was analysed by native-PAGE (A.) and SDS-PAGE (B.). A. An aliquot (5 μg) of purified Strep-HyaB (lane labelled Hyd-1) was separated in native PAGE as described in the legend to Fig. 1 and stained for hydrogenase enzyme activity. For comparison an aliquot (15 μg of total protein) of a crude extract derived from HDK200 was applied to the gel and labelled Wt. B. Purified Strep-HyaB (10 μg protein; lane labelled Hyd-1) was separated by 10% SDS-PAGE and stained for protein with Coomassie Brilliant Blue. The locations of Strep-HyaB and HyaA polypeptides are indicated on the right side of the figure. The polypeptide labelled HyaA' is a proteolytic degradation product identified as HyaA by mass spectrometry. Molecular mass markers (M) are indicated in kDa. C. Native-PAGE analysis of purified Strep-HybC (5 μg protein) is shown. Aliquots of crude extracts (15 μg protein) preparations derived from

HDK100 (Δ*hya*) (lane 1) and FTD147 (Δ*hyaB* Δ*hybC* Δ*hycE*) (lane 2) were run in parallel as controls. D. Analysis of purified Strep-HybC (10 µg protein) by 10% SDS-PAGE identified Strep-HybC and the subunits HybO and HybA, the identities of which were confirmed by mass spectrometry. Molecular mass markers (M) are indicated in kDa. The asterisk represents a weak hydrogen-dependent BV reductase activity unrelated to the [NiFe]-hydrogenases.
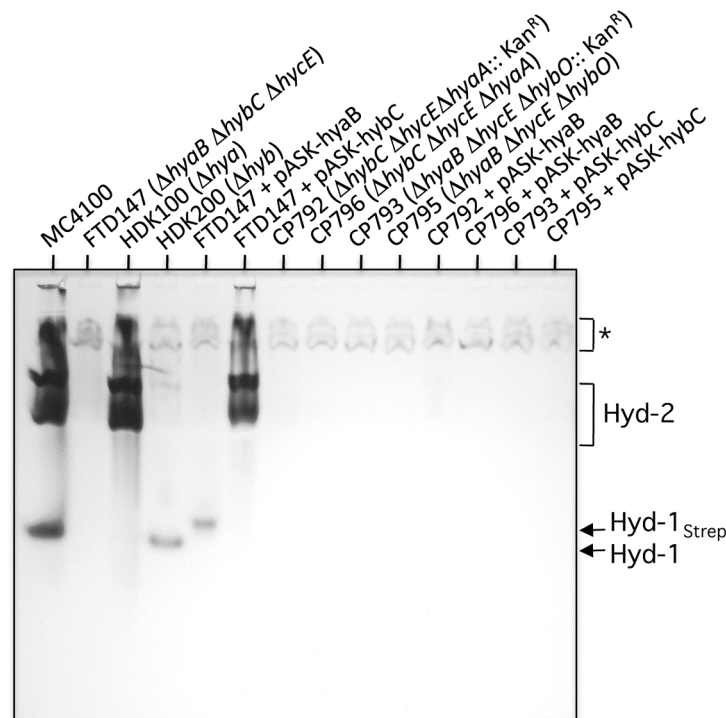
Figure 3. The small subunits of Hyd-1 and Hyd-2 are required for hydrogen-dependent BV reduction. A native PAGE analysis of crude extracts (15 µg protein) stained to reveal hydrogenase enzyme activity is shown. Lanes: MC4100 is wild type; FTD147 (Δ*hyaB* Δ*hybC* Δ*hycE*) is a negative control; HDK100 lacks Hyd-1 but retains Hyd-2 and Hyd-3; HDK200 lacks Hyd-2 but retains Hyd-1 and Hyd-3 activity; FTD147 + pASK-hyaB; FTD147 + pASK-hybC; CP792 (Δ*hybC*Δ*hycE* Δ*hyaA*::Kan[R]) carries a kanamycin-resistance cassette in the *hyaA* gene; in CP796 the kanamycin-resistance cassette was removed; CP793 (Δ*hyaB* Δ*hycE* Δ*hybO*::Kan[R]) carries a kanamycin-resistance cassette in the *hybO* gene; CP795 has the same genotype as CP793 but the kanamycin-resistance cassette has been removed from Δ*hybO*; CP792 containing pASK-hyaB CP796 containing pASK-hyaB; CP793 containing pASK-hybC CP795 containing pASK-hybC. The migration locations of Hyd-1, Hyd-2 and the Strep-HyaB-containing Hyd-1 (Hyd-1$_{Strep}$) are indicated. The asterisk represents a weak hydrogen-dependent BV reductase activity unrelated to the [NiFe]-hydrogenases.

Figure 4. Restoration of hydrogenase activity by transformation of the small subunit genes. Crude extracts (15 µg protein) of the strains shown were separated by native PAGE on 7.5% (w/v) polyacrylamide gels and subsequently stained for hydogenase enzyme activity. The gel in panel A shows extracts derived from MC4100 (wild type), CP734 (Δ*hyaB* Δ*hybC*), CP796 (Δ*hyaA* Δ*hybC* Δ*hycE*), CP796 transformed with pCAN-hyaA, encoding a His-tagged derivative of HyaA. The location of Hyd-1 in the gel is shown. The arrow in the top half of the gel signifies an active intermediate form of Hyd-1, designated Hyd-1', that is only observed when the small subunit HyaA carries an N-terminal His-tag. In panel B. a similar experiment was carried out for Hyd-2. The lanes include: CP795 (Δ*hyaB* Δ*hybO* Δ*hycE*); CP795 transformed with pCAN-hybO; CP734 (Δ*hyaB* Δ*hybC*) transformed with pASK-hybC; and CP795 transformed with pASK-hybC. The location of the Hyd-2 activity bands is defined by the bar and the asterisk indicates the location of the hydrogenase-independent, hydrogen-dependent BV reductase activity.

Figure 4

A. Lanes: MC4100, CP734 (ΔhyaBΔhybC), CP796 (ΔhyaAΔhyaBΔhybC), CP796 + pCAN-hyaA; arrows indicating Hyd-1' and Hyd-1

B. Lanes: CP795 (ΔhyaBΔhybOΔhycE), CP795 + pCAN-hybO, CP734 + pASK-hybC, CP795 + pASK-hybC; markings * and Hyd-2

A. Lanes: DHP-F2 (ΔhypF), MC4100, FTD147 (ΔhyaBΔhybCΔhycE), CP734 (ΔhyaBΔhybC), CP792 (ΔhybCΔhycE ΔhyaA::Kan^R), CP795 (ΔhybC ΔhycE ΔhyaA), CP793 (ΔhyaB ΔhycE ΔhybO)

unprocessed * / processed — Hyd-1
unprocessed * / processed — Hyd-2

B. kDa markers 180, 130, 100, 70, 55, 45, 35, 25; Lanes 1, 2; unprocessed/processed

Figure 5. The large subunits of both Hyd-1 (HyaB) and Hyd-2 (HybC) are processed in the absence of the small subunits. A. Western blots in which the large subunits of Hyd-1 and Hyd-2 in crude extracts (50 μg of protein) of different strains are shown. The positions of the unprocessed and processed forms of the polypeptides, indicating incorporation of the [NiFe] cofactor, are indicated on the left of the figure. Polypeptides were separated in 10% (w/v) SDS-PAGE and incubated with antibodies specific for the respective enzymes. The asterisks signify uncharacterised cross-reacting polypeptides. B. Strep-HybC (5 μg) purified from strain CP734 (ΔhyaB ΔhybO) as described in the Materials and Methods section was separated on 10% (w/v) SDS-PAGE and stained with Coomassie Brilliant Blue. Molecular mass markers (M) are indicated in kDa.

2.4.3 Zusätzliche Ergebnisse

Die Reinigung des aktiven FHL Komplexes ist eine Herausforderung für die Entwicklung enzymgestützter Wasserstoffbrennstoffzellen. Die Reinigungsstrategie von H_2-produzierenden Zellen mit einem *N*-terminalen Fusionstranskript an der großen Untereinheit HycE lieferte größtenteils nur inaktives Enzym (vgl. Abb. 11), welches nach dem gängigen Reifungsmodell nicht mit den übrigen FHL Komponenten assoziiert ist. Es konnte immunologisch eine Assoziation des Prä-Proteins mit den Hyp-Reifungsproteinen HypF, HypD und HypE nachgewiesen werden (nicht gezeigt), die Analyse ko-gereinigter Proteine mittels Massenspektrometrie ergab jedoch hauptsächlich eine Assoziation mit Chaperonen und Enzymen des anaeroben Stoffwechsels (Tabelle zu Abb. 11).
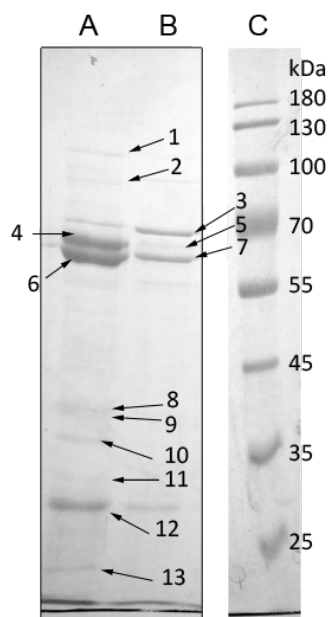
Abbildung 11: Reinigung von anaerob angezogenem His-HycE aus PM08 (Δ*pflA*) ohne Formiatzugabe. Der Stamm PM08 mit Plasmid-kodiertem HycE (ASKA Plasmid (Kitagawa *et al.*, 2005)) wurde anaerob in TGYEP, pH 6,5 angezogen und nach Erreichen der $OD_{600 nm}$ von 0,8 mit 250 μM IPTG induziert und anaerob bei 30 °C für weitere 3 h inkubiert. Die Reinigung erfolgte über eine 1 ml Nickel-NTA Säule und die Elution erfolgte mit 30 mM (Spur A) und 300 mM (Spur B) Imidazol im Puffer und Analyse im 10 % (w/v) SDS-Page. Spur C enthält den Marker PageRuler Prestained von Fermentas. Die markierten Banden wurden aus dem Gel ausgeschnitten und mittels Massenspektrometrie von der AG Sinz/ Christian Ihling analysiert. Korrespondierende Proteine mit ihrer jeweiligen prozentualen Abdeckung der Peptide durch die Massenspektrometrie und ihre berechneten molekularen Massen (kDa) sind unten angegeben. Die hier gewählten Anzuchtbedingungen liefern hauptsächlich unprozessiertes Polypeptid, Reinigungen aus MC4100 oder mit Zugabe von Formiat ergeben jedoch das gleiche Elutionsmuster.

	Abdeckung der Peptide	kDa	
Bande 1	39 %	96	AdhE - Alkoholdehydrogenase
	20 %	102	SecA - Protein Translokase
	13 %	112	FdoG - Fdh-O große Untereinheit (keine Tat-Signalpeptide)
	7 %	113	FdnG - Fdh-N große Untereinheit (keine Tat-Signalpeptide)
Bande 2	36 %	85	PflB - Pyruvat Formiat Lyase
Bande 3	51 %	67	GlmS- L-Glutamin:D-Fruktose-6-phosphat Aminotransferase
Bande 4	54 %	65	HycE - Peptid des unprozessierten *C*-Terminus identifiziert
Bande 5	46 %	65	HycE
Bande 6	69 %	57	GroL - Chaperon
Bande 7	50 %	57	GroL - Chaperon
Bande 8	42 %	40	OmpC - Porin C der äußeren Membran (keine Signalpeptide)
Bande 9	33 %	40	OmpC - Porin C der äußeren Membran (keine Signalpeptide)
	24 %	33	Rob - transkriptioneller Regulator
Bande 10	45 %	37	OmpA - Porin A der äußeren Membran
Bande 11	54 %	30	50S ribosomales Protein L2
Bande 12	61%	27	30S ribosomales Protein S2
	17 %	21	SlyD – Peptidyl-Prolyl *cis*/*trans* Isomerase
Bande 13	68 %	24	cAMP-Rezeptorprotein - transkriptioneller Regulator
	12 %	21	SlyD – Peptidyl-Prolyl *cis*/*trans* Isomerase

Die im Artikel bestimmten Hydrogenaseaktivitäten wurden als H_2 abhängige BV Reduktion bestimmt. Der eigentliche Anteil der H_2-Oxidation während des Wachstums geht daraus nicht hervor. Deshalb wurde weiterführend während des Wachstums die Wasserstoffmenge in der Gasphase einer anaeroben Kultur bestimmt und mit einer Mutante verglichen (CP734 – MC4100 $\Delta hyaB\ hybC$), die genetisch nicht befähigt ist H_2 zu oxidieren (Abb. 12). Es zeigte sich, dass es keinen Wachstumsunterschied zwischen den beiden Stämmen gibt und die H_2-Produktion genau wie die Aktivität der Hyd-1 und Hyd-2 im Nativen Gel bereits nach 3 h einsetzt, also nicht auf den Eintritt in die stationäre Phase angewiesen war. Des Weiteren wird jedoch aus der Differenz der Mengen des gebildeten H_2 zwischen den zwei Stämmen deutlich, dass etwa die Hälfte des vom FHL Komplex gebildeten H_2 wieder aufgenommen wurde und die resultierenden Elektronen vermutlich auf intern gebildetes Fumarat übertragen wurden.

A
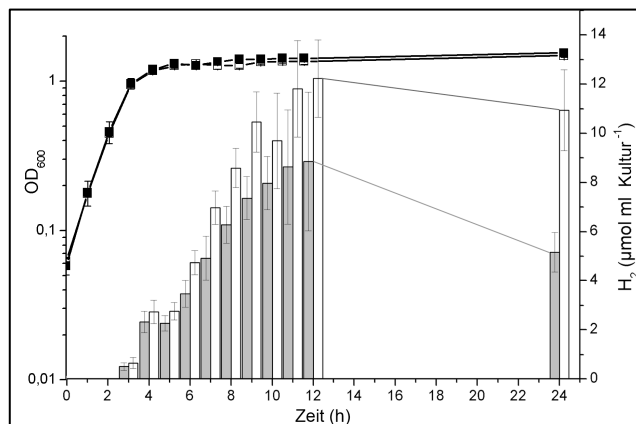
B
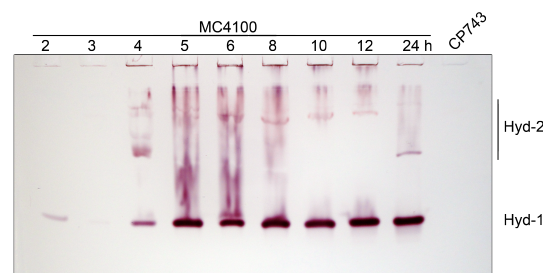
Abbildung 12: Wachstumskurve, H_2-Produktion und Aktivität der H_2-oxidierenden Enzyme. Die Stämme MC4100 **(gefüllte Symbole)** und CP743 ($\Delta hyaB\ hybC$) **(offene Symbole)** wurden als 10 ml Kulturen in 15 ml mit N_2 begasten Hungate Röhrchen angezogen. A: Zu den angegebenen Zeitintervallen wurde die $OD_{600\ nm}$ bestimmt (Kurve und linke Achse) und der H_2 in der Gasphase mittels Gaschromatographie gemessen und auf das Kulturvolumen berechnet (Balken und rechte Achse). B: Aus den gleichen Kulturen wurden zu den angegebenen Zeitintervallen Proben entnommen und 25 μg Protein auf ein 7,5 % (w/v) Natives-Page aufgetragen und die Aktivitäten von Hyd-1 und Hyd-2 angefärbt.

2.5 Enthüllung von Stoffwechseldefekten des biotechnologisch-bedeutsamen Modelbakteriums *Escherichia coli* **BL21(DE3).**

2.5.1 Zusammenfassung

Zur heterologen Überproduktion von Proteinen werden wegen der Deletion der *lon* und *ompT* Proteasen oftmals BL21(DE3) und dessen Derivate verwendet (Terpe, 2006). Dennoch sind diese Stämme keine gut charakterisierten K-12 Derivate, sondern B-Stämme, die durch ihre unterschiedliche Physiologie Komplikationen verursachen können. So war bisher zwar bekannt, dass BL21(DE3) keine Wasserstoffproduktion aufweist, jedoch der Grund war unbekannt. Durch die Genomsequenzierung 2009 wurde die Möglichkeit geschaffen den Stamm mit einer Kombination von bioinformatischen mit physiologischen Ansätzen zu untersuchen (Jeong *et al.*, 2009). Es wurden 78 Gensequenzen ausgewählt, deren Genprodukte direkt oder indirekt in die Reifung und Aktivität der [NiFe]-Hydrogenasen involviert sind. Von diesen wiesen 39 der abgeleiteten Proteinsequenzen insgesamt 74 Aminosäureaustausche im Vergleich zu MG1655, einem K-12 Stamm mit intakter Hydrogenase, auf. Weitere 6 Proteine konnten nicht funktionell exprimiert werden. Unter diesen stellte sich heraus, dass das für Fnr kodierende Gen ein internes Stopp-Codon an Codon-Position 141 enthält und damit der durch Fnr regulierte Nickel-Transporter nicht exprimiert wird. Durch Zugabe hoher Nickelmengen zum Medium konnte dieser Phänotyp supprimiert und die Aktivität der Hydrogenasen 1 und 2 wiederhergestellt werden. Durch Komplementation mit Plasmid-kodiertem Fnr konnte der gleiche Phänotyp hervorgerufen werden. Für die Expression des FHL Systems war jedoch zusätzlich zur Zugabe von Fnr noch die Supplementation mit Molybdationen (MoO_4^{2-}) erforderlich. Das *mod*-Operon mit den benachbarten Genen ist durch die Transduktion des DE3 Prophagen und angrenzender Bereiche aus einem Stamm, der als Gal$^-$ selektiert wurde, deletiert worden (Daegelen *et al.*, 2009). Es konnte gezeigt werden, dass für Restoration von 29 % FHL Aktivität in Anwesenheit von Fnr nicht der Regulator ModE, sondern hauptsächlich MoO_4^{2-} benötigt wurden und weitere Aktivitätssteigerung nur durch Zugabe von Formiat zum Medium erreicht werden konnte. Ebenso konnte die Abhängigkeit der Aktivität der Nitratreduktase von Fnr und MoO_4^{2-} belegt werden. Die Aktivitäten der Fdh-N und Fdh-H waren unter allen getesteten Bedingungen nicht zum Wildtypniveau wiederherstellbar, wobei jedoch ein Mangel dieser Aktivitäten durch Funktionsverlust der *sel*-Genprodukte nicht bestätigt werden konnte. Wahrscheinlich ist die Fdh-H Aktivität der limitierende Faktor für die Wiederherstellung voller FHL Aktivität.

2.5.2 Artikelkopie (weiterführende Online-Ergebnisse im Anhang 2)

PLoS one

Metabolic Deficiences Revealed in the Biotechnologically Important Model Bacterium *Escherichia coli* BL21(DE3)

Constanze Pinske[1], Markus Bönn[2], Sara Krüger[1], Ute Lindenstrauß[1], R. Gary Sawers[1]*

1 Institute for Microbiology, Martin-Luther University Halle-Wittenberg, Halle (Saale), Germany, 2 Institute of Computer Science, Martin-Luther University Halle-Wittenberg, Halle (Saale), Germany

Abstract

The *Escherichia coli* B strain BL21(DE3) has had a profound impact on biotechnology through its use in the production of recombinant proteins. Little is understood, however, regarding the physiology of this important *E. coli* strain. We show here that BL21(DE3) totally lacks activity of the four [NiFe]-hydrogenases, the three molybdenum- and selenium-containing formate dehydrogenases and molybdenum-dependent nitrate reductase. Nevertheless, all of the structural genes necessary for the synthesis of the respective anaerobic metalloenzymes are present in the genome. However, the genes encoding the high-affinity molybdate transport system and the molybdenum-responsive transcriptional regulator ModE are absent from the genome. Moreover, BL21(DE3) has a nonsense mutation in the gene encoding the global oxygen-responsive transcriptional regulator FNR. The activities of the two hydrogen-oxidizing hydrogenases, therefore, could be restored to BL21(DE3) by supplementing the growth medium with high concentrations of Ni^{2+} (Ni^{2+}-transport is FNR-dependent) or by introducing a wild-type copy of the *fnr* gene. Only combined addition of plasmid-encoded *fnr* and high concentrations of MoO_4^{2-} ions could restore hydrogen production to BL21(DE3); however, to only 25–30% of a K-12 wildtype. We could show that limited hydrogen production from the enzyme complex responsible for formate-dependent hydrogen evolution was due solely to reduced activity of the formate dehydrogenase (FDH-H), not the hydrogenase component. The activity of the FNR-dependent formate dehydrogenase, FDH-N, could not be restored, even when the *fnr* gene and MoO_4^{2-} were supplied; however, nitrate reductase activity could be recovered by combined addition of MoO_4^{2-} and the *fnr* gene. This suggested that a further component specific for biosynthesis or activity of formate dehydrogenases H and N was missing. Re-introduction of the gene encoding ModE could only partially restore the activities of both enzymes. Taken together these results demonstrate that BL21(DE3) has major defects in anaerobic metabolism, metal ion transport and metalloprotein biosynthesis.

Introduction

Escherichia coli is a facultative anaerobic enterobacterium that can grow both in the presence and in the absence of oxygen. When oxygen becomes limiting, *E. coli* can use nitrate or several alternative electron acceptors but if no exogenous electron acceptors are present it can resort to fermentation [1]. One of the key players in activating anaerobic gene expression is the global transcriptional regulator FNR (<u>f</u>umarate-<u>n</u>itrate <u>r</u>egulator). FNR regulates, directly or indirectly, the expression of a very large number of genes and operons [2] whose products ensure that the optimal electron acceptor is utilized to allow maximum energy conservation. Many of the genes whose expression is induced by FNR encode complex metalloproteins, which have different metal cofactors in their active sites. Biosynthesis of these metal cofactors often requires the concerted action of a large number of accessory proteins. During nitrate respiration, for example, the FNR- and nitrate-dependent formate dehydrogenase (FDH) N and nitrate reductase (NAR) respiratory pathway is induced. Both enzymes have an array of iron-sulfur cluster, as well as the bis-molybdopterin guanidine dinucleotide (bis-MGD) cofactor [3].

Additionally, FDH-N requires co-translational insertion of seleno-cysteine in the polypeptide chain [4]. On the other hand, during fermentative growth *E. coli* has an active hydrogen metabolism and each of the three hydrogenases synthesized under these conditions has a [NiFe] cofactor. This cofactor must also be carefully assembled and inserted into the apo-enzyme [5]. Metals such as molybdenum and nickel must also be transported into the cell to allow synthesis of the appropriate metalloenzymes to occur. FNR exerts global control over many aspects of metalloprotein biosynthesis in *E. coli* and this is summarized in Fig. 1.

Hydrogenases catalyze the reversible oxidation of hydrogen and *E. coli* encodes four [NiFe]-hydrogenases (Hyd) in its genome, only three of which have been characterized [5]. All three enzymes are membrane-associated. Hyd-1 and Hyd-2 have their active site oriented toward the periplasm. Both enzymes contribute to generation of a proton gradient by oxidizing hydrogen on the periplasmic side of the cytoplasmic membrane and delivering the electrons from hydrogen oxidation directly into the respiratory chain. Hyd-3, together with the second molybdoselenoenzyme FDH-H, forms the hydrogen-evolving formate hydrogenlyase (FHL) complex, which has its active site localized towards the
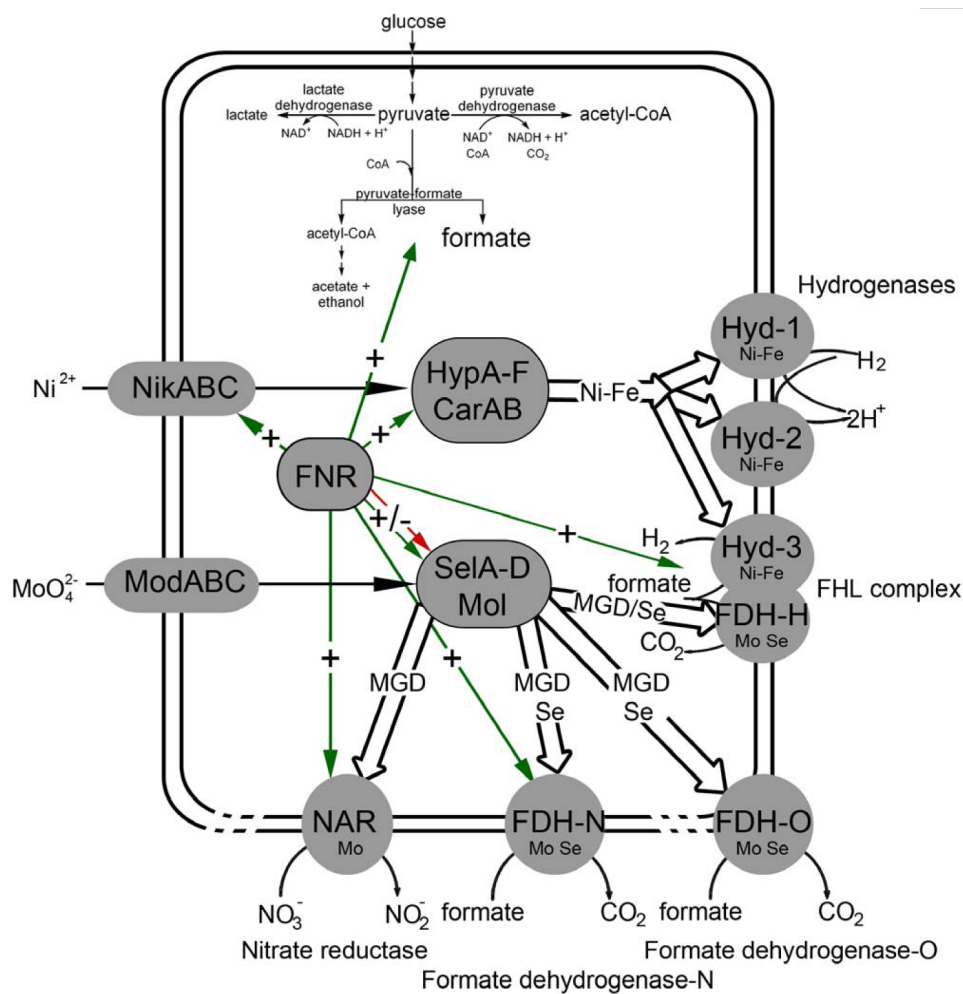
Figure 1. An overview of anaerobic hydrogen metabolism and nitrate respiration metabolism in *E. coli*. The metabolism of pyruvate under anaerobic conditions is shown in the upper portion of the Figure. The cellular locations of the three main [NiFe]-hydrogenases, the three molybdoselenium formate dehydrogenases and the principle nitrate reductase are shown, as are the transport systems for nickel and molybdate. The metal ion requirement and regulation with respect to the global regulator FNR are also indicated by arrows.
doi:10.1371/journal.pone.0022830.g001

cytoplasm [6]. The substrate of the FHL complex is formate, which is generated during fermentation of sugar substrates such as glucose by the anaerobically inducible pyruvate formate-lyase (PflB) [1]. Formate is disproportionated into carbon dioxide and hydrogen by the FHL complex, thus off-setting acidification of the cytoplasm during fermentation.

The [NiFe]-cofactor in K-12 strains of *E. coli* such as MC4100 or MG1655 is common to all three hydrogenase enzymes. Thus, the majority of the accessory enzymes, referred to as Hyp proteins, required to synthesize this cofactor govern the biosynthesis of each hydrogenase [5,7]. The Hyp proteins are involved in the synthesis of the non-proteinogenic ligands cyanide (CN^-) and carbon monoxide (CO), which are coordinated to the iron atom in the [NiFe]-cofactor (for a review see [7]). The two CN^- ligands are derived from carbamoylphosphate (CP) [8,9] while the source of the CO ligand is unclear. After synthesis and insertion of the modified iron atom into the large subunit precursor, nickel is then inserted through the action of HypA, HypB and SlyD [10]. The nickel required for biosynthesis of the active site is delivered by a specific ATP-binding cassette (ABC) transporter encoded by the FNR-regulated *nik* operon [11]. Lesions in the genes encoding the

HypA and HypB enzymes, the nickel transporter, or indeed the global oxygen-responsive transcriptional regulator FNR can be phenotypically complemented by the addition of excess nickel ions to the medium [12].

Together with FDH-H, which is encoded by the *fdhF* gene [13], and FDH-N there is a third molybdenum- and selenium-containing formate dehydrogenase in *E. coli*, which is referred to as FDH-O (for a review see [14]). FDH-O is synthesized at low levels, preferentially in the presence of oxygen or nitrate [4,15,16]. Selenocysteine insertion in all three FDH enzymes occurs co-translationally with a sequence of reactions requiring the SelA, SelB and SelD proteins together with a specific tRNA^{Sec} encoded by *selC* [17]. Post-translational insertion of molybdenum in the form of the bis-molybdopterin guanidine dinucleotide (bis-MGD) cofactor [18] into the active site is also required for the activity of all three FDHs, and consequently hydrogen-evolving FHL complex activity.

While hydrogenase research in *E. coli* has focused on K-12 strains, comparatively little is known about hydrogen metabolism of B strains of *E. coli*. Research in the 1940's by Delbrück focused on *E. coli* B strains to study T phage function [19]. The commonly

used BL21(DE3) strain was derived from an early isolate of *E. coli* B and was developed for T7 RNA polymerase-based gene expression after early isolation of a derivative carrying the DE3 prophage in its lambda attachment site [20,21]. The DE3 prophage was introduced by P1 transduction from strain Bc258 and this was isolated as a non-reverting Gal⁻ derivative of Bc251, which had been obtained by UV treatment [22]. This UV treatment resulted in the loss of some genes important to metalloprotein biosynthesis, as described in this study.

Meanwhile BL21(DE3) has become established worldwide as a host for recombinant protein over-production. Despite this fact, it is surprising to note that the biology of BL21(DE3) is poorly characterized. Clearly, the strain does not have a wildtype phenotype because it has been shown that BL21(DE3) is unable to produce hydrogen gas [23], and indeed completely lacks hydrogenase activity, which we demonstrate in this study. This is despite BL21(DE3) having an apparently full complement of hydrogenase structural genes in its genome [24]. The genetic and metabolic reasons underlying this lack of hydrogen production are unclear. Here we demonstrate that the reasons for this metabolic deficiency of BL21(DE3) result from a lack of the global oxygen-responsive transcription factor FNR [11,12,25,26], as well as severe deficiences in metalloprotein biosynthesis. This means that not only hydrogen metabolism but also nitrate respiration is compromised in the strain. These features have important implications for the use of BL21(DE3) and its derivatives in recombinant protein production, particularly for proteins of unknown function.

Results

BL21(DE3) is devoid of hydrogen metabolism

Only three of the four [NiFe]-hydrogenases (Hyd-1, Hyd-2 and Hyd-3) in *E. coli* K-12 strains are synthesized under standard laboratory conditions [6,27]. Total hydrogenase enzyme activity in K-12 wildtype strains such as MC4100 or BW25113 can be readily determined by measuring hydrogen-dependent reduction of the artificial electron acceptor benzyl viologen (BV) [6,27]. After anaerobic growth in buffered rich medium with glucose (TGYEP, pH 6.5) crude extracts derived from either strain had a total hydrogenase specific activity in the range of 3 U mg of protein⁻¹ (Table 1). A crude extract derived from strain DHP-F2 (Δ*hypF*), which is unable to synthesize the HypF carbamoyltransferase essential for biosynthesis of the [NiFe]-cofactor of all three enzymes [28], lacked hydrogenase activity. Extracts of BL21(DE3) grown anaerobically in TGYEP were also devoid of hydrogen-dependent BV oxidoreductase activity (Table 1).

The activity of the FHL complex can be determined in whole cells by measuring hydrogen evolution [29]. While the FHL activity of MC4100 after fermentative growth with glucose attained levels of 28 mU mg of protein⁻¹, BL21(DE3) failed to show any FHL activity, even after supplementation of the growth medium with formate, which is obligately required for the induction of the FHL complex [30]. DHP-F2 (Δ*hypF*) also lacked FHL activity, as anticipated and provided a negative control (Table 1).

Bioinformatic analysis of the genes associated with hydrogen metabolism in the genome of BL21(DE3)

Initially, a total of 86 candidate genes that are known to have either a direct or indirect influence on hydrogenase activity in *E. coli* MC4100 or its sequenced counterpart MG1655 were chosen for comparison with the corresponding gene products in BL21(DE3). The deduced amino acid sequences of all 86 genes were examined to identify amino acid exchanges or deletions.

Silent mutations that did not alter the amino acid sequence were ignored. Of the 86 candidate proteins examined with direct relevance to hydrogen metabolism only 42 proteins exhibited altogether 78 amino acid exchanges (missense mutations in the corresponding genes) and in 5 instances the corresponding genes were missing from the genome of BL21(DE3) completely (Table S1). Of this total carrying amino acid exchanges (or a nonsense mutation in the case of *fnr*), CarB, HypF, FNR, NikA, NikE, and NikD are the only putative candidates that could have a pleiotropic effect on hydrogenase activity resulting in a hydrogenase-negative phenotype.

The activities of Hyd-1 and Hyd-2 in BL21(DE3) can be restored by nickel ion supplementation

The *nik* operon codes for a specific ATP-binding cassette (ABC) transporter comprising a periplasmic binding protein NikA, the membrane components NikB and NikC, as well as the ATP-binding components NikD and NikE [31]. Defects in nickel-ion transport or HypA and HypB function, which are required for active hydrogenase biosynthesis can be phenotypically suppressed by addition of high concentrations of nickel ions to the growth medium [11,32,33] whereby non-specific Ni²⁺ ion uptake is mediated by the magnesium transport system [34]. The membrane components NikB and NikC showed no amino acid exchanges in BL21(DE3) compared to MG1655; however, the periplasmic binding protein NikA, as well as the ATP-binding components NikD and NikE had amino acid exchanges, with NikE having alterations in a total of six amino acids (see Table S1). In order to test first of all whether addition of high concentrations of Ni²⁺ ions to the growth medium could restore hydrogenase activity to BL21(DE3) we analysed hydrogen-dependent BV reduction (henceforth referred to as total hydrogenase activity) in crude extracts derived from BL21(DE3) grown anaerobically in the presence of 0.5 mM NiCl₂. Only very low total hydrogenase activity could be determined and no hydrogen-evolving FHL activity could be measured (Table 1). Analysis of the activities of Hyd-1 and Hyd-2 after non-denaturing gel-electrophoretic separation of proteins in crude extracts of BL21(DE3) grown in the presence or absence of 0.5 mM NiCl₂ (Fig. 2) revealed that while no activity could be visualised in BL21(DE3) grown without Ni²⁺ ion supplementation, addition of Ni²⁺ restored weak activities corresponding to Hyd-1 and Hyd-2; addition of formate, which was previously observed to result in increased Hyd-1 activity [6], had no effect on the activity band pattern (Fig. 2). This result suggested that nickel transport was indeed affected in BL21(DE3); however, addition of nickel at high concentrations could circumvent this phenotypic defect only partially.

To determine whether the mutations in *nikA*, *nikD* or *nikE* were responsible for the phenotypic defect in Ni²⁺, plasmids pJW3441, pJW3444 and pJW3445 (Keio collection; [35]), encoding NikA, NikD and NikE, respectively, were transformed into BL21(DE3) and total hydrogenase enzyme activity in crude extracts was determined (data not shown). None of the plasmids could restore hydrogenase activity, nor could activity bands corresponding to Hyd-1 or Hyd-2 be detected after native-PAGE (data not shown). It could be shown in complementation studies using the corresponding specific in-frame knockout mutants of *nikA*, *nikD* and *nikE* in the MG1655 derivative BW25113 (Keio collection; [35]) that their phenotype was hydrogenase-negative, that addition of 0.5 mM NiCl₂ could restore hydrogenase activity to each mutant and that introduction of the respective plasmids encoding the *nikA*, *nikD* or *nikE* genes restored functional Hyd-1 and Hyd-2 either totally or partially (Fig. S1). This result demonstrates that

Table 1. Total Hydrogenase, hydrogen evolving formate hydrogen lyase activity and formate dehydrogenase-H (FDH-H).

Strain/Condition[1]	Specific Hydrogenase Activity in U mg protein^{-1} ± SD	Specific Hydrogen evolving Activity in mU mg protein^{-1} ± SD	Specific FDH-H Activity in U mg protein^{-1} ± SD
MC4100	3.01±0.59	28±20	0.42±0.08
CP971 (ΔhycAl)	0.14±0.08	<0.01	<0.01
CP971 (ΔhycAl)/p31hycA-I	8.12±0.40	19±1	0.05±0.01
DHP-F2 (ΔhypF)	<0.01	<0.01	0.04±0.01
BL21(DE3)	0.02±0.01 (0.004±0.003)	0.7±0.1 (<0.01)	<0.01 (<0.01)
BL21(DE3)/500 µM NiCl$_2$	0.01±0.002	<0.01	<0.01
BL21(DE3)/15 mM formate	<0.01	<0.01	<0.01
BL21(DE3)/500 µM NiCl$_2$/15 mM formate	0.01±0.01 (0.02±0.01)	<0.01 (3±2)	<0.01 (<0.01)
BL21(DE3)/pCH21 (fnr$^+$)	0.05±0.02 (2.22±0.44)	0.2±0.1 (8±3)	<0.01 (0.04±0.02)
BL21(DE3)/p1fnr	0.04±0.003 (2.84±0.69)	0.8±0.8 (7±2)	<0.01 (0.07±0.01)
BL21(DE3)/p10fnr	0.03±0.02 (0.02±0.01)	0.1±0.1 (0.3±0.3)	<0.01 (<0.01)
BL21(DE3)/p13fnr	0.03±0.02 (0.03±0.02)	<0.01 (0.6±1)	<0.01 (<0.01)
BL21(DE3)/p31hycA-I	<0.01	0.6±0.4	<0.01
BL21(DE3)/p31hycA-I/p1fnr	n. d.[2]	(2±0.5)	n. d.
BL21(DE3)/p7modE	0.02±0.01 (0.05±0.003)	<0.01 (0.5±0.6)	<0.01 (<0.01)
BL21(DE3)/p7modE/500 µM NiCl$_2$/15 mM formate	0.01±0.003	<0.01	<0.01
BL21(DE3)/p7modE/p13fnr	0.03±0.003 (1.16±0.66)	<0.01 (6±2)	<0.01 (0.03±0.03)
BL21(DE3)/p7modE/p13fnr/500 µM NiCl$_2$/15 mM formate	(3.71±1.92)	(15±3)	(0.08±0.01)
PB1000	0.13±0.21	5±3	<0.01
PB1000/500 µM NiCl$_2$/15 mM formate	2.70±1.06	16±11	0.03±0.03
PB1000/pCH21	5.44±1.73	20±11	0.12±0.01
PB1000/p1fnr	6.16±1.30	34±6	0.50±0.06
PB1000/p10fnr	0.29±0.16	12±5	<0.01
PB1000/p13fnr	2.15±1.04 (2.59±1.20)	26±8 (21±2)	0.11±0.10 (0.10±0.04)

[1]Cells were grown in TGYEP pH 6.5. Values in parenthesis were obtained when cells were grown in the presence of 1 mM sodium molybdate.
[2]n. d. – not determined.
doi:10.1371/journal.pone.0022830.t001

the amino acid exchanges alone were not responsible for the defective nickel transport phenotype.

Despite missense mutations in the respective genes carbamoylphosphate synthetase and HypF are functional in BL21(DE3)

CarB is the large subunit of the carbamoylphosphate synthetase providing carbamoylphosphate as the substrate for the cyanide ligand in the hydrogenase large subunits [36]. A defect in CarB function can be phenotypically suppressed by the addition of citrulline to the medium [36]. Although addition of citrulline did not restore hydrogenase activity to BL21(DE3) (Fig. 2), the fact that Ni^{2+} supplementation could partially restore hydrogenase function indicated that carbamoylphosphate synthetase must be functional in the bacterium and thus the two amino acid exchanges in CarB did not prevent enzyme function. Moreover, although addition of the hypF gene from MC4100 [37] did not restore active Hyd-1 or Hyd-2 (Fig. 2), by the same argument as brought above, the HypF of BL21(DE3) must nevertheless be functional.

HypF of BL21(DE3) shows 5 amino acid exchanges compared to MG1655 and 4 of these are also found in the HypF protein of E. coli O157:H7 (R51L/Y62H/K214N/S565P); however this protein retains its function [38]. As Hyd-1 and Hyd-2 activities can be restored in BL21(DE3) through supplementation of nickel ions

without further addition of plasmid-encoded HypF it can be assumed that the 5th amino acid exchange (D258E) has no influence on Hyd activities.

The ability to recover Hyd-2 enzyme activity by adding Ni^{2+} (see above) also obviated the missense mutations in the hybD and hybF genes (Table S1) as possible reasons why Hyd-2 was inactive in BL21(DE3). This was further confirmed by the fact that introduction of these genes from MG1655 failed to restore Hyd-2 activity to BL21(DE3) extracts (data not shown).

BL21(DE3) is a fnr mutant

Expression of the nik operon is dependent on the global transcriptional regulator FNR [12]. Furthermore, FNR also positively regulates the expression of the hyp operon [39,40]. Analysis of the DNA sequence of the fnr gene in BL21(DE3) revealed a nonsense mutation (C→T transition) at codon 141, which resulted in an amber (UAG) stop codon [21]. Notably, many E. coli B strains carry this mutation [21,24]. Western blot analysis of a crude extract derived from BL21(DE3) confirmed that full length FNR could not be detected (Fig. 3A).

We isolated a spontaneous fnr mutant (PB1000, Table 1) of MC4100 that carried a 3550 bp deletion from insH-4 to the fnr gene and analysed the hydrogenase activity of this mutant. Total hydrogenase activity in extracts of PB1000 was reduced by >95% compared with the wildtype MC4100, FHL activity was reduced
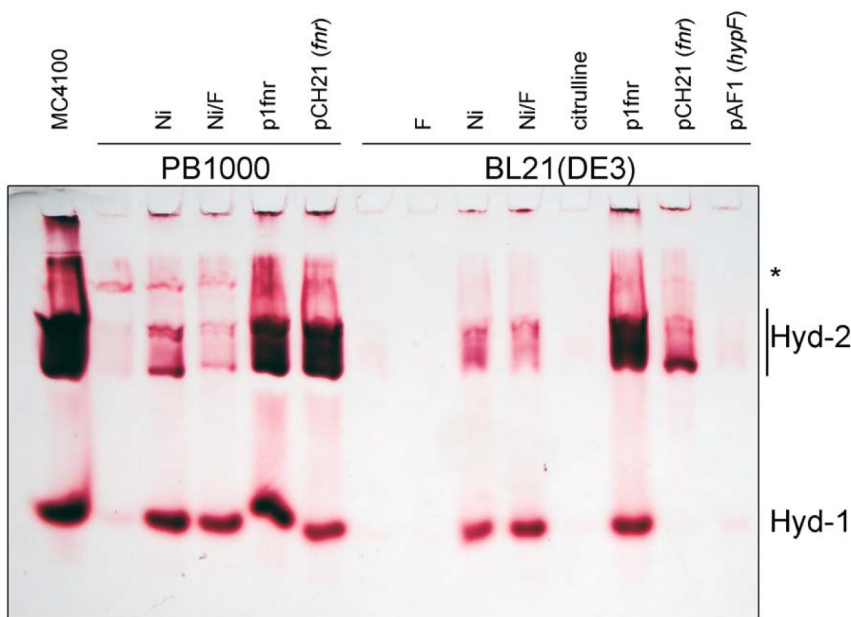
Figure 2. Hydrogenase 1 and 2 activity-staining after native-PAGE. Aliquots (25 µg of protein) of crude extracts derived from MC4100 (wild type), PB1000 (Δfnr) and BL21(DE3) after anaerobic growth in TGYEP with or without supplementation of 500 µM nickel(II)-chloride (Ni), 15 mM formate (F) or 0.3 mM citrulline addition of plasmid-coded fnr (p1fnr, pCH21) and hypF (pAF1) were applied to 7.5% (w/v) native-PAGE. On the right hand the migration positions of Hyd-1 and Hyd-2 are given. The band designated with an asterisk is due to a side-reaction of FDH-O/FDH-N and this activity is hydrogenase-independent.
doi:10.1371/journal.pone.0022830.g002
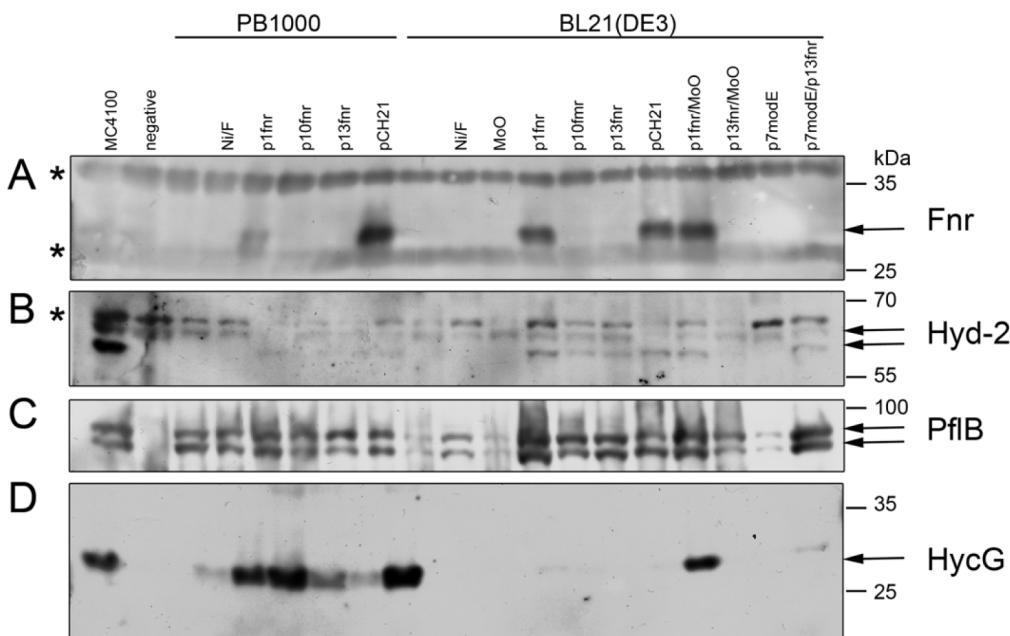
Figure 3. Western blot analysis of anaerobic enzymes in BL21(DE3). 25 µg Polypeptides in crude extracts derived from MC4100, PB1000 (Δfnr), BL21(DE3) with and without supplementation of 500 µM nickel(II)-chloride (Ni), 15 mM formate (F), 1 mM sodium-molybdate (MoO) or addition of plasmid encoded fnr (p1fnr, p10fnr, p13fnr, pCH21) and modE (p7modE) after anaerobic growth in TGYEP, pH 6.5 were separated by 10% (w/v) SDS-PAGE and transferred to nitrocellulose membranes. The samples were treated with antiserum raised against **A:** FNR, **B:** Hyd-2 (the upper arrows represents precursor and the lower arrow mature form of the Hyd-2 large subunit), **C:** PflB (the arrows mark the two different migrating forms typical for active protein after contact with oxygen), **D:** HycG (the Hyd-3 small subunit). The lane indicating the negative control contains PB1000 (Δfnr), DHP-F2 (ΔhypF), RM220 (ΔpflAB) and CP971 (ΔhycAI), from top to bottom, respectively. The asterisks signify unidentified cross-reacting species. On the right hand are given the sizes of the respective molecular mass marker (Prestained PageRuler, Fermentas).
doi:10.1371/journal.pone.0022830.g003

by 80% (Table 1) and the activity bands corresponding to Hyd-1 and Hyd-2 were barely detectable (Fig. 2). Introduction of the *fnr* gene on plasmid p1fnr into PB1000 restored total hydrogenase and FHL activities to wild type levels (Table 1). Transformation of BL21(DE3) with p1fnr resulted in a total hydrogenase specific activity of only 0.04 U mg^{-1} (compared with 3 U mg^{-1} for MC4100), while FHL activity was not restored at all by the plasmid. Although total hydrogenase activity was low, this activity nevertheless clearly represented fully active Hyd-1 and Hyd-2 under these growth conditions because activity-stained gels revealed active Hyd-1 and Hyd-2, which were restored to levels similar to those observed in K-12 wild type levels by p1fnr (Fig. 2). Because a *nik* operon mutation cannot be complemented by expression of the *fnr* gene [12] this allowed us to conclude that the missense mutations in the *nikA*, *nikD* and *nikE* genes of BL21(DE3) do not affect the function of the respective gene products.

The *fnr* gene on plasmid pCH21 is derived from MG1655 and includes the complete *fnr* regulatory region [41], while the *fnr* gene in p1fnr has a foreshortened and incomplete regulatory region with the consequence that there is 3 to 4-fold less FNR protein in MC4100 compared with MG1655 [42]. Transformation of BL21(DE3) with pCH21 also failed to restore hydrogen gas production or high level hydrogenase activity to the strain (Table 1). Surprisingly, however, although Hyd-2 enzyme activity could be visualised in crude extracts of BL21(DE3) transformed with pCH21 (Fig. 2), Hyd-1 was absent. Transformation of PB1000 with the same pCH21 restored total hydrogenase activity to wild type levels (Table 1 and Fig. 2). To ensure that plasmid-encoded FNR was synthesized in BL21(DE3), crude extracts of the transformed strain were analysed by Western blotting using anti-FNR antibodies. Plasmids p1fnr and pCH21 both resulted in high-level overproduction of the FNR protein (Fig. 3A). It was noted that the BL21(DE3) cells carrying pCH21 grew more slowly ($\mu = 0.56$ h^{-1}) than the plasmid-free strain, or BL21(DE3) transformed with pBR322 ($\mu = 0.77$ h^{-1}). In contrast, PB1000 ($\mu = 0.57$ h^{-1}) grew better when transformed with pCH21 ($\mu = 0.72$ h^{-1}). This might suggest that, because Hyd-1 synthesis is optimal in the stationary phase [43,44], lack of induction of *hya* operon expression might account for this discrepancy.

Plasmids that had lower expression of the *fnr* gene compared with p1fnr or pCH21 were analysed to determine if too much FNR had a deleterious effect on expression of particular hydrogenase-related genes. The *fnr* gene from MC4100 was cloned without its regulatory region into a medium-copy vector (pBluescript SK+), delivering p10fnr, or into a low-copy vector (pACYC184), delivering p13fnr. The level of FNR protein synthesized in BL21(DE3) transformed with these two plasmids was similar to the wild type MC4100 or slightly less in the case of p13fnr (Fig. 3A). Total hydrogenase activity in the BL21(DE3) strain transformed with either of these plasmids was also very low and had a similar level of activity as observed with p1fnr or pCH21 (Table 1). Hyd-1 and Hyd-2 were barely detectable after activity-staining following native PAGE (data not shown). Thus, something else was limiting biosynthesis of active hydrogenases in BL21(DE3) and the effect was not caused by over-expression of *fnr*.

The presence of mature, processed large subunits of the hydrogenases can be used as an indicator as to whether the [NiFe]-cofactor maturation machinery is functional [7]. As expression of the *hyp* operon is FNR-dependent [39], we examined by Western blot analysis with antibodies raised against Hyd-2 whether transformation of BL21(DE3) with all four plasmids encoding FNR restored processing of the Hyd-2 large subunit precursor to the strain (Fig. 3B). The result confirmed that the *fnr* genes encoded on p10fnr and p13fnr were expressed and that the

amount of FNR clearly did not limit Hyp protein synthesis or hydrogenase maturation activity because BL21(DE3) transformed with each plasmid showed clear processing of the Hyd-2 large subunit precursor.

Lack of FNR and nickel transport does not explain why BL21(DE3) is devoid of FHL complex activity

The total hydrogenase activity in MC4100 grown under glucose fermentation conditions is 3.0 U mg^{-1}, with the bulk of this activity being due to Hyd-3 activity, as can be seen from the activity in extracts of the $\Delta hycAI$ mutant, CP971, which has an activity of 0.14 U mg^{-1} (Table 1). Hyd-2 activity contributes less than 5% to the total hydrogenase activity and Hyd-1 activity contributes below 1% to the total under these conditions. This suggests that in BL21(DE3) only partial Hyd-1 and Hyd-2 activities were restored in the presence of *fnr* plasmids and Hyd-3 was inactive.

Exogenously added formate and nickel can phenotypically suppress the effect of *fnr* mutations on Hyd-3 and consequently FHL activity [6]. This is because FNR regulates PflB synthesis and consequently in a *fnr* mutant intracellular formate levels are reduced [45]. Western blot analysis of PflB levels in extracts of BL21(DE3) revealed that the protein was significantly reduced (Fig. 3C). Exogenous formate increased the level of PflB in the cell extracts and this is presumably due to build up of pyruvate, which induces *focApflB* operon expression [46]. All four plasmids encoding FNR also restored high-level PflB synthesis to BL21(DE3) (Fig. 3C).

Hydrogen gas production and total hydrogenase activity could be restored to near wild-type levels in PB1000 (Δfnr) by supplementation of formate and Ni^{2+} to the growth medium (Table 1). In contrast, however, formate and Ni^{2+} supplementation alone could not restore Hyd-3 or FHL activity to BL21(DE3) (Table 1). Taken together, these findings indicate that, although BL21(DE3) has reduced levels of intracellular formate due to reduced PflB synthesis, this is not the only reason why an active FHL complex could not be synthesized.

Five of the *hyc* genes carry missense mutations (Table S1). To rule out that these limit Hyd-3 activity we cloned the complete *hyc* operon from the genome of MC4100 and introduced this on plasmid p31hycA-I into BL21(DE3) and determined total hydrogenase and FHL activities (Table 1). Although p31hycA-I complemented the $\Delta hycA-I$ mutation in CP971, when transformed into BL21(DE3) the plasmid failed to restore either Hyd-3 activity or hydrogen gas production (Table 1). Indeed, simultaneously introducing the *fnr* gene on p1fnr also failed to restore either activity. This result indicates that something else limits development of both FHL and Hyd-3 activity in BL21(DE3).

Molybdenum uptake and metabolism are compromised in BL21(DE3)

As well as the requirement of [NiFe]-cofactor biosynthesis for hydrogen evolution there is also a necessity for co-translational selenocysteine incorporation and molybdenum cofactor biosynthesis for the FDH-H component of the FHL complex [47]. Further, the FdhD and FdhE proteins have been proposed to have chaperone-like functions and they are required for generation of functional FDH in *E. coli* [48].

Examination of the genome of BL21(DE3) revealed that five genes (*modABC*, *modE* and *modF*) are absent. The DE3 prophage insertion site is located directly in the region of the *mod* genes and it has been proposed that the deletion is due to an UV treatment in another strain and subsequent recombinant transfer by P1

transduction [21]. The ModABC proteins form the basis of the ABC transport system for the molybdate anion, while ModE is a molybdenum-responsive transcriptional regulator that represses expression of the *modABC* operon and activates expression of genes and operons whose products are either components of molyb-doenzymes or are functional together with molybdoenzymes [49].

Initial experiments were conducted in which excess molybdate was added to cultures, whereby the molybdate anion can be taken up non-specifically by the sulphate transport system [50]. Molybdate had no effect on total hydrogenase activity when added alone or in combination with nickel and formate (Table 1). Total hydrogenase activity was, however, restored to levels approximating those of wild type K-12 strains when molybdate was added to BL21(DE3) transformed with pCH21 or p1fnr. These same cells also produced hydrogen at a level approximately 25% of the K-12 wildtype (Table 1).

Western Blot analyses revealed that although low amounts of HycG, the small subunit of Hyd-3, were detected in extracts of BL21(DE3) without addition of metal ions, HycG levels were significantly increased in BL21(DE3) transformed with p1fnr, but only when 1 mM molybdate was included in the growth medium (Fig. 3D).

Activity of the molybdenum cofactor-dependent FDH-H enzyme was partially recovered after growth of BL21(DE3) transformed with pCH21 or p1fnr, but only when 1 mM molybdate was included in the growth medium, which is consistent with the requirement of molybdate for active enzyme synthesis (Table 1). Nevertheless, this activity attained levels of at best only 10% of the activity determined in K-12 strains. This suggests that the amount of active FDH-H limits the activity of the H_2-evolving FHL complex. Introduction of the *fdhF* gene on a plasmid had no effect on the FDH-H enzyme activity (data not shown), suggesting that maturation of the enzyme is what hinders a higher activity being attained.

ModE is a Mo-dependent transcriptional activator of genes and operons encoding many molybdenum cofactor-dependent en-zymes [51–53]. Introduction of the *modE* gene on a multicopy plasmid into BL21(DE3) already containing the *fnr* gene on the low-copy number plasmid p13fnr, together with the addition of molybdate to the growth medium restored total hydrogenase activity to 30% of the K-12 wildtype and FHL activity to 20% of the K-12 wildtype level. This result demonstrates clearly that ModE regulates Hyd-3 biosynthesis [52] because omission of the p7modE plasmid resulted in recovery of neither high hydrogenase activity nor H_2 production (Table 1). Finally, supplementation of the growth medium of BL21(DE3) transformed with p7modE and p13fnr with molybdate, nickel and formate resulted in H_2 production that was roughly 50% that of the K-12 strains (Table 1). Moreover, FDH-H polypeptide could be detected in extracts of this strain, indicating that selenocysteine incorporation [54] was functional in BL21(DE3); further addition of selenite or selenate to the growth medium failed to increase formate dehydrogenase enzyme activity further, suggesting that transport of the anion was not limiting (data not shown).

BL21(DE3) derivatives from other sources also have a hydrogenase-negative phenotype

To ensure that the phenotypes identified here to be associated with BL21(DE3) are not restricted to a strain from a particular source, we analyzed the ability of two BL21(DE3) derivatives from other sources for their ability to generate hydrogen. The Rosetta strain of BL21(DE3) (Novagen) has optimized codon usage for heterologous protein overproduction, while C41(DE3) was isolated specifically for the recombinant overproduction of membrane proteins [55] and is a derivative of the BL21(DE3) strain originally used by Studier and Moffatt [14]. Both BL21(DE3) were

transformed with plasmid pCH21 carrying the *fnr* gene and were grown in the presence and absence of 1 mM molybdate. Hydrogen was only produced by the strains when the additional copies of the *fnr* gene were introduced and molybdate was present in the growth medium (Table S2), indicating that other BL21(DE3) derivatives share the metabolic defects identified for BL21(DE3) obtained from Novagen.

BL21(DE3) cannot respire with nitrate

Three further bis-MGD-containing enzymes present in *E. coli* and which influence anaerobic growth are nitrate reductase (NAR), and FDH-N and FDH-O, the latter two are also selenoenzymes [14]. FDH-N and NAR are inducible in the presence of nitrate and allow the bacterium to respire anaerobi-cally with nitrate as electron acceptor [56]. FDH-O is phyloge-netically related to FDH-N; however, the enzyme is synthesized at a low level both aerobically as well an anaerobically in the presence of nitrate [57,58].

Crude extracts of BL21(DE3) grown anaerobically in rich medium in the presence of nitrate exhibited neither FDH-N nor NAR enzyme activity (Table 2). In contrast, extracts derived from the K-12 strain MC4100 grown under the same conditions had high activities of both enzymes. After transformation of BL21(DE3) with pCH21 or p1fnr neither enzyme activity could be detected. Addition of sodium molybdate to these cultures restored NAR activity but, surprisingly, not the activity of FDH-N (Table 2). Western blots revealed that the large subunit of the NAR enzyme (NarG) was only detected in the presence of multicopy *fnr* and molybdate (Fig. 4A).

A low activity of the nitrate-inducible FDH-N, attaining levels of 10% of K-12 strains, was only measurable in the presence of plasmids encoding FNR and ModE and when molybdate was added to the growth medium (Table 2). FDH-N activity could not be restored to this strain by introducing functional *selB, selD, fdhD* or *fdhE* genes on plasmids (Table 2 and data not shown). No condition could be identified that resulted in high FDH-N enzyme activity, which clearly would limit growth of BL21(DE3) by nitrate respiration using formate as electron donor. Although a FDH-N activity of 10% of the K-12 wild MC4100 could be recorded when the *fnr* and *modE* genes were introduced into BL21(DE3) and molybdate was added to the growth medium (Table 2), the large subunit of FDH-N was below the threshold of detection by Western blotting (Fig. 4B).

The activity of FDH-O can be visualized after native-PAGE using formate as a substrate and nitroblue tetrazolium (NBT) as an artificial electron acceptor [59]. No activity of this enzyme could be detected in extracts of BL21(DE3) grown anaerobically (Fig. 5). Bioinformatic analysis of the genes encoding *fdoGHI* revealed that no missense mutations were present (Table S1), indicating that this could not be the reason for the lack of enzyme activity. However, supplementation of the growth medium with molybdate restored FDH-O enzyme activity. Addition of the *fnr* gene into BL21(DE3) on a plasmid had no effect, which is in accord with the *fdoGHI* operon not being FNR-dependent [15]. The restoration of FDH-O activity also confirmed that the *sel* and *fdhD* and *fdhE* gene products of BL21(DE3) have sufficient activity to allow synthesis of active FDH-O.

Discussion

Although BL21(DE3) is an *fnr* mutant this is not the sole explanation for complete lack of hydrogen metabolism in the strain. For example, while the spontaneously isolated *fnr* deletion mutant, PB1000, of the K-12 strain MC4100 described in this study has significantly reduced hydrogenase activity, nevertheless,

Table 2. Specific activities of Nitrate reductase and Formate dehydrogenase N (FDH-N).

Strain/Condition[1]	Specific Nitrate reductase activity in U mg protein^{-1} ± standard deviation	Specific FDH-N Activity in U mg protein^{-1} ± standard deviation
MC4100	0.60±0.28	0.39±0.12
BL21(DE3)	0.01±0.02 (<0.01)	<0.01 (<0.01)
BL21(DE3)/pCH21 (fnr$^+$)	<0.01 (0.54±0.17)	<0.01 (<0.01)
BL21(DE3)/p1fnr	0.02±0.02 (0.40±0.23)	<0.01 (<0.01)
BL21(DE3)/p10fnr	<0.01 (0.08±0.08)	<0.01 (0.01±0.01)
BL21(DE3)/p13fnr	<0.01 (0.11±0.08)	<0.01 (<0.01)
BL21(DE3)/p7modE	<0.01 (<0.01)	<0.01 (0.05±0.04)
BL21(DE3)/p7modE/p13fnr	<0.01 (<0.01)	<0.01 (0.04±0.03)
BL21(DE3)/pJW3563 (selB$^+$)/p1fnr	0.02±0.01 (0.11±0.24)	<0.01 (0.01±0.002)
BL21(DE3)/pJW1753 (selD$^+$)/p1fnr	0.03±0.01 (0.13±0.12)	<0.01 (<0.01)
PB1000	0.01±0.01	0.04±0.02
PB1000/pCH21	0.59±0.15	0.19±0.03
PB1000/p1fnr	0.47±0.15	0.24±0.05
PB1000/p10fnr	0.02±0.02	0.16±0.09
PB1000/p13fnr	0.16±0.06 (0.13±0.01)	0.15±0.08 (0.16±0.06)

[1]Cells were grown in TGYEP pH 6.5 supplemented with 100 mM KNO$_3$. Values in parenthesis were obtained when cells were grown in the presence of 1 mM sodium molybdate.
doi:10.1371/journal.pone.0022830.t002

a low activity was still measurable. In contrast, no hydrogenase activity whatsoever in extracts or whole cells of BL21(DE3) could be detected, despite a full complement of structural genes being present in the genome [24]. Analysis of the deduced structural gene products revealed that, while Hyd-1 lacks amino acid exchanges, components of Hyd-2 carry some substitutions. In particular, however, a considerably higher number of mutations in Hyd-3 components could be identified. Nevertheless, all of these amino acid substitutions could be ruled out as the reasons for the lack of hydrogenase activity. Rather, in the cases of Hyd-1 and Hyd-2, the lack of FNR caused restricted nickel import with the consequence that the biosynthesis of the active site of these enzymes could not be completed. In the case of Hyd-3 neither nickel nor FNR augmentation was enough to restore enzyme activity. This proved to be, at least in part, due to impaired

molybdenum transport activity as well as due to the lack of the modE gene. ModE is a molybdenum-responsive transcriptional regulator that was identified to be required, along with FHLA and formate, to allow maximal expression of the fdhF gene and the hyc operon [52,60]. The observed partial dependence on molybdate and ModE for FHL biosynthesis could be verified in this study.

Nevertheless, although Hyd-3 activity could be restored to levels equivalent to K-12 wildtype strains grown under the same conditions, it was not possible to restore the hydrogen evolution activity of the FHL complex to wildtype levels. This proved to be due to a limitation in the activity of FDH-H, which could only be recovered to maximally 10–15% of that measured for MC4100. Analysis of FDH-N, which, along with nitrate reductase, is induced in the presence of nitrate and allows *E. coli* to grow by nitrate respiration, was also completely inactive in extracts of
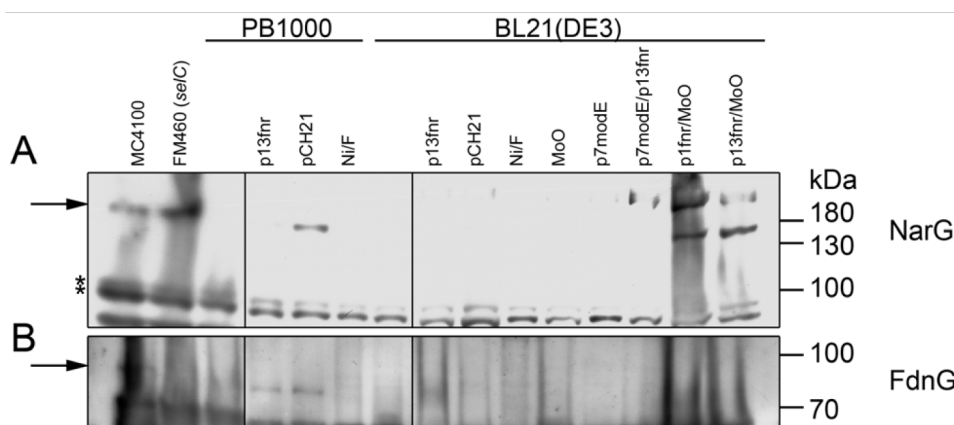
Figure 4. Western blot analysis of the large subunits of NAR and FDH-N. Crude extracts (25 μg protein) of MC4100, FM460 (ΔselC), PB1000 and BL21(DE3) bearing plasmids p13fnr (fnr$^+$), pCH21 (fnr$^+$), p7modE (modE$^+$) or supplemented with 500 μM nickel(II)-chloride (Ni), 15 mM formate (F) or 1 mM molybdate (MoO), when indicated were separated on 10% (w/v) SDS-PAGE after anaerobic growth in TGYEP, pH 6.5 with 100 mM potassium-nitrate. and treated with antiserum raised against **A:** Nar or **B:** FdnG.
doi:10.1371/journal.pone.0022830.g004
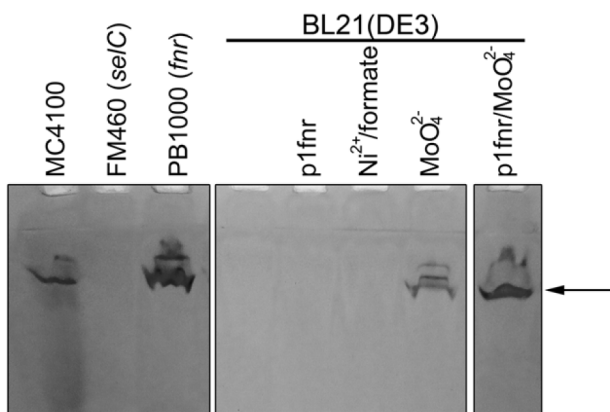
Figure 5. The activity of FDH-O in BL21(DE3) is restored with high concentrations of molybdate. Crude extracts (25 µg of protein) of the various strains indicated were separated in non-denaturing PAGE and stained specifically for FDH-O activity as described in the methods section. The arrow indicates the position of the active FDH-O enzyme.
doi:10.1371/journal.pone.0022830.g005

BL21(DE3) unless a combination of FNR, ModE and molybdate was supplied to the strain. Nevertheless, like FDH-H, which was also induced under these conditions, the activity reached maximally 15% of K-12 wild type. That nitrate reductase activity was induced to K-12 wildtype levels by the introduction of *fnr* on a plasmid, along with supplementation of the growth medium with molybdate, indicated that the limitation in the activities of both FDH selenomolybdoenzymes was not in bis-MGD biosynthesis or insertion or in gene expression of the corresponding structural genes. Moreover, the fact that the third FDH-O could be actively synthesized simply by adding only molybdate confirmed that selenocysteine biosynthesis and insertion is not compromised in BL21(DE3); it should be noted, however, that the amounts of the FDH-O enzyme in MC4100 extracts are considerably lower than those of the other two FDHs [58,61]. Biosynthesis of both FDH-H and FDH-N requires the private chaperones FdhD and FdhE [48,62,63]. Although the corresponding genes are present in the genome of BL21(DE3) both have single amino acid deletions, which could influence the efficiency with which both enzymes function. Additionally, both enzymes are iron-sulfur proteins and interact with components of the iron-sulfur biosynthetic machinery [64]. It is therefore theoretically possible that insufficient supply of iron could compromise the activities of these proteins. Notably, however, the gene encoding the IscR regulator and the iron-sulfur cluster insertion protein IscA do not carry any mutations when compared with their MG1655 counterparts (Table S1). Nevertheless, a further in-depth study will be required to determine whether the iron-sulfur biogenesis machinery is fully functional in BL21(DE3).

As well as having defects in nickel enzyme biosynthesis through the lack of FNR, molybdenum acquisition is also compromised, as is cobalt uptake through the nonsense mutation in the *btuB* gene [21]. Clearly, the extent to which maturation of other metalloproteins with further metal requirements is compromised in BL21(DE3) was outside the scope of this study. Nevertheless, this is an important issue to address in future metalloproteomic analyses using BL21(DE3). Moreover, it should be emphasized that all derivatives of the BL21(DE3) strain analyzed in this study lack a functional *fnr* gene, are deleted in the genes encoding molybdenum transport function and as we could demonstrate here have a

similar hydrogenase-negative phenotype to the Novogen strain of BL21(DE3).

The results of metalloproteomic studies have estimated that at least 40% of all proteins in all organisms are metalloproteins [65]. This is likely to be a conservative estimate because through the development of new high-throughput tandem mass and inductively coupled plasma mass spectrometry techniques combined with classical protein purification new, previously undiscovered metalloenzymes, (including new nickel- and molybdenum-containing enzymes) with as yet unknown functions, are being discovered [66]. The inevitable transfer of the genes encoding these novel metalloproteins into recombinant expression hosts, such as BL21(DE3), for large-scale protein production necessitates an appreciation of the limits of an expression system, particularly when trying to identify new protein functions with previously uncharacterized metal ion cofactors.

The influence of the *fnr* mutation on growth and metabolism of BL21(DE3) also should not be underestimated. Large-scale transcriptome studies have shown that FNR controls, directly or indirectly, the expression of at least one third of all the genes in the *E. coli* K-12 genome and this includes a large contingent of 'aerobic' genes [67,68]. Moreover, although BL21(DE3) is usually cultured for recombinant protein production in rich medium in the presence of air, it is very difficult, even in shake flasks, to supply *E. coli* with sufficient oxygen when growing in rich medium to maintain aerobiosis and cultures inevitably become oxygen-limited very quickly [69].

E. coli B was isolated, probably as a commensal of the human intestinal tract, in the early part of the 20th century [22]. Hydrogen generation by commensal or pathogenic strains could pose an evolutionary disadvantage in the host. For example, neither *Yersinia pestis*, *Shigella flexneri* nor *S. dysenteriae* produce hydrogen gas [70]; all three are pathogens. Moreover, the human pathogenic strain *Salmonella enterica* does not release hydrogen gas, because the uptake hydrogenase is extremely efficient [71]. On the other hand, hydrogen oxidation possibly provides a growth advantage for pathogenic bacteria. It has been shown for *Helicobacter pylori* that in the presence of hydrogen, growth and colonization of the stomach was improved [72] while *Campylobacter* spp. are also able to oxidize hydrogen [73]. *E. coli* strain BL21(DE3) is not listed as a pathogenic strain; however, being closely related to pathogenic strains like O157:H7 it is not surprising that evolutionary hydrogen gas production was perhaps counter-selected as can be deduced from the accumulation of amino acid exchanges within the FHL complex. The loss of FNR apparently occurred before *E. coli* B strains entered the laboratory [22]. We noted that when the *fnr* gene was reintroduced into BL21(DE3) anaerobic growth slowed, which contrasts with what is normally observed with K-12 strains [74]. The reasons for the better growth of BL21(DE3) lacking FNR are intriguing and worthy of further elucidation. The recent demonstration [75] that synthesis of the other global redox-sensing regulator ArcA [76][22] is possibly limiting in BL21(DE3) might also impact significantly on these metabolic deficiences.

Methods

Strains and growth conditions

All strains and plasmids used in this study are listed in Table 3. Aerobic growth was carried out in LB medium [77] in shaking cultures at 37°C. For growth on agar plates media were solidified by inclusion of 1.5% (w/v) agar. For qualitative hydrogen gas production 10 ml of LB medium with 0.8% (w/v) glucose with Durham tubes were used as described [78]. Anaerobic growths to determine hydrogenase activity were done in 100 ml of TGYEP,

pH 6.5 as described [79] and for growth curves the optical density at 600 nm was measured in a NOVOStar plate-reader (BMG Labtech, Germany) in sealed 96-well microtiter plates at 37°C. Anaerobic growth in microtiter plates was verified by native-PAGE with subsequent staining for hydrogenase activity [27]. When needed, kanamycin, chloramphenicol or ampicillin was added to the medium to final concentrations of 50, 12.5 and 100 µg ml^{-1}, respectively. Where indicated, addition of nickel(II)-chloride was done to a final concentration of 500 µM, of sodium molybdate ($MoO_4{}^{2-}$) to 1 mM, of formate to 15 mM and of KNO_3 to 100 mM.

Genetic manipulations and plasmid construction

Transformation of plasmids and recombinant DNA work was done as described [80]. Construction of the reference strain CP938 (BW25113 Δ*hycA-I*) was done as described in [81] with the strain BW25113 carrying plasmid pKD46. PCR with Phusion DNA polymerase (Finnzymes, Germany) was conducted using the chloramphenicol resistance cassette from plasmid pKD4 as template and the oligonucleotides hycA_5′ 5′-GCT TAA AGC TGG CAT CTC TGT TAA ACG GGT AAC CTG ACA *CCA*

TGG TCC ATA TGA ATA TCC TCC-3′ and hycI_3′ 5′-CCC ATC AAG AAC ATC CCT GTC CTG ATT CCT TAA TGA AAA *AGC GAT TGT GTA GGC TGG AGC T*-3′ (Metabion, Germany). The replacement of the *hyc* operon with the chloramphenicol-resistance cassette was verified by PCR amplification with oligonucleotides outside of the operon (hyp_K 5′-CTC *GGA TCC* TGT CAC CAT GAC ACT GTG GA-3′ and hycI_K 5′-CAG CGC ATC GGG CAA TTT AG-3′). The *hyc*-operon deletion allele was then transduced by phage P1*kc* transduction [77] into MC4100 resulting in strain CP971.

Three different plasmids containing the *fnr* gene from MC4100 were isolated or constructed for complementation of the *fnr* mutations in PB1000 and BL21(DE3). The *fnr* gene present on pCH21 [41] was also used for complementation analyses. Plasmid p1fnr was isolated from a gene library derived from MC4100 genomic DNA [82] by complementing the *fnr* mutation in PB1000 and screening for restoration of hydrogen-dependent reduction of benzyl viologen activity [83]. The DNA insert in plasmid p1fnr encompassed the *insH-4*, *ynaJ*, *uspE* and *fnr* genes (4.3 kb insert). Amplification of the *fnr* gene from MC4100 genomic DNA was done with Phusion DNA polymerase and oligonucleotides

Table 3. Strains and plasmids used in this study.

Strains	Genotype	Reference
MC4100	F- *araD139* Δ(*argF-lac*)*U169 ptsF25 deoC1 relA1 flbB5301 rspL150*-	[89]
DHP-F2	MC4100 Δ*hypF*	[28]
JW1753	BW25113 Δ*selD*	National BioResource Project (NBRP) – *E. coli* at National Institute of Genetics (NIG)
JW3563	BW25113 Δ*selB*	NBRP-*E.coli* at NIG
BL21(DE3)	F⁻ *ompT gal dcm lon hsdS$_B$*($r_B{}^-$ $m_B{}^-$) λ(DE3 [*lacI lacUV5-T7 gene 1 ind1 sam7 nin5*])	Novagen, USA
Rosetta(DE3) pLysS	F⁻ *ompT hsdS$_B$* ($r_B{}^-$ $m_B{}^-$) *gal dcm* λ(DE3 [*lacI lacUV5-T7 gene 1 ind1 sam7 nin5*]) pLysSRARE	Novagen, USA
C41(DE3)	F⁻ *ompT gal dcm hsdS$_B$* ($r_B{}^-$ $m_B{}^-$) λ(DE3), Like BL21(DE3) but with an uncharacterized mutation affecting membrane protein synthesis	[55]
CP938	BW25113 Δ*hycA-I*::Kan	This work
CP971	MC4100 Δ*hycA-I*::Kan	This work
PB1000	MC4100 Δ*purT* Δ*purU* Δ*insH4-fnr*	This work
FM460	MC4100 Δ(*selC*)*400*::Kan	[58]
RM220	MC4100 Δ*pflB-pflA*	[90]
Plasmids		
pAF1	Cm^R, *hypF*	[37]
pJW3563	ASKA Clone(-) *selB*	[35]
pJW1753	ASKA Clone(-) *selD*	[35]
pJW3441	ASKA Clone(-) *nikA*	[35]
pJW2444	ASKA Clone(-) *nikD*	[35]
pJW3445	ASKA Clone(-) *nikE*	[35]
pCH21	Ap^R, Cm^R, *fnr*	[41]
pBR322	cloning vector	[91]
p1fnr	genomic *E. coli* Sau3IIA fragments in pBR322, containing *fnr*	[37], This work
p10fnr	pBluescript SK(+) containing *fnr* in HindIII and BamHI site; Amp^R	This work
p13fnr	pACYC184 containing *fnr* in HindIII and BamHI site; Cm^R	This work
pACYCM	pACYC184 with A1845T exchange in *tetA*; Cm^R	This work
p31hycAI	8365 bp MluI insert from *hycAI* into pACYCM; withershins *tetA*; Cm^R	This work
p7modE	pBluescript SK(+) containing *modE* in BamHI and EcoRI site; Amp^R	This work
p2modE	pACYC184 containing *modE* from p7modE in BamHI and EcoRV site; Cm^R	This work

Fnr_HindIII_FW 5′-GTG *AAG CTT* ATG ATC CCG GAA AAG CGA ATT A-3′ and Fnr_BamHI_RW 5′-GTG *GGA TCC* TCA GGC AAC GTT ACG CGT ATG-3′. The resulting 765 bp DNA fragment was digested with HindIII and BanHI and ligated into pre-digested pBluescript SK(+) and pACYC184 vectors resulting in plasmids p10fnr and p13fnr, respectively. The cloning of the *modE* gene from MC4100 was performed in a similar manner except that the oligonucleotides modE_FW_BamHI 5′-CGC *GGA TCC* ATG CAG GCC GAA ATC CTT C-3′ and modE_RW_EcoRI 5′-CGC *GAA TTC* TTA GCA CAG CGT GGC GAT AAT C-3′ were used. The resulting 807 bp DNA fragment was digested with BamHI and EcoRI and ligated into BamHI-HindIII-digested pBluescript SK(+) resulting in p7modeE. The *modE* gene was subcloned into pACYC184 via BamHI and EcoRV digestion resulting in the plasmid p2modE. The DNA sequences of the cloned genes were verified (Seqlab). The cloning of the *hycA-I* operon was done by direct digestion of genomic DNA from strain MC4100 with MluI, which resulted in an approximate 8500 bp DNA fragment that was excised from an agarose gel and ligated into a modified pACYC184 vector (pACYCM). To generate pACYCM, the *tetA* gene of pACYC184 was modified to include a MluI restriction site by exchanging A1845T with the oligonucleotides pACY-C184_A1845T_FW 5′-CTA TCG ACT ACG CG**T** TCA TGG CGA CCA CAC-3′ and pACYC184_A1845T_RW 5′-GTG TGG TCG CCA TGA **A**CG CGT AGT CGA TAG-3′ using the QuickChange site-directed mutagenesis procedure (Stratagene). The orientation of the insert in p31hycA-I with respect to the *tetA* gene was verified by PCR and partial DNA sequence analysis. The functionality of the insert was tested by transforming p31hycA-I into strain CP971 (Δ*hycA-I*), which restored hydrogen gas production.

Determination of enzyme activities

Dye overlay methods for colony screening were applied as has been described for formate dehydrogenase activity [83] with 0.5 mM benzyl viologen and a hydrogen atmosphere for hydrogenase activity or 2.5 mM benzyl viologen and 250 mM formate for formate dehydrogenase activity after anaerobic growth on agar plates in GasPak anaerobic jars (Oxoid, UK).

Anaerobic cultures were harvested at an $OD_{600\,nm}$ of approximately 0.8. Cells from cultures were harvested by centrifugation at $4000\times$ g for 10 min at 4°C. The cell pellet was resuspended in 1% (v/v) of the culture volume of 50 mM MOPS buffer pH 7.0 and lysed on ice by sonication (30 W power for 5 min with 0.5 s pulses). Unbroken cells and cell debris were removed by centrifugation for 15 min at $10,000\times$ g and 4°C and the supernatant was carefully decanted and used as the crude cell extract. Total enzyme activities were measured using 1 cm path-length anaerobic cuvettes in an Uvicon 900 dual-wavelength spectrophotometer according to [27] except that the buffer used was 50 mM MOPS buffer, pH 7.0 with 4 mM benzyl viologen. To determine hydrogenase activity the gas phase of the cuvettes was replaced with 100% hydrogen gas and the detection wavelength used was 578 nm and an $E_{M,\,578}$ value of 8,600 M^{-1} cm^{-1} was assumed for reduced benzyl viologen. Formate dehydrogenase H (FDH-H) activity was measured under the same conditions except that the cuvettes were flushed with nitrogen. The reaction was started by the addition 30 mM sodium formate. Nitrate reductase (NAR) enzyme activity was measured using 0.4 mM benzyl viologen reduced to an OD_{600} of 2 with freshly prepared 10 mM sodium dithionite solution. The reaction was started by the addition of 9 mM sodium nitrate as described [84] with an $E_{M,600\,nm}$ value of 7,400 M^{-1} cm^{-1} assumed for reduced benzyl viologen. Formate dehydrogenase N (FDH-N) activity was measured using final concentrations of 75 μM 2,6-dichlorophenolindophenol (DCPIP) and 288 μM phenazine meth-

osulfate (PMS) and the reaction was started by the addition of 40 mM formate [84]. An $E_{M,\,600\,nm}$ of 20,000 M^{-1} cm^{-1} for oxidised DCPIP was assumed. The specific activity of the FHL complex, measured as hydrogen evolution, was assayed in whole cells as described [29]. One unit of activity was defined as the oxidation of 1 μmol of the respective substrate per min. All activities were determined from 3 independent cultures. Protein concentration was determined [85] with bovine serum albumin as standard.

Polyacrylamide gel electrophoresis and in-gel hydrogenase activity-staining

For Western blot analysis, aliquots of 50 μg protein from crude extracts were separated in 10 or 12.5% (w/v) SDS-polyacrylamide gels (SDS-PAGE) [86] and transferred to nitrocellulose membranes as described [87]. Antibodies raised against FNR (1:3000; a kind gift from G. Unden, Mainz, Germany), PflB (1:3000), Hyd-2 (1:20,000; a kind gift of F. Sargent, Dundee, Scotland), HycG (1:3000; [88]), NAR (1:3000) and FDH-N (1:3000) were used. Secondary antibody conjugated to horseradish peroxidase was obtained from Bio-Rad. Visualisation was done by the enhanced chemiluminescent reaction (Stratagene). Detection of hydrogenase enzyme activity after non-denaturing PAGE (native-PAGE) was performed as described [27]. Gels for hydrogenase activity-staining were loaded with 25 μg protein per lane. In-gel activity of FDH-O was determined using 50 mM sodium formate and 978 mM nitroblue tetrazolium (NBT) as described [59].

Bioinformatic analysis of BL21(DE3) and MG1655 genome

The global alignment of the analysed gene products against all translated potential open reading frames (ORF) in BL21(DE3) was based on an *ad hoc* implementation of the Needleman-Wunsch algorithm. The scoring function used in this implementation was chosen in such a way that it resulted in a similarity score being equal to the length of the protein in MG1655, if the translated potential ORF in BL21(DE3) matched the protein exactly. This indicated the existence of the respective gene product in BL21(DE3). If for a given protein in MG1655 no exact match was detected in any translated potential ORF in BL21(DE3), the maximal similarity score out of all calculated global alignments was chosen.

Supporting Information

Figure S1   Partial complementation of nickel transport- and hydrogenase maturation-defective mutants. Shown is an activity-stained gel after non-denaturing PAGE analysis of extracts derived from the indicated strains, which were grown anaerobically as described in the methods section of the main text. The locations of Hyd-1 and Hyd-2 are indicated as is a hydrogen-independent activity band (*) frequently observed under these growth conditions. D, original mutant without addition; Ni, growth in the presence of 0.5 mM $NiCl_2$; growth of the mutant after transformation with a plasmid carrying the gene that is deleted from the chromosome in the respective mutant (See Table 3 of main text). Strains JW3441 (*nikA*), JW2444 (*nikD*), JW3445 (*nikE*), JW2961 (*hybD*) and JW5493 (*hybF*) were described in [35].
(TIF)

Table S1   Amino acid exchanges in BL21(DE3) gene products compared to MG1655 with a function in hydrogen metabolism. * see [92]
(DOCX)

Table S2   Phenotypic analysis of hydrogen metabolism in different of BL21(DE3) derivatives. [1] Cells were grown in

TGYEP pH 6.5. Values in parenthesis were obtained after growth of cells in the presence of 1 mM sodium molybdate. [2] The mean and standard deviation of three independent experiments are shown. [3] Gas production was measured qualitatively with inverted Durham tubes.
(DOCX)

Author Contributions

Conceived and designed the experiments: CP RGS. Performed the experiments: CP SK UL. Analyzed the data: CP MB SK UL RGS. Wrote the paper: CP RGS.

References

1. Sawers R, Clark D, Böck A (2004) Fermentative Pyruvate and Acetyl-Coenzyme A Metabolism. EcoSal - *Escherichia coli* and *Salmonella*: cellular and molecular biology.
2. Spiro S, Guest JR (1991) Adaptive responses to oxygen limitation in *Escherichia coli*. Trends Biochem Sci 16: 310–314.
3. Schindelin H, Kisker C, Rajagopalan KV (2001) Molybdopterin from molybdenum and tungsten enzymes. Adv Protein Chem 58: 47–94.
4. Berg BL, Stewart V (1990) Structural genes for nitrate-inducible formate dehydrogenase in *Escherichia coli* K-12. Genetics 125: 691–702.
5. Forzi L, Sawers RG (2007) Maturation of [NiFe]-hydrogenases in *Escherichia coli*. Biometals 20: 565–578.
6. Sawers R, Ballantine S, Boxer D (1985) Differential expression of hydrogenase isoenzymes in *Escherichia coli* K-12: evidence for a third isoenzyme. J Bacteriol 164: 1324–1331.
7. Böck A, King P, Blokesch M, Posewitz M (2006) Maturation of hydrogenases. Adv Microb Physiol 51: 1–71.
8. Forzi L, Hellwig P, Thauer RK, Sawers RG (2007) The CO and CN(-) ligands to the active site Fe in [NiFe]-hydrogenase of *Escherichia coli* have different metabolic origins. FEBS Lett 581: 3317–3321.
9. Lenz O, Zebger I, Hamann J, Hildebrandt P, Friedrich B (2007) Carbamoyl-phosphate serves as the source of CN(-), but not of the intrinsic CO in the active site of the regulatory [NiFe]-hydrogenase from *Ralstonia eutropha*. FEBS Lett 581: 3322–3326.
10. Kaluarachchi H, Chan Chung KC, Zamble DB (2010) Microbial nickel proteins. Nat Prod Rep 27: 681–694.
11. Wu L, Mandrand-Berthelot M (1986) Genetic and physiological characterization of new *Escherichia coli* mutants impaired in hydrogenase activity. Biochimie 68: 167–179.
12. Wu L, Mandrand-Berthelot M, Waugh R, Edmonds C, Holt S, et al. (1989) Nickel deficiency gives rise to the defective hydrogenase phenotype of *hydC* and *fnr* mutants in *Escherichia coli*. Mol Microbiol 3: 1709–1718.
13. Sauter M, Böhm R, Böck A (1992) Mutational analysis of the operon (*hyc*) determining hydrogenase 3 formation in *Escherichia coli*. Mol Microbiol 6: 1523–1532.
14. Sawers G (1994) The hydrogenases and formate dehydrogenases of *Escherichia coli*. Antonie Van Leeuwenhoek 66: 57–88.
15. Abaibou H, Pommier J, Benoit S, Giordano G, Mandrand-Berthelot MA (1995) Expression and characterization of the *Escherichia coli fdo* locus and a possible physiological role for aerobic formate dehydrogenase. J Bacteriol 177: 7141–7149.
16. Ruiz-Herrera J, DeMoss JA (1969) Nitrate reductase complex of *Escherichia coli* K-12: participation of specific formate dehydrogenase and cytochrome *b1* components in nitrate reduction. J Bacteriol 99: 720–729.
17. Böck A, Forchhammer K, Heider J, Leinfelder W, Sawers G, et al. (1991) Selenocysteine: the 21st amino acid. Mol Microbiol 5: 515–520.
18. Schwarz G, Mendel RR, Ribbe MW (2009) Molybdenum cofactors, enzymes and pathways. Nature 460: 839–847.
19. Delbrück M (1940) The growth of bacteriophage and lysis of the host. J Gen Physiol 23: 643–660.
20. Studier FW, Moffatt BA (1986) Use of bacteriophage T7 RNA polymerase to direct selective high-level expression of cloned genes. J Mol Biol 189: 113–130.
21. Studier FW, Daegelen P, Lenski RE, Maslov S, Kim JF (2009) Understanding the differences between genome sequences of *Escherichia coli* B strains REL606 and BL21(DE3) and comparison of the *E. coli* B and K-12 genomes. J Mol Biol 394: 653–680.
22. Daegelen P, Studier FW, Lenski RE, Cure S, Kim JF (2009) Tracing ancestors and relatives of *Escherichia coli* B, and the derivation of B strains REL606 and BL21(DE3). J Mol Biol 394: 634–643.
23. Akhtar MK, Jones PR (2008) Deletion of *iscR* stimulates recombinant clostridial Fe-Fe hydrogenase activity and H$_2$-accumulation in *Escherichia coli* BL21(DE3). Appl Microbiol Biotechnol 78: 853–862.
24. Jeong H, Barbe V, Lee CH, Vallenet D, Yu DS, et al. (2009) Genome sequences of *Escherichia coli* B strains REL606 and BL21(DE3). J Mol Biol 394: 644–652.
25. Schlensog V, Birkmann A, Böck A (1989) Mutations in *trans* which affect the anaerobic expression of a formate dehydrogenase (*fdhF*) structural gene. Arch Microbiol 152: 83–89.
26. Birkmann A, Zinoni F, Sawers R, Böck A (1987) Factors affecting transcriptional regulation of the formate-hydrogen-lyase pathway of *Escherichia coli*. Arch Microbiol 148: 44–51.
27. Ballantine S, Boxer D (1985) Nickel-containing hydrogenase isoenzymes from anaerobically grown *Escherichia coli* K-12. J Bacteriol 163: 454–459.
28. Paschos A, Bauer A, Zimmermann A, Zehelein E, Böck A (2002) HypF, a carbamoyl phosphate-converting enzyme involved in [NiFe] hydrogenase maturation. J Biol Chem 277: 49945–49951.
29. Pinske C, Sawers RG (2010) The role of the ferric-uptake regulator Fur and iron homeostasis in controlling levels of the [NiFe]-hydrogenases in *Escherichia coli*. International Journal of Hydrogen Energy 35: 8938–8944.
30. Rossmann R, Sawers G, Böck A (1991) Mechanism of regulation of the formate-hydrogenlyase pathway by oxygen, nitrate, and pH: definition of the formate regulon. Mol Microbiol 5: 2807–2814.
31. Navarro C, Wu LF, Mandrand-Berthelot MA (1993) The *nik* operon of *Escherichia coli* encodes a periplasmic binding-protein-dependent transport system for nickel. Mol Microbiol 9: 1181–1191.
32. Hube M, Blokesch M, Böck A (2002) Network of hydrogenase maturation in *Escherichia coli*: role of accessory proteins HypA and HybF. J Bacteriol 184: 3879–3885.
33. Waugh R, Boxer D (1986) Pleiotropic hydrogenase mutants of *Escherichia coli* K12: growth in the presence of nickel can restore hydrogenase activity. Biochimie 68: 157–166.
34. Hausinger RP (1987) Nickel utilization by microorganisms. Microbiol Rev 51: 22–42.
35. Kitagawa M, Ara T, Arifuzzaman M, Ioka-Nakamichi T, Inamoto E, et al. (2005) Complete set of ORF clones of *Escherichia coli* ASKA library (a complete set of *E. coli* K-12 ORF archive): unique resources for biological research. DNA Res 12: 291–299.
36. Paschos A, Glass R, Böck A (2001) Carbamoylphosphate requirement for synthesis of the active center of [NiFe]-hydrogenases. FEBS Lett 488: 9–12.
37. Maier T, Binder U, Böck A (1996) Analysis of the *hydA* locus of *Escherichia coli*: two genes (*hydN* and *hypF*) involved in formate and hydrogen metabolism. Arch Microbiol 165: 333–341.
38. Rangarajan E, Asinas A, Proteau A, Munger C, Baardsnes J, et al. (2008) Structure of [NiFe] hydrogenase maturation protein HypE from *Escherichia coli* and its interaction with HypF. J Bacteriol 190: 1447–1458.
39. Messenger S, Green J (2003) FNR-mediated regulation of *hyp* expression in *Escherichia coli*. FEMS Microbiol Lett 228: 81–86.
40. Lutz S, Jacobi A, Schlensog V, Böhm R, Sawers G, et al. (1991) Molecular characterization of an operon (*hyp*) necessary for the activity of the three hydrogenase isoenzymes in *Escherichia coli*. Mol Microbiol 5: 123–135.
41. Jamieson DJ, Higgins CF (1984) Anaerobic and leucine-dependent expression of a peptide transport gene in *Salmonella typhimurium*. J Bacteriol 160: 131–136.
42. Sawers RG (2005) Expression of *fnr* is constrained by an upstream IS*5* insertion in certain *Escherichia coli* K-12 strains. J Bacteriol 187: 2609–2617.
43. Richard D, Sawers G, Sargent F, McWalter L, Boxer D (1999) Transcriptional regulation in response to oxygen and nitrate of the operons encoding the [NiFe] hydrogenases 1 and 2 of *Escherichia coli*. Microbiology 145: 2903–2912.
44. Brøndsted L, Atlung T (1994) Anaerobic regulation of the hydrogenase 1 (*hya*) operon of *Escherichia coli*. J Bacteriol 176: 5423–5428.
45. Sawers G, Böck A (1988) Anaerobic regulation of pyruvate formate-lyase from *Escherichia coli* K-12. J Bacteriol 170: 5330–5336.
46. Sawers G, Böck A (1989) Novel transcriptional control of the pyruvate formate-lyase gene: upstream regulatory sequences and multiple promoters regulate anaerobic expression. J Bacteriol 171: 2485–2498.
47. Boyington JC, Gladyshev VN, Khangulov SV, Stadtman TC, Sun PD (1997) Crystal structure of formate dehydrogenase H: catalysis involving Mo, molybdopterin, selenocysteine, and an Fe$_4$S$_4$ cluster. Science 275: 1305–1308.
48. Schlindwein C, Giordano G, Santini CL, Mandrand MA (1990) Identification and expression of the *Escherichia coli fdhD* and *fdhE* genes, which are involved in the formation of respiratory formate dehydrogenase. J Bacteriol 172: 6112–6121.
49. Hall DR, Gourley DG, Leonard GA, Duke EM, Anderson LA, et al. (1999) The high-resolution crystal structure of the molybdate-dependent transcriptional regulator (ModE) from *Escherichia coli*: a novel combination of domain folds. EMBO J 18: 1435–1446.
50. Rosentel JK, Healy F, Maupin-Furlow JA, Lee JH, Shanmugam KT (1995) Molybdate and regulation of *mod* (molybdate transport), *fdhF*, and *hyc* (formate hydrogenlyase) operons in *Escherichia coli*. J Bacteriol 177: 4857–4864.
51. Anderson LA, McNairn E, Lubke T, Pau RN, Boxer DH, et al. (2000) ModE-dependent molybdate regulation of the molybdenum cofactor operon *moa* in *Escherichia coli*. J Bacteriol 182: 7035–7043.

52. Hasona A, Self WT, Ray RM, Shanmugam KT (1998) Molybdate-dependent transcription of *hyc* and *nar* operons of *Escherichia coli* requires MoeA protein and ModE-molybdate. FEMS Microbiol Lett 169: 111–116.

53. McNicholas PM, Gunsalus RP (2002) The molybdate-responsive *Escherichia coli* ModE transcriptional regulator coordinates periplasmic nitrate reductase (*napFDAGHBC*) operon expression with nitrate and molybdate availability. J Bacteriol 184: 3253–3259.

54. Zinoni F, Birkmann A, Leinfelder W, Böck A (1987) Cotranslational insertion of selenocysteine into formate dehydrogenase from *Escherichia coli* directed by a UGA codon. Proc Natl Acad Sci U S A 84: 3156–3160.

55. Miroux B, Walker JE (1996) Over-production of proteins in *Escherichia coli*: mutant hosts that allow synthesis of some membrane proteins and globular proteins at high levels. J Mol Biol 260: 289–298.

56. Darwin A, Tormay P, Page L, Griffiths L, Cole J (1993) Identification of the formate dehydrogenases and genetic determinants of formate-dependent nitrite reduction by *Escherichia coli* K12. J Gen Microbiol 139: 1829–1840.

57. Rolfe MD, Beek Ter A, Graham AI, Trotter EW, Asif HMS, et al. (2011) Transcript profiling and inference of *Escherichia coli* K-12 ArcA activity across the range of physiologically relevant oxygen concentrations. J Biol Chem 286: 10147–10154.

58. Sawers G, Heider J, Zehelein E, Böck A (1991) Expression and operon structure of the *sel* genes of *Escherichia coli* and identification of a third selenium-containing formate dehydrogenase isoenzyme. J Bacteriol 173: 4983–4993.

59. Enoch HG, Lester RL (1975) The purification and properties of formate dehydrogenase and nitrate reductase from *Escherichia coli*. J Biol Chem 250: 6693–6705.

60. Self WT, Grunden AM, Hasona A, Shanmugam KT (1999) Transcriptional regulation of molybdoenzyme synthesis in *Escherichia coli* in response to molybdenum: ModE-molybdate, a repressor of the *modABCD* (molybdate transport) operon is a secondary transcriptional activator for the *hyc* and *nar* operons. Microbiology 145: 41–55.

61. Pinsent J (1954) The need for selenite and molybdate in the formation of formic dehydrogenase by members of the *coli-aerogenes* group of bacteria. Biochem J 57: 10–16.

62. Lüke I, Butland G, Moore K, Buchanan G, Lyall V, et al. (2008) Biosynthesis of the respiratory formate dehydrogenases from *Escherichia coli*: characterization of the FdhE protein. Arch Microbiol 190: 685–696.

63. Mandrand-Berthelot MA, Couchoux-Luthaud G, Santini CL, Giordano G (1988) Mutants of *Escherichia coli* specifically deficient in respiratory formate dehydrogenase activity. J Gen Microbiol 134: 3129–3139.

64. Butland G, Peregrín-Alvarez JM, Li J, Yang W, Yang X, et al. (2005) Interaction network containing conserved and essential protein complexes in *Escherichia coli*. Nature 433: 531–537.

65. Andreini C, Bertini I, Rosato A (2009) Metalloproteomes: a bioinformatic approach. Acc Chem Res 42: 1471–1479.

66. Cvetkovic A, Menon AL, Thorgersen MP, Scott JW, Poole Ii FL, et al. (2010) Microbial metalloproteomes are largely uncharacterized. Nature 466: 779–782.

67. Salmon K, Hung S-P, Mekjian K, Baldi P, Hatfield GW, et al. (2003) Global gene expression profiling in *Escherichia coli* K12. The effects of oxygen availability and FNR. J Biol Chem 278: 29837–29855.

68. Constantinidou C, Hobman JL, Griffiths L, Patel MD, Penn CW, et al. (2006) A reassessment of the FNR regulon and transcriptomic analysis of the effects of nitrate, nitrite, NarXL, and NarQP as *Escherichia coli* K12 adapts from aerobic to anaerobic growth. J Biol Chem 281: 4802–4815.

69. McDaniel LE, Bailey EG (1969) Effect of shaking speed and type of closure on shake flask cultures. Appl Microbiol 17: 286–290.

70. Holt JG (1989) Bergey's manual of systematic bacteriology Lippincott Williams & Wilkins. 2648 p.

71. Zbell AL, Maier RJ (2009) Role of the Hya hydrogenase in recycling of anaerobically produced H₂ in *Salmonella enterica* serovar Typhimurium. Appl Environ Microbiol 75: 1456–1459.

72. Olson JW, Maier RJ (2002) Molecular hydrogen as an energy source for *Helicobacter pylori*. Science 298: 1788–1790.

73. Goodman TG, Hoffman PS (1983) Hydrogenase activity in catalase-positive strains of *Campylobacter* spp. J Clin Microbiol 18: 825–829.

74. Shaw DJ, Guest JR (1982) Amplification and product identification of the *fnr* gene of *Escherichia coli*. J Gen Microbiol 128: 2221–2228.

75. Waegeman H, Beauprez J, Moens H, Maertens J, De Mey M, et al. (2011) Effect of *iclR* and *arcA* knockouts on biomass formation and metabolic fluxes in *Escherichia coli* K12 and its implications on understanding the metabolism of *Escherichia coli* BL21 (DE3). BMC Microbiol 11: 70.

76. Sawers G (1999) The aerobic/anaerobic interface. Curr Opin Microbiol 2: 181–187.

77. Miller J (1972) Experiments in Molecular Genetics. 466 p.

78. Guest JR (1969) Biochemical and genetic studies with nitrate reductase *C*-gene mutants of *Escherichia coli*. Mol Gen Genet 105: 285–297.

79. Begg Y, Whyte J, Haddock B (1977) The identification of mutants of *Escherichia coli* deficient in formate dehydrogenase and nitrate reductase activities using dye indicator plates. FEMS Microbiol Lett 2: 47–50.

80. Sambrook J, Russell D (2001) Molecular Cloning: A Laboratory Manual.

81. Datsenko K, Wanner B (2000) One-step inactivation of chromosomal genes in *Escherichia coli* K-12 using PCR products. Proc Natl Acad Sci U S A 97: 6640–6645.

82. Hesslinger C, Fairhurst S, Sawers G (1998) Novel keto acid formate-lyase and propionate kinase enzymes are components of an anaerobic pathway in *Escherichia coli* that degrades L-threonine to propionate. Mol Microbiol 27: 477–492.

83. Mandrand-Berthelot M-A, Wee M, Haddock B (1978) An improved method for the Identification and Characterization of Mutants of *Escherichia coli* deficient in formate dehydrogenase activity. FEMS Microbiol Lett 4: 37–40.

84. Lester RL, DeMoss JA (1971) Effects of molybdate and selenite on formate and nitrate metabolism in *Escherichia coli*. J Bacteriol 105: 1006–1014.

85. Lowry O, Rosebrough N, Farr A, Randall R (1951) Protein measurement with the Folin phenol reagent. J Biol Chem 193: 265–275.

86. Laemmli U (1970) Cleavage of structural proteins during the assembly of the head of bacteriophage T4. Nature 227: 680–685.

87. Towbin H, Staehelin T, Gordon J (1979) Electrophoretic transfer of proteins from polyacrylamide gels to nitrocellulose sheets: procedure and some applications. Proc Natl Acad Sci U S A 76: 4350–4354.

88. Magalon A, Böck A (2000) Dissection of the maturation reactions of the [NiFe] hydrogenase 3 from *Escherichia coli* taking place after nickel incorporation. FEBS Lett 473: 254–258.

89. Casadaban MJ (1976) Transposition and fusion of the *lac* genes to selected promoters in *Escherichia coli* using bacteriophage lambda and Mu. J Mol Biol 104: 541–555.

90. Kaiser M, Sawers G (1994) Pyruvate formate-lyase is not essential for nitrate respiration by *Escherichia coli*. FEMS Microbiol Lett 117: 163–168.

91. Balbás P, Soberon X, Merino E, Zurita M, Lomeli H, et al. (1986) Plasmid vector pBR322 and its special-purpose derivatives–a review. Gene 50: 3–40.

92. Self W, Hasona A, Shanmugam K (2004) Expression and regulation of a silent operon, *hyf*, coding for hydrogenase 4 isoenzyme in *Escherichia coli*. J Bacteriol 186: 580–587.

2.5.4 Zusätzliche Ergebnisse

2.5.4.1 Wiederherstellung der Fdh Aktivität
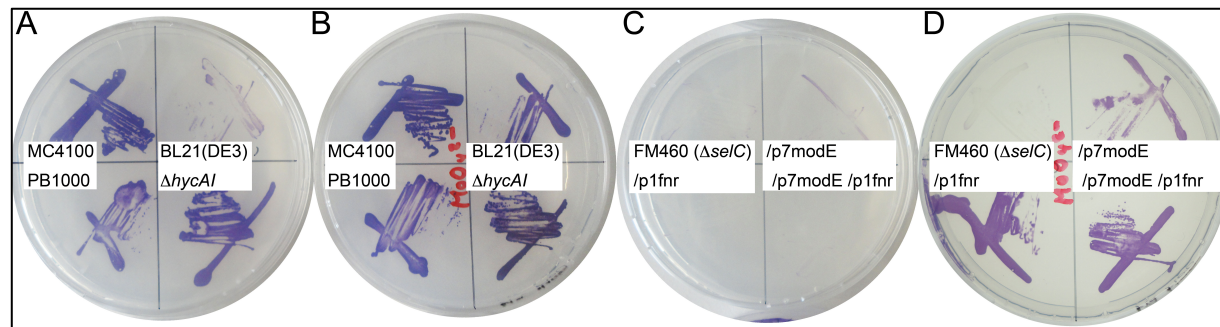
Abbildung 13 Benzylviologen Formiatdehydrogenase Überschichtungstest. Die Stämme A/B: MC4100 (Wildtyp), BL21(DE3), PB1000 (Δ*fnr*), CP971 (Δ*hycAI*), C/D: FM460 (Δ*selC*) und BL21(DE3) transformiert mit *modE* (/p7modE), *fnr* (/p1fnr) oder beiden Plasmiden wurden auf M9-Minimalmedium-Platten in denen kein (**A/C**) oder 1 mM MoO$_4^{2-}$ (**B/D**) enthalten war, ausplattiert, unter N$_2$ Atmosphäre inkubiert und mit Weichagar, der 2,5 mM Benzylviologen und 250 mM Formiat enthielt überschichtet. Formiatdehydrogenase Aktivität erscheint als violette Verfärbung.

Die Formiatdehydrogenase Aktivität konnte zwar nicht quantifiziert werden, war dennoch deutlich in einer qualitativen Analyse nachweisbar. Wie in Abb. 13 zu erkennen ist, besitzen eine *selC* Mutante und BL21(DE3) keine Fdh-H Aktivität. Die Aktivität von BL21(DE3) kann jedoch im Gegensatz zur *selC* Mutante durch Zugabe von MoO$_4^{2-}$ wieder hergestellt werden. Zugabe von *modE* und *fnr* hatten keinen Effekt solange kein MoO$_4^{2-}$ im Medium war, zudem eine Fnr Mutation (PB1000) allein nicht zum Verlust der Fdh-H Aktivität führte. Damit konnte abschließend bewiesen werden, dass Fdh-H Aktivität in BL21(DE3) vorhanden und ausschließlich MoO$_4^{2-}$ abhängig ist.

2.5.4.3 pH-Phänotyp einer Fnr Mutante

Bezogen auf ihren [NiFe]-Hydrogenase Phänotyp konnte die MC4100 Δ*fnr* Mutante charakterisiert werden und eine ausgeprägte pH Abhängigkeit festgestellt werden (Abb. 14). Während in MC4100 die Expression der Gene für die gemischte Säuregärung bei niedrigem pH verstärkt wird (Rossmann *et al.*, 1991), findet diese Regulation in PB1000 nicht statt. So konnte sowohl eine Erhöhung der Proteinmenge von Hyd-2, als auch ein Anstieg der Gesamthydrogenase Aktivität und der FHL Aktivität bei Erhöhung des pH im Medium beobachtet werden. Ebenfalls konnte in einem Nativ-Gel nach Anzucht bei pH 8,0 geringe Aktivität von Hyd-1 sichtbar gemacht werden (nicht gezeigt). Die Detektion von H$_2$ bei hohem pH steht im Gegensatz zur H$_2$-Synthese im MC4100 bei niedrigem pH (Mnatsakanyan *et al.*, 2004), konnte jedoch durch zusätzliche Einführung einer Deletion in *hycG* vollständig unterbunden werden und ist damit FHL abhängig. Die Reifung der Hyd-2 und Hyd-3, sowie die nominale Aktivität sind jedoch geringer als im MC4100 (Tab. 1), weil sowohl der Nickel-

Transport (Wu *et al.*, 1989) als auch die Verfügbarkeit von Formiat durch die partielle Fnr Regulation des *focA-pflB* Operons (Sawers, 2006) limitierend sind. Dies wird durch die verringerten PflB Proteinmengen einer Fnr Mutante sichtbar (Abb. 14C).
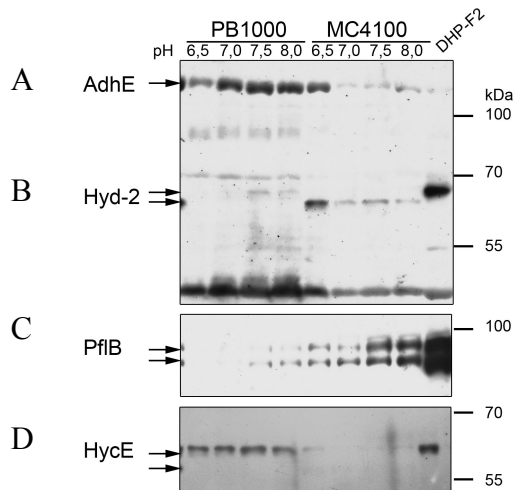
Abbildung 14 Abhängigkeit der Hydrogenase Reifung und Hyd-2, PflB und HycE Enzymmengen von pH und Fnr. Proben von 25 µg Protein nach anaeroben Wachstum in TGYEP mit verschiedenen pH Werten von PB1000 (Δ*fnr*) und MC4100 wurden in 10 % (w/v) SDS-Page aufgetrennt, auf Nitrocellulose trensferiert und mittels Antikörpern gegen **(B)** Hydrogenase 2 (Kreuzreaktion gegen AdhE/**A**), PflB **(C)** und HycE **(D)** detektiert.

Tabelle 1 Fermentative Enzym-Aktivitäten einer Δ*fnr* Mutante (PB1000) und MC41000 in Abhängigkeit vom pH.

Stamm/pH [a]	spezifische Gesamthydrogenase Aktivität (U mg^{-1})	spezifische Formiatdehydrogenase-H Aktivität (U mg^{-1})	spezifische FHL abgängige H$_2$ Produktion (mU mg^{-1})
MC4100/ pH 6,0	4,26 ± 0,87	0,31 ± 0,05	36 ± 9
MC4100/ pH 6,5	2,95 ± 0,74	0,24 ± 0,06	28 ± 20
MC4100/ pH 7,0	2,02 ± 0,59	0,12 ± 0,04	20 ± 2
MC4100/ pH 7,5	1,70 ± 0,87	0,09 ± 0,02	20 ± 14
PB1000/ pH 6,0	0,01 ± 0,01	< 0,01	2 ± 1
PB1000/ pH 6,5	0,03 ± 0,02	< 0,01	2 ± 1
PB1000/ pH 7,0	0,05 ± 0,04	< 0,01	3 ± 1
PB1000/ pH 7,5	0,07 ± 0,05	< 0,01	3 ± 2

[a] Anzucht von MC4100 und PB1000 (Δ*fnr*) erfolgte in TGYEP mit Kaliumphosphatpuffer mit den angegebenen pH Werten. Messung der Aktivitäten wurden in Dreifachbestimmungen ermittelt.

2.6 Die respiratorischen Molybdän-Selenoproteine der Formiatdehydrogenasen von *Escherichia coli* besitzen Wasserstoff: Benzylviologen Oxidoreduktase Aktivität.

2.6.1 Zusammenfassung

In *E. coli* Stämmen, die genetisch nicht fähig waren aktive [NiFe]-Hydrogenasen zu synthetisieren, konnte in nicht denaturierenden Gelen durch Aktivitätsfärbung eine Migrationsbande visualisiert werden, die wasserstoffabhängig Benzylviologen (BV) reduziert. Unter einer Stickstoffatmosphäre konnte die Bande nicht sichtbar gemacht werden, solange kein Formiat als Elektronendonor vorhanden war. Nach Reinigung dieser Aktivität aus der Membran und anschließender massenspektrometrischer Analyse, konnten Peptidfragmente der Formiatdehydrogenasen N und O (Fdh-N/-O) identifiziert werden (FdoG/H/I/FdnG/H). Um die Spezifität der Analyse zu bestätigen wurde eine *selC* Mutante untersucht, die nicht mehr in der Lage ist Formiatdehydrogenasen zu synthetisieren. In Extrakten dieses Stammes konnte die Aktivitätsbande nicht detektiert werden.

Weiterhin wurde eine *fnr* Mutation in einen Hydrogenase-defizienten Stamm eingebracht und eine Intensivierung der Bande unter fermentativen Bedingungen beobachtet. Die Transkription des *fdn*-Operons ist Fnr abhängig, während die für Fdh-O kodierenden Gene von Fnr unabhängig exprimiert werden. Dass Fdh-O den Hauptanteil der Aktivität in dieser Bande ausmacht, beweist die Einführung einer Deletion in das Gen für die Fdh-O große Untereinheit (*fdoG*), welche die Aktivität fast vollständig vermindert. Eine Deletion des Gens für die große Untereinheit von Fdh-N (*fdnG*) hatte unter fermentativen Anzuchtbedingungen keinen Einfluss, verringerte jedoch die Intensität der Aktivitätsbande nach Anzucht unter Nitratrespiratorischen Bedingungen. Die für die akzessorischen Proteine FdhD und FdhE kodierenden Gene werden in Nachbarschaft vom *fdo*-Operon exprimiert und obwohl die Funktion beider Genprodukte nicht genau bekannt ist, sind sie essentiell für die Aktivitäten von Fdh-O und Fdh-N. Die Deletion dieser Gene verhinderte ebenfalls den Nachweis der Aktivitätsbande. Einen Polaritätseffekt von einer *fdo*-Deletion auf die Expression des stromabwärts gelegenen *fdhE*-Gens konnte ausgeschlossen werden, da die Zugabe von *fdhE in trans* keinen Effekt auf Intensität der Fdh-O/-N Bande hatte (Paper Abb. 4, rechte Spur).

Bei den Färbungen war es möglich die Aktivität sowohl mit Phenazinmethosulfat (PMS):Nitroblautetrazoliumchlorid (NBT) als auch mit BV:2,3,5-Triphenyltetrazoliumchlorid (TTC) sichtbar zu machen. Zusätzlich konnte mit PMS auch die Aktivität von Hyd-1 detektiert werden, während Hyd-2 jedoch ausschließlich mit BV reagiert (Daten nicht gezeigt).

Obwohl beide Enzyme gemeinsam zur Aktivtätsbande beitragen, sie gleiches Migrationsverhalten im Gel aufweisen, FdnH *in vitro* sowohl mit FdnG als auch FdoG interagiert und ihre Identität 74 % beträgt, konnten bisher keine Vermischung der Untereinheiten festgestellt werden (Lüke *et al.*, 2008), jedoch besteht theoretisch die Möglichkeit, dass bei der Trimerisierung der Trimere zu ihrer Quartärstruktur verschiedene Enzyme einen Anteil beitragen.

2.6.2 Artikelkopie

BMC
Microbiology

RESEARCH ARTICLE

Open Access

The respiratory molybdo-selenoprotein formate dehydrogenases of *Escherichia coli* have hydrogen: benzyl viologen oxidoreductase activity

Basem Soboh[1†], Constanze Pinske[1†], Martin Kuhns[1], Mandy Waclawek[1], Christian Ihling[2], Karen Trchounian[3], Armen Trchounian[3], Andrea Sinz[2] and Gary Sawers[1*]

Abstract

Background: *Escherichia coli* synthesizes three membrane-bound molybdenum- and selenocysteine-containing formate dehydrogenases, as well as up to four membrane-bound [NiFe]-hydrogenases. Two of the formate dehydrogenases (Fdh-N and Fdh-O) and two of the hydrogenases (Hyd-1 and Hyd-2) have their respective catalytic subunits located in the periplasm and these enzymes have been shown previously to oxidize formate and hydrogen, respectively, and thus function in energy metabolism. Mutants unable to synthesize the [NiFe]-hydrogenases retain a H_2: benzyl viologen oxidoreductase activity. The aim of this study was to identify the enzyme or enzymes responsible for this activity.

Results: Here we report the identification of a new H_2: benzyl viologen oxidoreductase enzyme activity in *E. coli* that is independent of the [NiFe]-hydrogenases. This enzyme activity was originally identified after non-denaturing polyacrylamide gel electrophoresis and visualization of hydrogen-oxidizing activity by specific staining. Analysis of a crude extract derived from a variety of *E. coli* mutants unable to synthesize any [NiFe]-hydrogenase-associated enzyme activity revealed that the mutants retained this specific hydrogen-oxidizing activity. Enrichment of this enzyme activity from solubilised membrane fractions of the hydrogenase-negative mutant FTD147 by ion-exchange, hydrophobic interaction and size-exclusion chromatographies followed by mass spectrometric analysis identified the enzymes Fdh-N and Fdh-O. Analysis of defined mutants devoid of selenocysteine biosynthetic capacity or carrying deletions in the genes encoding the catalytic subunits of Fdh-N and Fdh-O demonstrated that both enzymes catalyze hydrogen activation. Fdh-N and Fdh-O can also transfer the electrons derived from oxidation of hydrogen to other redox dyes.

Conclusions: The related respiratory molybdo-selenoproteins Fdh-N and Fdh-O of *Escherichia coli* have hydrogen-oxidizing activity. These findings demonstrate that the energy-conserving selenium- and molybdenum-dependent formate dehydrogenases Fdh-N and Fdh-O exhibit a degree of promiscuity with respect to the electron donor they use and identify a new class of dihydrogen-oxidizing enzyme.

* Correspondence: gary.sawers@mikrobiologie.uni-halle.de
† Contributed equally
[1]Institute for Microbiology, Martin-Luther University Halle-Wittenberg, Kurt-Mothes-Str. 3, 06110 Halle (Saale), Germany
Full list of author information is available at the end of the article

BioMed Central

Background

Hydrogen and formate are electron donors frequently used by anaerobic microorganisms. Metabolism of hydrogen and formate is often highly interlinked in many bacteria that can oxidize both compounds. This is exemplified in the fermentative metabolism of the enterobacterium *Escherichia coli* where up to one third of the carbon from glucose is converted to formate; formate is then disproportionated to H_2 and CO_2 [1-3]. Formate can be metabolized by three membrane-associated, molybdo-seleno formate dehydrogenases (Fdh), termed Fdh-H (associated with hydrogen production), Fdh-N (induced in the presence nitrate) and Fdh-O (also detected during aerobic growth). Fdh-H is encoded by the *fdhF* gene and together with one of the four [NiFe]-hydrogenases (Hyd) of *E. coli*, Hyd-3, forms the hydrogen-evolving formate hydrogenlyase (FHL) enzyme complex.

Fdh-N (FdnGHI) and Fdh-O (FdoGHI) are highly related enzymes at both the amino acid sequence and functional levels [1,4]. They are multi-subunit oxidoreductases each comprising a large catalytic subunit (FdnG or FdoG), an electron-transfer subunit (FdnH or FdoH) and a membrane-anchoring subunit (FdnI or FdoI); the latter has a quinone-binding site that allows transfer of electrons derived from formate oxidation into the respiratory chain [4-6]. Both enzymes have their respective active site located on the periplasmic face of the cytoplasmic membrane and they couple formate oxidation to energy conservation. A key feature of all three Fdh enzymes is the presence of selenocysteine, a *bis*-molybdopterin guanine dinucleotide (*bis*-MGD) cofactor and a [4Fe-4S] cluster in their respective catalytic subunit [4,7]. Although the synthesis of the Fdh-N enzyme is induced to maximal levels during growth in the presence of nitrate, the enzyme is also present at lower levels during fermentative growth [1,5,8]. Fdh-O is synthesized constitutively and is present at low levels aerobically, during fermentative growth and nitrate respiration [6,9].

E. coli has also the coding capacity to synthesize four membrane-associated, multi-subunit Hyd enzymes, which are termed Hyd-1 through Hyd-4 [2,10]. Hyd-1, Hyd-2 and Hyd-3 have been characterized in detail. Like Fdh-N and Fdh-O, Hyd-1 and Hyd-2 have their active sites located facing the periplasm [11]. Both enzymes oxidize hydrogen and contribute to energy conservation. Due to the fact that hydrogenases catalyze the reversible oxidation of dihydrogen *in vitro*, the activities of all three characterized [NiFe]-hydrogenases of *E. coli* can be determined simultaneously in a single reaction using hydrogen as electron donor and the artificial electron acceptor benzyl viologen (BV) [12,13]. Moreover, the hydrogen-oxidizing activities of Hyd-1 and Hyd-2 can also be visualized after electrophoretic separation under non-denaturing conditions in the presence of detergent [12]. Because of its apparent labile nature the activity of Hyd-3 cannot be visualized after gel electrophoresis.

It was noted many years ago [14] that in non-denaturing polyacrylamide gels a slowly-migrating protein complex with a hydrogen: BV oxidoreductase enzyme activity, apparently unrelated to either Hyd-1 or Hyd-2, could be visualized after electrophoretic separation of membrane fractions derived from *E. coli* grown under anaerobic conditions. In this study, this hydrogenase-independent enzyme activity could be identified as being catalyzed by the highly related Fdh-N and Fdh-O enzymes.

Results

Hydrogenase-independent hydrogen: BV oxidoreductase activity in *E. coli* membranes

Membrane fractions derived from anaerobically cultured wild-type *E. coli* K-12 strains such as P4X [12,15] and MC4100 [16] exhibit a slowly migrating hydrogen: benzyl viologen (BV) oxidoreductase activity that cannot be assigned to either Hyd-1 or Hyd-2. Previous findings based on non-denaturing PAGE [16] estimated a size of approximately 500 kDa for this complex. To demonstrate the hydrogenase-independent nature of this enzyme activity, extracts derived from a *hypF* mutant, which lacks the central hydrogenase maturase HypF and consequently is unable to synthesize active [NiFe]-hydrogenases [17], retained this single slowly migrating species exhibiting hydrogen:BV oxidoreductase activity, while the activity bands corresponding to Hyd-1 and Hyd-2 were no longer visible (Figure 1). This result demonstrates that the activity of this slowly migrating band is completely unrelated to the [NiFe]-hydrogenases Hyd-1, Hyd-2, Hyd-3 or Hyd-4. Note that no active, stained bands were observed when this experiment was performed with a nitrogen gas atmosphere (data not shown).

Formate dehydrogenases N and O catalyze hydrogen:BV oxidoreduction

In order to identify the enzyme(s) responsible for this new hydrogen: BV oxidoreductase activity, the *hypF* deletion mutant was grown anaerobically and the membrane fraction was prepared (see Methods). The hydrogen: BV oxidoreductase activity could be released from the membrane in soluble form by treatment with the detergent Triton X-100. Enrichment of the activity was achieved by separation from contaminating membrane proteins using Q-sepharose anion exchange, phenyl sepharose hydrophobic interaction chromatography and
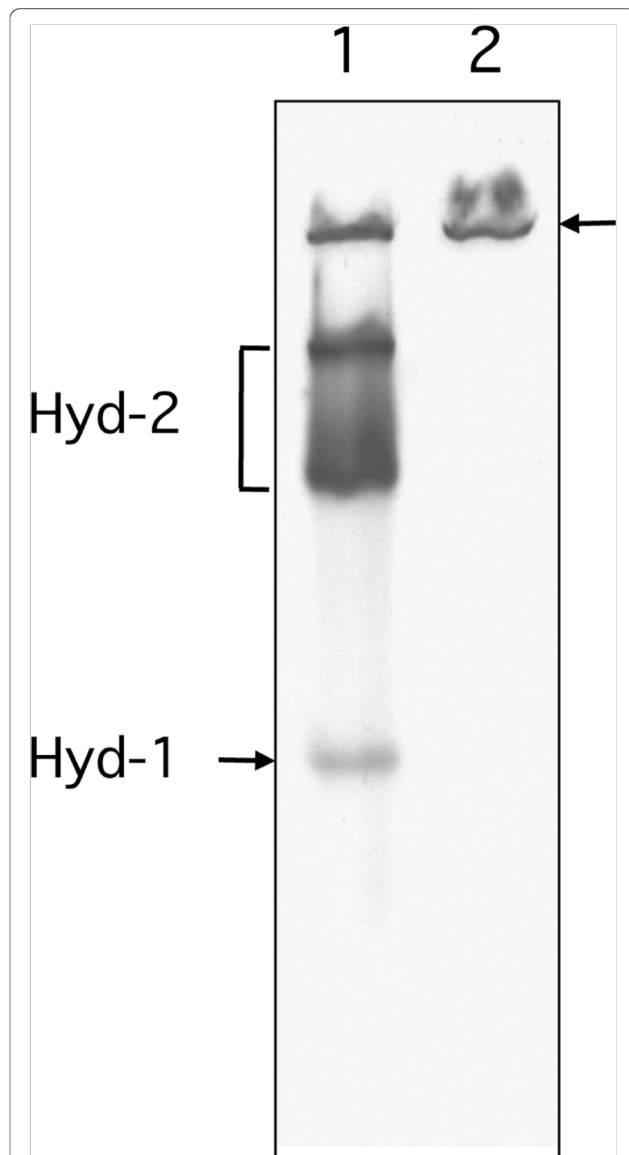
Figure 1 A *hypF* mutant retains hydrogenase-independent H$_2$: BV oxidoreductase activity. Extracts derived from MC4100 (lane 1) and the isogenic Δ*hypF* mutant DHP-F2 (lane 2) were separated by non-denaturing PAGE and subsequently stained for hydrogenase enzyme activity as described in the Methods section. Strains were grown in TYEP medium with 0.8% (w/v) glucose, pH 6.5. Equivalent amounts of Triton X-100-treated crude extract (50 μg of protein) were applied to each lane. The activity bands corresponding to Hyd-1 and Hyd-2 are indicated, as is the slowly migrating activity band (designated by an arrow) that corresponds to a hydrogenase-independent H$_2$:BV oxidoreductase enzyme activity.

activity gel identifying the active enzyme, are shown in Figure 2. Two distinct peaks that absorbed at 280 nm could be separated (Figure 2A) and the hydrogen: BV oxidoreductase activity was found to be exclusively associated with the higher molecular mass symmetric peak labelled P1 (Figure 2B). This peak eluted after 47 ml (V$_o$ = 45 ml) and was estimated to have a mass of between 500-550 kDa (data not shown).

The band showing hydrogen: BV oxidoreductase activity in Figure 2B was carefully excised and the polypeptides within the fraction were analyzed by mass
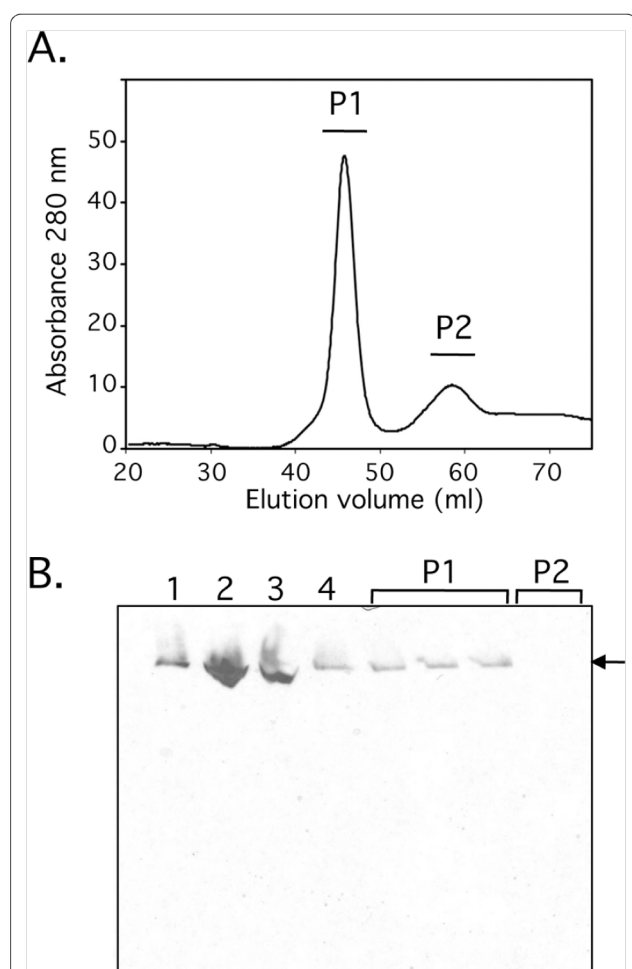
Figure 2 Chromatographic separation of the H$_2$: BV oxidoreductase activity on a Superdex-S200 column. A. A representative elution profile of the enriched H$_2$: BV oxidoreductase enzyme activity after size exclusion chromatography on Superdex-S200 is shown. The absorbance at 280 nm was monitored and the two main elution peaks were labelled P1 and P2. B. Samples of the fractions across the elution peaks P1 and P2 were separated by non-denaturing PAGE and subsequently stained for hydrogenase enzyme activity. Lane 1, crude cell extract (50 μg protein); lane 2, membrane fraction (50 μg protein); lane 3, solubilised membrane fraction (50 μg protein); lane 4, aliquot of the 400 mM fraction from the Q-sepharose column. The arrow identifies the H$_2$: BV oxidoreductase enzyme activity.

finally gel filtration on a Superdex-200 size exclusion column (see Methods for details). Fractions with enzyme activity were monitored during the enrichment procedure using activity-staining after non-denaturing PAGE. A representative elution profile from the Superdex-200 chromatography step, together with the corresponding

spectrometry. Both Fdh-O and Fdh-N enzymes were unambiguously identified: the polypeptides FdoG, FdoH, FdoI, FdnG, and FdnH were identified. The catalytic subunits of Fdh-O and Fdh-N share 74% amino acid identity and both enzymes are synthesized at low levels during fermentative growth. Fdh-N is a trimer of trimers ($\alpha\beta\gamma$) with molecular mass of 510 kDa [4] and this correlates well with the estimated size of the protein complex showing H_2: BV oxidoreductase activity as revealed by non-denaturing PAGE and size exclusion chromatography.

Both Fdh-N and Fdh-O can catalyze the formate-dependent reduction of either BV or DCPIP (2,6-dichlorophenolindophenol) [8,9], whereby Fdh-N transfers electrons much more readily to DCPIP than to BV [8]. Analysis of fraction P1 from the gel filtration experiment revealed a formate: BV oxidoreductase activity of 67 mU mg protein^{-1} and a formate: DCPIP oxidoreductase activity of 0.64 U mg protein^{-1} (Table 1). In comparison, the H_2: BV oxidoreductase activity of fraction P1 was 15 mU mg protein^{-1}, while no enzyme activity could be detected when hydrogen gas was replaced with nitrogen gas.

All three Fdh enzymes in *E. coli* are selenocysteine-containing proteins [1,2,18]. Therefore, a mutant unable to incorporate selenocysteine co-translationally into the polypeptides should lack this slow-migrating enzyme H_2-oxidizing activity. Analysis of crude extracts derived from the *selC* mutant FM460, which is unable to synthesize the selenocysteine-inserting tRNA^{SEC} [19], lacked the hydrogenase-independent activity band observed in the wild-type (Figure 3), consistent with the activity being selenium-dependent. Notably Hyd-1 and Hyd-2 both retained activity in the *selC* mutant.

Fdh-N and Fdh-O can also transfer the electrons from hydrogen to other redox dyes

The catalytic subunits of Fdh-N and Fdh-O are encoded by the *fdnG* and *fdoG* genes, respectively [5,6]. To analyse the extent to which Fdh-N and Fdh-O contributed

Table 1 Activity of enriched enzyme fraction with different electron donors

Electron donor and acceptor[a]	Specific Activity (mU mg protein^{-1})[b]
H_2 and benzyl viologen	14.8 ± 2.3
Benzyl viologen without an electron donor	< 0.20
Formate and benzyl viologen	1.24 ± 1.0
Formate and PMS/DCPIP	638.3 ± 69

[a] The buffer used was 50 mM sodium phosphate pH 7.2; BV was used at a final concentration of 4 mM; formate was added to a final concentration of 18 mM; and PMS/DCPIP were added at final concentrations of 20 μM and 78 μM, respectively.
[b] The mean and standard deviation (±) of at least three independent experiments are shown.
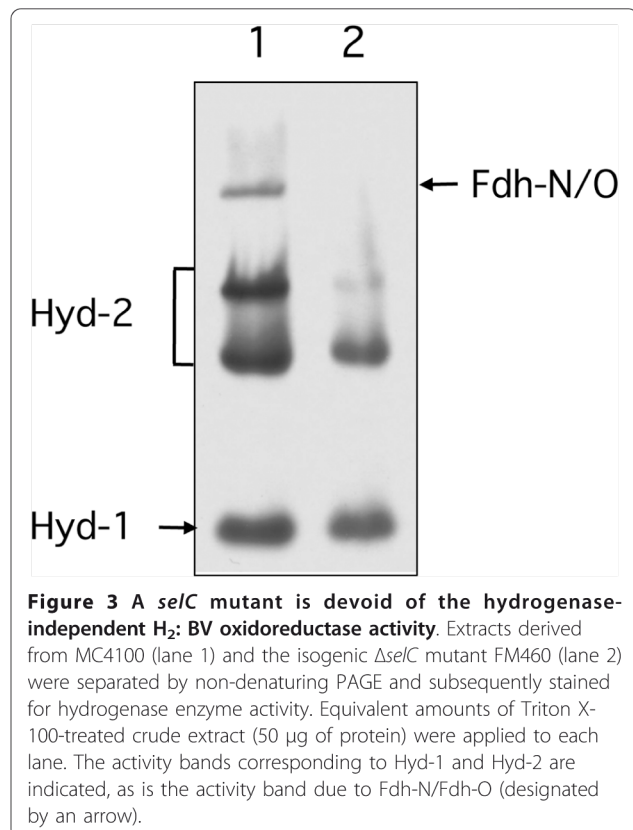
Figure 3 A *selC* mutant is devoid of the hydrogenase-independent H_2: BV oxidoreductase activity. Extracts derived from MC4100 (lane 1) and the isogenic ΔselC mutant FM460 (lane 2) were separated by non-denaturing PAGE and subsequently stained for hydrogenase enzyme activity. Equivalent amounts of Triton X-100-treated crude extract (50 μg of protein) were applied to each lane. The activity bands corresponding to Hyd-1 and Hyd-2 are indicated, as is the activity band due to Fdh-N/Fdh-O (designated by an arrow).

to hydrogen: BV oxidoreductase activity after fermentative growth the activity in mutants with a deletion mutation either in *fdnG* or in *fdoG* was analyzed. Introduction of a deletion mutation in the *fdnG* gene resulted in a slight reduction in intensity of the H_2: BV oxidoreductase activity band (Figure 4A). The *fdoG* mutation also resulted in a similar phenotype (Figure 4A). Introduction of the *fdnG* or *fdoG* genes on plasmids into the respective mutants restored full activity. An activity band associated with Hyd-2 was used as a loading control for these experiments. Strain FTD147, which has mutations in the genes encoding the catalytic subunits of Hyd-1, Hyd-2 and Hyd-3 [20], and thus cannot synthesize active [NiFe]-hydrogenases, lacked the Hyd-2 activity band but retained the Fdh-N/O hydrogen-oxidizing activity (Figure 4A top panel). Note that the isogenic wild type BW25113 of the JW series of strains had an identical phenotype to that of MC4100 (data not shown). These experiments demonstrate that under fermentative growth conditions Fdh-N and Fdh-O both contribute to the H_2: BV oxidoreductase enzyme activity.

Fdh-N and Fdh-O catalyze the formate-dependent reduction of phenazine methosulphate/nitroblue tetrazolium (PMS/NBT), which can be used to visualize Fdh enzyme activity after non-denaturing PAGE [8]. Staining

Figure 4 Analysis of H$_2$- and formate-oxidizing activities of Fdh-N/O in different mutant backgrounds. Small-scale cultures of each strain were grown in TGYEP medium in the absence (A) or presence of nitrate (B). Extracts derived from the strains indicated were separated by non-denaturing PAGE and subsequently stained for H$_2$: BV oxidoreductase (top panel), H$_2$: PMS/NBT oxidoreductase (middle panel) or formate: PMS/NBT oxidoreductase (bottom panel) enzyme activity as described in the Methods section. Equivalent amounts of Triton X-100-treated crude extract (25 μg of protein) were applied to each lane. The activity band due to Fdh-N/Fdh-O is labelled by an arrow. The activity band due to hydrogenase 2 (Hyd-2) is also labelled in the top panel of part A and was used as a loading control for the experiment. Note the Hyd-2 activity can only be identified as a H$_2$: BV oxidoreductase activity. The asterisk indicates hydrogenase activity associated with incompletely solubilised membrane material. The gel stained for H$_2$: BV oxidoreductase activity was incubated for 8 h, while the gels stained with PMS/NBT were incubated for 1 h. In the interests of clarity, lanes were labelled based on the key genotype of the strain used. Lanes: MC4100 (wild type); FTD147 (Δ*hyaB* Δ*hybC* Δ*hycE*); FTD147 Δ*fnr* signifies CP1104; Δ*fdhE* signifies JW3862 (Δ*fdhE*); Δ*fdhE*/pfdhE signifies JW3862 complemented with plasmid pCA24N-*fdhE*[+]; Δ*fdhD* signifies JW3866 (Δ*fdhD*); Δ*fdhD*/pfdhD signifies JW3866 complemented with plasmid pCA24N-*fdhD*[+]; Δ*fdnG* signifies JW1470 (Δ*fdnG*); Δ*fdnG*/pfdnG signifies JW1470 complemented with plasmid pCA24N-*fdnG*[+]; Δ*fdoG* signifies JW3865 (Δ*fdoG*); Δ*fdoG*/pfdoG signifies JW3865 complemented with plasmid pCA24N-*fdoG*[+]; Δ*fdoG*/pfdhE signifies JW3865 complemented with plasmid pCA24N-*fdhE*[+]. Note that BW25113 had an identical phenotype in these experiments to MC4100.

for formate: PMS/NBT oxidoreductase enzyme activity (Figure 4A, bottom panel) revealed that after growth under fermentative conditions, Fdh-O had a stronger contribution to the overall intensity of the activity band than Fdh-N, because while extracts derived from the *fdnG* mutant had similar activity to the wild type, the activity in an extract from the *fdoG* mutant was considerably reduced. Introduction of the *fdoG* gene on a plasmid, however, restored the activity to the mutant (Figure 4A bottom panel). Notably, replacing formate with hydrogen as electron donor revealed that both enzymes also catalyzed the hydrogen-dependent reduction of PMS/NBT (Figure 4A, middle panel). A similar pattern for H_2: PMS/NBT oxidoreductase activity was observed as was seen for formate: PMS/NBT oxidoreductase activity (compare the middle and bottom panels in Figure 4A). Taken together, these findings suggest that Fdh-N is the more effective enzyme at transferring the electrons from H_2 to BV/TTC than to PMS/NBT. That Fdh-O is nevertheless effective at catalyzing H_2-dependent BV reduction is shown in the lane containing an extract derived from CP1104 (labelled FTD147Δ*fnr* in Figure 4) in which an *fnr* mutation was introduced into the hydrogenase-negative strain FTD147 (Figure 4, top panel). Synthesis of Fdh-N is absolutely dependent on the redox regulator FNR [1,21] and thus is absent in an *fnr* mutant. In contrast, Fdh-O activity is apparently up-regulated in the *fnr* mutant (Figure 4A).

Fdh-N/O show H_2: BV and H_2: PMS/NBT oxidoreductase activities in extracts after respiratory growth with nitrate

Biosynthesis of Fdh-N is enhanced when *E. coli* is grown anaerobically in the presence of nitrate [1,5,21], while synthesis of Fdh-O is essentially constitutive [9]. The same strains analyzed in Figure 4A were grown anaerobically in the presence of nitrate and aliquots of crude extracts were separated by non-denaturing PAGE followed by staining for H_2: BV oxidoreductase, H_2: PMS/NBT oxidoreductase and formate: PMS/NBT oxidoreductase activities. The gel presented in the top panel of Figure 4B shows clearly a H_2: BV oxidoreductase activity in extracts of strains FTD147, CP1104 (FTD147Δ*fnr*), as well as in the *fdoG* mutant. The activity in extracts of MC4100 shown in this experiment was only weakly discernable (Figure 4B, top panel, first lane). As anticipated [13], synthesis of Hyd-1 and Hyd-2 was strongly reduced in MC4100 after growth in the presence of nitrate (data not shown). The mutant with a deletion in the *fdnG* gene essentially lacked H_2: BV oxidoreductase activity but this could be recovered by introduction of the *fdnG* gene on plasmid pCA24N-*fdnG*⁺ (Figure 4B, top panel).

Aliquots of the same extracts specifically stained to visualize H_2: PMS/NBT oxidoreductase and formate: PMS/NBT oxidoreductase activities showed a strong

Fdh-N-dependent H_2: PMS/NBT oxidoreductase activity (Figure 4B, middle panel). Substituting hydrogen with formate as electron donor delivered a similar staining pattern (Figure 4B, bottom panel).

Hydrogen oxidation by Fdh-N and Fdh-O is dependent on the accessory proteins FdhD and FdhE

The *fdoGHI* operon encoding Fdh-O is flanked by *fdhD* and *fdhE*, both of which encode accessory enzymes required for the synthesis of active Fdh enzymes [22,23]. To demonstrate the dependence of the H_2-oxidizing activities of both Fdhs on FdhD and FdhE, individual mutants lacking either the *fdhD* or the *fdhE* gene were analyzed under the same conditions as described above for the wild type and *fdoG* and *fdnG* mutants. All three activities were absolutely dependent on both FdhD and FdhE (Figure 4). Complementation experiments revealed that while FdhD on a plasmid fully complemented the *fdhD* mutation, plasmid-encoded FdhE only partially complemented the *fdhE* mutation.

Discussion

We demonstrate here that both of the respiratory formate dehydrogenases Fdh-N and Fdh-O have hydrogen-oxidizing enzyme activity. Together with the three characterized [NiFe]-hydrogenases, these are the only two enzymes in *E. coli* crude extracts that had this activity. These results suggest that the Fdh-N and Fdh-O enzymes show a degree of non-specificity with regard to the electron donor they can use. Notably, formate and dihydrogen (CO_2/formate, E_o' = -432 mV [24]) and (H^+/hydrogen, E_o' = -414 mV) are both strong reductants.

Previous studies have demonstrated that *E. coli* can couple hydrogen oxidation to nitrate reduction and Hyd-1 and Hyd-2 participate in this process [25]. However, attempts to demonstrate significant hydrogen-dependent nitrate reduction in the absence of Hyd-1 and Hyd-2 did not deliver reproducible levels of hydrogen oxidation, presumably due to the limited hydrogen-oxidizing activity of Fdh-N and Fdh-O. Nevertheless, the findings reported here might have physiological relevance in other microorganisms. For example, enzymes with subunits orthologous to FdnG are found in the obligate dehalorespiring and hydrogen-oxidizing *Dehalococcoides* spp., e.g. strain CBDB1, and have an associated subunit with similarity to hydrogenase membrane-anchoring subunits [26]. Rather than having a selenocysteinyl residue in their presumptive active site they have a seryl residue. It is established that in *E. coli* replacement of selenocysteine with serine abolishes the formate-oxidizing activity of Fdh-H [27]. Moreover, it is also clear that *Dehalococcoides* strain CBDB1 cannot use formate as a substrate, suggesting that this formate dehydrogenase-like enzyme might have another

function. One possibility based on the findings presented here might be that it accepts H_2 as substrate.

As both Fdh enzymes are selenium-dependent, impaired co-translational insertion of selenocysteine prevented synthesis of either enzyme and concomitantly abolished the [NiFe]-hydrogenase-independent H_2: BV oxidoreductase activity. Moreover, because both Fdh-N and Fdh-O are absolutely dependent on the FdhE and FdhD proteins for activity of the enzyme [22,23], deletion of *fdhE* and *fdhD* also abolished specifically this H_2: BV oxidoreductase activity. The precise functions of FdhD and FdhE in formate dehydrogenase biosynthesis remain to be established; however, it is likely that they perform a function in post-translational maturation of the enzymes [22].

While it is established that the iron-molybdenum cofactor in nitrogenase catalyzes unidirectional proton reduction as an inevitable consequence of nitrogen reduction [28], the studies here present the first report of a seleno-molybdenum enzyme catalyzing dihydrogen activation. Recent studies have shown that high-valence (oxidation state VI) oxo-molybdenum model complexes can activate dihydrogen at high temperature and H_2 pressure [29]. The crystal structure of Fdh-N [4] also reveals a similar geometry of the molybdenum atom to these model complexes; however, along with the four *cis* thiolate groups, which are derived from the two MGD cofactors, a hydroxyl from a water molecule and the selenate group from selenocysteine coordinate the Mo atom. The coordination geometry might play an important role in conferring hydrogen activation capability, as the molybdoenzyme nitrate reductase from *E. coli* [30] cannot oxidize dihydrogen. Instead of the selenate ligand, nitrate reductase has an oxo ligand to the Mo, which is contributed by an aspartate residue. In this regard, however, it should be noted that although the third formate dehydrogenase Fdh-H also has similar active site geometry to Fdh-N [4,7], we could not detect a dihydrogen-activating activity associated with this enzyme in our gel system. In contrast to other molybdopterin-containing molybdoenzymes catalyzing oxo-transfer of the oxygen from H_2O to the substrate, Fdh-H, and presumably also Fdh-N and Fdh-O, catalyze the direct release of CO_2 and not bicarbonate from formate [31]. The transfer of the proton from formate to a histidine and concomitant reduction of Mo(VI) to Mo(IV) facilitates direct release of CO_2 with the cofactor returning to the oxidized Mo(VI) state after electron transfer to the iron-sulfur cluster [31]. Such a dehydrogenation reaction could explain the inefficient oxidation of H_2 by Fdh-N/O demonstrated here. Future studies will focus on testing this hypothesis to characterize the mechanism of dihydrogen activation.

Conclusions

The energy-conserving formate dehydrogenases of *E. coli* can use dihydrogen as an enzyme substrate. Apart from the [NiFe]-hydrogenases, these enzymes were the only ones in extracts of anaerobically grown *E. coli* that could oxidize hydrogen and transfer the electrons to benzyl viologen or phenazine methosulfate/nitroblue tetrazolium. While the possible significance of this activity to the general anaerobic physiology of *E. coli* remains to be established, this finding has potentially important implications for our understanding of the hydrogen metabolism of other anaerobic microorganisms.

Methods

Strains, plasmids and growth conditions

All bacterial strains and plasmids used in this study are listed in Table 2. Bacterial growth of all *E. coli* strains was performed at 37°C. *E. coli* cells were cultivated anaerobically in buffered TYEP medium [32] supplemented with 0.8% (w/v) glucose. Where indicated formate was added to a final concentration of 15 mM and nitrate to 15 mM. Aerobic cultures were grown in flasks filled maximally to 10% of their volume, while anaerobic cultures were grown in stoppered bottles filled to the top with medium. When required, kanamycin was added to a final concentration of 50 μg/ml and chloramphenicol to a final concentration 15 μg/ml. Cultures were harvested after reaching an optical density at 600 nm of 0.9 was attained. Cells were collected by

Table 2 Strains and plasmids used in this study

Strains	Genotype	Reference or source
MC4100	F⁻ *araD139* Δ(*argF-lac*)*U169 ptsF25 deoC1 relA1 flbB5301 rspL150⁻*	[38]
MC-NG	Like MC4100, but Δ*fdnG*	This work
MC-OG	Like MC4100, but Δ*fdoG*	This work
FM460	Like MC4100, but Δ*selC*	[34]
DHP-F2	Like MC4100, but Δ*hypF*	[17]
FTD147	Like MC4100, but Δ*hyaB*, Δ*hybC*, Δ*hycE*	[19]
CP1104	Like FTD147, but Δ*fnr*	This work
JW1328	BW25113 Δ*fnr*	[39]
JW3862	BW25113 Δ*fdhE*	[39]
JW3866	BW25113 Δ*fdhD*	[39]
JW1470	BW25113 Δ*fdnG*	[39]
JW3865	BW25113 Δ*fdoG*	[39]
Plasmids		
pfdhE	pCA24N *fdhE*⁺	[39]
pfdhD	pCA24N *fdhD*⁺	[39]
pfdnG	pCA24N *fdnG*⁺	[39]
pfdoG	pCA24N *fdoG*⁺	[39]

centrifugation at 50,000 xg for 20 min at 4°C. Harvested cell pellets were suspended in 50 ml 50 mM MOPS pH 7.5 and re-centrifuged under the same conditions. Washed cell pellets were either used immediately or stored at -20°C until use.

Strain construction

Deletions in the *fdnG* and *fdoG* genes were introduced into appropriate strains by $P1_{kc}$ transduction [33] using strains JW1470 ($\Delta fdnG$::Kan^R) or JW3865 ($\Delta fdoG$::Kan^R) (obtained from the National BioResources Project, Japan) as donors. The *selC* mutation from FM460 [34] was moved in a similar manner into clean genetic backgrounds. Similarly, the *fnr* mutation from JW1328 was transduced into FTD147 to create FTD147Δfnr.

Measurement of enzyme activity

Hydrogen-dependent reduction of benzyl viologen (referred to as hydrogenase activity) was determined as described [12] using 50 mM sodium phosphate pH 7.2. One unit of enzyme activity is defined as that which reduces 1 µmol of dihydrogen min^{-1}. Formate dehydrogenase enzyme activity was assayed spectrophotometrically at RT by monitoring the formate-dependent, PMS-mediated reduction of 2, 6- dichlorophenolindophenol (DCPIP) exactly as described [35] or the formate-dependent reduction of benzyl viologen. The latter assay was performed exactly as for the hydrogenase assay with the exception that 50 mM formate replaced hydrogen as enzyme substrate. One unit of enzyme activity is defined as that which oxidizes 1 µmol of formate min^{-1}.

Protein concentration was determined [36] with bovine serum albumin as standard.

In-gel visualization of enzyme activity

Detection of hydrogenase enzyme activity after non-denaturing PAGE was performed as described [12]. Samples of crude extract or fractions after Q-sepharose, phenyl sepharose and Superdex 200 (5 to 50 µg of protein) were incubated with 4% (v/v) Triton X-100 for 30 min prior to application to the gels. After electrophoretic separation of the proteins, the gels were incubated in 50 mM MOPS pH 7.2 containing 0.5 mM BV and 1 mM 2, 3, 5-triphenyltetrazolium chloride and they were incubated under a hydrogen: nitrogen atmosphere (5% H$_2$: 95% N$_2$) at room temperature for 8 h. This assay was used to identify the hydrogen-oxidizing activity during the enrichment procedure described below.

Visualization of formate dehydrogenase enzyme activity was performed exactly as described [8] using phenazine methosulfate as mediator and nitroblue tetrazolium as electron acceptor. Visualization of the hydrogen: PMS/NBT oxidoreductase activity associated with Fdh-N and Fdh-O was performed exactly for formate

dehydrogenase but formate was replaced by hydrogen gas as enzyme substrate.

Preparation of cell extracts and enrichment of the hydrogenase-independent hydrogen-oxidizing activity

Unless indicated otherwise, all steps were carried out under anaerobic conditions in a Coy™ anaerobic chamber under a N$_2$ atmosphere (95% N$_2$: 5% H$_2$) and at 4°C. All buffers were boiled, flushed with N$_2$, and maintained under a slight overpressure of N$_2$.

For routine experiments and enzyme assay determination, washed cells (1 g wet weight) were resuspended in 3 ml of 50 mM MOPS pH 7.5 including 5 µg DNase/ml and 0.2 mM phenylmethylsulfonyl fluoride. Cells were disrupted by sonication (30W power for 5 min with 0.5 sec pulses). Unbroken cell and cell debris were removed by centrifugation for 30 min at 50 000 xg at 4°C and the supernatant (crude extract) was decanted. Small-scale analyses were carried out with 0.1-0.2 g wet weight of cells suspended in a volume of 1 ml MOPS buffer as described above. Cell disruption was done by sonication as described above.

To enrich the protein(s) responsible for the hydrogenase-independent hydrogen-oxidizing activity, crude membranes were isolated from cell extracts routinely prepared from 20 g (wet weight) of cells by ultracentrifugation at 145 000 × g for 2 h. Crude membranes were then suspended in 60 ml of 50 mM MOPS, pH 7.5 (buffer A). Triton X-100 was added to the suspended membrane fraction to a final concentration of 4% (v/v) and the mixture was incubated for 4 h at 4°C with gentle swirling. After centrifugation at 145 000 xg for 1 h to remove insoluble membrane particles, the solubilized membrane proteins present in the supernatant were loaded onto a Q-Sepharose HiLoad column (2.6 x15 cm) equilibrated with buffer A. Unbound protein was washed from the column with 60 ml of buffer A. Protein was eluted from the column with a stepwise NaCl gradient (80 ml each of 0.1 M, 0.2 M, 0.3 M, 0.4 M, 0.5 M and 1 M) in buffer A at a flow rate of 5 ml min^{-1}. Activity was recovered in the fractions eluting with 0.4 M NaCl. The fractions containing enzyme activity were brought to a concentration of 0.5 M ammonium sulfate and loaded onto a hydrophobic interaction chromatography column (Phenyl-Sepharose HiLoad; 2.6 × 10 cm) equilibrated with 0.5 M ammonium sulfate in buffer A. Protein was eluted using a stepped ammonium sulfate gradient (60 ml each of 0.4 M, 0.3 M, 0.2 M, 0.1 M and without ammonium sulfate) in buffer A and at a flow rate of 5 ml min^{-1}. The hydrogen-oxidizing activity was recovered in the fractions eluting with only buffer A. Fractions containing enzyme activity were concentrated by centrifugation at 7,500 × g in centrifugal filters (Amicon Ultra, 50 K, Millipore, Eschborn, Germany) and

applied to a Hi-Load Superdex-200 gel filtration column (2.6 × 60 cm) equilibrated with buffer A containing 0.1 M NaCl. Fractions containing the hydrogen-oxidizing activity eluted after 47 ml (peak maximum); the void volume V_o of the column was 45 ml and the separation range was from 60-600 kDa. Protein was stored in buffer A containing 0.1 M NaCl at a concentration of 3 mg protein ml^{-1}. The activity was stable for several months when stored at -80°C.

Mass spectrometric identification of proteins

For mass spectrometric analysis the gel band showing H_2: BV oxidoreductase activity after hydrophobic interaction chromatography was excised and the proteins within the band were *in-gel* digested following standard protocols [37]. Briefly, protein disulfides were reduced with DTT and cysteines were alkylated with iodoacetamide. Digestion was performed at 37°C for two hours using trypsin as protease. ProteaseMax® surfactant was used in the digestion and extraction solutions to improve the recovery of hydrophobic peptides. The peptide extracts were analyzed by LC/MS on an UltiMate Nano-HPLC system (LC Packings/Dionex) coupled to an LTQ-Orbitrap XL mass spectrometer (ThermoFisher Scientific) equipped with a nanoelectrospray ionization source (Proxeon). The samples were loaded onto a trapping column (Acclaim PepMap C18, 300 μm × 5 mm, 5 μm, 100Å, LC Packings) and washed for 15 min with 0.1% trifluoroacetic acid at a flow rate of 30 μl/min. Trapped peptides were eluted using a separation column (Acclaim PepMap C18, 75 μm × 150 mm, 3 μm, 100Å, LC Packings) that had been equilibrated with 100% A (5% acetonitrile, 0.1% formic acid). Peptides were separated with a linear gradient: 0-50% B (80% acetonitrile, 0.1% formic acid) in 90 min, 50-100% B in 1 min, remain at 100% B for 5 min. The column was kept at 30°C and the flow-rate was 300 nl/min. During the duration of the gradient, *online* MS data were acquired in data-dependent MS/MS mode: Each high-resolution full scan (*m/z* 300 to 2000, resolution 60,000) in the orbitrap analyzer was followed by five product ion scans (collision-induced dissociation (CID)-MS/MS) in the linear ion trap for the five most intense signals of the full scan mass spectrum (isolation window 2 Th). Both precursor and fragment ions were analyzed in the orbitrap analyzer. Dynamic exclusion (repeat count was 3, exclusion duration 180 s) was enabled to allow detection of less abundant ions. Data analysis was performed using the Proteome Discoverer 1.0 (Thermo Fisher Scientific), MS/MS data of precursor ions in the *m/z* range 350-8000 were searched against the SwissProt Database (version 53.3, taxonomy *E. coli*, 8,852 entries) using Mascot (version 2.2, Matrixscience), mass accuracy was set to 3 ppm and 0.01 Da for precursor and fragment ions, respectively. Carbamidomethylation of cysteines was set as static modification and oxidation of methionine as potential modification. Up to four missed cleavages of trypsin were allowed. Proteins identified by at least two peptides with an expectation value < 0.01 were considered as unambiguously identified.

Author details
[1]Institute for Microbiology, Martin-Luther University Halle-Wittenberg, Kurt-Mothes-Str. 3, 06120 Halle (Saale), Germany. [2]Institute of Pharmacy, Martin-Luther University Halle-Wittenberg, Wolfgang-Langenbeck-Str. 1 06120 Halle (Saale), Germany. [3]Department of Biophysics, Yerevan State University, 1 A. Manoukian Str., Yerevan 0025, Armenia.

Authors' contributions
BS, MK, MW, CP and KT carried out the biochemical studies. CI performed the mass spectrometric analyses and CI and AS interpreted the data. BS, CP, AT, AS and RGS conceived the study and helped draft the manuscript. RGS wrote the manuscript. All authors have read and approved the manuscript.

Competing interests
The authors declare that they have no competing interests.

References
1. Sawers G: **The hydrogenases and formate dehydrogenases of** *Escherichia coli. Antonie van Leeuwenhoek* 1994, **66**:57-88.
2. Sawers G, Blokesch M, Böck A: **Anaerobic formate and hydrogen metabolism.** In *EcoSal- Escherichia coli and Salmonella: Cellular and Molecular Biology.* Edited by: Curtiss III R.(Editor in Chief). ASM Press, Washington, D.C; [http://www.ecosal.org], September 2004, posting date.
3. Sawers RG: **Formate and its role in hydrogen production in** *Escherichia coli. Biochem Soc Trans* 2005, **33**:42-46.
4. Jormakka M, Törnroth S, Byrne B, Iwata S: **Molecular basis of proton motive force generation: structure of formate dehydrogenase-N.** *Science* 2002, **295**:1863-1868.
5. Berg BL, Li J, Heider J, Stewart V: **Nitrate-inducible formate dehydrogenase in** *Escherichia coli* **K-12. I. Nucleotide sequence of the** *fdnGHI* **operon and evidence that opal (UGA) encodes selenocysteine.** *J Biol Chem* 1991, **266**:22380-22385.
6. Abaibou H, Pommier J, Benoit S, Giordano G, Mandrand-Berthelot MA: **Expression and characterization of the** *Escherichia coli fdo* **locus and a possible physiological role for aerobic formate dehydrogenase.** *J Bacteriol* 1995, **177**:7141-7149.
7. Boyington JC, Gladyshev VN, Khangulov SV, Stadtman TC, Sun PD: **Crystal structure of formate dehydrogenase H: catalysis involving Mo, molybdopterin, selenocysteine, and an** Fe_4S_4 **cluster.** *Science* 1997, **275**:1305-1308.
8. Enoch HG, Lester RL: **The purification and properties of formate dehydrogenase and nitrate reductase from** *Escherichia coli. J Biol Chem* 1975, **250**:6693-6705.
9. Sawers G, Heider J, Zehelein E, Böck A: **Expression and operon structure of the** *sel* **genes of** *Escherichia coli* **and identification of a third selenium-containing formate dehydrogenase isoenzyme.** *J Bacteriol* 1991, **173**:4983-4993.
10. Forzi L, Sawers RG: **Maturation of [NiFe]-hydrogenases in** *Escherichia coli. Biometals* 2007, **20**:565-578.
11. Sargent F: **Constructing the wonders of the bacterial world: biosynthesis of complex enzymes.** *Microbiology* 2007, **153**:633-651.

12. Ballantine SP, Boxer DH: **Nickel-containing hydrogenase isoenzymes from** anaerobically grown *Escherichia coli* K-12. *J Bacteriol* 1985, **163**:454-459.

13. Sawers RG, Ballantine SP, Boxer DH: **Differential expression of** hydrogenase isoenzymes in *Escherichia coli* K-12: evidence for a third isoenzyme. *J Bacteriol* 1985, **164**:1324-1331.

14. Sawers RG: **Membrane-bound hydrogenase isoenzymes from** *Escherichia coli*. *PhD Thesis* University of Dundee; 1985.

15. Sawers RG, Boxer DH: **Purification and properties of membrane-bound** hydrogenase isoenzyme 1 from anaerobically grown *Escherichia coli* K12. *Eur J Biochem* 1986, **156**:265-275.

16. Pinske C, Sawers RG: **The role of the ferric-uptake regulator Fur and iron** homeostasis in controlling levels of the [NiFe]-hydrogenases in *Escherichia coli*. *Int J Hydrogen Energy* 2010, **35**:8938-8944.

17. Paschos A, Bauer A, Zimmermann A, Zehelein E, Böck A: **HypF, a** carbamoyl phosphate-converting enzyme involved in [NiFe] hydrogenase maturation. *J Biol Chem* 2002, **277**:49945-4995.

18. Böck A, Forchhammer K, Heider J, Baron C: **Selenoprotein synthesis: an** expansion of the genetic code. *Trends Biochem Sci* 1991, **16**:463-467.

19. Leinfelder W, Zehelein E, Mandrand-Berthelot M-A, Böck A: **Gene for a** novel tRNA species that accepts L-serine and co-translationally inserts selenocysteine. *Nature* 1988, **331**:723-725.

20. Redwood MD, Mikheenko IP, Sargent F, Macaskie LE: **Dissecting the roles** of *Escherichia coli* hydrogenases in biohydrogen production. *FEMS Microbiol Lett* 2008, **278**:48-55.

21. Berg BL, Stewart V: **Structural genes for nitrate-inducible formate** dehydrogenase in *Escherichia coli* K-12. *Genetics* 1990, **125**:691-702.

22. Lüke I, Butland G, Moore K, Buchanan G, Lyall V, Fairhurst SA, Greenblatt JF, Emili A, Palmer T, Sargent F: **Biosynthesis of the respiratory formate** dehydrogenases from *Escherichia coli*: characterization of the FdhE protein. *Arch Microbiol* 2010, **190**:685-696.

23. Schlindwein C, Giordano G, Santini CL, Mandrand MA: **Identification and** expression of the *Escherichia coli fdhD* and *fdhE* genes, which are involved in the formation of respiratory formate dehydrogenase. *J Bacteriol* 1993, **172**:6112-6121.

24. Thauer RK, Jungermann K, Decker K: **Energy conservation in chemotrophic** anaerobic bacteria. *Bacteriol Rev* 1977, **41**:100-180.

25. Laurinavichene TV, Tsygankov AA: **The involvement of hydrogenases 1** and 2 in the hydrogen-dependent nitrate respiration of *Escherichia coli*. *Microbiology (Mikrobiologiya, Russia)* 2003, **72**:740-745.

26. Kube M, Zinder SH, Kuhl H, Reinhardt R, Adrian L: **Genome sequence of** the chlorinated compound-respiring bacterium *Dehalococcoides* species strain CBDB1. *Nature Biotechnol* 2005, **23**:1269-1273.

27. Zinoni F, Birkmann A, Leinfelder W, Böck A: **Cotranslational insertion of** selenocysteine into formate dehydrogenase from *Escherichia coli* directed by a UGA codon. *Proc Natl Acad Sci USA* 1987, **84**:3156-3160.

28. Seefeldt LC, Hoffman BM, Dean DR: **Mechanism of Mo-dependent** nitrogenase. *Annu Rev Biochem* 2009, **78**:701-722.

29. Reis PM, Paulo Costa J, Romão CC, Fernandes JA, Calhorda MJ, Royo B: **Hydrogen activation by high-valent oxo-molybdenum(VI) and -rhenium** (VII) and -(V) compounds. *Dalton Trans* 2008, **13**:1727-1733.

30. Bertero MG, Rothery RA, Palak M, Hou C, Lim D, Blasco F, Weiner JH, Strynadka NCJ: **Insights into the respiratory electron transfer pathway** from the structure of nitrate reductase A. *Nature Struct Biol* 2003, **10**:681-687.

31. Khangulov SV, Gladyshev VN, Dismukes GC, Stadtman TC: **Selenium-** containing formate dehydrogenase H from *Escherichia coli*: a molybdopterin enzyme that catalyzes formate oxidation without oxygen transfer. *Biochemistry* 1998, **37**:3518-3528.

32. Begg YA, Whyte JN, Haddock BA: **The identification of mutants of** *Escherichia coli* deficient in formate dehydrogenase and nitrate reductase activities using dye indicator plates. *FEMS Microbiol Lett* 1977, **2**:47-50.

33. Miller JH: *Experiments in Molecular Genetics* Cold Spring Harbor, Cold Spring Harbor Press; 1972.

34. Leinfelder W, Forchhammer K, Zinoni F, Sawers G, Mandrand-Berthelot M-A, Böck A: *Escherichia coli* genes whose products are involved in selenium metabolism. *J Bacteriol* 1988, **170**:540-546.

35. Lester RL, DeMoss JA: **Effects of molybdate and selenite on formate and** nitrate metabolism in *Escherichia coli*. *J Bacteriol* 1971, **105**:1006-1014.

36. Lowry OH, Rosebrough NJ, Farr AL, Randall RJ: **Protein measurement with** the Folin phenol reagent. *J Biol Chem* 1951, **193**:265-275.

37. Shevchenko A, Tomas H, Havliš J, Olsen JV, Mann M: **In-gel digestion for** mass spectrometric characterization of proteins and proteomes. *Nature Protocols* 2007, **1**:2856-60.

38. Casadaban MJ: **Transposition and fusion of the** *lac* **genes to selected** promoters in *Escherichia coli* using bacteriophage lambda and Mu. *J Mol Biol* 1976, **104**:541-555.

39. Kitagawa M, Ara T, Arifuzzaman M, Ioka-Nakamichi T, Inamoto E, *et al*: **Complete set of ORF clones of** *Escherichia coli* ASKA library (a complete set of *E. coli* K-12 ORF archive): unique resources for biological research. *DNA Res* 2005, **12**:291-299.

2.7 Das A-typ Träger-Protein ErpA ist essentiell für die Ausbildung aktiver Formiat-Nitrat Respiration in *Escherichia coli* K-12.

2.7.1 Zusammenfassung

Die Eisen-Schwefel-Cluster Biosynthese in *E. coli* erfolgt entweder durch das Isc oder das Suf System. Dabei werden vorgefertigte [FeS]-Cluster mit Hilfe von A-typ Träger (*A-type carrier* - ATC) Proteinen auf Zielproteine übertragen. Einige Deletionen der Gene für diese ATC Proteine sind aerob letal, während unter anaeroben Bedingungen Wachstum möglich ist (Loiseau *et al.*, 2007). Es konnte hier gezeigt werden, dass auch die anaerobe Nitratatmung durch Deletion von *iscA* stark reduziert und durch Deletion von *erpA* nicht nachweisbar war. Die *iscU* Mutante, mit Deletion des für die zentrale Isc Gerüst-Komponente IscU kodierenden Gens, hatte den gleichen Phänotyp wie die *erpA* Mutante, während eine *sufA* Deletion keinen Effekt zeigte. Als Grund für diesen Phänotyp konnte gezeigt werden, dass die kleinen [FeS]-Cluster haltigen Untereinheiten FdnH und NarH immunologisch nicht mehr nachweisbar waren. Da die letzte Proteinkomponente des *fdnGHI* Operons detektierbar war, ist die komplette Translation des Operons gewährleistet und es muss sich deshalb bei der Abwesenheit von FdnH um post-translationelle Kontrolle handeln. Die großen Untereinheiten NarG und FdnG besitzen ohne ihre kleinen Untereinheiten keine Aktivität und im Fall von FdnG wurde der Transport ins Periplasma verhindert, was sich immunologisch durch ein Laufverhalten des Polypeptides zeigte, welches dem einer Tat Mutante gleicht. Beide großen Untereinheiten besitzen neben dem Molybdopterin-Kofaktor ebenfalls ein [FeS]-Cluster über dessen Assemblierung *in vivo* jedoch keine Aussagen getroffen werden konnten. Lediglich die große Untereinheit der Nitratreduktase NarG weist in den *erpA* und *iscU* Mutanten und in der *erpA iscA* Doppelmutante aberrantes Laufverhalten auf, was auf Instabilität des Polypeptides in diesem Hintergrund hindeutet. Um zu untersuchen, ob die Effekte ausschließlich auf den eingebrachten Deletionen beruhen und ob die ATC-Proteine untereinander austauschbar sind, wurden die Gene *erpA* und *iscA* in Plasmide kloniert und diese in Mutanten transformiert. Dabei konnten die entsprechenden Plasmide die jeweiligen Mutationen komplementieren und zusätzlich konnte mit *iscA* die Aktivität von Fdh-N in einer *erpA* Mutante komplementiert werden. Komplementation mit *sufA* konnte die Aktivität in einer *iscA* oder *erpA* Mutante nicht wieder herstellen. Bisher ist der Übertragungsweg der [FeS]-Cluster vom IscU x IscS Komplex zum Apoprotein nicht geklärt, die Ergebnisse deuten jedoch auf eine gemeinsame oder überlappende Funktion von IscA und ErpA hin.

2.7.2 Artikelkopie

The A-type Carrier Protein ErpA is Essential for Formation of an Active Formate-Nitrate Respiratory Pathway in *Escherichia coli* K-12

Constanze Pinske and R. Gary Sawers[*]

Institute for Biology/ Microbiology, Martin-Luther University Halle-Wittenberg, Kurt-Mothes-Str. 3, 06120 Halle (Saale) Germany

Running title: Iron-sulfur cluster biogenesis in anaerobic enzymes

[*] Address correspondence to: R.G. Sawers, Institute for Biology/ Microbiology, Martin-Luther University Halle-Wittenberg, Kurt-Mothes-Str. 3, 06120 Halle (Saale) Germany
Tel., +49 345 5526350; Fax., +49 345 5527010; Email, gary.sawers@mikrobiologie.uni-halle.de

Abstract.
A-type carrier (ATC) proteins of the Isc (iron-sulfur-cluster) and Suf (sulfur mobilization) iron-sulfur ([Fe-S]) cluster biogenesis pathways are proposed to traffic pre-formed [Fe-S] clusters to apoprotein targets. In this study we analyzed the roles of the ATC proteins ErpA, IscA and SufA in the maturation of the nitrate-inducible, multi-subunit anaerobic respiratory enzymes formate dehydrogenase-N (Fdh-N) and nitrate reductase (Nar). Mutants lacking SufA had enhanced activities of both enzymes. While both Fdh-N and Nar activities were strongly reduced in an *iscA* mutant, both enzymes were inactive in an *erpA* mutant and in a mutant unable to synthesize the [Fe-S] cluster scaffold protein IscU. It could be shown for both Fdh-N and Nar that loss of enzyme activity correlated with absence of the [Fe-S] cluster-containing small subunit. Moreover, a slowly migrating form of the catalytic subunit FdnG of Fdh-N was observed, consistent with impeded TAT-dependent transport. The highly related Fdh-O enzyme was also inactive in the *erpA* mutant. Although the Nar enzyme has its catalytic subunit NarG localized in the cytoplasm, it also exhibited an aberrant migration in an *erpAiscA* mutant suggesting that these modular enzymes lack catalytic integrity due to impaired cofactor bioynthesis. Cross-complementation experiments demonstrated that multicopy IscA could partially compensate for lack of ErpA with respect to Fdh-N activity but not Nar activity. These findings suggest that ErpA and IscA have overlapping roles in assembly of these anaerobic respiratory enzymes but demonstrate that ErpA is essential for the production of active enzymes.

Introduction.

Iron-sulfur ([Fe-S]) clusters are ubiquitous prosthetic groups of many metalloenzymes in almost all life-forms and have a variety of functions in diverse cellular processes. They play a particularly important role in electron transfer in the diverse respiratory oxidoreductases found in microorganisms. Generation of [Fe-S] clusters does not occur spontaneously but requires dedicated machineries that orchestrate their assembly and subsequent transfer to the apoprotein substrates (for reviews see (3, 20, 36)). There are at least three different [Fe-S] biosynthetic systems known in microbes and they are referred to as Nif (nitrogen fixation-associated), Isc (iron sulfur cluster) and Suf (sulfur mobilization). The initial discovery of the specialized NifUS proteins for the generation of [Fe-S] clusters in the nitrogenase enzyme of the nitrogen-fixing bacterium *Azotobacter vinelandii* (19) made it immediately clear that further generalized [Fe-S] machineries in bacteria must exist and these are represented by the Isc and Suf systems in many microbes (45, 53).

The protein components of the Isc and Suf biogenesis systems can be roughly divided into those proteins dedicated to [Fe-S] assembly and those involved in the subsequent trafficking of the pre-formed cluster to the ultimate apo-protein acceptor (36). The proteins proposed to be involved in transfer or trafficking of the [Fe-S] are referred to as A-type carrier (ATC) proteins and the bacterium *Escherichia coli* has three of these, termed IscA, SufA and ErpA (26), which are phylogenetically related (50). There is, however, some debate as to whether these proteins actually might be iron chaperones delivering iron to the respective assembly machineries (52) but current evidence is consistent with a role in direct cluster transfer (33, 36).

An *erpA* mutation severely affects the ability of *E. coli* to respire both in the presence of oxygen or in the presence of alternative electron acceptors such as nitrate (26). This appears to contrast with *iscA* or *sufA* mutants, which can grow anaerobically (50). *E. coli* must be, however, at least partially dependent on the Isc system for nitrate respiration because a mutant lacking the *isc* operon exhibited a 60% reduction in activtiy of the global regulator FNR (31). FNR has an oxygen-sensitive [4Fe-4S] clusters and the protein controls expression of genes required for nitrate respiration (15, 25, 51) (Fig. 1). The extent to which *iscA* and *erpA* mutations affect the maturation and activities of the key enzymes of nitrate respiration has not been examined.

When grown anaerobically in the presence of nitrate *E. coli* induces the synthesis of two large membrane-associated multienzyme complexes, formate dehydrogenase N (Fdh-N) and nitrate reductase (Nar) (40). A further aerobic enzyme, Fdh-O, highly similar to Fdh-N with regard to physiological function, is also synthesized in the presence of nitrate (1, 44). Making use of endogenously generated formate as an electron donor and coupling this to nitrate reduction allows the bacterium to generate a proton gradient using a classical redox-loop chemiosmotic mechanism (8, 21-23, 32, 37) (Fig. 1). Fdh-N, Fdh-O and Nar have a similar modular architecture comprising a large membrane extrinsic catalytic subunit, a small electron-transferring subunit and a membrane-anchoring subunit with a menaquinone/(-ol)-binding site (Fig. 1). The enzymes are arranged on opposite sides of the cytoplasmic membrane, which affords vectorial electron transport but subsequent to biosynthesis requires transport of the FdnGH dimer across the membrane by the TAT-translocon where it subsequently interacts with the integral FdnI subunit to form the final active Fdh-N enzyme (34, 39). Fdh-N/O and Nar have an array of metal-containing prosthetic groups that facilitate electron transfer through each enzyme complex. All three enzymes have a molybdo-bis(molybdopterin guanine dinucleotide) (Mo-bis-MGD) cofactor and a [4Fe-4S] (iron sulfur) cluster in the catalytic subunit, four [4Fe-4S] clusters (or 3 x [4Fe-4S] + 1 x [3Fe-4S] in the case of Nar) in the small subunit and two low-potential heme groups in the membrane anchor subunit. Additionally, Fdh-N (and presumably also Fdh-O) has a selenocysteinyl residue coordinated to the Mo-bis-MGD cofactor and this is required for enzyme activity (1, 7, 21, 22). While a considerable amount is known regarding the biosynthesis and incorporation of selenocysteine and Mo-bis-MGD into these enzymes (40, 41, 43), much less is known about the requirements for biosynthesis of the [4Fe-4S] clusters. In this study we analyzed the biosynthesis and activities of Fdh-N and Nar during nitrate respiration of *E. coli* mutants devoid of the three ATC paralogues IscA, SufA and ErpA.

Materials and Methods.

Strains, plasmids and growth conditions. All bacterial strains and plasmids used in this study are listed in Table 1. Strain CP1223 (MC4100 Δ*sufA::cat*) was constructed by introducing a 327 bp deletion within the *sufA* gene in BW25113 carrying plasmid pKD46 as described (13). PCR with Phusion DNA polymerase (Finnzymes, Germany) was carried out using the chloramphenicol resistance cassette from pKD3 as template and the primers 5'_sufA 5'-CGA TGA AGT GAG GTA AAT CGA TGG ACA TGC ATT CAG GAA C*CC ATG GTC CAT ATG AAT ATC CTC C*-3' and 3'_sufA 5'-TAC GAG ACA TAG TAC CGC CTA TAC CCC AAA GCT TTC GCC A*GC GAT TGT GTA GGC TGG AGC T*-3' (Metabion, Germany). The mutant *sufA* allele was transduced by phage P1*kc* into strain MC4100 resulting in strain CP1223 and the replacement with the 1028 bp pKD3 fragment was verified by PCR using the *sufA* cloning primers.

E. coli was grown aerobically in Erlenmeyer flasks filled to maximally 10% of their volume with TGYEP medium (6) on a rotary shaker (250 rpm) and incubated at 37°C. Anaerobic growths were performed at 37°C in sealed bottles filled with anaerobic growth medium under a nitrogen gas atmosphere. To elicit induction of Fdh-N and Nar enzyme synthesis 100 mM potassium nitrate was added to the growth medium. When required, the growth medium was solidified with 1.5 % (w/v) agar. All growth media were supplemented with 0.1% (v/v) SLA trace element solution (17). When growing strain DV1151 culture media were supplemented with 0.1 mM mevalonate (50). The antibiotics chloramphenicol, kanamycin and ampicillin, when required, were added to the medium at the final concentrations of 12.5 $\mu g\ ml^{-1}$, 50 $\mu g\ ml^{-1}$ and 100 $\mu g\ ml^{-1}$, respectively. Where indicated 0.2% (w/v) L-arabinose was added to cultures to induce *erpA* expression in the strain LL401 (*ara$_p$::erpA*) (26).

When required, the Kan^R cassette of certain mutants was deleted by transforming with pCP20 encoding a Flp-recombinase (12). Mutants were subsequently tested for sensitivity to kanamycin.

Recombinant DNA work was carried out according to published methods (38). Plasmids containing *sufA*, *iscA* and *erpA* genes were constructed by PCR amplification of the respective DNA fragments from genomic DNA of MC4100 using Phusion DNA polymerase (Finnzymes, Germany) and the oligonucleotides sufA_FW_BamHI 5'-CGC GGA TCC atg GAC ATG CAT TCA GGA AC-3'; sufA_RW_EcoRI 5'-CGC GAA TTC cta TAC CCC AAA GCT TTC GC-3'; iscA_FW_BamHI 5'-CGC GGA TCC atg TCG ATT ACA CTG AGC GAC-3'; iscA_RW_EcoRI 5'-CGC GAA TTC tca AAC GTG GAA GCT TTC GC-3'; erpA_FW_BamHI 5'-GCG GGA TCC atg AGT GAT GAC GTA GCA CTG-3' and erpA_RW_EcoRI 5'-GCG GAA TTC tta GAT ACT AAA GGA AGA ACC-3'. The resulting 388 bp (*sufA*), 337 bp (*iscA*) and 358 bp (*erpA*) PCR fragments and the pBluescript SK(+) vector (Stratagene) were digested with BamHI and EcoRI and ligated resulting in psufA, piscA and perpA, respectively. The DNA sequence of each insert was verified (Seqlab, Germany).

Preparation of cell extracts and determination of enzyme activities. Anaerobic cultures were harvested at an OD_{600nm} of approximately 0.8. Cells from cultures were harvested by centrifugation at 4000 x g for 10 min at 4°C, resuspended in 2-3 ml of MOPS pH 7.0 buffer and lysed on ice by sonication (30W power for 5 minutes with 0.5 sec pulses). Unbroken cells and cell debris were removed by centrifugation for 15 min at 10 000 x g and at 4°C and the supernatant was used as the crude cell extract. Formate dehydrogenase N and nitrate reductase enzyme activities were determined according to (14) using MOPS pH 7.0 buffer. Protein concentration of crude extracts was determined (27) with bovine serum albumin as standard.

Polyacrylamide gel electrophoresis, activity-staining and immunoblotting. Aliquots of 25-50 µg of protein from the indicated fractions were separated by SDS-polyacrylamide gel electrophoresis (PAGE) using 10% (w/v) polyacrylamide (24) and transferred to nitrocellulose membranes as described (48). Antibodies raised against Fdh-N (1:5000 a kind gift from F. Sargent), and Nar (1:3000; a kind gift from A. Magalon) were used. Secondary antibody conjugated to

horseradish peroxidase was obtained from Bio-Rad. Visualisation was done by the enhanced chemiluminesent reaction (Stratagene).

Non-denaturing PAGE was performed using 5% (w/v) polyacrylamide gels pH 8.5 and included 0.1% (w/v) Triton X-100 in the gels (5). Samples (25 μg of protein) were incubated with 5% (w/v) Triton X-100 prior to application to the gels. Activity-staining to reveal Fdh-O using phenazinemethosulfate, nitrobluetetrazolium (PMS-NBT) and formate was done as described in (14) and Nar was done as described in (18) using nitrate , dithionite and benzyl viologen (BV) in 50 mM MOPS pH 7.0 as buffer.

Results.

The iron-sulfur cluster trafficking protein SufA is dispensable for formate dehydrogenase and nitrate reductase maturation. The Fdh-N/O and Nar enzymes each have five [Fe-S] clusters and we wanted to determine whether the Isc or Suf systems were required during maturation of either enzyme. Initially, we examined the effects of *sufA* and *iscA* mutations individually on Fdh-N and Nar enzyme activities in anaerobically respiring *E. coli*. Under the assay conditions, Fdh-O contributes only a small percentage to the overall activity and therefore activity will be referred to as Fdh-N only (44). The *sufA* mutation (strain CP1123) caused an approximate 5-fold increase in both Nar and Fdh-N activity when compared with the activity measured in extracts of MC4100 and MG1655 (Table 2). This data suggests that wild-type SufA has a negative influence on either activity or synthesis of Fdh-N and Nar, possibly due to competition for [Fe-S] clusters.

Effect of mutations in *iscU* and *iscA* on nitrate-dependent enzyme activities.

Determination of enzymes activities in a crude extract derived from a mutant unable to synthesize the ATC protein IscA after anaerobic growth in the presence of glucose and nitrate showed a reduction in Fdh-N activity of approximately 50% and in Nar activity of 80% (Table 2). Clearly Nar activity was more strongly affected by the defect in IscA synthesis than Fdh-N activity. That the activity of both enzymes was absolutely dependent on the Isc machinery was, however, demonstrated by examining enzymes activities in extracts of a mutant unable to synthesize the [Fe-S] scaffold protein IscU (2, 16), which completely lacked activity of either enzyme (Table 2). These data indicate that in the absence of IscA another ATC protein, possibly ErpA can accept and traffic [Fe-S] to the Fdh-N and Nar enzymes.

ErpA is essential for Fdh-N and Nar enzyme activities in nitrate-respiring *E. coli*. Extracts of two different *erpA* mutants were totally devoid of Nar and Fdh-N activities (Table 2). As anticipated, activities of both enzymes were also absent in extracts derived from strain DV1151 (50), which carries mutations in both *iscA* and *erpA*. This result corroborates the findings described above for the *iscU* mutant and indicates that the Isc machinery is necessary for [Fe-S] cluster biosynthesis and delivery to the key enzymes of nitrate respiration.

Expression of the *erpA* gene in strain LL401 is conditional because it is under the control of the *ara*$_P$

promoter (26). Addition of L-arabinose to the anaerobic culture medium restored Fdh-N activity to approximately 60% of the wild type, while Nar activity was restored to 55% of that of MG1655 (Table 2). Complementation experiments with plasmids encoding IscA and ErpA revealed that multicopy *iscA* complemented the *iscA* mutation and multicopy *erpA* complemented the *erpA* mutation, restoring Fdh-N activity to levels that were 2 fold and 3 fold that of the wild-type, respectively (Table 2). ErpA and IscA also restored Nar activity to the respective mutants, but only to levels of between 50 and 80% of the wild type activity (Table 2). While multicopy *erpA* could not restore either Fdh-N or Nar activity in the *iscA* mutant CP477, multicopy *iscA* could restore Nar activity to approximately 20% of wild type activity in the *erpA* mutant (Table 2). Introduction of *sufA* on plasmid psufA had no signficant influence on the activities of either Fdh-N or Nar in the respective mutants (data not shown). These findings imply a partial functional substitution of *iscA* for *erpA* when it is provided in excess, but only for Nar activity. Interestingly, introduction of plasmid piscA into the *erpA* mutant LL401 failed to result in restoration of any Fdh-N activity (Table 2).

Neither multicopy ErpA nor multicopy SufA could complement the *iscA erpA* double mutations in DV1151 (data not shown).

Taken together, these findings demonstrate that the Isc machinery but not the Suf system is required for [Fe-S] cluster insertion into the Fdh-N and Nar enzymes.

It is important to note that extracts derived from the K-12 derivatives MC4100, BW25113 and MG1655 all showed similar Nar and Fdh-N activities (Table 2). They also showed similar regulation patterns in all respects that we have tested and thus in our hands the findings presented allow direct comparison between the strains. Furthermore, the absence of either activity did not influence the activity of the other enzyme, e.g. deletion of *fdnG* did not affect Nar. This indicates that the *erpA* and *iscA* mutations affected both enzyme activities separately.

Enzyme-specific staining after native-PAGE reveals that ErpA and IscA are essential for Nar and Fdh activity. Nar enzyme activity can be visualized after non-denaturing PAGE (28). Analysis of crude extracts derived from various strains grown anaerobically with nitrate revealed a single nitrate-dependent active enzyme complex (Fig. 2A) that was absent in extracts of mutants lacking either the *narG* gene or *fnr*, which encodes the oxygen-responsive transcriptional regulator FNR of the *narGHJI* operon (15, 51). Extracts from the MC4100, JW3815 (Δ*tatC*) and CP1223 (Δ*sufA*) had similarly intense activity bands like that observed in a *fdnG* mutant (Fig. 2A), confirming that Nar maturation does not depend on the Suf machinery. In contrast, the *iscA* mutant CP477 had a significantly weaker activity while the *erpA* (LL402) and *iscU* (JW2513) mutants had a barely detectable activity band. No active Nar enzyme could be detected in an extract of the *erpA iscA* double null mutant

(DV1151) (Fig. 2A). Complementation studies with plasmids piscA and perpA revealed that only piscA could restore Nar activity to strain CP477 (*iscA*) and only perpA could restore activity to detectable levels in the conditional *erpA* mutant LL401 (Fig. 2C). In contrast to the weak restoration of Nar activity measured in extracts (see Table 2), plasmid piscA did not result in a clearly visible, active Nar enzyme. The reason for this discrepancy might be due to the activity being below the threshold that can be detected by this method. Introduction of *sufA* on plasmid psufA had no signficant influence on Nar activity in the respective mutants (data not shown).

The activities of the highly similar Fdh-N and Fdh-O enzymes cannot be readily distinguished using standard enzyme assays; however, by specific staining using formate and PMS-NBT after non-denaturing PAGE the Fdh-O enzyme complex can be readily visualized (44). A single active enzyme complex present in extracts from *fdnG, narG, sufA* and *fnr* mutants could be clearly distinguished and had a similar intensity to that seen in extracts of MC4100 (Fig. 2B). Expression of the *fdoGHI* operon is independent of the FNR regulator (1, 44).

In contrast to Nar, however, but like Fdh-N, maturation of Fdh-O is completely dependent on a functional TAT-translocon (49) as no enzyme activity could be detected in extracts derived from the *tatC* mutant JW3815 (Fig. 2B). No Fdh-O enzyme activity could be visualized in extracts derived from *iscA, erpA, iscU* or *erpA iscA* mutants, which demonstrates that Fdh-O activity was strongly dependent on both ErpA and IscA.

Extracts derived from the single knock-out mutants CP477 (Δ*iscA*) and LL401 (conditional *erpA* mutant) complemented with plasmids perpA or piscA were analyzed using the same approach as described above. Each plasmid could restore Fdh-O enzyme activity to the respective mutant (Fig. 2D). Although this assay determines activity using a cummulative approach, and is therefore only semi-quantitative, some weak cross-complementation was observed for each plasmid. The findings of this experiment indicate that with respect to Fdh-O enzyme activity, ErpA and IscA exhibit a degree of redundancy.

Mutants lacking ErpA or IscA are devoid of the small electron-transferring subunit and exhibit aberrant Fdh-N and Nar polypeptide patterns. In an attempt to understand the reason for the lack of Fdh-N and Nar enzyme activity in the [Fe-S] cluster trafficking mutants, extracts derived from the various mutants grown under nitrate-respiring conditions were prepared and subjected to western blot analysis with antiserum raised against either Fdh-N or Nar (Fig. 3). The Fdh-N enzyme comprises the 113 kDa FdnG catalytic subunit, the 32.2 kDa FdnH electron transfer subunit and the 25.3 kDa FdnI membrane anchor subunit (22), while the Nar enzyme comprises the 140.5 kDa NarG catalytic subunit, the 58.6 kDa NarH electron transfer subunit and the 25.5 kDa NarI membrane anchor (8). Like the catalytic

subunit of Fdh-N, the catalytic subunit of Nar has a [4Fe-4S] cluster (8, 23), however, in contrast to FdnG, NarG lacks a TAT-signal peptide. Western blot analysis of extracts from MC4100 and PB1000 (Δ*fnr*) allowed unequivocal identification of the NarG subunit in a MC4100 crude extract (Fig. 3A). A mutant lacking either Fdh-N (Δ*fdnG*) or TatC exhibited very strong signals in western blots for the NarG polypeptide (Fig. 3A). This might suggest that in the absence of active Fdh-N, Nar is more efficiently assembled.

In extracts derived from mutants that had signficantly reduced, or that lacked, Nar enzyme activity, a second, faster migrating NarG polypeptide species could occasionally be observed. This is best exemplified in an extract derived from the *erpA iscA* double null mutant DV1151 (see right-hand lane of Fig. 3A). Extracts derived from strains CP477 and LL401 phenotypically or genotypically complemented revealed that multicopy *iscA* restored high-levels of of the more slowly migrating NarG polypeptide species to the *iscA* mutant and similarly multicopy *erpA* restored NarG to LL401 (Fig. 3C) in correlation with the restoration of Nar enzyme activity in the extract (Table 2).

The antiserum raised against Nar also recognized the 58.6 kDa electron-transferring subunit of Nar, NarH (Fig. 3B). Analysis of crude extracts from the various strains revealed a direct correlation between loss of Nar enzyme activity (see Table 2) and the absence of detectable NarH polypeptide (Fig. 3B). Extracts of the *fnr* mutant PB1000 acted as a negative control and, as anticipated (51), no NarH polypeptide could be detected. Similarly, no NarH could be detected in a mutant lacking the gene encoding the large subunit, suggesting that the NarH polypeptide was unstable in the absence of the catalytic subunit. Importantly, extracts derived from mutants devoid of ErpA, IscA or IscU also lacked NarH and upon reintroduction of the piscA or perpA, NarH could be restored to the corresponding mutants CP477 (*iscA*) and LL401, respectively (Fig. 3B). These results suggest that one reason for the lack of Nar activity in mutants devoid of ATC proteins is due to the absence of the iron sulfur-containing, electron transfer subunit.

In the western blots of Fdh-N shown in Fig. 3 FdnG, FdnH and FdnI could all be identified to migrate as single polypeptides in crude extracts of MC4100, each with the approximate size predicted from the deduced molecular mass (Fig. 3C, D and E). The identity of all three subunits was confirmed by analysis of an extract derived from the *fnr* mutant PB1000, which lacked all three polypeptides. No transcription of the *fdnGHI* operon occurs in a *fnr* mutant (25, 51). An extract from a *sufA* mutant revealed a polypeptide pattern like that seen for MC4100 (Fig. 3C, D and E), which was anticipated because the mutant showed increased rather then decreased Fdh-N enzyme activity (see Table 2). In an extract derived from the *iscA* mutant CP477, the FdnG polypeptide migrated as two forms, the lower of which

corresponded to that in MC4100 while the second form of the polypeptide migrated marginally more slowly with a molecular mass that would be expected if the TAT signal peptide were not cleaved (49). The two mutants (*erpA* and *iscU*) devoid of any measureable Fdh-N enzyme activity (see Table 2) showed only the more slowly migrating polypeptide, suggesting that in these strains FdnG could not pass the TAT-translocon (Fig. 3A). Analysis of the migration pattern of FdnG in the *tatC* mutant JW3815 (Fig. 4) revealed that only the more slowly migrating form of the FdnG polypeptide could be identified, thus strongly supporting the contention that in the *erpA* and *iscU* mutants FdnG was not transported across the cytoplasmic membrane.

Analysis of the electron-transferring subunit FdnH of the Fdh-N enzyme revealed that in the crude extracts of CP477 (Δ*iscA*), LL402 (Δ*erpA*) and JW2513 (Δ*iscU*) no, or barely detectable, FdnH polypeptide could be visualized (Fig. 3B).

With the exception of the *fnr* mutant PB1000 all of the strains analyzed had essentially comparable levels of the membrane anchor subunit FdnI (Fig. 3B). This indicates that the reason for the lower amount, or absence, of FdnH was more rapid degradation.

Discussion.

In this study we have provided a plausible explanation for the observation originally made by Loiseau *et al.* (26) that an *E. coli erpA* mutant is unable to grow by nitrate respiration. In the absence of this proposed [Fe-S] cluster trafficking protein the maturation through metal cofactor insertion of the key respiratory enzymes Fdh-N and Nar cannot be completed and the enzymes are essentially inactive. Because transcription of both the *fdnGHI* and *narGHJI* operons is absolutely dependent on the [Fe-S] protein FNR (15, 25, 51), it was conceivable that this could have been the explanation for the respiratory defect in the *erpA* mutant. However, identification of both the FdnG and FdnI polypeptides in the *erpA* single and *erpA iscA* double mutants indicated that FNR function was not completely compromised and implies that insertion of the [4Fe-4S] cluster into FNR is not totally dependent on the Isc system or ErpA (31). Western blot analysis confirmed the presence of essentially wild-type levels of FNR in extracts of the ATC protein mutants (data not shown). These findings support the results of Mettert *et al.* (31) who demonstrated that Isc⁻ mutants retain 40% functionality of FNR. As the Suf machinery does not appear to be involved [Fe-S] cluster assembly into FNR, this might suggest the existence of another route of delivery for particular clusters also under anaerobic conditions. FNR as a key [Fe-S] protein controlling expression of a comparatively large regulon is clearly not reliant on only one pathway for cluster assembly and delivery, whereas for cluster insertion into the electron-transfer subunits of the anaerobic oxidoreductases the Isc system appears to be the main route.

We could demonstrate for both Fdh-N and Nar that the likely reason for the lack of activity and incomplete maturation of the enzymes is presumably because the electron-transferring small subunit, and possibly also the large catalytic subunit, fails to receive its complement of [4Fe-4S] clusters. This conclusion is based on the apparent enhanced turnover of the FdnH and NarH subunits and the appearance of a slowly migrating form of the FdnG catalytic subunit that correlates in its migration characteristics with the species observed in a *tatC* mutant. Isolation and spectroscopic characterization of the FdnG polypeptide from an *erpA* or an *iscU* mutant, which shared the same phenotype with respect to nitrate respiration, will be required to demonstrate whether the catalytic subunit indeed lacks its [4Fe-4S] cluster or whether the reason for the apparent lack of TAT-dependent transport is because the small subunit was absent. The identification of the intact FdnI anchor polypeptide in the various mutants confirmed that the mature FdnGH dimer is first transported by the TAT machinery and then forms the final active Fdh-N complex post-membrane translocation (39).

Supporting evidence that the [4Fe-4S] cluster might indeed be missing or aberrantly inserted into the large subunit of these enzymes was provided by the observation of a faster migrating form of the NarG polypeptide detectable in *iscU* and *erpAiscA* double mutants. In this instance, however, because Nar is not a TAT substrate (39), the faster migrating form of the protein cannot result from lack of processing. Rather, this suggests that either the [4Fe-4S] cluster or the Mo-bis-MGD cofactor (or both) was not properly inserted into the protein in the mutant, thus making the protein more susceptible to endoproteolytic cleavage. Why only maximally half of the population of NarG polypeptides migrated more rapidly in the gel, despite the enzyme being completely inactive, is currently unclear.

It should be noted that in the assembly of Fdh-N, Fdh-O and Nar, [Fe-S] cluster-containing proteins also play a role in Mo-bis-MGD cofactor biosynthesis (43), while in the case of Fdh-N and Fdh-O maturation the [Fe-S] protein FdhE has a chaperone function (29) and mutants unable to synthesize FdhE have no Fdh-N enzyme activity (30, 42). Thus, there are several possible steps along the maturation pathway of these enzymes that could be affected in mutants deficient in [Fe-S] cluster trafficking function (see Fig. 1).

The stronger dependence on ErpA than on IscA for Fdh and Nar maturation, together with the similar phenotypes of *erpA* and *iscU* mutants, indicates that ErpA is central to [Fe-S] cluster insertion by the Isc machinery in nitrate-respiring cells (36, 50). That ErpA and IscA have different but overlapping apoprotein targets is suggested by the fact that, although the approximately 110 amino acid ErpA and IscA proteins are phylogenetically related, they share only 40% amino acid sequence identity. Increasing the amount of IscA in an *erpA* mutant by

introducing the *iscA* gene on a plasmid demonstrated that IscA can, to a certain extent, functionally substitute for ErpA and confirms that the proteins have overlapping functions. This has been previously suggested (36). Interestingly, a *sufA* mutation increased both Nar and Fdh enzyme activites, which suggests that although SufA is not required for iron-sulfur cluster insertion into Nar or Fdh-N polypeptides, it might compete with the IscA and ErpA ATC proteins for iron-sulfur cluster substrate. Notably, SufA shares 32% amino acid identity with ErpA and 48% amino acid identity with IscA. Taken together, these findings suggest that the absolute levels of each ATC protein in the cell, together with variations in primary sequence, governs apoprotein substrate-specificity.

With regard to anaerobic respiration IscU sits above IscA, and most probably also ErpA, in the hierarchy of [Fe-S] cluster biogenesis. It has been shown that IscU can transfer a [Fe-S] cluster to IscA but not *vice versa* (33). The transfer does not occur directly, as IscA and IscU do not interact (47), but occurs possibly via the chaperone HscA, which is encoded at the *isc* locus on the chromosome. IscU has been proposed to transfer [Fe-S] clusters indirectly to ErpA via IscA in aerobically growing cells (50). The findings presented in this study strongly suggest that IscU can transfer [Fe-S] clusters to ErpA independently of IscA; however, whether this occurs via an intermediate protein, e.g. HscA, remains to be established. In analogy with IscU, the SufBCD scaffold complex donates [Fe-S] clusters to SufA (11) under oxidative stress and during iron limitation (36). SufA appeared only to impede transfer of [Fe-S] clusters to the Fdh-N, Fdh-O and Nar apoproteins via IscA and ErpA, based on enzyme activity data, indicating a high degree specificity of the ErpA/ IscA for the respective anaerobic apoproteins targets. It will be interesting to determine what controls this specificity and whether apoprotein target-specific chaperone proteins might recruit specific ATC proteins.

Finally, the question arises whether any of the ATC proteins might transfer [3Fe-4S] clusters preferentially compared to [4Fe-4S] clusters into the electron transfer subunits of the enzymes or whether ErpA and IscA do not distinguish between these cluster types. For example, recent studies looking at the roles of IscA and SufA in aerobic metabolism have indicated that a distinct and as yet undefined [Fe-S] cluster assembly pathway is responsible for introduction of [2Fe-2S] clusters into FhuF and the SoxR regulator (46). The overlapping, yet differential dependence on both IscA and ErpA also might be consistent with the suggestion that IscA and ErpA assemble different [Fe-S] clusters into certain apo-protein substrates with different efficiency. While Fdh-N only has [4Fe-4S] clusters in the holoenzyme, Nar has a single [3Fe-4S] cluster, as well as [4Fe-4S] clusters. Whether ErpA and IscA exhibit differential cluster transfer to different apoprotein targets will be one of the questions addressed in future studies.

References.
1.   **Abaibou, H.**, **J. Pommier**, **S. Benoit**, **G. Giordano**, **and M. A. Mandrand-Berthelot**. 1995. Expression and characterization of the *Escherichia coli fdo* locus and a possible physiological role for aerobic formate dehydrogenase. J. Bacteriol. **177**:7141–7149.
2.   **Agar, J. N.**, **C. Krebs**, **J. Frazzon**, **B. H. Huynh**, **D. R. Dean**, **and M. K. Johnson**. 2000. IscU as a scaffold for iron-sulfur cluster biosynthesis: sequential assembly of [2Fe-2S] and [4Fe-4S] clusters in IscU. Biochemistry **39**:7856–7862.
3.   **Ayala-Castro, C.**, **A. Saini**, **and F. W. Outten**. 2008. Fe-S cluster assembly pathways in bacteria. Microbiol. Mol. Biol. Rev. **72**:110–125.
4.   **Baba, T.**, **T. Ara**, **M. Hasegawa**, **Y. Takai**, **Y. Okumura**, **M. Baba**, **K. Datsenko**, **M. Tomita**, **B. Wanner**, **and H. Mori**. 2006. Construction of *Escherichia coli* K-12 in-frame, single-gene knockout mutants: the Keio collection. Mol. Syst. Biol. **2**:2006 0008.
5.   **Ballantine, S.**, **and D. Boxer**. 1985. Nickel-containing hydrogenase isoenzymes from anaerobically grown *Escherichia coli* K-12. J. Bacteriol. **163**:454–459.
6.   **Begg, Y.**, **J. Whyte**, **and B. Haddock**. 1977. The identification of mutants of *Escherichia coli* deficient in formate dehydrogenase and nitrate reductase activities using dye indicator plates. FEMS Microbiol. Lett. **2**:47–50.
7.   **Berg, B. L.**, **J. Li**, **J. Heider**, **and V. Stewart**. 1991. Nitrate-inducible formate dehydrogenase in *Escherichia coli* K-12. I. Nucleotide sequence of the *fdnGHI* operon and evidence that opal (UGA) encodes selenocysteine. J. Biol. Chem. **266**:22380–22385.
8.   **Bertero, M. G.**, **R. A. Rothery**, **M. Palak**, **C. Hou**, **D. Lim**, **F. Blasco**, **J. H. Weiner**, **and N. C. J. Strynadka**. 2003. Insights into the respiratory electron transfer pathway from the structure of nitrate reductase A. Nat. Struct. Biol. **10**:681–687.
9.   **Blattner, F. R.**, **G. Plunkett**, **C. A. Bloch**, **N. T. Perna**, **V. Burland**, **M. Riley**, **J. Collado-Vides**, **J. D. Glasner**, **C. K. Rode**, **G. F. Mayhew**, **J. Gregor**, **N. W. Davis**, **H. A. Kirkpatrick**, **M. A. Goeden**, **D. J. Rose**, **B. Mau**, **and Y. Shao**. 1997. The complete genome sequence of *Escherichia coli* K-12. Science **277**:1453–1462.
10.   **Casadaban, M. J.** 1976. Transposition and fusion of the *lac* genes to selected promoters in *Escherichia coli* using bacteriophage lambda and Mu. J. Mol. Biol. **104**:541–555.
11.   **Chahal, H. K.**, **Y. Dai**, **A. Saini**, **C. Ayala-Castro**, **and F. W. Outten**. 2009. The SufBCD Fe−S Scaffold Complex Interacts with SufA for Fe−S Cluster Transfer. Biochemistry **48**:10644–10653.
12.   **Cherepanov, P.**, **and W. Wackernagel**. 1995. Gene disruption in *Escherichia coli*: Tc^R and Km^R cassettes with the option of Flp-catalyzed excision of the antibiotic-resistance determinant. Gene **158**:9–14.
13.   **Datsenko, K.**, **and B. Wanner**. 2000. One-step inactivation of chromosomal genes in *Escherichia coli* K-12 using PCR products. Proc. Natl. Acad. Sci. U S A **97**:6640–6645.
14.   **Enoch, H. G.**, **and R. L. Lester**. 1975. The purification and properties of formate dehydrogenase and nitrate reductase from *Escherichia coli*. J. Biol. Chem. **250**:6693–6705.
15.   **Green, J.**, **and M. S. Paget**. 2004. Bacterial redox sensors. Nat. Rev. Microbiol. **2**:954–966.
16.   **Hoff, K. G.**, **J. J. Silberg**, **and L. E. Vickery**. 2000. Interaction of the iron-sulfur cluster assembly protein IscU with the

Hsc66/Hsc20 molecular chaperone system of *Escherichia coli*. Proc. Natl. Acad. Sci. USA **97**:7790–7795.

17.   **Hormann, K.**, and **J. Andreesen**. 1989. Reductive cleavage of sarcosine and betaine by *Eubaterium acidaminophilum* via enzyme systems different from glycine reductase. Arch. Microbiol. **153**:50–59.

18.   **Hucklesby, D. P.**, and **R. H. Hageman**. 1973. A staining method for nitrite reductase on polyacrylamide gels after electrophoresis. Anal. Biochem. **56**:591–592.

19.   **Jacobson, M. R.**, **V. L. Cash**, **M. C. Weiss**, **N. F. Laird**, **W. E. Newton**, and **D. R. Dean**. 1989. Biochemical and genetic analysis of the *nifUSVWZM* cluster from *Azotobacter vinelandii*. Mol. Gen. Genet. **219**:49–57.

20.   **Johnson, D. C.**, **D. R. Dean**, **A. D. Smith**, and **M. K. Johnson**. 2005. Structure, function, and formation of biological iron-sulfur clusters. Annu. Rev. Biochem. **74**:247–281.

21.   **Jormakka, M.**, **S. Törnroth**, **B. Byrne**, and **S. Iwata** 2002. Molecular Basis of Proton Motive Force Generation: Structure of Formate Dehydrogenase-N. Science **295**:1863–1868.

22.   **Jormakka, M.**, **B. Byrne**, and **S. Iwata**. 2003. Formate dehydrogenase--a versatile enzyme in changing environments. Curr. Opin. Struct. Biol. **13**:418–423.

23.   **Jormakka, M.**, **D. Richardson**, **B. Byrne**, and **S. Iwata**. 2004. Architecture of NarGH reveals a structural classification of Mo-bisMGD enzymes. Structure **12**:95–104.

24.   **Laemmli, U.** 1970. Cleavage of structural proteins during the assembly of the head of bacteriophage T4. Nature **227**:680–685.

25.   **Li, J.**, and **V. Stewart**. 1992. Localization of upstream sequence elements required for nitrate and anaerobic induction of *fdn* (formate dehydrogenase-N) operon expression in *Escherichia coli* K-12. J. Bacteriol. **174**:4935–4942.

26.   **Loiseau, L.**, **C. Gerez**, **M. Bekker**, **S. Ollagnier-de Choudens**, **B. Py**, **Y. Sanakis**, **J. Teixeira de Mattos**, **M. Fontecave**, and **F. Barras**. 2007. ErpA, an iron sulfur (Fe S) protein of the A-type essential for respiratory metabolism in *Escherichia coli*. Proc. Natl. Acad. Sci. USA **104**:13626–13631.

27.   **Lowry, O.**, **N. Rosebrough**, **A. Farr**, and **R. Randall**. 1951. Protein measurement with the Folin phenol reagent. J. Biol. Chem. **193**:265–275.

28.   **Lund, K.**, and **J. A. DeMoss**. 1976. Association-dissociation behavior and subunit structure of heat-released nitrate reductase from *Escherichia coli*. J. Biol. Chem. **251**:2207–2216.

29.   **Lüke, I.**, **G. Butland**, **K. Moore**, **G. Buchanan**, **V. Lyall**, **S. A. Fairhurst**, **J. F. Greenblatt**, **A. Emili**, **T. Palmer**, and **F. Sargent**. 2008. Biosynthesis of the respiratory formate dehydrogenases from *Escherichia coli*: characterization of the FdhE protein. Arch. Microbiol. **190**:685–696.

30.   **Mandrand-Berthelot, M. A.**, **G. Couchoux-Luthaud**, **C. L. Santini**, and **G. Giordano**. 1988. Mutants of *Escherichia coli* specifically deficient in respiratory formate dehydrogenase activity. J. Gen. Microbiol. **134**:3129–3139.

31.   **Mettert, E. L.**, **F. W. Outten**, **B. Wanta**, and **P. J. Kiley**. 2008. The impact of O_2 on the Fe-S cluster biogenesis requirements of *Escherichia coli* FNR. J. Mol. Biol. **384**:798–811.

32.   **Mitchell, P.** 1979. Keilin's respiratory chain concept and its chemiosmotic consequences. Science **206**:1148-1159.

33.   **Ollagnier-de Choudens, S.**, **Y. Sanakis**, and **M. Fontecave**. 2004. SufA/IscA: reactivity studies of a class of scaffold proteins involved in [Fe-S] cluster assembly. J. Biol. Inorg. Chem. **9**:828–838.

34.   **Palmer, T.**, **F. Sargent**, and **B. Berks**. 2005. Export of complex cofactor-containing proteins by the bacterial Tat pathway. Trends. Microbiol. **13**:175–180.

35.   **Pinske, C.**, **M. Bönn**, **S. Krüger**, **U. Lindenstrauß**, and **R.**

36.   **G. Sawers**. 2011. Metabolic deficiences revealed in the biotechnologically important model bacterium *Escherichia coli* BL21(DE3). PLoS ONE **6**:e22830.

36.   **Py, B.**, and **F. Barras**. 2010. Building Fe-S proteins: bacterial strategies. Nat. Rev. Microbiol. **8**:436–446.

37.   **Richardson, D.**, and **R. G. Sawers**. 2002. Structural biology. PMF through the redox loop. Science **295**:1842–1843.

38.   **Sambrook, J.**, and **D. Russell**. 2001. Molecular Cloning: A Laboratory Manual.

39.   **Sargent, F.** 2007. Constructing the wonders of the bacterial world: biosynthesis of complex enzymes. Microbiology **153**:633–651.

40.   **Sawers, R. G.** 1994. The hydrogenases and formate dehydrogenases of *Escherichia coli*. Antonie Van Leeuwenhoek **66**:57–88.

41.   **Sawers, R. G.**, **D. Clark**, and **A. Böck**. 2004. Fermentative Pyruvate and Acetyl-Coenzyme A Metabolism. EcoSal - *Escherichia coli* and *Salmonella*: cellular and molecular biology.

42.   **Schlindwein, C.**, **G. Giordano**, **C. L. Santini**, and **M. A. Mandrand**. 1990. Identification and expression of the *Escherichia coli fdhD* and *fdhE* genes, which are involved in the formation of respiratory formate dehydrogenase. J. Bacteriol. **172**:6112–6121.

43.   **Schwarz, G.**, **R. R. Mendel**, and **M. W. Ribbe**. 2009. Molybdenum cofactors, enzymes and pathways. Nature **460**:839–847.

44.   **Soboh, B.**, **C. Pinske**, **M. Kuhns**, **M. Waclawek**, **C. Ihling**, **K. Trchounian**, **A. Trchounian**, **A. Sinz**, and **G. Sawers**. 2011. The respiratory molybdo-selenoprotein formate dehydrogenases of *Escherichia coli* have hydrogen: benzyl viologen oxidoreductase activity. BMC Microbiol. **11**:173.

45.   **Takahashi, Y.**, and **U. Tokumoto**. 2002. A third bacterial system for the assembly of iron-sulfur clusters with homologs in archaea and plastids. J. Biol. Chem. **277**:28380–28383.

46.   **Tan, G.**, **J. Lu**, **J. P. Bitoun**, **H. Huang**, and **H. Ding**. 2009. IscA/SufA paralogues are required for the [4Fe-4S] cluster assembly in enzymes of multiple physiological pathways in *Escherichia coli* under aerobic growth conditions. Biochem. J. **420**:463–472.

47.   **Tokumoto, U.**, **S. Nomura**, **Y. Minami**, **H. Mihara**, **S.-I. Kato**, **T. Kurihara**, **N. Esaki**, **H. Kanazawa**, **H. Matsubara**, and **Y. Takahashi**. 2002. Network of protein-protein interactions among iron-sulfur cluster assembly proteins in *Escherichia coli*. J. Biochem. **131**:713–719.

48.   **Towbin, H.**, **T. Staehelin**, and **J. Gordon**. 1979. Electrophoretic transfer of proteins from polyacrylamide gels to nitrocellulose sheets: procedure and some applications. Proc. Natl. Acad. Sci. U S A **76**:4350–4354.

49.   **Tullman-Ercek, D.**, **DeLisa, M. P.**, **Kawarasaki, Y.**, **Iranpour, P.**, **Ribnicky, B.**, **Palmer, T.** & **Georgiou, G.** (2007). Export pathway selectivity of *Escherichia coli* twin arginine translocation signal peptides *J Biol Chem* **282**, 8309–8316.

50.   **Vinella, D.**, **C. Brochier-Armanet**, **L. Loiseau**, **E. Talla**, and **F. Barras**. 2009. Iron-sulfur (Fe/S) protein biogenesis: phylogenomic and genetic studies of A-type carriers. PLoS Genet **5**:e1000497.

51.   **Walker, M. S.**, and **J. A. DeMoss**. 1991. Promoter sequence requirements for Fnr-dependent activation of transcription of the *narGHJI* operon. Mol. Microbiol. **5**:353–360.

52.   **Yang, J.**, **J. P. Bitoun**, and **H. Ding**. 2006. Interplay of IscA and IscU in biogenesis of iron-sulfur clusters. J. Biol. Chem. **281**:27956–27963.

53.   **Zheng, L.**, **V. L. Cash**, **D. H. Flint**, and **D. R. Dean**. 1998. Assembly of iron-sulfur clusters. Identification of an *iscSUA-hscBA-fdx* gene cluster from *Azotobacter vinelandii*. J. Biol. Chem. **273**:13264–13272.

Table 1. Strains and plasmids used in this study

Strains/ plasmids	Genotype[a]	Reference/ Source
MC4100	F$^-$ *araD139* Δ(*argF-lac*)*U169 ptsF25 deoC1 relA1 flbB5301 rspL150*$^-$	(10)
MG1655	F$^-$ λ$^-$ *ilvG*$^-$ *rfb*-50 *rph*-1	(9)
BW25113	F$^-$ Δ(*araD-araB*)*567* Δ*lacZ4787*(::*rrnB-3*) λ$^-$ *rph-1* Δ(*rhaD-rhaB*)*568 hsdR514*	(4, 13)
CP477	As MC4100 but Δ*iscA*::Kan^R; ECK2525	This study
CP1221	As BW25113 but Δ*sufA*::*cat*	This study
CP1223	As MC4100 but Δ*sufA*::*cat*	This study
PB1000	As MC4100 but Δ*fnr*	(35)
LL401	MG1655 *cat*RExBAD*erpA*, *erpA* placed under control of the pBAD promoter	(26)
LL402	MG1655 Δ*erpA*::Cm^R; ECK0155	(26)
DV1151	MG1655 Δ*erpA*::Cm^R *iscA*	(49)
JW2512	BW25113 Δ*iscA*::Kan^R; ECK2525	+
JW2513	BW25113 Δ*iscU*::Kan^R; ECK2526	+
JW1470	BW25113 Δ*fdnG*::Kan^R; ECK1468	+
JW1215	BW25113 Δ*narG*::Kan^R; ECK1218	+
JW3815	BW25113 Δ*tatC*::Kan^R; ECK3832	+
Plasmids		
pCP20	*FLP*$^+$, λcI857$^+$, λ*p*$_R$ Rep^{ts}, Amp^R, Cm^R	(12)
perpA	pBluescript SK(+) containing *erpA* in BamHI and EcoRI site; Amp^R	This study
pLUE-A	pUC18 expressing *erpA*, Amp^R	(26)
piscA	pBluescript SK(+) containing *iscA* in BamHI and EcoRI site; Amp^R	This study
psufA	pBluescript SK(+) containing *sufA* in BamHI and EcoRI site; Amp^R	This study

+ National BioResources Project (NIG, Japan): E. coli
[a] Allele numbers are given for single gene mutants and refer to the K-12 nomenclature.

Table 2: Activities of formate dehydrogenase and nitrate reductase are ErpA- and IscA-dependent.

Strain and genotype[a]	Specific Fdh-N Activity in U mg protein^{-1} ± standard deviation[b]	Specific Nar activity in U mg protein^{-1} ± standard deviation[b]
MC4100	0.15 ± 0.08	0.40 ± 0.09
MG1655	0.15 ± 0.03	0.55 ± 0.40
BW25113	0.13 ± 0.04	0.55 ± 0.16
JW1215 (*narG*)	0.21 ± 0.12	< 0.01
JW1470 (*fdnG*)	0.03 ± 0.03	0.43 ± 0.30
CP477 (*iscA*)	0.08 ± 0.03	0.08 ± 0.04
CP477 (*iscA*) piscA	0.37 ± 0.29	0.32 ± 0.12
CP477 (*iscA*) perpA	0.08 ± 0.01	0.02 ± 0.01
LL402 (*erpA*)	< 0,01	0.02 ± 0.02
LL401 (*erpA*)	0.01 ± 0.01	0.02 ± 0.02
LL401 + L-Arabinose	0.10 ± 0.06	0.3 ± 0.08
LL401 + piscA	0.01 ± 0.01	0.11 ± 0.04
LL401 + piscA + L-Ara	0.07 ± 0.01	0.27 ± 0.05
LL401 + perpA[c]	0.52 ± 0.14	0.24 ± 0.03
CP1223 (*sufA*)	0.71 ± 0.29	1.19 ± 0.25
DV1151 (*iscA erpA*)	< 0.01	0.02 ± 0.03
JW2513 (*iscU*)	< 0.01	0.01 ± 0.04

[a] Cells were grown anaerobically in TGYEP pH 6.5 supplemented with 100 mM KNO$_3$
[b] The mean and standard error of at least three independent experiments are shown.
[c] Performed with two different plasmids encoding ErpA (perpA and pLUE-A) with both delivering similar results.
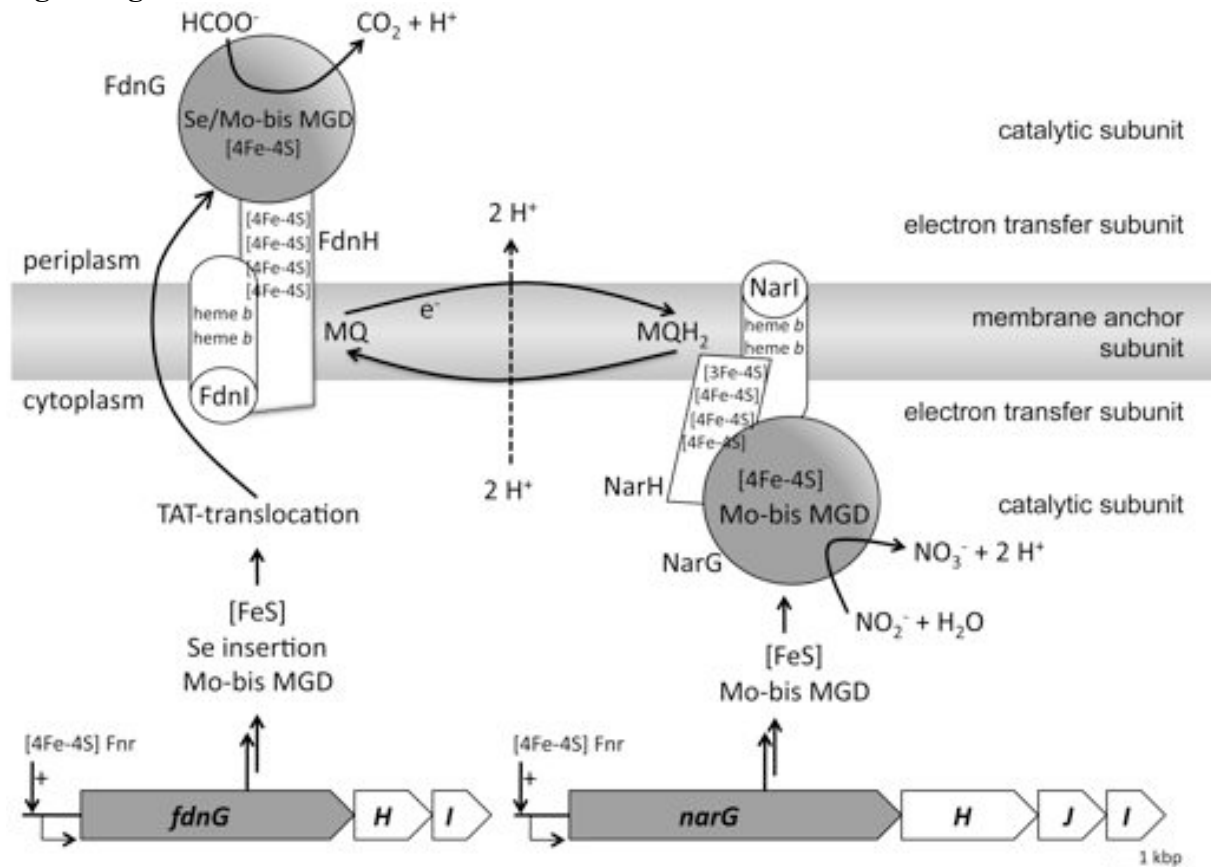
Figure legends

Fig. 1. Schematic representation of the organization of the formate dehydrogenase-N and nitrate reductase enzymes in the cytoplasmic membrane of *Escherichia coli*. Shown are the FNR-regulated structural gene operons for Fdh-N (*fdnGHI*) and Nar (*narGHJI*) and the steps required from protein synthesis via cofactor insertion ([Fe-S] cluster, selenocysteine (Se), molybdo-bis-molybdopterin guanine dinucleotide (Mo-bis-MGD)) to Tat-dependent membrane transport for Fdh-N. The membrane anchor subunits FdnI and NarI further contain heme *b* cofactors, the electron transfer subunits FdnH and NarH have several [FeS]-clusters and the catalytic subunits FdnG and NarG have Mo-bis MGD, [4Fe-4S] and Se (only FdnG). The reaction catalyzed by each enzyme and the connecting menaquinone (MQ)-menaquinol (MQH$_2$)-based redox loop is shown.
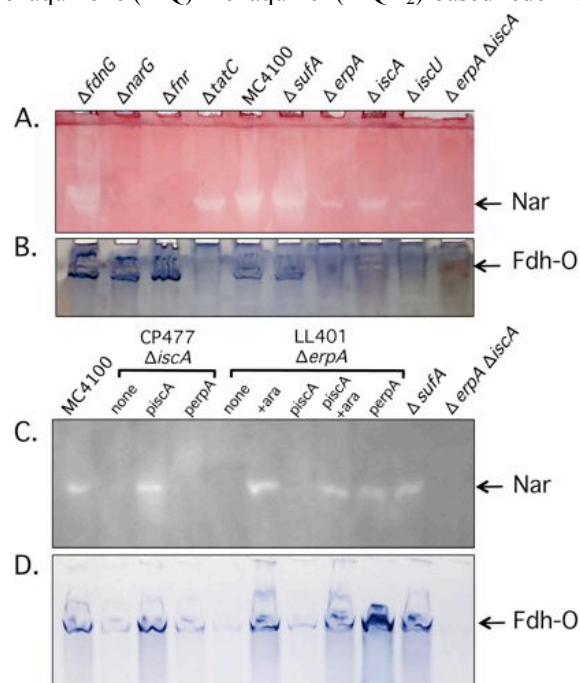
Fig. 2. Staining for Nar and Fdh-O activities. In the interest of clarity only the genotypes of the strains analyzed are shown. Samples (50 µg protein) of crude extracts from strains JW1470 (Δ*fdnG*), JW1215 (Δ*narG*), PB1000 (Δ*fnr*), JW3815 (Δ*tatC*), MC4100 (wild type), CP1223 (Δ*sufA*), LL401 (conditional *erpA*), LL402 (Δ*erpA*), CP477 (Δ*iscA*), JW2513 (Δ*iscU*) and DV1151 (Δ*erpA iscA*) after anaerobic growth in TGYEP, pH 6.5/ 100 mM nitrate were separated in 7.5 % (w/v polyacrylamide)-PAGE and stained for Nar **(A, C)** or Fdh-O **(B, D)** activities as described in the Methods section. In a similar manner crude extract samples (25 µg protein) derived from strains CP477 (Δ*iscA*) and LL401 (*ara*$_P$::*erpA*) transformed with plasmids piscA (*iscA*$^+$) or perpA (*erpA*$^+$) as indicated were stained for Nar **(C)** or Fdh-O **(D)** activity. Conditional recovery of *erpA* gene expression in LL401 was induced by supplementing the growth medium with 0.2% (w/v) L-arabinose (26).
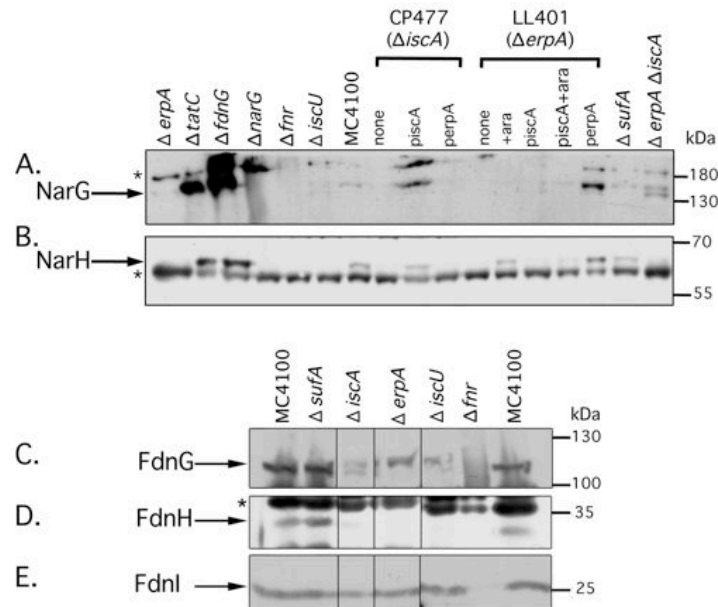

Fig. 3. Western blot analysis of Nar and Fdh-N proteins. In the interest of clarity only the genotypes of the strains analyzed are shown. Crude extracts (25 µg protein) derived from strains MC4100 (wild type), CP1223 (Δ*sufA*), CP477 (Δ*iscA*), LL401 (conditional *erpA*), LL402 (Δ*erpA*), DV1151 (Δ*erpA iscA*), JW2513 (Δ*iscU*), JW1470 (Δ*fdnG*), JW1215 (Δ*narG*), PB1000 (Δ*fnr*) and JW3815 (Δ*tatC*) and where indicated transformed with plasmids piscA (*iscA*$^+$) or perpA (*erpA*$^+$), grown in TGYEP, pH 6.5/ 100 mM nitrate were separated in 10 % (w/v polyacrylamide) SDS-PAGE (12.5% w/v in panel B) and transferred to nitrocellulose membranes. Samples were probed with antiserum raised against **A**: NarG, **B**: NarH, **C**: FdnG, **D**: FdnH, or **E**: FdnI. The asterisks signify unidentified polypeptide species that show cross-reaction with the antiserum and were used as loading controls in the experiments. On the right hand are given the sizes of the respective molecular mass standards (PageRuler Prestained, Fermentas). On the left of the Figure the polypeptides corresponding to the respective Nar and Fdh-N subunits are indicated.
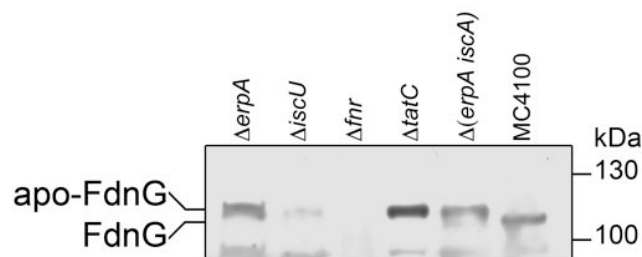
Fig. 4 Correlation between the slower migrating FdnG polypeptide species identified in certain ATC trafficking mutants with that observed in a Δ*tatC* strain. In the interest of clarity only the genotypes of the strains analyzed are shown. Samples (50 µg protein) of crude extracts derived from strains LL402 (Δ*erpA*), JW2513 (Δ*iscU*), PB1000 (Δ*fnr*) JW3815 (Δ*tatC*), DV1151 (Δ*erpA iscA*) and MC4100 (wild type) after anaerobic growth in TGYEP, pH 6.5/ 100 mM nitrate were separated in 8% (w/v polyacrylamide) SDS-PAGE, transferred to nitrocellulose membrane and probed with antiserum raised against FdnG. On the left hand side of the Figure the migration of the apoprotein form (apo-FdnG) and the processed species of FdnG are indicated and on the right side the sizes of the molecular mass standard (PageRuler Prestained, Fermentas) are given.

2.8 Der Transfer von Eisen-Schwefel Clustern zu [NiFe]-Hydrogenasen in *Escherichia coli* benötigt die A-typ Träger-Proteine ErpA und IscA.

2.8.1 Zusammenfassung

Analog zur Untersuchung der nitratrespiratorischen Enzyme in *erpA* und *iscA* Mutanten (Abschnitt 2.7), wurde der Effekt der Deletionen auf die fermentativen Enzyme des H_2-Stoffwechsels in *E. coli* untersucht. So besitzen die kleinen Hydrogenase Untereinheiten Elektronen-transferierende [FeS]-Cluster, während die großen Untereinheiten das [NiFe]-Zentrum enthalten. Es zeigte sich, dass Mutanten mit Deletionen der *erpA* und *iscA* Gene keine Hyd-1 und Hyd-2 Aktivitäten haben, während eine Deletion des *sufA* Gens ohne Effekt blieb. Der Mangel an Aktivität ist auf den wahrscheinlich proteolytischen Abbau der kleinen Untereinheiten in Abwesenheit ihrer [FeS]-Cluster zurückzuführen, ohne die keine Aktivität sichtbar ist (vgl. Abschnitt 2.4). Ein immunologischer Nachweis der großen Untereinheiten ergab, dass Prozessierung in Abwesenheit von *iscA* und *erpA* zwar erfolgte, die Proteinmengen der großen Untereinheiten jedoch stark reduziert waren, während die kleinen Untereinheiten nicht mehr detektierbar waren. Dies belegt einerseits die Translation des gesamten Operons, dessen erstes Gen für die kleinen Untereinheiten kodiert, und andererseits eine Unabhängigkeit oder Redundanz der Reifung vom Isc System.

Für die Aktivität des FHL Komplexes konnte eine teilweise Abhängigkeit von *iscA* und eine vollständige Abhängigkeit von *erpA* belegt werden. Dennoch konnten alle untersuchten Proteinkomponenten immunologisch nachgewiesenen werden und die Abwesenheit der Aktivität lediglich auf mangelnde Assoziation mit der Cytoplasmamembran zurückgeführt werden. Offenbar sind im Gegensatz zu den kleinen Untereinheiten von Hyd-1 und Hyd-2 die [FeS]-Cluster haltigen Proteine des FHL Komplexes in Abwesenheit des Isc Systems vor Proteolyse geschützt. Dies steht im Gegensatz zum Proteinmuster einer *hypF* Mutante, deren große Hyd Untereinheiten durch mangelnde Reifung stabilisiert wurden, deren kleine Hyd Untereinheiten jedoch ebenfalls nicht detektiert werden konnten. So werden offensichtlich sowohl die Assoziation mit der prozessierten großen Untereinheit als auch die Insertion der [FeS]-Cluster benötigt, um die kleinen Untereinheiten nachzuweisen. Die Ergebnisse dieser Mutanten zeigten einmal mehr, dass FHL-Komplex und Wasserstoff-oxidierende Enzyme verschiedene Prioritäten haben und unter Limitierung der Reifungsmaschinerie die Assemblierung des FHL Komplexes Vorrang hat.

2.8.2 Artikelkopie (Manuskript)

Delivery of Iron-Sulfur Clusters to [NiFe]-Hydrogenases in *Escherichia coli* Requires the A-Type Carrier Proteins ErpA and IscA

Constanze Pinske and R. Gary Sawers[*]

Institute for Biology/ Microbiology, Martin-Luther University Halle-Wittenberg, Kurt-Mothes-Str. 3, 06120 Halle (Saale) Germany

[*] For correspondence: R.G. Sawers, Institute for Biology/ Microbiology, Martin-Luther University Halle-Wittenberg, Kurt-Mothes-Str. 3, 06120 Halle (Saale) Germany
Tel., +49 345 5526350; Fax., +49 345 5527010; Email, gary.sawers@mikrobiologie.uni-halle.de

Abstract.
During fermentation *Escherichia coli* synthesizes three [NiFe]-hydrogenases. Hydrogenase-1 (Hyd-1) and Hyd-2 have a hydrogen-uptake function while Hyd-3 forms part of the hydrogen-evolving formate hydrogenlyase (FHL) enzyme complex. The catalytic subunit of each enzyme has a single Fe atom that forms part of the [NiFe] prosthetic group, while each enzyme also has an electron-transferring small subunit with a particular complement of [Fe-S] clusters. How iron is delivered to these enzymes is unclear. A-type carrier (ATC) proteins of the Isc (iron-sulfur-cluster) and Suf (sulfur mobilization) iron-sulfur ([Fe-S]) cluster biogenesis pathways are proposed to traffic pre-formed [Fe-S] clusters to apoprotein targets. While mutants lacking SufA were unaffected in hydrogenase biosynthesis, *iscA* or *erpA* mutants were devoid of Hyd-1 and Hyd-2 activity. This was due to a lack of the [Fe-S]-cluster-containing small subunit, apparently caused by enhanced degradation of the apoprotein. Processing of the large, catalytic subunit, which is characteristic of [NiFe] cluster insertion and which is independent of the small subunit, was still observed in the mutants. Although hydrogen evolution catalyzed by the FHL complex was completely dependent on ErpA, also little activity was retained in an *iscA* mutant. Our findings demonstrate different dependencies on IscA and ErpA for [Fe-S] cluster delivery to hydrogen-oxidizing and hydrogen-evolving enzymes.

Introduction.

Iron-sulfur ([Fe-S]) clusters are ubiquitous prosthetic groups of many metalloenzymes in almost all life-forms and they have a variety of functions in diverse cellular processes. Generation of [Fe-S] clusters does not occur spontaneously but requires dedicated machineries that orchestrate their assembly and subsequent transfer to apoprotein substrates (for reviews see [1-3]. There are at least three different [Fe-S] biosynthetic systems known and they are referred to as Nif (nitrogen fixation-associated), Isc (iron sulfur cluster) and Suf (sulfur mobilization). The initial discovery of the specialized NifUS proteins for the generation of [Fe-S] clusters in the nitrogenase enzyme of the nitrogen-fixing bacterium *Azotobacter vinelandii* [4] made it immediately clear that further generalized [Fe-S] machineries in bacteria must exist and these are represented by the Isc and Suf systems in many microbes [5,6].
The protein components of the Isc and Suf biogenesis systems can be roughly divided into those proteins dedicated to [Fe-S] assembly and those proposed to be involved in the subsequent trafficking of the pre-formed cluster to the ultimate apoprotein acceptor [3]. The proteins involved in transfer or trafficking of [Fe-S] are referred to as A-type carrier (ATC) proteins and the bacterium *Escherichia coli* has three of these, which are phylogenetically related [7], and are termed IscA, SufA and ErpA [8]. Current evidence is consistent with a role in cluster transfer between the Isc or Suf scaffold machinery and apoprotein substrates [3,9,10]; however, it has been also proposed that the ATC proteins deliver iron to the scaffold proteins [11].
An *erpA* mutation severely impairs aerobic growth of *E. coli* while single mutations in the *sufA* and *iscA* genes are viable [8]. Individual knock-out mutations in the *iscA, erpA* or *sufA* genes have a limited effect on anaerobic growth [8], suggesting redundancy of function for [Fe-S] cluster insertion into key iron-sulfur proteins. This contrasts with *iscA sufA* double null mutants, which generally are non-viable aerobically unless another means of [Fe-S] cluster

assembly is present, such as heterologously expressed *nifUS* [3,12]. Similarly, *iscA erpA* double mutants require introduction of the eukaryal isoprenoid biosynthetic pathway together with supplementation of mevalonate to restore growth [7,8]. Taken together these genetic studies suggest that IscA and SufA are functionally redundant during aerobic growth of *E. coli*, while IscA and ErpA show redundancy even anaerobically. Little is known, however, about which apoproteins these putative [Fe-S] cluster-delivery proteins have as substrates.

[NiFe]-hydrogenases are evolutionarily ancient [Fe-S] cluster-containing proteins that catalyze the reduction of protons to molecular hydrogen or the oxidation of hydrogen to protons and electrons [13,14]. The genome of *E. coli* encodes four membrane-associated [NiFe]-hydrogenases, only three of which are synthesized under anaerobic growth conditions. Hydrogenase 1 (Hyd-1) and Hyd-2 have their respective active site located in the periplasm and catalyze hydrogen oxidation. Hyd-3 forms part of the multi-subunit, hydrogen-evolving formate hydrogenlyase (FHL) complex [15], which disproportionates formic acid into CO_2 and H_2 during fermentation and which has its active sites in the cytoplasm (Fig. 1). The hydrogen-oxidizing enzymes comprise a large catalytic subunit, which lacks a [Fe-S] cluster but has a [NiFe] prosthetic group that catalyzes hydrogen activation, a small, electron-transfer subunit with one [3Fe-4S] and two [4Fe-4S] clusters, as well as a membrane-anchor subunit that carries menaquinone-binding sites [15-18]. Hyd-2 has an additional [Fe-S] cluster subunit, HybA, which is not a typical small subunit, but has been shown to be required for growth on hydrogen and fumarate [19].

The FHL complex has four protein subunits that are predicted to have [Fe-S] clusters [20,21]. The HycG protein is the small subunit of Hyd-3 and has a [4Fe-4S] cluster. The molybdenum-bis-molybdopterin guanine dinucleotide cofactor- and selenocysteine-containing formate dehydrogenase component, Fdh-H, encoded by the *fdhF* gene [22] has one [4Fe-4S] cluster [23], while the small subunit of the Fdh-H is encoded by *hycB* and is predicted to have four [4Fe-4S] clusters. A further ferredoxin-like subunit HycF also is predicted to have multiple [4Fe-4S] clusters [20]. Finally, biosynthesis of the FHL complex is absolutely dependent on the metabolite formate [24], which is generated by the glycyl radical enzyme pyruvate formate-lyase (PflB) [25]. PflB is converted to its active, radical-containing form by the radical SAM enzyme PflA and this enzyme also has a [4Fe-4S] cluster as prosthetic group [25].

The large subunit of [NiFe]-hydrogenases contains the hetero-bimetallic [NiFe] active site that usually has one CO and 2 CN⁻ ligands bound to the iron atom. The maturation of the [NiFe]-center requires the action of at least one [4Fe-4S] cluster-containing protein, HypD [26,27], which is essential for [NiFe]-center biosynthesis although its precise role in the process is still unclear [13].

The involvment of [Fe-S] clusters in the biosynthesis and activity of the [NiFe]-hydrogenases is therefore extensive and is summarized in Fig. 1. While a considerable amount of information is available concerning the biosynthesis of the [NiFe]-center and the associated diatomic ligands by the Hyp maturases (for reviews see [13,15], as well as the route of nickel incorporation [28], virtually nothing is known about either the routes of incorporation of the [Fe-S] clusters into the small subunits or where the iron atom in the active site originates. In this study, we have examined the biosynthesis of the [NiFe]-hydrogenases of *E. coli* with respect to the potential involvement of the three ATC paralogues IscA, SufA and ErpA. Our results reveal that IscA and ErpA are both required for assembly of active [NiFe]-hydrogenases but the dependence on each differs according to the physiological function of the hydrogenase.

Results.

The iron-sulphur cluster trafficking proteins IscA and ErpA are required for hydrogen-oxidizing enzyme function.

Initially we examined the effect of deleting the genes encoding the ATC proteins IscA, SufA and ErpA on total hydrogenase enzyme activity in fermenting *E. coli* cells. The *sufA* mutation had no effect either on total hydrogenase enzyme activity (Table 2), which measures the activities of all three hydrogenases concomitantly [29], or on the hydrogen-evolving Hyd-3-dependent FHL activity (Table 3). In contrast, an *iscA* mutation or an *erpA* mutation reduced total hydrogenase activity by 95% (Table 2) and FHL activity by minimally 85% (Table 3). Combining the *iscA* and *erpA* mutations in strain DV1151 [7] abolished both hydrogenase and FHL activity (Tables 2 and 3). The same overall hydrogen metabolism phenotype was observed in an *iscU* mutant. These findings indicates that IscA and ErpA exhibit a degree of redundancy with regard to total hydrogenase activity and that the Isc machinery is essential for hydrogen-oxidizing and –evolution activities in fermentatively growing *E. coli*.

Because Hyd-1 and Hyd-2 contribute approximately only 10% to the total hydrogenase activity measured in fermenting cells, while Hyd-3 contributes the remainder [29], it was important to determine whether the activities of the three Hyd enzymes were differentially affected in the different ATC mutants. Hyd-1 and Hyd-2 can be distinguished after separation

in native PAGE followed by specific hydrogenase activity-staining [29,30]; Hyd-3 enzyme activity is labile under these conditions and cannot be detected after native-PAGE. Extracts derived from a *sufA* mutant had wild type Hyd-1 and Hyd-2 activity profiles (Fig. 2). In contrast, extracts derived from the *iscA* and *erpA* mutants were devoid of both activities. This is a similar phenotype to that of the Δ*hypF* mutant DHP-F2, which cannot synthesize the [NiFe]-center and therefore lacks all hydrogenase enzyme activities [31] (Table 2, Fig. 2). This finding suggests that the residual hydrogenase enzyme activity measured in the *iscA* and *erpA* mutants (see Table 2) was due to Hyd-3 and indicates that, in contrast to Hyd-1 and Hyd-2, the Hyd-3 enzyme activity showed some redundancy with regard to IscA and ErpA. In order to confirm the first assumption, a mutant was constructed that lacked both *iscA* as well as the *hycABCDEFGHI* operon (strain CP967 in Table 2), which encodes Hyd-3 [20,21]. No significant hydrogenase activity could be measured in extracts of CP967. This result confirmed that the bulk of enzyme activity measured with benzyl viologen as electron acceptor under these growth conditions was due to Hyd-3 and that Hyd-3 was solely responsible for hydrogen gas production (Table 3). To determine whether IscA and ErpA showed some redundancy with regard to Hyd-3 biosynthesis, extracts of the *erpA iscA* double null mutant (strain DV1151 in Table 1) were examined for total hydrogenase activity and for hydrogen gas production (Tables 2 and 3). Neither activity could be determined in the mutant, confirming that IscA and ErpA exhibit redundancy.

A mutation in the *cyaY* gene encoding the frataxin-like protein [32] proposed to be involved in assembly of [2Fe-2S] clusters had no major effect on hydrogen metabolism (Tables 2 and 3).

It should be noted that various *E. coli* K-12 wild type strains, including MC4100, MG1655 and BW25113 and mutants thereof, share the same hydrogen metabolism phenotype and are therefore directly comparable (Fig. S1).

Complementation analysis. Introduction of the *iscA* gene on a multicopy plasmid (piscA) into the *iscA* mutant CP477 restored total hydrogenase enzyme activity to MC4100 levels (Table 2). Similarly, introduction of the *erpA* gene on plasmid perpA restored total hydrogenase activity to the conditional *erpA* mutant LL401. Because the *erpA* gene in LL401 is under the control of the *ara*$_P$ promoter [8], growth of the strain in the presence of arabinose induces *erpA* expression and restored hydrogenase activity (Table 2). While multicopy *iscA* could not restore hydrogenase activity in strain LL401, multicopy *erpA* could restore some hydrogenase activity (approximately 10% of MC4100) to strain CP477 (*iscA*) (Table 2). Both plasmids could restore between 5 and 10% total

hydrogenase activity to the *erpA iscA* double null mutant DV1151.

Analysis of extracts derived from CP477 and LL401 transformed with either piscA or perpA (Fig. 2) revealed that only multicopy *iscA* restored Hyd-1 and Hyd-2 activity to CP477, while only growth in the presence of arabinose (or less effectively perpA) restored Hyd-1 and Hyd-2 activities to LL401. This result suggests that the partial restoration of total hydrogenase activity in the cross-complementation experiments resulted from minor Hyd-3 activity, not Hyd-1 or Hyd-2. FHL activity, however, was not restored by introduction of piscA into LL401 or perpA into CP477 (Table 3).

Low levels of the processed hydrogenase catalytic subunit in *iscA* and *erpA* mutants. It is possible to distinguish two forms of the hydrogenase catalytic subunits using western blot analysis after SDS-PAGE [13]. The two forms of the approximately 65 kDa large subunit represent an unprocessed polypeptide and a processed form of the polypeptide, which lacks a short C-terminal peptide that results from a specific endoproteolytic cleavage event [13,33] and which only occurs after insertion of the [NiFe]-center has been completed [34]. Western blot analysis of the catalytic subunit of Hyd-1 (HyaB) in crude extracts derived from the wild type MC4100 revealed mainly the faster-migrating, processed polypeptide (Fig. 3A). In contrast, a mutant unable to make the HypF maturase, which provides the cyanide ligands to the iron atom of the active site, shows only the unprocessed form of the polypeptide because the [NiFe]-center cannot be synthesized [31]. Analysis of the Hyd-1 large subunit in a crude extract derived from the *sufA* mutant revealed both unprocessed and processed forms at levels similar to those observed for MC4100 (Fig. 3A). This is consistent with the wild type level of Hyd-1 activity seen in the *sufA* mutant (see Fig. 2). Analysis of extracts derived from the *iscA* and *erpA* mutants revealed that there were much lower amounts of the unprocessed and processed forms of the polypeptide in the mutants (Fig. 3A). Nevertheless, these results clearly show that, despite the reduced levels of Hyd-1 protein, the reason for the lack of detectable enzyme activity was not because the catalytic subunit could not receive the completed [NiFe] cofactor. Similar observations were made for the catalytic subunit (HybC) of Hyd-2 (see below and Fig. 4).

The respective [Fe-S] cluster-containing small subunit of both hydrogen-uptake hydrogenases is absent in a *hypF* mutant.

The antisera raised against Hyd-1 and Hyd-2 also recognize the [Fe-S] cluster-containing small subunits. Western blot analysis of crude extracts derived from MC4100 grown under fermentative conditions using antiserum raised against Hyd-1 (Fig. 3B) or Hyd-2

(Fig. 3C) identified the HyaA and HybO polypeptides, respectively, with molecular masses of approximately 35 kDa [35,36]. As a control, no HybO polypeptide could be observed in extracts of the *hybO* mutant CP795 (Fig. 3C). Surprisingly, in extracts derived from the Δ*hypF* strain DHP-F2 neither HyaA nor HybO could be detected (Fig. 3B, C). This suggests that in the absence of the processed form of the catalytic subunit, the small subunit is subject to rapid degradation.

The respective [Fe-S] cluster-containing small subunit of both hydrogen-uptake hydrogenases is absent in *iscA* and *erpA* mutants.

Recent studies have demonstrated that the [Fe-S] cluster-containing small subunit is essential to allow measurement of hydrogen-dependent benzyl viologen (BV) reduction of the Hyd-1, Hyd-2 and Hyd-3 enzymes [37]. Western blot analysis of extracts derived from the *iscA* mutant CP477 and the *erpA* mutant LL402 [8] also lacked the small subunits of Hyd-2 (Fig. 3D) and Hyd-1 (Fig. 3B and data not shown). In contrast, extracts of a *sufA* mutant showed wild type levels of both subunits (Fig. 3B, D). These data demonstrate a direct correlation between the presence of the hydrogenase small subunit and the detection of enzyme activity and suggest that the reason no Hyd-1 or Hyd-2 enzyme activity could be detected in the *iscA* or *erpA* mutants (see Fig. 2) was due to the absence of the small subunit. Thus, the data suggest that in the ATC mutants the small subunits of the hydrogenases are more rapidly degraded, possibly because they lack a full complement of [Fe-S] clusters.

The processed catalytic HybC subunit of hydrogenase-2 is not membrane-associated in *erpA* and *iscA* mutants.

Convincing evidence has been presented to indicate that the hydrogenase small subunit associates with the large subunit only after the [NiFe]-center has been inserted [13,38]. As the small subunits HyaA and HybO bear the signal peptide for recognition and membrane transport to the periplasmic side of the membrane by the Tat translocon, membrane translocation can only take place after complex formation between the mature catalytic subunit and the mature small subunit has occurred. To examine the subcellular localization of the HybC catalytic subunit in the various ATC mutants, extracts of the respective mutants were fractionated into soluble and membrane fractions and analyzed by western blot (Fig. 4). In extracts derived from MC4100, both Hyd-1 and Hyd-2 activities were associated with the cytoplasmic membrane (Fig. 4A). The processed form of the large subunit HybC was also found associated with the membrane fraction (Fig. 4B). In contrast, after fractionation of extracts from *iscA* and *erpA* mutants, processed HybC was primarily found in the soluble

fraction (Fig. 4B) and no active Hyd-2 could be identified in any sub-cellular fraction (Fig. 4A). It should be noted that only very low amounts of processed HybC were detected in both ATC mutants. Fractionated extracts derived from the *sufA* mutant revealed that the processed form of HybC was associated with the membrane fraction and essentially none was detected in the soluble fraction (Fig. 4B).

While a clear membrane association of the HybO small subunit was observed for MC4100 and the *sufA* mutant (Fig. 4B), no HybO could be detected in any sub-cellular fraction, or in whole cells, of the *erpA* or *iscA* or indeed *hypF* mutants. Introduction of the *iscA* gene on piscA into CP477 restored both Hyd-1 and Hyd-2 enzymes activities as well as the appearance of membrane-associated, processed HybC and the small subunit HybO (Fig. 4B).

The ability to generate formate intracellularly is not affected by *erpA* or *iscA* mutations.

One possible reason for the reduced FHL complex activity in *erpA* and *iscA* mutants could conceivably be due to lack of formate, which is essential for induction of *fdhF* and *hyc* gene expression [24]. Formate is generated by pyruvate formate-lyase (PflB) whose specific, activating radical-SAM enzyme PflA has an [Fe-S] cluster [25]. The presence of the active form of PflB can be readily visualized by western blotting with antibodies raised against PflB because in the presence of oxygen a specific scission of the PflB polpeptide occurs at amino acid position 733-734 resulting in a C-terminal truncation of the polypeptide chain [39]. Extracts derived from MC4100 (wild type), and the *iscA* and *erpA* mutants all showed the double band characteristic of the radical-bearing PflB species (Fig. S2), indicating that PflB was active in these strains and therefore lack of formate was not the reason for the reduction in FHL enzyme activity.

Membrane association of the HycG small subunit of Hyd-3 is compromised in *erpA* and *iscA* mutants.

The FHL complex is located on the cytoplasmic side of the membrane and consists of 7 proteins of which 4 (HycB, HycF, HycG and FdhF) have at least one [4Fe-4S] cluster [21] (Fig. 1). It is known that association of HycE with HycG, the large and small Hyd-3 subunits, respectively, occurs only after insertion of the active site into HycE [34]. The FHL complex retains approximately 15% of the wild-type activity in an *iscA* mutant (Table 3) indicating that, in contrast to what was observed for Hyd-1 and Hyd-2, the Hyd-3 enzyme showed at least partial activity. Western blot analysis with anti-HycG antibodies revealed that HycG levels were reduced in extracts of CP477 (*iscA*) and LL401 (*erpA*) compared with MC4100 (Fig. 5A). As a negative control an extract of the *hycA-I* deletion mutant CP971 showed no polypeptide signal corresponding to HycG. Notably, an extract of the

hypF mutant DHP-F2 also completely lacked HycG (Fig. 5A). Re-introduction of the *iscA* gene into CP477 (on piscA) restored HycG levels to the mutant while addition of L-arabinose or introduction of multicopy *erpA* or indeed multicopy *iscA* also restored HycG levels. This result suggests that with respect to HycG an increased dosage of *iscA* can compensate for the absence of ErpA but not *vice versa* (Fig. 5A).

Sub-cellular fractionation studies demonstrated that HycG was membrane-associated in both MC4100 and the *sufA* mutant CP1223 after fermentative growth with glucose (Fig. 5B). Analysis of whole cells, crude extracts, membrane and soluble fractions derived from the *iscA* and *erpA* mutants using HycG-specific antibodies revealed an altered sub-cellular distribution of HycG compared to that seen in MC4100, with the bulk of the polypeptide being in the soluble fraction (Fig. 5B). While a small amount of HycG was membrane-associated in CP477, no HycG could be observed in the membrane fraction of the *erpA* mutant. This finding indicates that the association of HycG with the FHL complex was compromised in the *iscA* and *erpA* mutants and it was not the amount of HycG *per se* that was limiting.

The FdhF component of the FHL complex is located mainly in the soluble fraction in *erpA* and *iscA* mutants and is enzymatically inactive.

With the aid of antibodies it was possible to examine the localization of the FdhF polypeptide (which is the catalytic subunit of the Fdh-H activity) in the various ATC mutants (Fig. 5C). The 80 kDa FdhF polypeptide was distributed evenly between the soluble and membrane fractions in MC4100, the Δ*hypF* mutant DHP-F2, as well as the *sufA* mutant CP1223. Crude extracts derived from these strains exhibited similar Fdh-H activity (Table 4), which is the formate dehydrogenase activity associated with the FHL complex and has been shown to be catalyzed by the FdhF catalytic subunit in association with the complex; FdhF is loosely associated with the membrane-associated FHL complex [23,25,29]. Analysis of the subcellular distribution of the FdhF polypeptide in the *erpA* mutant revealed that the bulk of the polypeptide was in the soluble fraction (Fig. 5C). In the *iscA* mutant CP477 FdhF was mainly localized in the soluble fraction but was still detectable in the membrane, but at lower levels than in MC4100. Perhaps this low-level association of FdhF with the membrane explains the residual, weak FHL activity measurable in *iscA* and *erpA* mutants (see Table 3), because neither mutant exibited measurable Fdh-H enzyme activity (Table 4). Complementation of the conditional *erpA* mutant LL401 by supplementing the growth medium with L-arabinose or transforming the strain with perpA restored Fdh-H activity (Table 4). Similarly, transformation of CP477 (*iscA*) with piscA

restored Fdh-H activity to extracts; however, both piscA in LL401 and perpA in CP477 failed to restore Fdh-H enzyme activity (Table 4), indicating that, like Hyd-1 and Hyd-2, Fdh-H enzyme activity is absolutely dependent on the activities of both ATC proteins.

The 20.5 kDa HycF polypeptide has similarity to ferredoxin-like proteins [20]. In contrast to either the FdhF or HycG FHL complex components, Western blot analysis of HycF revealed that it remained tightly associated with the membrane in MC4100 and the *iscA* and *erpA* mutants (Fig. 5D).

The [Fe-S] cluster-containing maturase HypD is present in *erpA* and *iscA* mutants but not in a strain lacking the scaffold protein IscU.

The [4Fe-4S] cluster-containing HypD maturase together with a number of other maturase enzymes are required for the biosynthesis of the [NiFe]-cofactor [26,27,40]. It was reported [13] that amino acid exchanges in a quartet of the C-terminally localized Cys residues in HypD, which coordinate the [4Fe-4S] cluster [27], destabilize the protein. Extracts derived from MC4100 and the [Fe-S] cluster-trafficking mutants were separated by SDS-PAGE and subjected to western blot analysis with anti-HypD antibodies (Fig. 6). HypD migrated as an approximately 40 kDa polypeptide in extracts from MC4100. An extract derived from the *hyp* operon deletion mutant BEF314 [41] showed no polypeptide that migrated at this position or that reacted with the anti-HypD antibodies (Fig. 6). While extracts from CP477 (Δ*iscA*) and CP1223 (Δ*sufA*) had essentially MC4100 levels of HypD, an extract derived from an *erpA* mutant showed a HypD polypeptide of reduced intensity. In contrast, extracts from the *iscU* mutant JW2513 showed no polypeptide, a result which would be consistent with a lack of the [Fe-S] cluster in HypD causing rapid turnover of the protein (see [13]).

Discussion.

Deficiences in anaerobic modular [Fe-S] cluster enzyme assembly

In this study we have shown that a mutant lacking the A-type carrier proteins ErpA and IscA cannot oxidize molecular hydrogen and have a severely reduced capability to evolve dihydrogen. A mutant unable to synthesize the [Fe-S] cluster scaffold protein IscU of the Isc machinery [3] was essentially deficient in [NiFe]-hydrogenase-dependent hydrogen metabolism. The fact that some FHL complex activity was retained in the *iscA* and *erpA* mutants suggests that the two ATC proteins may have overlapping functions with respect to Hyd-3 maturation; however, both proteins appear to be essential for synthesis of active hydrogen-oxidizing hydrogenases. Together, these findings indicate that these proteins exhibit distinctions in the range of their apoprotein targets. The severe reduction

in overall hydrogenase enzyme activity, measured as hydrogen-dependent BV reduction, as well as the complete loss specifically of Hyd-1 and Hyd-2 activities, presents a clear phenotype for individual *iscA* and *erpA* mutants with respect to hydrogen metabolism. The lack of an effect of a *sufA* mutation on hydrogen metabolism rules out any direct involvement of the SufA protein in anaerobic hydrogen metabolism and underscores and extends the genetic evidence indicating that IscA and ErpA are solely involved in the biogenesis of [Fe-S] clusters during both anaerobic respiratory and fermentative metabolism [3]. The findings of the current study are also supported by the recent demonstration that the modular anaerobic respiratory enzymes formate dehydrogenase and nitrate reductase are inactive in *erpA* mutants but retain partial activity in *iscA* mutants [42]. Taken together these data indicate that the Isc machinery is crucial for the biosynthesis and assembly of functional modular anaerobic oxidoreductases that depend on [Fe-S] clusters for electron transfer processes.

Three [Fe-S] cluster insertion phenotypes are associated with *iscA* and *erpA* mutations

The *iscA* and *erpA* mutants exhibit three phenotypes with respect to hydrogen metabolism. Firstly, stability of, and by implication [Fe-S] cluster insertion into, the respective small subunit of Hyd-1 and Hyd-2 is absolutely dependent on both ErpA and IscA, indicating a requirement for the function of both proteins in enzyme maturation. A similar requirement was observed for the activity of the formate dehydrogenase H associated with the FHL complex. Second, in the case of the maturation of the FHL complex, there is partial redundancy between ErpA and IscA. Third, with respect to [Fe-S] cluster insertion into HypD, a clear redundancy between IscA and ErpA is observed because either can stabilize the polypeptide; an absolute dependence on the Isc machinery is, however, demonstrated because in an *iscU* mutant HypD cannot be detected, presumably due to enhanced degradation [13,40].

Absence of the small subunit is the reason for the lack of hydrogenase enzyme activity

The lack of hydrogenase enzyme activity (measured as benzyl viologen: oxidoreduction) in the individual ATC mutants proved in each enzyme analyzed to be due to the absence of the small, electron-transferring subunit, which relays electrons between the catalytic site in the large subunit and the quinone pool [15,43,44]. In the respiratory Hyd-1 and Hyd-2 enzymes each small subunit has three [Fe-S] clusters with the medial one being a [3Fe-4S] cluster flanked by [4Fe-4S] clusters [44]. We believe it is valid to assume that if the [Fe-S] clusters cannot be inserted

into these proteins they are rapidly degraded. This is strongly supported by the apparent instability of the [Fe-S] cluster-containing [NiFe]-hydrogenase maturase HypD observed previously, which is caused by substitution of the Cys residues that coordinate the cluster [40] and the lack of HypD in an *iscU* mutant (see Fig. 6). Our recent demonstration that in the absence of the small subunit hydrogen-dependent benzyl viologen reduction is abolished [37] explains why enzyme activity could not be detected in the ATC mutants.

Because the HyaA and HybO small subunits of Hyd-1 and Hyd-2, respectively, carry Tat signal peptides [45], if they are rapidly degraded then they are unavailable to associate with the mature catalytic subunit and thus the HyaA-HyaB and HybO-HybC dimeric complexes cannot be translocated through the Tat translocon. Our ability to detect the mature forms of the HyaB and HybC large subunits, albeit in signficantly lower amounts compared with the MC4100, supports the contention that the matured large subunits of Hyd-1 and Hyd-2 become trapped in the cytoplasmic compartment. Moreover, because the mature HybC large subunit, which lacks a Tat signal peptide, could be detected in the soluble fraction, this indicates that biosynthesis of the [NiFe] active site was not compromised in the ATC mutants and provides futher proof that the large subunit is matured independently of the small subunit. The findings also indicate that both proteins form a complex only after maturation of each has been completed (Fig. 7).

The detection of processed, mature forms of the catalytic subunits of Hyd-1 and Hyd-2 indicates that delivery of the iron for biosynthesis of the [NiFe] active site is either independent of the [Fe-S] cluster biogenesis machinery, or that the IscA and ErpA proteins show redundancy in this function. In this regard, it should be noted that the ATC proteins have been proposed to function in iron donation to the Isc machinery and possibly other proteins [46,47]. The question of whether the ATC proteins might be involved in Fe delivery for active site biosynthesis unfortunately cannot be resolved by the findings presented in this study because an *iscU* mutant lacks detectable levels of the [Fe-S] cluster-containing HypD maturase. Without HypD it is not possible to synthesize and introduce the [NiFe]-center into the hydrogenase catalytic subunits. This problem will require the development of an *in vitro* system [48] to address the origin of the iron ion in the [NiFe] center.

Do ErpA and IscA deliver different [FeS] clusters to apoprotein targets?

The association of the FHL components FdhF (the catalytic subunit of the Fdh-H enzyme activity) and the Hyd-3 small subunit HycG with the membrane-

associated core complex is absolutely dependent on the presence of ErpA. Presumably the lack of association of FdhF with the core FHL complex was due either to aberrant maturation of the HycB [Fe-S] small subunit of Fdh-H or incomplete maturation of FdhF itself, which has a [4Fe-4S] cluster as well as a molybdo-bis molybdopterin guanine dinucleotide cofacter [23]. We have shown recently that the other two related formate dehydrogenases Fdh-N and Fdh-O showed aberrant maturation in an *erpA* mutant [42], also probably reflecting defective cofactor insertion.

It is perhaps noteworthy that the predicted [Fe-S] cluster-containing HycF protein did not exhibit rapid turnover, or an inability to associate with the membrane in the ATC mutants, or aberrant migration upon SDS-PAGE. Clearly, HycF represents a predicted [Fe-S] protein that either receives its [Fe-S] cluster from a source other than IscA or ErpA (an *erpA iscA* double mutant also shows membrane-associated HycF (data not shown)), or its apoprotein is not subject to rapid degradation and even in the absence of [Fe-S] clusters associates with the membrane. It is also possible, but unlikely based on the primary sequence, that it has no [Fe-S] cluster. Further analyses will be required to resolve this issue.

An *iscA* mutation also caused a signficant reduction in FHL activity as measured by hydrogen gas evolution but activity was never observed to be completely absent in the mutant. This non-redundant phenotype suggests distinct roles for both IscA and ErpA in [Fe-S] cluster trafficking to the small subunits, as has been recently suggested during aerobic growth [3,8]. Moreover, it should be noted that, although the approximately 110 amino acid ErpA and IscA proteins are phylogenetically related, they share only 40% amino acid sequence identity (57% similarity), which would be consistent with them having different apoprotein substrates. Pye and Barras have proposed that in aerobically growing cells IscA accepts a pre-formed [Fe-S] cluster from IscU and transfers this cluster via ErpA to the apo-protein substrate [3]. This model would be consistent with the findings observed for Hyd-1 and Hyd-2; however, [Fe-S] cluster transfer from IscA to ErpA cannot explain the other phenotypes of the *iscA* and *erpA* mutations on FHL maturation. Rather, it is possible that ErpA might transfer [4Fe-4S] clusters more efficiently while IscA can transfer either [4Fe-4S] or [3Fe-4S] clusters. Based on sequence analysis FdhF, HycB, HycF and HycG of the FHL complex have only [4Fe-4S] clusters, while the HybO and HyaA small subunits of the hydrogen-oxidizing enzymes have both [4Fe-4S] and [3Fe-4S] clusters. The partial overlap of ATC function in FHL complex assembly suggests that both ATCs can fullfil the role of [4Fe-4S] cluster insertion, although there seems to

be a greater dependence on ErpA. Recent studies looking at the roles of IscA and SufA in aerobic metabolism have indicated that a distinct and as yet undefined [Fe-S] cluster assembly pathway is responsible for introduction of [2Fe-2S] clusters into particular apoprotein substrates, e.g. FhuF and the SoxR regulator [49], which might also be consistent with the suggestion that IscA and ErpA assemble different [Fe-S] clusters into certain apoprotein substrates. Moreover, the recent, exciting discovery of a new type of [4Fe-3S] cluster in the small subunit of the oxygen-tolerant, membrane-associated respiratory [NiFe]-hydrogenase of *Ralstonia eutropha* [50] and *Hydrogenovibrio marinus* [51] underscores the possible existence of further trafficking systems in other organsims. Our future studies will be directed towards addressing the possibility of differential cluster transfer by the ATC proteins.

The paradoxical phenotype of a *hypF* mutant and the spatio-temporal assembly of hydrogenases

HypF is central to the maturation of [NiFe]-hydrogenases because it synthesizes the CN⁻ ligands to the Fe atom in the active site of these enzymes [13]. The consequence of deleting the *hypF* gene is that the catalytic subunits do not receive the [NiFe]-cofactor and consequently remain unprocessed and are enzymatically inactive. The results of this study demonstrate that the small subunits of Hyd-1, Hyd-2 and Hyd-3 cannot be detected in a *hypF* mutant, which is the same phenotype as observed in Isc⁻ mutants. While in *iscA* and *erpA* mutants the residual large subunit is processed and mature, in the *hypF* mutant the large subunit remains unprocessed. These results underscore the importance of prior maturation of the catalytic subunit before it can interact with the mature, [Fe-S] cluster-containing form of the small subunit. If the large subunit cannot be matured the small subunit is rapidly degraded; trancriptional regulation can be ruled out as a reason for lack of the small subunit polypeptides because the genes encoding the small subunits are the first genes in the operons [16,17,20]. Equally, if the small subunit does not receive its complement of [Fe-S] clusters then it is rapidly degraded and the large subunit is then also degraded, albeit more slowly. The apparent paradox lies in the fact that the unprocessed large subunit is clearly comparatively stable in a *hypF* mutant but is not stable in, for example, an *erpA* mutant (see Fig. 4). This suggests that a protein, which must be dependent on a component of the functional Isc machinery, stabilizes the immature catalytic subunit, preventing it from degradation. In this regard it is possible that products of *hya, hyb* and *hyc* operon genes have specific chaperone functions, e.g. HycH (see [13]). This is in analogy to observations made for the small subunit of

the [NiFe]-hydrogenase in the nitrogen-fixing symbiotic bacterium *Rhizobium leguminosarum* [52] where a mutation in an accessory gene *hupH* resulted in significantly reduced levels of the small subunit. HupH has been proposed to have a chaperone-like function in the maturation of the hydrogenase small subunit, possibly subsequent to [Fe-S] cluster delivery. Notably HyaF encoded in the *hya* operon is an orthologue of HupH and might perform a similar function during the maturation of HyaA [13,52].

A working hypothesis for hydrogenase maturation, using Hyd-2 as a model, is presented in Fig. 7. We assume a similar model for the maturation of Hyd-1. Either IscA or ErpA can deliver the [Fe-S] cluster to apo-HypD and together with the other Hyp maturases [13] synthesizes the [NiFe]-cofactor and inserts it into the pre-HybC large subunit. Whether the Fe atom in the active site is derived from the Isc machinery or is delivered by the Hyp protein machinery remains to be elucidated. After processing of the catalytic subunit by removal of the C-terminal peptide, along with the associated conformational change, maturation is complete. In a presumably independent, but temporally orchestrated, reaction the apo-HypO small subunit receives its complement of [Fe-S] clusters from the combined actions of IscA and ErpA. Whether further specific chaperones are involved in this process also remains to be established. Only once maturation is completed can holo-HybO interact with mature HybC to form the holo-HybO-HybC dimer that is a proficient substrate for the Tat translocon. If insuffient [Fe-S] clusters are available the small subunit is directed to the protein degradation machinery. Precisely which proteins are involved in turnover of improperly matured hydrogenase subunits also remains to be determined.

In the case of FHL complex assembly, the maturation of HycE (Hyd-3 catalytic subunit) follows a similar path to HybC (Fig. 7). In the case of FdhF and the electron-transferring small subunits HycG and HycB, however, ErpA is the main route of [Fe-S] cluster delivery with IscA playing a more subsidiary role. Future studies will be directed toward verifying the proposed roles of IscA and ErpA in [Fe-S] cluster delivery to these proteins and to determining whether all of these processes occur in a single multienzyme assembly complex or whether they are prepared in separate sub-complexes prior to assembly.

Methods.

Strains, plasmids and growth conditions. All bacterial strains and plasmids used in this study are listed in Table 1.
E. coli was grown aerobically in Erlenmeyer flasks filled to maximally 10% of their volume with TGYEP medium [53]. Cultures were incubated on a rotary shaker (250 rpm) and at 37°C. Anaerobic growths were performed at 37°C in sealed bottles filled with anaerobic growth medium under a nitrogen gas atmosphere.

When required, the growth medium was solidified with 1.5 % (w/v) agar. All growth media were supplemented with 0.1% (v/v) SLA trace element solution [54]. The antibiotics chloramphenicol, kanamycin and ampicillin, when required, were added to the medium at the final concentrations of 12.5 $\mu g\ ml^{-1}$, 50 $\mu g\ ml^{-1}$ and 100 $\mu g\ ml^{-1}$, respectively. Where indicated, L-arabinose was added to the growth medium to 0.2% (w/v).
When required, the Kan^{R} cassette of certain mutants was removed by transforming the strain in question with pCP20 encoding a Flp-recombinase [55]. Mutants were subsequently tested for sensitivity to kanamycin.

Preparation of cell extracts and determination of enzyme activities. Anaerobic cultures were harvested at an $OD_{600\ nm}$ of approximately 0.8. Cells from cultures were harvested by centrifugation at 4000 x g for 10 min at 4°C, resuspended in 2-3 ml of MOPS buffer pH 7.0 and lysed on ice by sonication (30W power for 5 minutes with 0.5 sec pulses). Unbroken cells and cell debris were removed by centrifugation for 15 min at 10 000 x g at 4°C and the supernatant was used as the crude cell extract. Membrane and soluble fractions were prepared as described [30]. Samples designated as cells in the figures indicates that whole cell samples were collected by centrifugation and the cell pellets were either resuspended directly in SDS sample buffer for western blot analysis or they were treated with 4% (v/v) Triton X-100 for 30 min on ice prior to being loaded directly onto non-denaturing polyacrylamide gels in 100 µl of the respective buffer at an optical density $OD_{600\ nm}$ equivalent to 1. Protein concentration of crude extracts was determined [56] with bovine serum albumin as standard. Hydrogenase activity was measured according to [30] and benzyl viologen-associated formate dehydrogenase activity according to [29] except that the buffer used was 50 mM MOPS, pH 7.0. The wavelength used in the hydrogenase enzyme assay was 578 nm and an E_{M} value of 8,600 $M^{-1}\ cm^{-1}$ was assumed for reduced benzyl viologen. One unit of activity corresponded to the oxidation of 1 µmol of hydrogen per min. Experiments were performed minimally three times and each time enzyme assays were perfomed in triplicate. Data are presented as standard deviation of the mean.
Quantitative determination of formate hydrogenlyase activity was performed as described [57].

Polyacrylamide gel electrophoresis and immunoblotting. Aliquots of 25-50 µg of protein from the indicated sub-cellular fractions were separated by SDS-polyacrylamide gel electrophoresis (PAGE) using 10% (w/v) polyacrylamide [58] and transferred to nitrocellulose membranes as described [59]. Antibodies raised against Hyd-1 (1: 10000; [36]), HycG (1:3000; [21]), Hyd-2 (1:20000; a kind gift from F. Sargent), FdhF (1:5000; [21]) and HycF (1:3000; a kind gift from A. Böck) were used. Secondary antibody conjugated to horseradish peroxidase was obtained from Bio-Rad. Visualisation was done by the enhanced chemiluminescent reaction (Stratagene).
Non-denaturing PAGE was performed using 5% (w/v) polyacrylamide gels pH 8.5 and included 0.1% (w/v) Triton X-100 in the gels and running buffer [30]. Samples (25 µg of protein) were incubated with 5% (w/v) Triton X-100 prior to application to the gels. Hydrogenase activity-staining was done as described in [30] except that the buffer used was 50 mM MOPS pH 7.0.

References.

1. Ayala-Castro C, Saini A, Outten FW (2008) Fe-S cluster assembly pathways in bacteria. Microbiol Mol Biol Rev 72: 110–125. doi:10.1128/MMBR.00034-07

2. Johnson DC, Dean DR, Smith AD, Johnson MK (2005) Structure, function, and formation of biological iron-sulfur clusters. Annu Rev Biochem 74: 247–281. doi:10.1146/annurev.biochem.74.082803.133518

3. Py B, Barras F (2010) Building Fe-S proteins: bacterial strategies. Nat Rev Microbiol 8: 436–446. doi:10.1038/nrmicro2356

4. Jacobson MR, Cash VL, Weiss MC, Laird NF, Newton WE, et al. (1989) Biochemical and genetic analysis of the nifUSVWZM cluster from Azotobacter vinelandii. Mol Gen Genet 219: 49–57.

5. Takahashi Y, Tokumoto U (2002) A third bacterial system for the assembly of iron-sulfur clusters with homologs in archaea and plastids. J Biol Chem 277: 28380–28383. doi:10.1074/jbc.C200365200

6. Zheng L, Cash VL, Flint DH, Dean DR (1998) Assembly of iron-sulfur clusters. Identification of an iscSUA-hscBA-fdx gene cluster from Azotobacter vinelandii. J Biol Chem 273: 13264–13272.

7. Vinella D, Brochier-Armanet C, Loiseau L, Talla E, Barras F (2009) Iron-sulfur (Fe/S) protein biogenesis: phylogenomic and genetic studies of A-type carriers. PLoS Genet 5: e1000497. doi:10.1371/journal.pgen.1000497

8. Loiseau L, Gerez C, Bekker M, Ollagnier-de Choudens S, Py B, et al. (2007) ErpA, an iron sulfur (Fe S) protein of the A-type essential for respiratory metabolism in Escherichia coli. Proc Natl Acad Sci USA 104: 13626–13631. doi:10.1073/pnas.0705829104

9. Ollagnier-de Choudens S, Sanakis Y, Fontecave M (2004) SufA/IscA: reactivity studies of a class of scaffold proteins involved in [Fe-S] cluster assembly. J Biol Inorg Chem 9: 828–838. doi:10.1007/s00775-004-0581-9

10. Chahal HK, Dai Y, Saini A, Ayala-Castro C, Outten FW (2009) The SufBCD Fe−S Scaffold Complex Interacts with SufA for Fe−S Cluster Transfer. Biochemistry 48: 10644–10653. doi:10.1021/bi901518y

11. Yang J, Bitoun JP, Ding H (2006) Interplay of IscA and IscU in biogenesis of iron-sulfur clusters. J Biol Chem 281: 27956–27963. doi:10.1074/jbc.M601356200

12. Tokumoto U, Kitamura S, Fukuyama K, Takahashi Y (2004) Interchangeability and distinct properties of bacterial Fe-S cluster assembly systems: functional replacement of the isc and suf operons in Escherichia coli with the nifSU-like operon from Helicobacter pylori. J Biochem 136: 199–209. doi:10.1093/jb/mvh104

13. Böck A, King P, Blokesch M, Posewitz M (2006) Maturation of hydrogenases. Adv Microb Physiol 51: 1–71.

14. Vignais PM, Billoud B (2007) Occurrence, classification, and biological function of hydrogenases: an overview. Chem Rev 107: 4206–4272. doi:10.1021/cr050196r

15. Forzi L, Sawers RG (2007) Maturation of [NiFe]-hydrogenases in Escherichia coli. Biometals 20: 565–578. doi:10.1007/s10534-006-9048-5

16. Menon NK, Robbins J, Wendt J, Shanmugam K, Przybyla A (1991) Mutational analysis and characterization of the Escherichia coli hya operon, which encodes [NiFe] hydrogenase 1. J Bacteriol 173: 4851–4861.

17. Menon NK, Chatelus CY, Dervartanian M, Wendt JC, Shanmugam KT, et al. (1994) Cloning, sequencing, and mutational analysis of the hyb operon encoding Escherichia coli hydrogenase 2. J Bacteriol 176: 4416–4423.

18. Sargent F, Ballantine S, Rugman P, Palmer T, Boxer D (1998) Reassignment of the gene encoding the Escherichia coli hydrogenase 2 small subunit-identification of a soluble precursor of the small subunit in a hypB mutant. Eur J Biochem 255: 746–754.

19. Dubini A, Pye R, Jack R, Palmer T, Sargent F (2002) How bacteria get energy from hydrogen: a genetic analysis of periplasmic hydrogen oxidation in Escherichia coli. International Journal of Hydrogen Energy 27: 1413–1420.

20. Böhm R, Sauter M, Böck A (1990) Nucleotide sequence and expression of an operon in Escherichia coli coding for formate hydrogenlyase components. Mol Microbiol 4: 231–243.

21. Sauter M, Böhm R, Böck A (1992) Mutational analysis of the operon (hyc) determining hydrogenase 3 formation in Escherichia coli. Mol Microbiol 6: 1523–1532.

22. Zinoni F, Birkmann A, Stadtman T, Böck A (1986) Nucleotide sequence and expression of the selenocysteine-containing polypeptide of formate dehydrogenase (formate-hydrogen-lyase-linked) from Escherichia coli. Proc Natl Acad Sci U S A 83: 4650–4654.

23. Boyington JC, Gladyshev VN, Khangulov SV, Stadtman TC, Sun PD (1997) Crystal structure of formate dehydrogenase H: catalysis involving Mo, molybdopterin, selenocysteine, and an Fe4S4 cluster. Science 275: 1305–1308.

24. Rossmann R, Sawers RG, Böck A (1991) Mechanism of regulation of the formate-hydrogenlyase pathway by oxygen, nitrate, and pH: definition of the formate regulon. Mol Microbiol 5: 2807–2814.

25. Sawers RG, Clark DP (2004) Fermentative pyruvate and acetyl CoA metabolism. July 2004, posting date. Chapter 3.5.3. In R. Curtiss III (Editor in Chief), EcoSal--Escherichia coli and Salmonella: Cellular and Molecular Biology. [Online.] http://www.ecosal.org. ASM Press, Washington, D.C..

26. Blokesch M, Albracht SPJ, Matzanke BF, Drapal NM, Jacobi A, et al. (2004) The complex between hydrogenase-maturation proteins HypC and HypD is an intermediate in the supply of cyanide to the active site iron of [NiFe]-hydrogenases. J Mol Biol 344: 155–167. doi:10.1016/j.jmb.2004.09.040

27. Watanabe S, Matsumi R, Arai T, Atomi H, Imanaka T, et al. (2007) Crystal structures of [NiFe] hydrogenase maturation proteins HypC, HypD, and HypE: insights into cyanation reaction by thiol redox signaling. Mol. Cell 27: 29–40. doi:10.1016/j.molcel.2007.05.039

28. Eitinger T, Mandrand-Berthelot MA (2000) Nickel transport systems in microorganisms. Arch Microbiol 173: 1–9.

29. Sawers RG, Ballantine S, Boxer D (1985) Differential expression of hydrogenase isoenzymes in Escherichia coli K-12: evidence for a third isoenzyme. J Bacteriol 164: 1324–1331.

30. Ballantine S, Boxer D (1985) Nickel-containing

hydrogenase isoenzymes from anaerobically grown *Escherichia coli* K-12. J Bacteriol 163: 454–459.

31. Paschos A, Bauer A, Zimmermann A, Zehelein E, Böck A (2002) HypF, a carbamoyl phosphate-converting enzyme involved in [NiFe] hydrogenase maturation. J Biol Chem 277: 49945–49951. doi:10.1074/jbc.M204601200

32. Layer G, Ollagnier-de Choudens S, Sanakis Y, Fontecave M (2006) Iron-sulfur cluster biosynthesis: characterization of *Escherichia coli* CyaY as an iron donor for the assembly of [2Fe-2S] clusters in the scaffold IscU. J Biol Chem 281: 16256–16263. doi:10.1074/jbc.M513569200

33. Rossmann R, Sauter M, Lottspeich F, Böck A (1994) Maturation of the large subunit (HYCE) of *Escherichia coli* hydrogenase 3 requires nickel incorporation followed by C-terminal processing at Arg537. Eur J Biochem 220: 377–384.

34. Magalon A, Böck A (2000) Dissection of the maturation reactions of the [NiFe] hydrogenase 3 from *Escherichia coli* taking place after nickel incorporation. FEBS Lett 473: 254–258.

35. Ballantine S, Boxer D (1986) Isolation and characterisation of a soluble active fragment of hydrogenase isoenzyme 2 from the membranes of anaerobically grown *Escherichia coli*. Eur J Biochem 156: 277–284.

36. Sawers RG, Boxer D (1986) Purification and properties of membrane-bound hydrogenase isoenzyme 1 from anaerobically grown *Escherichia coli* K12. Eur J Biochem 156: 265–275.

37. Pinske C, Krüger S, Soboh B, Ihling C, Kuhns M, *et al.* (2011) Efficient electron transfer from hydrogen to benzyl viologen by the [NiFe]-hydrogenases of *Escherichia coli* is dependent on the coexpression of the iron-sulfur cluster-containing small subunit. Arch Microbiol. Epub: 21717143, doi:10.1007/s00203-011-0726-5

38. Jack RL, Buchanan G, Dubini A, Hatzixanthis K, Palmer T, *et al.* (2004) Coordinating assembly and export of complex bacterial proteins. EMBO J 23: 3962–3972. doi:10.1038/sj.emboj.7600409

39. Wagner A, Frey M, Neugebauer F, Schafer W, Knappe J (1992) The free radical in pyruvate formate-lyase is located on glycine-734. Proc Natl Acad Sci U S A 89: 996–1000.

40. Blokesch M, Böck A (2006) Properties of the [NiFe]-hydrogenase maturation protein HypD. FEBS Lett 580: 4065–4068. doi:10.1016/j.febslet.2006.06.045

41. Jacobi A, Rossmann R, Böck A (1992) The *hyp* operon gene products are required for the maturation of catalytically active hydrogenase isoenzymes in *Escherichia coli*. Arch Microbiol 158: 444–451.

42. Pinske C, Sawers RG (2011) The A-type carrier protein ErpA is essential for formation of an active formate-nitrate respiratory pathway in *Escherichia coli* K-12. J Bacteriol.

43. Sawers RG (1994) The hydrogenases and formate dehydrogenases of *Escherichia coli*. Antonie Van Leeuwenhoek 66: 57–88.

44. Volbeda A, Charon M, Piras C, Hatchikian E, Frey M, *et al.* (1995) Crystal structure of the nickel-iron hydrogenase from *Desulfovibrio gigas*. Nature 373: 580–587.

45. Sargent F (2007) Constructing the wonders of the bacterial world: biosynthesis of complex enzymes. Microbiology (Reading, Engl) 153: 633–651. doi:10.1099/mic.0.2006/004762-0

46. Ding H, Clark RJ (2004) Characterization of iron binding in IscA, an ancient iron-sulphur cluster assembly protein. Biochem J 379: 433–440. doi:10.1042/BJ20031702

47. Ding H, Yang J, Coleman LC, Yeung S (2007) Distinct iron binding property of two putative iron donors for the iron-sulfur cluster assembly: IscA and the bacterial frataxin ortholog CyaY under physiological and oxidative stress conditions. J Biol Chem 282: 7997–8004. doi:10.1074/jbc.M609665200

48. Soboh B, Krüger S, Kuhns M, Pinske C, Lehmann A, *et al.* (2010) Development of a cell-free system reveals an oxygen-labile step in the maturation of [NiFe]-hydrogenase 2 of *Escherichia coli*. FEBS Lett 584: 4109–4114. doi:10.1016/j.febslet.2010.08.037

49. Tan G, Lu J, Bitoun JP, Huang H, Ding H (2009) IscA/SufA paralogues are required for the [4Fe-4S] cluster assembly in enzymes of multiple physiological pathways in *Escherichia coli* under aerobic growth conditions. Biochem J 420: 463–472. doi:10.1042/BJ20090206

50. Fritsch J, Scheerer P, Frielingsdorf S, Kroschinsky S, Friedrich B, *et al.* (2011) The crystal structure of an oxygen-tolerant hydrogenase uncovers a novel iron-sulphur centre. Nature. doi:10.1038/nature10505

51. Shomura Y, Yoon K-S, Nishihara H, Higuchi Y (2011) Structural basis for a [4Fe-3S] cluster in the oxygen-tolerant membrane-bound [NiFe]-hydrogenase. Nature. doi:10.1038/nature10504

52. Manyani H, Rey L, Palacios JM, Imperial J, Ruiz-Argüeso T (2005) Gene products of the *hupGHIJ* operon are involved in maturation of the iron-sulfur subunit of the [NiFe] hydrogenase from *Rhizobium leguminosarum* bv. viciae. J Bacteriol 187: 7018–7026. doi:10.1128/JB.187.20.7018-7026.2005

53. Begg Y, Whyte J, Haddock B (1977) The identification of mutants of *Escherichia coli* deficient in formate dehydrogenase and nitrate reductase activities using dye indicator plates. FEMS Microbiol Lett 2: 47–50.

54. Hormann K, Andreesen J (1989) Reductive cleavage of sarcosine and betaine by *Eubaterium acidaminophilum* via enzyme systems different from glycine reductase. Arch Microbiol 153: 50–59.

55. Cherepanov P, Wackernagel W (1995) Gene disruption in *Escherichia coli*: Tc^R and Km^R cassettes with the option of Flp-catalyzed excision of the antibiotic-resistance determinant. Gene 158: 9–14.

56. Lowry O, Rosebrough N, Farr A, Randall R (1951) Protein measurement with the Folin phenol reagent. J Biol Chem 193: 265–275.

57. Pinske C, Sawers RG (2010) The role of the ferric-uptake regulator Fur and iron homeostasis in controlling levels of the [NiFe]-hydrogenases in *Escherichia coli*. International Journal of Hydrogen Energy 35: 8938–8944. doi:10.1016/j.ijhydene.2010.06.030

58. Laemmli U (1970) Cleavage of structural proteins during the assembly of the head of bacteriophage T4. Nature 227: 680–685.

59. Towbin H, Staehelin T, Gordon J (1979) Electrophoretic transfer of proteins from polyacrylamide gels to nitrocellulose sheets: procedure and some applications. Proc Natl Acad Sci U S A 76: 4350–4354.

60. Casadaban MJ (1976) Transposition and fusion of the *lac* genes to selected promoters in *Escherichia coli* using bacteriophage lambda and Mu. J Mol Biol 104: 541–555.

61. Pinske C, Bönn M, Krüger S, Lindenstrauß U, Sawers RG (2011) Metabolic deficiences revealed in the biotechnologically important model bacterium *Escherichia coli* BL21(DE3). PLoS ONE 6: e22830. doi:10.1371/journal.pone.0022830

62. Redwood M, Mikheenko I, Sargent F, Macaskie L (2007) Dissecting the roles of *Escherichia coli* hydrogenases in biohydrogen production. FEMS Microbiol Lett 278 : 48–55.

63. Soboh B, Pinske C, Kuhns M, Waclawek M, Ihling C, *et al.* (2011) The respiratory molybdo-selenoprotein formate dehydrogenases of *Escherichia coli* have hydrogen: benzyl viologen oxidoreductase activity. BMC Microbiol 11,173.

Table 1. Strains and plasmids used in this study

Strains/ plasmids	Genotype[a]	Reference/ Source
MC4100	F$^-$ *araD139* Δ(*argF-lac*)*U169 ptsF25 deoC1 relA1 flbB5301 rspL150* $^-$	[60]
BEF314	MC4100 Δ*hypB-hypE2 (hyp :: cat* pACYC184)	[41]
DHP-F2	MC4100 Δ*hypF* 59-629AA; ECK2707	[31]
PB1000	MC4100 Δ*purT* Δ*purU* Δ*insH4-fnr*	[61]
FTD147	MC4100 Δ*hyaB hybC hycE*	[62]
CP795	MC4100 Δ*hyaB hybO hycE*	[37]
CP477	As MC4100 but Δ*iscA*::Kan^R; ECK2525	[42]
CP1223	As MC4100 but Δ*sufA*::Cm^R; ECK1680	[42]
CP545	As MC4100 but Δ*cyaY*::Kan^R; ECK3801	This study
CP971	As MC4100 but Δ*hycA-I*:Kan^R	[61]
CP967	As MC4100 but Δ*iscA*::Kan^R *hycAI*::Cm^R	This study
LL401	MG1655 conditional *ara$_P$*::*erpA*	[8]
LL402	MG1655 Δ*erpA*::Cm^R	[8]
DV1151	MG1655 Δ*erpA*::Cm^R *iscA*	[7]
JW3779	BW25113 Δ*cyaY*::Kan^R; ECK3801	+
JW2513	BW25113 Δ*iscU*::Kan^R; ECK2526	+
Plasmids		
pCP20	*FLP$^+$,* λcI857$^+$, λp_R Rep^{ts}, Amp^R, Cm^R	[55]
perpA	pBluescript SK(+) containing *erpA* in BamHI and EcoRI site; Amp^R	[42]
piscA	pBluescript SK(+) containing *iscA* in BamHI and EcoRI site; Amp^R	[42]

+ National BioResources Project (NIG, Japan): E. coli
[a] Allele numbers are given for single gene mutants and refer to the K-12 nomenclature.

Table 2: Total hydrogenase activity of mutants lacking [Fe-S] trafficking A-type carrier proteins.

Strain and genotype[a]	Specific Hydrogenase Activity in U mg protein^{-1} ± SD[b]		
	no addition	piscA	perpA
MC4100	3.00 ± 0.59	1.65 ± 0.49	2.78 ± 0.71
DHP-F2	0.01	n.d.	n.d.
CP477 (*iscA*)	0.12 ± 0.07	3.59 ± 0.19	0.28 ± 0.07
LL401 (conditional *erpA*)[c]	0.13 ± 0.16	0.07 ± 0.04	3.37 ± 1.45
CP1223 (*sufA*)	4.17 ± 0.12	n.d	n.d.
DV1151 (*iscA erpA*)	< 0.01	0.18 ± 0.23	0.27 ± 0.13
JW2513 (*iscU*)	0.01 ± 0.01	n.d.	n.d.
CP545 (*cyaY*)	3.58 ± 0.11	n.d.	n.d.
CP971 (*hycAI*)	0.14 ± 0.08	n.d.	n.d.
CP967 (*iscA hycAI*)	< 0.01	n.d.	n.d.

[a] Cells were grown anaerobically in TGYEP.
[b] The mean and standard error of at least three independent experiments are shown.
[c] The activity measured after growth in the presence of 0.2% (w/v) L-arabinose was 5.34 ± 1.02 U mg protein^{-1}
n.d. – Activity in this combination was not determined.

Table 3: Hydrogen evolving activity of mutants lacking [Fe-S] trafficking A-type carrier proteins.

Strain and genotype[a]	Specific Hydrogen evolving Activity in mU mg protein^{-1} ± SD[b]		
	no addition	piscA	perpA
MC4100	30 ± 7	32 ± 8	23 ± 12
DHP-F2	< 1	n.d.	n.d.
CP971 (*hycAI*)	< 1	n.d.	n.d.
CP477 (*iscA*)	5 ± 1	20 ± 15	2 ± 1
LL401 (conditional *erpA*)[c]	2 ± 1	1 ± 1	6 ± 0.4
CP1223 (*sufA*)	15 ± 5	n.d.	n.d.
DV1151 (*iscA erpA*)	< 1	n.d.	n.d.
JW2513 (*iscU*)	< 1	n.d.	n.d.
CP545 (*cyaY*)	16 ± 4	n.d.	n.d.

[a] Cells were grown anaerobically in TGYEP.

[b] The mean and standard error of at least three independent experiments are shown.

[c] The activity measured after growth in the presence of 0.2% (w/v) L-arabinose was 13 ± 2 mU mg protein^{-1}

n.d. – Activity in this combination was not determined.

Table 4: Mutants lacking the ATC proteins IscA and ErpA have deficiences in fermentative formate dehydrogenase activity.

Strain (genotype)[a]	A_S Fdh-H (U mg protein^{-1})[b]
MC4100	0.24 ± 0.06
BW25113	0.20 ± 0.02
LL401 (conditional *erpA*)	< 0.01
LL401 L-arabinose	0.35 ± 0.14
LL401 piscA	< 0.01
LL401 piscA L-arabinose	0.13 ± 0.16
LL401 perpA	0.22 ± 0.07
CP477 (*iscA*)	< 0.01
Δ*iscA* piscA	0.12 ± 0.01
Δ*iscA* perpA	< 0.01
CP1223 (Δ*sufA*)	0.14 ± 0.12

[a] Cells were grown anaerobically in TGYEP.

[b] The mean and standard error of at least three independent experiments are shown.
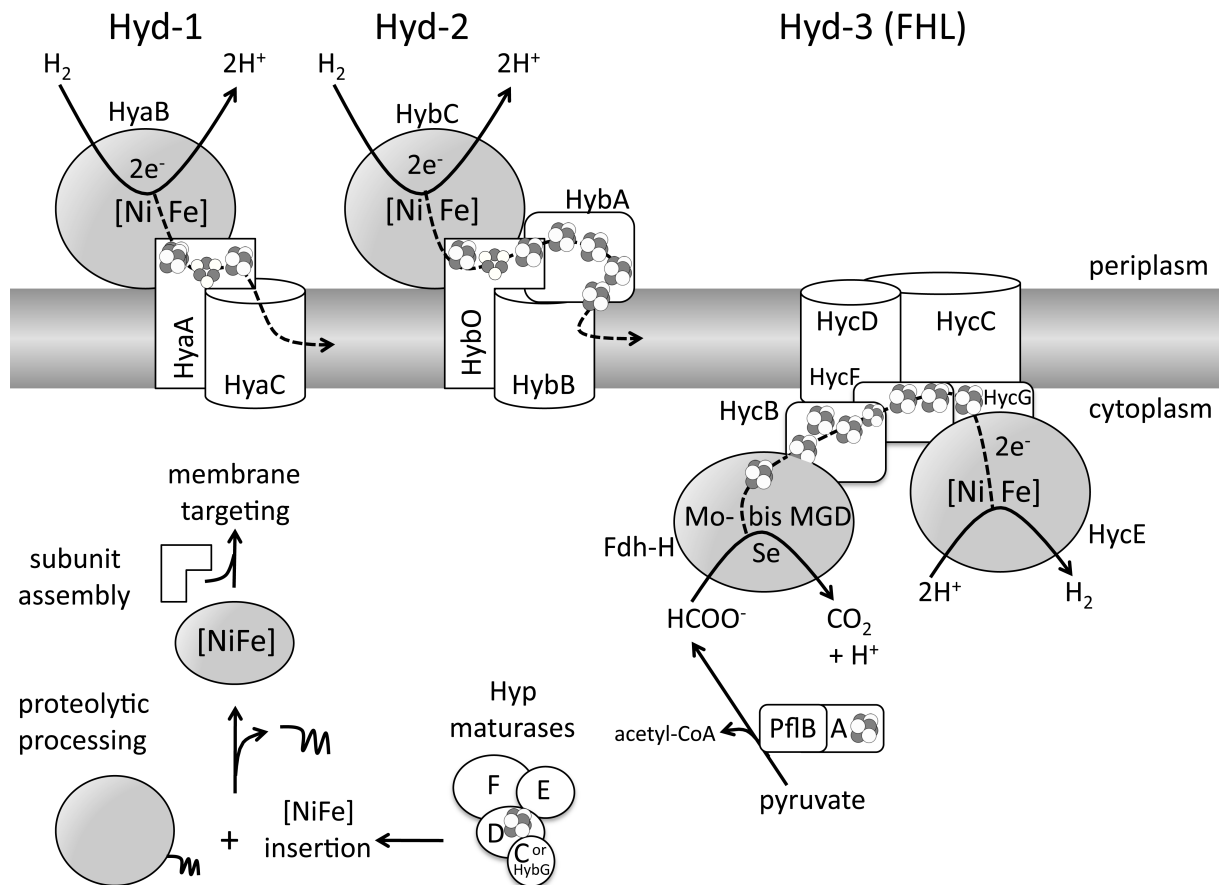
Figure legends

Figure 1. Schematic representation of the iron-sulphur cluster-containing proteins involved in the hydrogen metabolism of *E. coli*. The three anaerobic, membrane-associated [NiFe]-hydrogenases are schematically represented with their associated subunit. The presence of iron-sulphur clusters is designated by the grouped spheres. No distinction is made between [3Fe-4S] and [4Fe-4S] clusters. The ‚squiggle' attached to the apoprotein form of the hydrogenase catalytic subunit (bottom left of the Figure) represents the C-terminal peptide that is removed subsequent to insertion of the [NiFe] prosthetic group. Mo-bis MGD in the Fdh-H protein designates the molydo-bis molybdopterin guanine dinucleotide cofactor and Se indicates selenocysteine. The dotted arrows indicate electron flow within the modular enzymes or to the quinone pool. PflB and PflA represent the enzymes pyruvate formate-lyase and its SAM-radical activating enzyme, respectively.
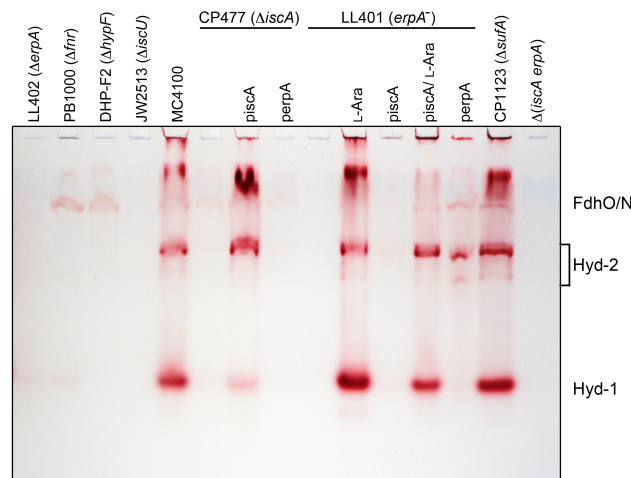

Figure 2. Hydrogenases 1 and 2 are inactive in *iscA* and *erpA* mutants. Aliquots of crude extracts (25 µg protein) derived from the bacterial stains shown were separated by non-denaturing PAGE (7.5% w/v polacrylamide) and subsequently stained for hydrogenase enzyme activity. Hyd-1 migrates

as a single active enzyme species while Hyd-2 shows multiple active forms, which are designated on the right of the panel. The weak hydrogen: benzyl viologen oxidoreductase activity that is independent of the [NiFe]-hydrogenases is associated with FDH-O/N [63] is also designated. In Strain DV1151 only the genotype is indicated as Δ(*erpA iscA*).
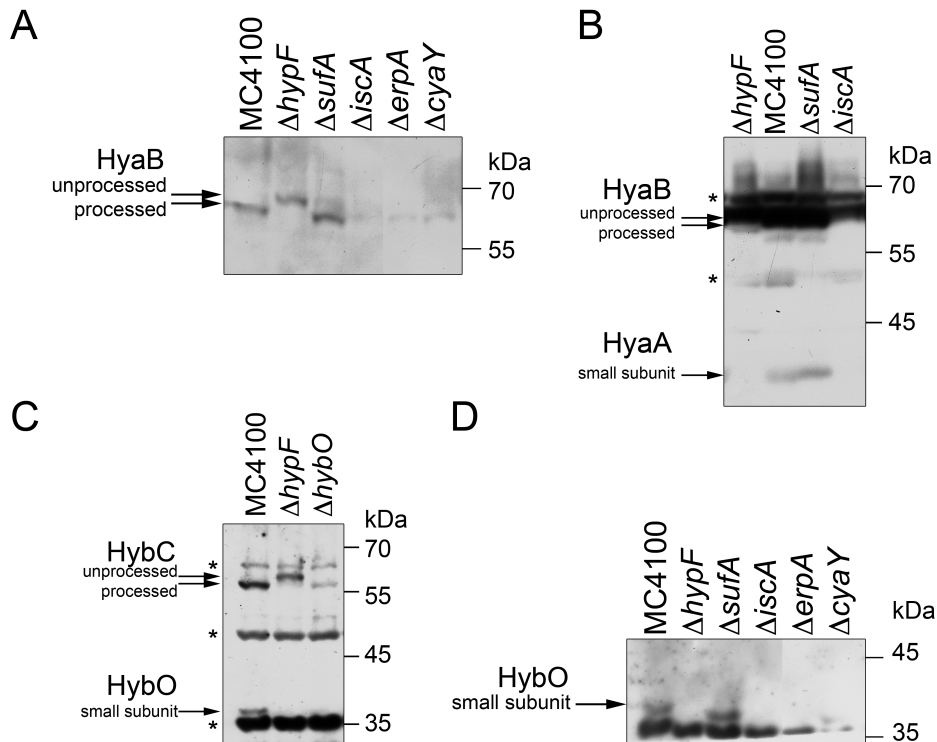

Figure 3. Immunological analysis reveals maturation of the catalytic subunit and absence of the small subunit of the hydrogen-uptake enzymes in *erpA* and *iscA* mutant. Samples of crude extracts (25 - 50 μg protein) derived from the strains (genotypes are shown above each lane) indicated were separated in 10% w/v SDS-PAGE, transferred to nitrocellulose membranes and probed with antibodies against the Hyd-1 large subunit (HyaB) (A) or the small subunit (B). The locations of the processed and unprocessed forms of the large subunit polypeptide are shown on the left of the panel and the migration position of molecular mass size markers are shown on the right. Results of a similar experiment showing Western blots of the large (HybC) and small (HybO) subunits of Hyd-2 are shown in C and D. Unspecific cross-reacting polypeptides that were used as internal loading controls are marked with an asterisk. MC4100, wild type; DHP-F2 (Δ*hypF*); CP1223 (Δ*sufA*); CP477 (Δ*iscA*); LL402 (Δ*erpA*); CP545 (Δ*cyaY*); CP975 (Δ*hyaB* Δ*hybO* Δ*hycE*).
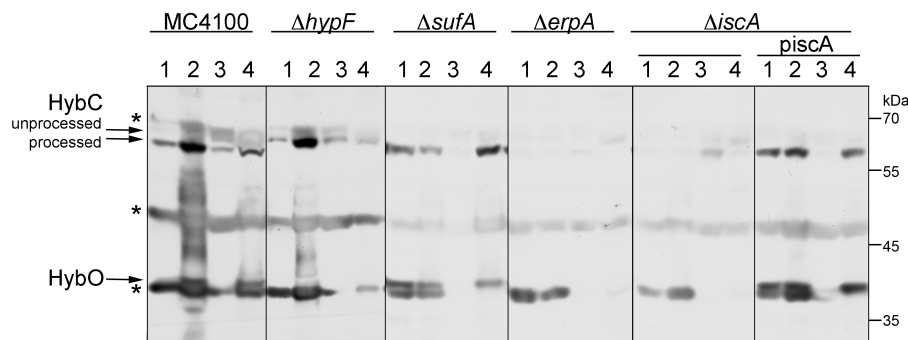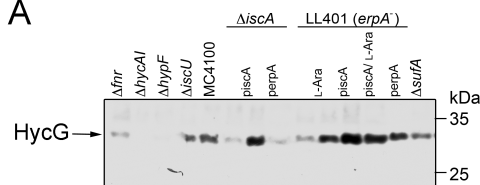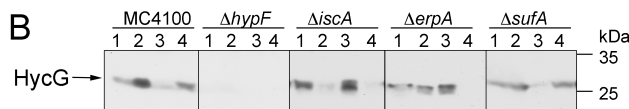
A
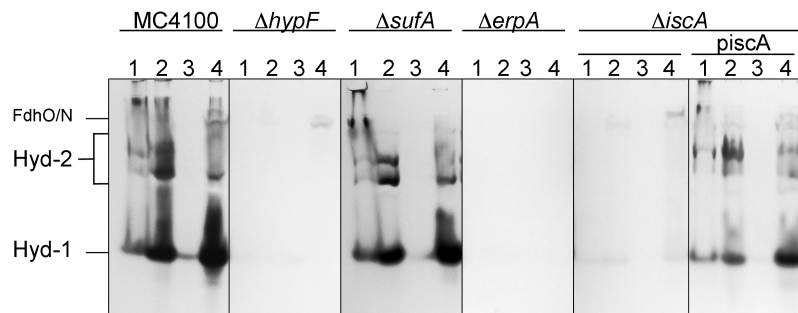
B

Figure 4. Subcellular localization of hydrogenase 2 in *iscA*, *sufA* and *erpA* mutants. Aliquots (25 µg protein) derived from whole cells (1), crude extracts (2), soluble fractions (3) or membrane fractions (4) from MC4100, DHP-F2 (Δ*hypF*), CP1223 (Δ*sufA*), LL402 (Δ*erpA*), CP477 (Δ*iscA*) and CP477 + piscA were separated either by native-PAGE (A) (7.5% w/v polyacrylamide) and stained for Hyd-1 and Hyd-2 activity, or by 10% SDS-PAGE (B) and subjected to Western blotting using anti-Hyd-2 antiserum. On the left side of panel A, the migration positions of Hyd-1, Hyd-2, and of the hydrogenase-independent FDH-O/N hydrogen-BV oxidoreductase activity are indicated. In panel B the migration positions of the unprocessed and processed forms of the catalytic subunit HybC and the small subunit HybO are shown. The asterisks indicate unspecifically cross-reacting polypeptides of unknown identity, which acted as internal loading controls. The migration positions of the molecular mass standards (in kDa) are indicated on the right of the Figure.

A

B

C
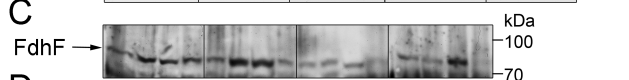
D
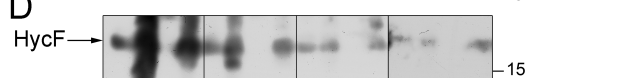
Figure 5. Subcellular localization of the formate hydrogenlyase components HycG, Fdh-H and HycF in *iscA*, *sufA* and *erpA* mutants. A. Aliquots (25 µg protein) derived from crude extracts of the strains PB1000 (*fnr*), CP971 (Δ*hycA-I*), DHP-F2 (Δ*hypF*), JW2513 (Δ*iscU*), MC4100, CP477 (Δ*iscA*), LL401 (conditional *erpA*) and CP1223 (Δ*sufA*) were separated in 10% SDS-PAGE and subjected to western blotting with anti-HycG antibodies. In parts B, C, and D aliquots (25 µg protein) derived from

cells (1), crude extracts (2), soluble fractions (3) or membrane fractions (4) from MC4100, DHP-F2 (Δ*hypF*), CP1223 (Δ*sufA*), LL402 (Δ*erpA*) and CP477 (Δ*iscA*) were separated by 10% SDS-PAGE and subjected to western blotting using anti-HycG (B), anti-Fdh-H (C) and anti-HycF (D) antisera. The arrows on the left side of the panels identify the relevant polypeptides. The migration positions of the molecular mass standards (in kDa) are indicated on the right of the Figure.
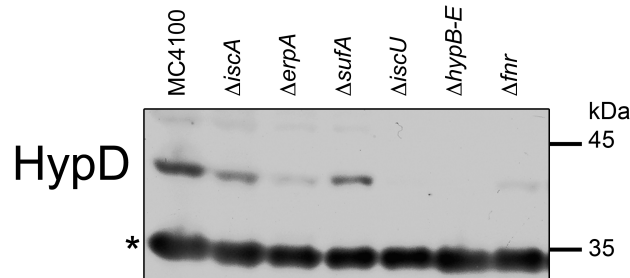
Figure 6. Identification of the HypD maturase in mutants defective in iron-sulphur cluster biogenesis. Aliquots (25 μg protein) derived from MC4100, CP477 (Δ*iscA*), LL402 (Δ*erpA*), CP1223 (Δ*sufA*), JW2513 (Δ*iscU*), BEF314 (Δ*hypB-E*) and PB1000 (Δ*fnr*) were separated by 10% SDS-PAGE and subjected to Western blotting using anti-HypD antiserum. The asterisk indicates an unidentified cross-reacting polypeptide that served as an internal loading control. The migration positions of the molecular mass standards (in kDa) are indicated on the right of the Figure.
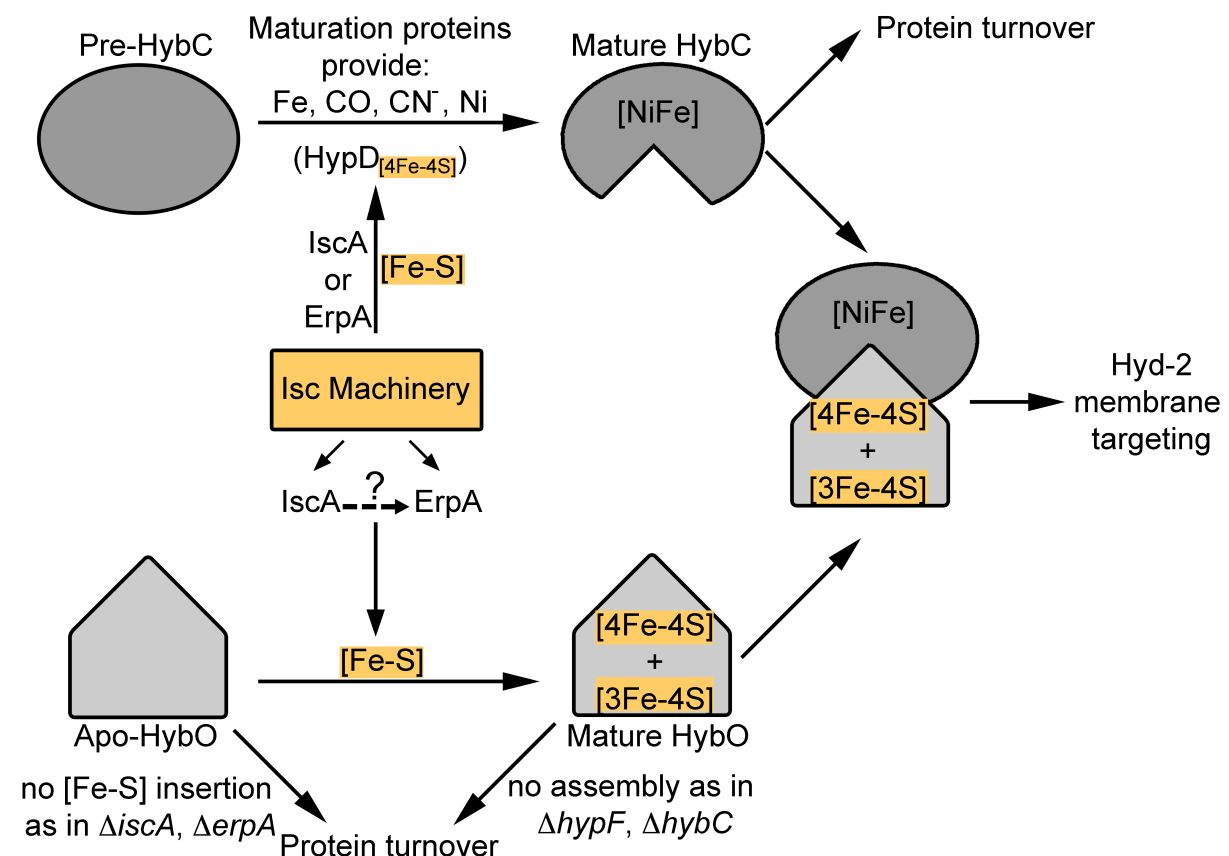

Figure 7. Model depicting the involvement of the [Fe-S] trafficking A-type carrier proteins IscA and ErpA in hydrogenase 2 biosynthesis. Isc machinery represents the *iscSU-hscBA-fdx* gene products. Pre-HybC and Apo-HybO signify the unprocessed, cluster-free apo-forms of the large and small subunit, respectively, while the completely processed forms are termed Mature. Full arrows signify directs routes of [Fe-S] cluster transfer while the dotted arrow with the question mark indicates an alternative route of transfer from IscA directly to ErpA. The mature form of HybC contains a complete [NiFe]-center, which includes the Fe and Ni atoms as well as the diatomic ligands CO and CN‾ as indicated above the arrow. Insertion of these requires the concerted action of the Hyp protein

machinery [13]. Only after maturation of the individual subunits has been completed do they interact and are then to be targeted to the membrane. When assembly is hindered both subunits are rapidly degraded at different points as indicated.
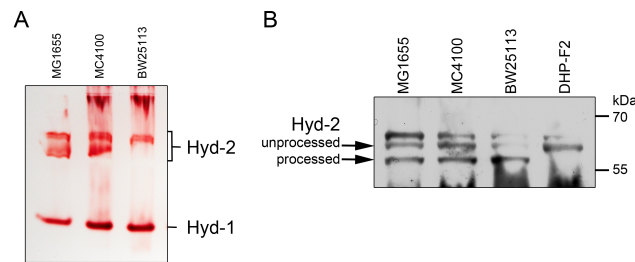
Figure S1. Comparative analysis of hydrogen-uptake hydrogenases in different *E. coli* K-12 derivatives. A. Aliquots of crude extracts (25 μg protein) derived from the bacterial stains shown were separated by non-denaturing PAGE (7.5% w/v polacrylamide) and subsequently stained for hydrogenase enzyme activity. The locations of Hyd-1 and Hyd-2 activity bands are shown. B. Western blot analysis of the unprocessed and processed forms of the HybC large subunit of Hyd-2 was performed using crude extracts (25 μg protein) derived from the bacterial strains indicated. Strain DHP-F2 is a derivative of carrying a deletion in the *hypF* gene.
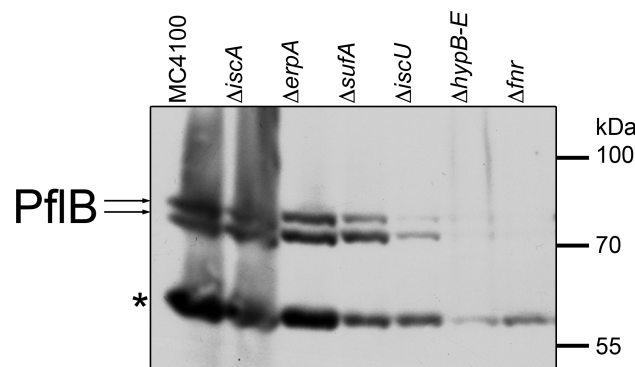
Figure S2. Western blot analysis of pyruvate formate-lyase levels in mutants defective in iron-sulphur cluster biogenesis. Aliquots (25 μg protein) derived from MC4100, DHP-F2 (Δ*hypF*), CP463 (Δ*sufA*), CP477 (Δ*iscA*), LL402 (Δ*erpA*), JW2513 (Δ*iscU*), BEF314 (Δ*hypB-E*) and PB1000 (Δ*fnr*) were separated by 10% SDS-PAGE and subjected to Western blotting using anti-PflB antiserum. The double band characteristic of the full-length and oxygenolytically cleaved polypeptide are indicated as PflB while the asterisk denotes an unidentified cross-reacting polypeptide that served as an internal loading control. The migration positions of the molecular mass standards (in kDa) are indicated on the right of the Figure.

3. Diskussion

Die Energiekonservierung in *E. coli* erfolgt durch membrangebundene terminale Oxidoreduktasen, zu denen streng genommen auch die [NiFe]-Hydrogenasen gehören. Die meisten dieser Enzyme besitzen Metalle als Kofaktoren (Unden & Bongaerts, 1997). Für den Transport und Assemblierung der Metalle synthetisieren Zellen spezielle Proteine, deren Funktion und Einfluss auf Metalloenzyme innerhalb dieser Arbeit untersucht wurden. Die Erkenntnisse und daraus resultierenden Fragen werden im Folgenden diskutiert.

3.1 Eisenverfügbarkeit und Fur

Eisen kommt in Proteinen in Häm-Kofaktoren, in [FeS]-Clustern des Elektronentransportes (Atmungsenzyme und Ferredoxine), des Tricarbonsäurezyklus (Aconitase und Succinat Dehydrogenase), von Proteinen der Biosynthese von DNA (Ribonukleotid-Reduktase) und Aminosäuren vor. Ebenso konnte Eisen in Zwei-Eisen Zentren von Rubredoxinen und Eisenspeicherproteinen wie Ferritinen nachgewiesen werden. Eisen und insbesondere Fe-S Verbindungen könnten einer Theorie entsprechend an der Entstehung des Lebens beteiligt gewesen sein (Huber & Wächtershäuser, 1997). Da freies Eisen(II) in der Zelle durch Fenton-Reaktionen mit H_2O_2 reaktive und schädigende Sauerstoffspezies wie Hydroxylradikale entstehen lassen kann (Earhart, 1996; Green & Paget, 2004), müssen Transport und Biosynthese kontrolliert erfolgen (Andrews *et al.*, 2003). Mittels genetischer Manipulation können die Funktionen dieser Systeme auf den Wasserstoff-Metabolismus untersucht werden.

Durch die Deletion des für den Fur Regulator kodierenden Gens, ist generell eine Deregulation der Eisenaufnahme zu erwarten, was durch die konstitutive Expression der Gene *fhuA* (Ferrichrom), *fecA* (Fe-Citrat) und teilweise auch *fepA* (Enterochelin) in einer *fur*-Mutante gezeigt werden konnte (Hantke, 1981). So ist ein durch Eisenmangel verursachter Phänotyp einer *fur*-Mutante auszuschließen. Die hier gemessene Reduktion der Transkription der Gene des FHL Komplexes und der daraus resultierenden geringeren Hyd-Aktivität, stellt eine plausible Erklärung eines in *Salmonella typhimurium*, einem eng verwandten Enterobakterium, beschriebenen Phänotyps einer *fur* Mutante dar. Dieser zeichnet sich durch erhöhte Sensitivität gegenüber pH Absenkung aus, konnte jedoch bisher nicht erklärt werden (Foster & Hall, 1992). Wie Fur die *hyc* und *fdhF* Regulation genau beeinflusst, kann nur spekuliert werden (Abb. 8), könnte aber zukünftig über Experimente durch eine Variation des beschriebene Fur-Titrationsassays mittels eines *hyc-lacZ* Konstruktes verifiziert werden

(Escolar *et al.*, 1999). So dient der FHL Komplex durch die Oxidation des toxischen Formiats und durch die Reduktion von Protonen der pH Regulation unter fermentativen Bedingungen (Rossmann *et al.*, 1991), weswegen Hyd defiziente Stämme Verlust der Säureresistenz zeigen (Hayes *et al.*, 2006). Zum Schutz vor Säurestress wurde, wie hier gezeigt, unter Eisenmangel oder in einer *fur*-Gendeletions Mutante noch Aktivität vom FHL Komplex aufrechterhalten, während die H_2-oxidierenden Hydrogenasen bereits nicht mehr nachweisbar waren. Die Funktion der [NiFe]-Hydrogenasen bei der Säureregulation wird durch deren Deletion deutlich. Diese hat zunächst außer der mangelnden Wasserstoffproduktion und vermindertem Wachstum auf H_2/Fumarat scheinbar keinen signifikanten Phänotyp (Krasna, 1984). Jedoch ist die regulatorische Antwort auf Deletion von Hydrogenaseaktivität, z.B. durch die Deletion von *hypF*, eine erhöhte Expression verschiedener Gene deren Genprodukte wie Decarboxylasen alternativ zum FHL Komplex der Antwort auf pH Absenkung dienen (Glutamatdecarboxylase *gadB* ca. 6-fach; Arginindecarboxylase *adiA* ca. 5-fach; Daten nicht gezeigt).

Die in *fur* Mutanten gemessene Reduktion der Hyd-1 und Hyd-2 Aktivitäten bei gleichzeitig konstanter Transkription deutet auf post-transkriptionelle Regulation hin. Solche Regulation auf Translationsebene wird in *E. coli* durch die Stabilität der mRNA, aber auch durch Paarungen mit kleinen regulatorischen RNAs vermittelt (Boysen *et al.*, 2010; Majdalani *et al.*, 2005; Vogel & Sharma, 2005). Neben den beschriebenen RNA-Paarungen mit RyhB, FnrS und OxyS geben die stromaufwärts gelegenen, regulatorischen RNA-Bereiche die Möglichkeit der Generierung stabiler Sekundärstrukturen vergleichbar derer, die für Fdh-N beschrieben wurden (Punginelli *et al.*, 2004). Solche Bereiche und Sekundärstrukturen existieren bei den [NiFe]-Hydrogenasen ebenfalls und bieten sich künftig für gerichtete Mutagenese mit anschließenden Regulationsstudien ähnlich solcher von Richard *et al.*, 1999 an.

Weiterhin wurde beschrieben, dass sich ein *fur*-Gendeletion ähnlicher Phänotyp durch die Deletion der Gene des Fe^{2+}-Aufnahme Systems FeoABC hervorrufen lässt, da vermutlich FeoABC die Hauptquelle des Fur gebundenen Eisens liefert (Earhart, 1996). Es konnte sowohl in Eisenaufnahme-Mutanten als auch in *fur*-Mutanten eine Reduktion der Aktivität der wasserstoffoxidierenden Enzyme Hyd-1 und Hyd-2 beobachtet werden, bei gleichzeitiger Reduktion der FHL Aktivität. Dabei war die Reduktion der Gesamthydrogenaseaktivität in Eisenaufnahme-Mutanten (*feoB entC*) um das Fünffache weniger signifikant als die zehnfache

Reduktion in der *fur*-Mutante, weil offensichtlich die Eisen-Aufnahme nicht vollständig unterbunden werden kann. Artifiziell kann ein Eisenmangel durch die Deletion der für Eisentransporter kodierenden Gene oder durch Zugabe von Chelatoren ins Medium hervorgerufen werden. So zeigte eine multiple Eisenaufnahmemutante (Δ*fecA-E zupT mntH feoB entC*) einen eindeutigen Effekt mit vollständiger Abwesenheit der Hydrogenase Aktivitäten. Dabei tragen die gemeinsame Deletion der Gene *feoB* und *entC* bereits zum Verlust von 80 % der Gesamtaktivität bei, weswegen sie die Hauptaufnahme für Eisen unter diesen Bedingungen darstellen. Phänotypische Komplementation nach Eisendepletion zeigten, dass Eisen(II) bevorzugt zur Reifung des aktiven Zentrums verwendet wurde.

Bisher wurde kein einzelner spezifischer Eisentransporter für die [NiFe]-Hydrogenase beschrieben wie er vergleichsweise für den Nickel Transport identifiziert werden konnte (Wu *et al.*, 1989). Vielmehr kann nach Reduktion zu Eisen(II) von einer generellen Eisenaufnahme in die Zelle ausgegangen werden, auf die eine rasche Insertion in das entsprechende Eisen-liefernde Protein folgt. Der direkte Einbau des Eisens könnte durch HypD innerhalb eines Komplexes mit dem Chaperon GroL stattfinden. Eine Interaktion des unprozessierten HycE-Polypeptides mit großen Mengen an GroL konnte bei der Reinigung festgestellt werden. GroL interagiert unspezifisch mit Fur und SlyD (Kerner *et al.*, 2005), aber auch spezifisch mit HypD (Arifuzzaman *et al.*, 2006) und bietet sich als hydrophober Insertionsort zum Schutz vor Fenton Reaktionen für das aktive Zentrum an. Indizien zum Einbau des Eisens ins aktive Zentrum über die Vorstufe eines [FeS]-Zentrums analog zur Nitrogenase-Kofaktorinsertion (Shepard *et al.*, 2011) oder wie es bereits für die [FeFe]-Hydrogenase von *C. reinhardtii* gezeigt wurde (Mulder *et al.*, 2010), konnten durch die gewonnenen *in vivo* Daten nicht verifiziert werden. Weiterhin wurde hier das Frataxin-ähnliche Protein CyaY als Eisen-lieferndes Protein für das aktive Zentrum erwogen. Dessen Funktion als Eisendonor für den IscU x IscS Komplex ist umstritten, denn viele der beschriebenen Effekte dieses Proteins lassen sich auf eine allosterische Regulation zurückführen und ein *in vitro* Eisen-Transfer konnte bisher nicht nachgewiesen werden (Ayala-Castro *et al.*, 2008; Lill, 2009). Einen signifikanten Effekt auf die Aktivität der [NiFe]-Hydrogenasen hatte die Deletion des *cyaY* Gens nicht. Neben CyaY wurden ursprünglich auch die ATC-Proteine als Eisendonoren in Erwägung gezogen (Ding *et al.*, 2004; 2007). Die Untersuchung deren Funktion ergab jedoch einen auf die kleinen Untereinheiten beschränkten Phänotyp.

3.2 Die kleinen Untereinheiten und [FeS]-Cluster

Eisen wird in den kleinen Untereinheiten für [FeS]-Cluster benötigt und diese scheinen ohne ihren Kofaktor instabil zu sein. Ähnliches konnte für HypD gezeigt werden, dessen Polypeptid ohne die [FeS]-Cluster bindenden Cysteine nicht nachweisbar war (Blokesch & Böck, 2006). Für Ferredoxin konnte andererseits gezeigt werden, dass sowohl Elektronentransfer als auch Cluster Stabilität in Cystein-austausch Varianten in reduziertem Maße gegeben sind (Hurley et al., 1997). Die [FeS]-Cluster koordinierenden Cysteine der kleinen Untereinheiten sind hoch-konserviert und können in den strukturell verwandten Untereinheiten des Komplex I aus Mitochondrien identifiziert werden (Albracht, 1993). Weiterhin war Instabilität der kleinen Untereinheiten, so dass diese immunologisch nicht mehr nachweisbar waren, auch bei Abwesenheit der großen Untereinheiten oder wenn diese ungereift vorlagen, zu beobachten. Dieser rasche Abbau unterliegt einer strengen Kontrolle. Da die kleinen Untereinheiten eine enge Kontaktfläche mit den großen Untereinheiten haben (Volbeda et al., 1995) und bei Hyd-1 und Hyd-2 auch den Tat-vermittelten Membrantransport koordinieren (Dubini & Sargent, 2003), müssen Assemblierung und Transport kontrolliert werden. Eine Reihe von Chaperonen wie HyaE und HybE interagieren dafür spezifisch mit den Tat-Signalen der kleinen und auch mit den C-terminalen Peptiden der großen Untereinheiten (Dubini & Sargent, 2003). Es konnte hier gezeigt werden, dass ohne die kleinen Untereinheiten HyaA, HybO oder HycG kein Elektronentransport vom aktiven Zentrum möglich ist und deshalb keine Aktivität messbar war. Die Annahme, dass Elektronen vom [NiFe]-Zentrum die kurze Distanz (≈ 14 Å) zu einem artifiziellen Elektronenakzeptor Benzylviologen oder zu einer Elektrode überbrücken können, gilt für die [NiFe]-Hydrogenasen aus E. coli nicht. Im Gegensatz dazu wird bei der monomeren C. reinhardtii [FeFe]-Hydrogenase dies durch den unterschiedlichen Aufbau des Enzyms ermöglicht (Silakov et al., 2009). Es besteht aus einem einzelnen Polypeptid in dem bereits eine Elektronentransportkette durch [FeS]-Cluster vorhanden ist, während bei den [NiFe]-Hydrogenasen keine [FeS]-Cluster in der großen Untereinheit zu finden sind. Dabei geht die Funktion der kleinen Untereinheiten über bloßen Elektronentransport hinaus. Das Redoxpotential der [FeS]-Cluster, insbesondere des proximalen, scheint in vivo die Katalyserichtung oder zumindest die Richtung des Elektronentransportes zu bestimmen und verleiht Schutz vor O_2 (Fritsch et al., 2011a).

Eine Inaktivierung von Hydrogenasen durch Sauerstoff lässt sich mittels Elektronenspinresonanz Spektroskopie (electron paramagnetic resonance, EPR) verfolgen,

indem für das oxidierte Ni(III) Signale erscheinen, die unterschiedlich schnell reaktivierbar sind (Armstrong & Albracht, 2005). Dabei wurden im sogenannten Ni-A („*unready*") Zustand ein Peroxid und im Ni-B („*ready*") Zustand ein Hydroxo-Ligand im aktiven Zentrum bestimmt, der bei Reaktivierung weiter zu Wasser reduziert wird (Fontecilla-Camps *et al.*, 2007). Daraus resultierend wurden zunächst bei den O_2-toleranten Hydrogenasen verschiedene Mechanismen vorgeschlagen. *Ralstonia eutropha,* ein Vertreter der sogenannten Knallgasbakterien, nutzt Sauerstoff als terminalen Elektronenakzeptor (Pohlmann *et al.*, 2006). Dabei werden die Gene von drei [NiFe]-Hydrogenasen, eine membrangebundene (MBH), eine lösliche (SH), sowie eine regulatorische Hydrogenase (RH), exprimiert (Cramm, 2009), die einen besonderen Schutz gegenüber O_2-Inaktivierung aufweisen. Im Vergleich zum Standard Ni-Fe(CN)$_2$CO-Zentrum (Volbeda *et al.*, 1996) wurden z.B. jeweils ein zusätzlicher Cyanidligand am Nickel und Eisenatom der SH postuliert (Happe *et al.*, 2000), die jedoch bei *in situ* Untersuchungen nicht bestätigt werden konnten (Horch *et al.*, 2010). Weiterhin wurde eine Verengung des Gaskanals durch große Aminosäureseitenketten an den Positionen 74 (Val) und 122 (Leu) der RH entdeckt (Liebgott *et al.*, 2010). Zudem wird das besonders positive Redoxpotential des proximalen [FeS]-Clusters der kleinen Untereinheit der MBH als O_2-Schutz beschrieben (Goris *et al.*, 2011). Dieses proximale Cluster der MBH konnte durch Strukturaufklärung als [4Fe-3S]-Cluster identifiziert werden, bei welchem zwei Cysteine zusätzlich zu den vier üblichen am [FeS]-Zentrum dazu dienen eines der Eisenatome zu delokalisieren, während das zweite die Koordination eines Schwefelatoms übernimmt (Fritsch *et al.*, 2011a; 2011b; Shomura *et al.*, 2011). Durch das veränderte Redoxpotential wird einen reverser Elektronenfluss zum aktiven Zentrum ermöglicht, um dort Sauerstoffspezies zu reduzieren (Fritsch et al., 2011b; Goris et al., 2011; Shomura et al., 2011). Die O_2-tolerante Hyd-1 von *E. coli* weist in der kleinen Untereinheit ebenfalls zusätzliche Cysteine am proximalen [FeS]-Cluster auf, die eine Toleranz gegenüber O_2 verleihen (Lukey *et al.*, 2011).

Es gibt für [FeS]-Cluster bisher nur drei in Mikroorganismen beschriebene universelle Einbaumaschinerien mit anschließender Modifikation (Johnson, 1998; Shepard *et al.*, 2011), von denen das Suf und das Isc System in *E. coli* existieren (Abb. 7). Für das Suf System konnte kein direkter Einfluss unter den hier verwendeten Bedingungen festgestellt werden. Der Einfluss der gesamten Isc Maschinerie wird durch die Deletion des *iscU* Gens, dessen Produkt die zentrale Isc Komponente darstellt (Abb. 7), sichtbar. In einem solchen Stamm sind keine Aktivitäten der [FeS]-Cluster haltigen Enzyme nachweisbar. Die beiden zur Isc Maschinerie gehörenden Genprodukte von *erpA* und *iscA* haben unabhängig voneinander

Einfluss auf die Aktivität der Hydrogenasen. In beiden Stämmen konnten keine Hyd-1 und Hyd-2 Aktivitäten detektiert werden, während in dem *iscA* Stamm wenig und in dem *erpA* Stamm keine FHL Aktivität nachweisbar war. Von den durchgeführten *in vivo* Versuchen kann jedoch nicht abgeleitet werden, ob beide Proteine konzertiert oder sukzessiv am Einbau der [FeS]-Cluster der kleinen Untereinheiten beteiligt sind (Vinella *et al.*, 2009). Ein Verlust der Aktivität in diesen Mutanten geht stets mit Instabilität des zugehörigen [FeS]-haltigen Polypeptides einher. Also ist es die mangelnde Insertion des [FeS]-Clusters, welches die kleinen Untereinheiten stabilisiert.

Wie die Differenzierung der Biosynthese von [4Fe-4S] und [3Fe-4S]-Clustern oder gar dem neuartigen [4Fe-3S]-Cluster (Fritsch *et al.*, 2011a; Shomura *et al.*, 2011) erfolgt, ist unbekannt und bedarf der Konstruktion [FeS]-modifizierter Modelluntereinheiten und anschließender *in vitro* Analyse. Wahrscheinlich existieren jedoch proteinspezifische Chaperone, die den Einbau in die Zielproteine dirigieren. So konnte für die Genprodukte von *hupGHIJ* aus *Rhizobium leguminosarum* gezeigt werden, dass sie spezifisch an der Reifung der kleinen Untereineheiten beteiligt sind (Manyani *et al.*, 2005). Ähnliche Proteine mit Thioredoxin-ähnlichem Aufbau in *E. coli* sind HyaE, HyaF und HybE (Menon *et al.*, 1991, 1994), deren Interaktion mit den Tat-Signal enthaltenen Vorstufen, nicht jedoch mit den gereiften kleinen Untereinheiten gezeigt werden konnte (Dubini & Sargent, 2003) und deshalb für sie eine Funktion bei der Kofaktor-Insertion denkbar wäre. Es ist bekannt, dass im FHL Komplex die Polypeptide HycB, F, G und FdhF ausschließlich [FeS]-Cluster des [4Fe-4S]-Typs enthalten und eine gewisse Unabhängigkeit von *iscA* existiert, was bedeuten könnte, dass *erpA* diese [4Fe-4S]-Cluster bereitstellt. Die bei Hyd-1 und Hyd-2 benötigte [FeS]-Modifikation zum [3Fe-4S]-Cluster könnte von *iscA* ausgeführt werden. Schlussfolgernd müssten in diesem Fall entweder funktionelle [FeS]-Cluster im FHL Komplex einer *iscA* Mutante vorhanden sein oder im Gegenzug eine Funktionalität der einzelnen Proteine des FHL-Komplexes ohne ihre [FeS]-Cluster bewiesen werden.

Die Aktivitätsdaten der [FeS]-Cluster Mutante *iscA* belegten, dass unter Limitierung der Insertionsmaschinerie für [FeS]-Cluster zunächst die Bereitstellung der [FeS]-Cluster des FHL Komplexes sichergestellt werden. Unter nitratrespiratorischen Bedingungen kann zwischen Fdh-N und Nar keine solche Präferenz festgestellt werden. Hier findet ohne eines der beiden Enzyme keine Nitratatmung statt und es bringt keinen Vorteil Kofaktoren für eines der beiden Enzyme vorrangig bereitzustellen. Ebenfalls war für Nar und Fdh-N eine

vollständige Abhängigkeit von *erpA* und *iscU* zu beobachten, während *iscA* die Aktivitäten nicht vollständig reduzierte. Es wurde früher bereits gezeigt, dass *isc* Deletionen die Transkription vom *narG* Promotor durch Verringerung der Fnr Aktivität senken, dabei zeigte allerdings eine *iscA* Mutante um 30 % verringerte *narG* Transkription und *iscU* knapp unter 50 % (Mettert *et al.*, 2008). Deshalb beruht der hier gezeigte Phänotyp dieser Mutanten nicht nur auf Reduktion der Transkription, sondern hauptsächlich auf Limitierung der Insertion der [FeS]-Cluster in die kleinen Untereinheiten. Diese waren immunologisch in *fnr*, *iscA*, *erpA* und *iscU* Stämmen nicht detektierbar. Es sind demnach durch Deletion des Isc Systems nicht nur einzelne, sondern allgemein [FeS]-abhängige Enzymaktivitäten betroffen. Jedoch kann Überproduktion von *iscA* eine teilweise Komplementation eines *erpA* Phänotyps bewirken, was auf eine gewisse Unabhängigkeit beider Proteine hindeutet und Hinweise auf eine Redundanz liefert. Sowohl die Hyd, als auch die Nar und Fdh Aktivitäten bieten sich zur Untersuchung für [FeS]-Biosynthese an und erweitern das bisherige Methodenspektrum um neue *in vivo* Enzymaktivitäten (Ayala-Castro *et al.*, 2008; Lill, 2009). Aus dem Vergleich zu Fdh-N und Nar geht außerdem hervor, dass die beobachteten Präferenzen der Hydrogenaseenzyme im H_2-Stoffwechsel der [FeS]-Mutanten spezifisch sind.

3.3 Fnr⁻ -Stämme haben nicht nur einen Hyd⁻ -Phänotyp

Es ist bekannt, dass die Verfügbarkeit von Metallen die Transkription beeinflusst. So konnte für die Expression Fnr abhängiger Promotoren gezeigt werden, dass Eisen-Chelatoren die DNA-Protein Komplexformation *in vivo* und *in vitro* hemmen, sich der Eisengehalt des Fnr Proteins abhängig von Sauerstoff ändert und Eisen(II) bevorzugt bei der Reaktivierung verwendet wird (Green & Guest, 1993a; 1993b; Spiro *et al.*, 1989). Der Einbau des redoxaktiven [4Fe-4S]-Clusters wird dabei vom Isc System durchgeführt und Deletion der Gene des *isc* Systems verringert Fnr Aktivität um 60 % (Mettert *et al.*, 2008). Das enthaltene [4Fe-4S]-Cluster ist sensitiv gegenüber O_2 und dient der Fnr Aktivierung durch Dimerisierung (Crack *et al.*, 2008).

Ähnlich dem BL21(DE3) Stamm kam es auch bei K-12 Stämmen wiederholt zu spontanen *fnr* Deletionen, die jedoch insofern ungewöhnlich sind, weil Zellen ohne Fnr eine Reihe von Genen nicht mehr exprimieren können und man einen Wachstumsnachteil erwarten würde. Das Phänomen der spontanen *fnr* Deletion ist unter *E. coli* Stämmen weit verbreitet und kann in verschiedenen Ausprägungen beobachtet werden (Soupene *et al.*, 2003). Im *E. coli* B-Stamm BL21(DE3) ist die *fnr* Expression durch ein internes Stopp-Codon verhindert (Jeong

et al., 2009) und im enteropathogenen Stamm O104:H4 durch eine Leserasterverschiebung (Mellmann *et al.*, 2011). Auch wurde 2003 zwischen zwei verschiedenen Derivaten des Stammes MG1655 unterschieden, von denen eines (NCM3105) eine ausgedehnte Deletion um das *fnr* Gen enthielt (vgl. Anhang 3) (Soupene *et al.*, 2003). Diese Deletion erstreckt sich von einer Rac-Prophagen Integrase bis zum IS*5* Element zwischen *ynaI* und *ynaJ* (Soupene *et al.*, 2003). In der vorliegenden Arbeit wurde eine als PB1000 bezeichnete Mutante isoliert, bei der eine Deletion zwischen *insH4* und *fnr* vorlag (vgl. Anhang 3). Die Eingrenzung der Deletion erfolgte mittels Southern-Blot und spezifischen Sonden, deren Signale in PB1000 nicht detektierbar waren. Weitere *fnr* Mutanten von MC4100 mit identischen Deletionen wurden wiederholt bei der Herstellung von unabhängigen Mehrfachdeletionsmutanten nach P1$_{vir}$ Phagentransduktion isoliert, jedoch erst anschließend an die aerobe Konstruktion der Stämme durch deren anaerobe Charakterisierung bemerkt. Auch die beschriebene Mutante RM102 (Birkmann *et al.*, 1987a), die zunächst mit einer Resistenz in *fnr* isoliert worden war, welche anschließend entfernt wurde, hat zwischen *insH4* und *fnr* eine identische Gendeletion. Eine *fnr* Expressionsregulation erfolgt in MC4100 durch die Integration eines zusätzlichen IS*5* Elementes stromaufwärts von *fnr*, welches die Transkription des *fnr* Gens verringert und einen *fnr* Phänotyp in einer *hfq* Mutante in MC4100 vermittelt (Sawers, 2005c). Das Protein Hfq (*host factor* für RNA-Phage Q) stabilisiert RNA-RNA Bindung und interagiert mit einer Reihe von kurzen regulatorischen RNAs wie FnrS, RyhB und OxyS (Boysen *et al.*, 2010; Durand & Storz, 2010; Zhang *et al.*, 1998). Dieses zusätzliche IS*5* Element in MC4100 (Sawers, 2005c) erleichtert chromosomale Veränderungen wie die Deletion des dazwischen liegenden Bereiches und ist ein sogenannter *hotspot* für Mutationen (Naas *et al.*, 1995). Generell entstehen fortlaufend Mutationen und werden durch Nährstoffmangel verstärkt, dennoch scheint ausgerechnet eine *fnr* Deletion unter den hier verwendeten Bedingungen zu schnellerem Wachstum und daraus resultierender Selektion unter Laborbedingungen zu führen. So reguliert Fnr gemeinsam mit ArcA die Expression einer Reihe von Genen für die aerobe Atmung wie Succinat-Dehydrogenase, NADH:Ubichinon Oxidoreduktase oder Cytochrom *bd*-I Oxidase, die bei einer *fnr* Deletion verstärkt exprimiert würden und das aerobe Wachstum verbessern (Iuchi & Lin, 1991; Shalel-Levanon *et al.*, 2005).

Der Hyd defiziente Phänotyp einer *fnr* Mutante wie BL21(DE3) lässt sich durch mangelnde Nickel-Aufnahme und *pfl* Expression erklären (Kaiser & Sawers, 1995; Sawers *et al.*, 1985; Wu *et al.*, 1989). Die Transkriptionregulation der Gene des FHL Komplexes ist nicht direkt Fnr abhängig, denn Transkription in einer *fnr* Mutante kann durch Formiatzugabe initiiert

werden (Birkmann *et al*., 1987b; Sawers *et al*., 1985). Die hier in einer *fnr* Mutante beobachtete Umkehrung der pH Regulation könnte dennoch durch den veränderten Formiatmetabolismus hervorgerufen werden. Durch geringen pH werden unter Anaerobiose viele der für Hyd Aktivität benötigten Gene induziert, während die für Fdh-O kodierenden Gene bei pH Erhöhung verstärkt exprimiert werden (Hayes *et al*., 2006). So kann Formiat bei hohem pH weder aus der Zelle diffundieren (pKa 3,8) noch wird es transportiert, obwohl die Kristallstruktur vom Formiattransporter FocA eine Strukturänderung zur offenen Form bei hohem pH zeigt (Lü *et al*., 2011; Waight *et al*., 2010). Das Metabolit häuft sich unter diesen Bedingungen an und kann dadurch bei hohem pH die durch die *fnr* Mutation bedingte fehlende Transkription der Gene für Hyd-1 und vom FHL Komplex initiieren (Rossmann *et al*., 1991; Sawers & Boxer, 1986). Gleichzeitig gibt es keine Induktion der Expression der Gene für die Formiat-verbrauchenden Fdh-N (Kang *et al*., 2005). Lediglich die Expression des *fdo* Operons ist in einer *fnr* Mutante nicht beeinflusst (Abaibou *et al*., 1995) und die *fdo* Genprodukte (Fdh-O) besitzen eine zusätzliche H_2 abhängige BV Reduktase Aktivität. Zusammen mit der *fdo*-Genexpression bei hohem pH, könnte das Enzym der Nutzung von H_2 als Elektronendonor unter Hydrogenase-reprimierenden Bedingungen dienen. Ein direkter H_2 Verbrauch durch die Fdh's in einem Hyd-negativen Stamm konnte jedoch experimentell nicht bestätigt werden (Daten nicht gezeigt). Lediglich eine alternative Atmungskette mit Formiatoxidation durch die drei Fdh's bei gleichzeitiger Nitrit Reduktion, wurde gezeigt (Hussain *et al*., 1994).

Die Verknüpfung der Hydrogenasen mit anderen Enzymen des Stoffwechsels wird außerdem durch Transkriptionsuntersuchungen (Daten nicht gezeigt) deutlich. Es werden in einer *hypF* Mutante innerhalb der Säureregulation die Gene des FHL Komplexes und der Hyp Reifungsproteine um ein Vielfaches hochreguliert, während die Transkription H_2-oxidierender Enzyme (*hyaA*) nicht einmal verdoppelt wird. Dieser Effekt ist größtenteils auf die durch FHL Dysfunktion begründete Acidifizierung und Formiatanhäufung zurückzuführen und kann anhand der verstärkten Expression von *gadB* verfolgt werden (Castanie-Cornet *et al*., 1999). Weiterhin wurden die Gene der Enzyme des Komplex I der Atmungskette, wie auch die *fdn*-Gene verstärkt exprimiert. Im Allgemeinen wird die Expression der Gene für Enzyme alternativer Atmungsketten zwar reguliert, jedoch ist stets basale Expression vorhanden, um schnell auf wechselnde Umweltbedingungen reagieren zu können (Cole, 1996). So wird bei Wachstum in Anwesenheit alternativer Elektronenakzeptoren die Hydrogenaseaktivität deutlich reduziert (Yamamoto & Ishimoto,

1978). Aber auch bei fermentierenden Zellen stoppte die H_2-Produktion sofort wenn Dimethylsulfoxid (DMSO) oder Nitrat zugegeben wurden (Daten nicht gezeigt). DMSO und Nitrat regulieren demnach nicht nur die Expression der Gene des H_2-Metabolismus (Richard *et al.*, 1999), sondern auch den Elektronenfluss innerhalb der Zelle, weil die Reduktion von DMSO ($E^{0'}$ +160 mV) und Nitrat ($E^{0'}$ +420 mV) mehr Energie konserviert als Fermentation (Thauer *et al.*, 1977; Unden & Bongaerts, 1997). Dabei ist Hyd-2 durch sein Redoxpotential theoretisch ebenfalls in der Lage Elektronen von H_2 auf DMSO, Trimethylamin-*N*-oxid oder Fumarat zu übertragen (Laurinavichene *et al.*, 2002; Lukey *et al.*, 2010) und dient damit als respiratorische Hydrogenase (Sawers *et al.*, 1985). Zwar wird durch H_2-Oxidation nicht direkt Energie konserviert, aber zumindest Wachstum auf Malat und Fumarat mit H_2 als Elektronendonor ist ohne Hyd-2 nicht möglich (Dubini *et al.*, 2002).

3.4 FHL im Formiatkonzept

Es stellt sich die Frage warum unter den oben beschriebenen Bedingungen des Fe-Mangels und der Limitierung der [FeS]-Maschinerie die nur drei bis vier Proteinkomponenten umfassenden Hyd-1 und Hyd-2 nicht funktionstüchtig sind, während gleichzeitig der 7 Proteinkomponenten umfassende FHL Komplex synthetisiert wird? Die Untersuchung des Stammes BL21(DE3) machte deutlich, dass wesentlich mehr zusätzliche Reifungsproteine für die ko-translationelle Insertion des Selenocysteins und die Bereitstellung des Molybdopterin-kofaktors der Fdh-H Komponente benötigt werden als für die H_2-oxidierenden Enzyme und dementsprechend die Regulation differenzierter ist (Hopper *et al.*, 1994; Rossmann *et al.*, 1991; Self *et al.*, 1999). Der FHL Komplex war ohne die Fdh-H Komponente nicht funktionell und selbst die Hyd-3 Aktivität war in Abwesenheit des Fdh-H Enzyms nicht detektierbar. Es scheint eine enge Verbindung vom H_2-Stoffwechsel zu Fdh's zu geben, der über die Assoziation von Fdh-H im FHL Komplex hinausgeht. So konnte durch Massenspektrometrie Analysen festgestellt werden, dass das unprozessierte Polypeptid der Hyd-3 großen Untereinheit mit Fdh-O und Fdh-N Polypeptiden assoziiert vorliegt. Die Verlässlichkeit dieser Daten zeigt sich durch die gleichzeitige Identifikation des SlyD Polypeptides, welches als Interaktionspartner der großen Untereinheit beschrieben wurde (Chan Chung & Zamble, 2011a; 2011b). Die gleichzeitig mit SlyD stattfindende Interaktion des HypA-HycE Komplexes zur Nickel-Insertion findet nur statt, wenn HypD und HypC vorhanden sind (Chan Chung & Zamble, 2011a), was den immunologischen Nachweis der Hyp Proteine bestätigt, die jedoch wegen ihrer geringen Abundanz durch MS nicht identifiziert werden konnten. Der FHL Komplex dissimiliert Formiat und konkurriert

theoretisch mit Fdh-O und Fdh-N um Formiat, was nur durch deren diametrale Membranlokalisation verhindert wird. Die periplasmatische Assoziation der Fdh's mit HycE stellt wahrscheinlich keinen enzymatisch aktiven Komplex dar, könnte aber der Stabilisierung der jeweiligen Polypeptide dienlich sein oder, wenn auch abwegig, eine Vorstufe wie HCO_3^- oder Formiat für den CO-Liganden des aktiven Zentrums liefern. Für eine mögliche Involvierung der Fdh's in den CO-Stoffwechsel spricht die Reduktion der Transkription der *fdo*-Gene um 50 % unter anaeroben Bedingungen, wenn CO freisetzende Substanzen im Medium enthalten waren (Davidge *et al.*, 2009).

Es konnte der Anteil der H_2-oxidierenden Hydrogenasen am H_2-Metabolismus während der Fermentation bestimmt und eine Reoxidation von ca. 50 % des gebildeten H_2 gemessen werden. Damit scheint anders als bei den Cyanobakterien der FHL Komplex unter den gewählten Anzuchtbedingungen mehr H_2 zu produzieren als in der gleichen Kultur wieder oxidiert werden kann. Dementsprechend ist *E. coli* in Mischkulturen im Darm ein H_2-Donor für den Interspezies-Wasserstoff Transfer. Derartige Syntrophie wird als Anlass für die Bildung der eukaryontischen Zelle vorgeschlagen (Martin & Müller, 1998) und ist bei den beiden Archaea *Ignicoccus hospitalis* und *Nanoarchaeum equitans* gut charakterisiert worden (Podar *et al.*, 2008).

3.5 Ausblick zur technischen Verwendbarkeit

Für die zukünftige Nutzung von Hydrogenasen bei der biotechnologischen Produktion von H_2 müssen noch Hürden genommen werden (Kim & Kim, 2011). So steht für die Entwicklung eines *in vitro* Systems von [NiFe]-Hydrogenasen noch die endgültige Identifizierung der Quelle für den CO Liganden aus (Bürstel *et al.*, 2011). Die rekombinante Reinigung des labilen FHL-Komplexes macht durch verbesserte Affinitätschromatographie Fortschritte (Sawers *et al.*, 1985), ist jedoch noch weit von einer effizienten Produktion entfernt. Bei den [FeFe]-Hydrogenasen ist die Biosynthese des aktiven Zentrums zwar weitestgehend geklärt (Mulder *et al.*, 2011) und die katalytischen Eigenschaften sprechen für das Enzym, demgegenüber stellt aber die O_2-Sensitivität eine Herausforderung dar. Ebenso müssen für die fermentative Photoevolution bei Cyanobakterien metabolische Abläufe geklärt werden (Oh *et al.*, 2011). Die Entwicklung von synthetischen Modellen des aktiven Zentrums ohne Protein hat in den letzten Jahren große Fortschritte gemacht (Carroll *et al.*, 2011; Rauchfuss, 2007). Dieser chemische Ansatz H_2 zu produzieren ist vielversprechend, muss aber, um erfolgreich zu sein, weiterhin an den biologischen Vorbildern orientiert werden (Tard *et al.*, 2005).

4. Zusammenfassung

Im Rahmen dieser Arbeit wurde der Einfluss der Eisenhomöostase auf die Regulation und Aktivität der [NiFe]-Hydrogenasen aus *E. coli* untersucht. Es konnten neue Erkenntnisse zur Präferenz des aufgenommenen Eisens und zur differenziellen Regulation der einzelnen Hydrogenasen gewonnen werden.

So beeinflusst die Deletion des Gens für den Fur Eisenaufnahme-Regulator die Aktivität der H_2-oxidierenden Hydrogenasen negativ und senkt die Transkription der Gene des FHL Komplexes. Aber auch die Eisen(II)-Aufnahme durch den FeoABC-Transporter ist wichtig für die Aktivitäten der H_2-oxidierenden Enzyme. Gemeinsam mit *entC* wird die Haupt-Eisenquelle für das aktive Zentrum der Hydrogenasen sichergestellt. Unter Metall-Limitierung wird bis zuletzt die FHL Aktivität aufrechterhalten, um der Anhäufung toxischer Metabolite wie Formiat entgegenzuwirken.

In Hydrogenasen wird Eisen für das aktive Zentrum und die [FeS]-Cluster der kleinen Untereinheiten benötigt. Ohne die kleinen Untereinheiten kann keine Hydrogenaseaktivität in Extrakten nachgewiesen werden. Die [FeS]-Cluster werden dabei vom Isc (*iron sulfur cluster*) System geliefert, wobei die *Trafficking* Proteine IscA und ErpA für die H_2-oxiderenden Hydrogenasen essentiell sind, während für FHL Aktivität hauptsächlich ErpA benötigt wird und Effekte einer *iscA* Mutante partiell sind. Die Polypeptide der kleinen Untereinheiten waren immunologisch nicht mehr nachweisbar. Ein ähnlicher Phänotyp konnte auch in respiratorischen Enzymen wie Nitratreduktase und Fdh-N beobachtet werden. Die kleinen Untereinheiten waren nicht mehr nachweisbar und die großen Untereinheiten zeigten keine Aktivität in Isc⁻ Mutanten. Auch hier war die Abhängigkeit von IscA nicht vollständig.

Ohne Hydrogenasen werden Fdh-O und Fdh-N verstärkt exprimiert. Diese lassen sich in der Aktivitätsfärbung mit einer Nebenaktivität als H_2 abhängige BV Reduktion sichtbar machen. Alternative respiratorische Enzyme werden im Zuge einer allgemeinen präventiven Stoffwechselumstellung exprimiert, um metabolisch auf Veränderungen reagieren zu können.

Der Stamm BL21(DE3) besitzt keine H_2-oxidierenden Hydrogeaseaktivitäten solange kein Nickel ins Medium gegeben wird. Für FHL Aktivität mussten zusätzlich Formiat und Molybdat zugegeben werden. Dies liegt darin begründet, dass BL21(DE3) eine *fnr* und *modA-E* Mutante ist, die keine Fnr abhängige Nickelaufnahme und keine ModABC abhängige

Molybdataufnahme mehr ausführen kann. Die Aufklärung des Hydrogenase-negativen Phänotyps in BL21(DE3) macht deutlich, dass bei Reinigung von Metalloproteinen die Physiologie des Stammes beachtet werden sollte.

5. Literaturverzeichnis

Abaibou, H., Pommier, J., Benoit, S., Giordano, G. & Mandrand-Berthelot, M. A. (1995). Expression and characterization of the *Escherichia coli fdo* locus and a possible physiological role for aerobic formate dehydrogenase. *J Bacteriol* **177**, 7141–7149.

Adams, M. (1990). The structure and mechanism of iron-hydrogenases. *Biochim Biophys Acta* **1020**, 115–145.

Adams, M., Mortenson, L. & Chen, J. (1981). Hydrogenase. *Biochim Biophys Acta* **594**, 105–176.

Adinolfi, S., Iannuzzi, C., Prischi, F., Pastore, C., Iametti, S., Martin, S. R., Bonomi, F. & Pastore, A. (2009). Bacterial frataxin CyaY is the gatekeeper of iron-sulfur cluster formation catalyzed by IscS. *Nat Struct Mol Biol* **16**, 390–396.

Albracht, S. P. (1993). Intimate relationships of the large and the small subunits of all nickel hydrogenases with two nuclear-encoded subunits of mitochondrial NADH: ubiquinone oxidoreductase. *Biochim Biophys Acta* **1144**, 221–224.

Anderson, L. A., McNairn, E., Lubke, T., Pau, R. N., Boxer, D. H. & Leubke, T. (2000). ModE-dependent molybdate regulation of the molybdenum cofactor operon *moa* in *Escherichia coli*. *J Bacteriol* **182**, 7035–7043.

Andreesen, J. R., Gottschalk, G. & Schlegel, H. G. (1970). *Clostridium formicoaceticum* nov. spec. isolation, description and distinction from *C. aceticum* and *C. thermoaceticum*. *Arch Mikrobiol* **72**, 154–174.

Andrews, S. C., Berks, B. C., McClay, J., Ambler, A., Quail, M. A., Golby, P. & Guest, J. R. (1997). A 12-cistron *Escherichia coli* operon (*hyf*) encoding a putative proton-translocating formate hydrogenlyase system. *Microbiology (Reading, Engl)* **143**, 3633–3647.

Andrews, S., Robinson, A. & Rodriguez-Quinones, F. (2003). Bacterial iron homeostasis. *FEMS Microbiol Rev* **27**, 215–237.

Arifuzzaman, M., Maeda, M., Itoh, A., Nishikata, K., Takita, C., Saito, R., Ara, T., Nakahigashi, K., Huang, H.-C., et al. (2006). Large-scale identification of protein-protein interaction of *Escherichia coli* K-12. *Genome Res* **16**, 686–691.

Armstrong, F. & Albracht, S. (2005). [NiFe]-hydrogenases: spectroscopic and electrochemical definition of reactions and intermediates. *Philos Transact A Math Phys Eng Sci* **363**, 937–54.

Ayala-Castro, C., Saini, A. & Outten, F. W. (2008). Fe-S cluster assembly pathways in bacteria. *Microbiol Mol Biol Rev* **72**, 110–125.

Bagg, A. & Neilands, J. B. (1987). Ferric uptake regulation protein acts as a repressor, employing iron (II) as a cofactor to bind the operator of an iron transport operon in *Escherichia coli*. *Biochemistry* **26**, 5471–5477.

Bagramyan, K. A. & Martirosov, S. M. (1989). Formation of an ion transport supercomplex in *Escherichia coli*. An experimental model of direct transduction of energy *FEBS Lett* **246**, 149–152.

Bagramyan, K., Mnatsakanyan, N., Poladian, A., Vassilian, A. & Trchounian, A. (2002). The roles of hydrogenases 3 and 4, and the F_0F_1-ATPase, in H_2 production by *Escherichia coli* at alkaline and acidic pH. *FEBS Lett* **516**, 172–178.

Ballantine, S. & Boxer, D. (1985). Nickel-containing hydrogenase isoenzymes from anaerobically grown *Escherichia coli* K-12. *J Bacteriol* **163**, 454–459.

Ballantine, S. & Boxer, D. (1986). Isolation and characterisation of a soluble active fragment of hydrogenase isoenzyme 2 from the membranes of anaerobically grown *Escherichia coli*. *Eur J Biochem* **156**, 277–284.

Berg, B. L. & Stewart, V. (1990). Structural genes for nitrate-inducible formate dehydrogenase in *Escherichia coli* K-12. *Genetics* **125**, 691–702.

Berks, B. C. (1996). A common export pathway for proteins binding complex redox cofactors. *Mol Microbiol* **22**, 393–404.

Bertero, M. G., Rothery, R. A., Palak, M., Hou, C., Lim, D., Blasco, F., Weiner, J. H. & Strynadka, N. C. J. (2003). Insights into the respiratory electron transfer pathway from the structure of nitrate reductase A. *Nat Struct Biol* **10**, 681–687.

Birkmann, A. & Böck, A. (1989). Characterization of a *cis* regulatory DNA element necessary for formate induction of the formate dehydrogenase gene (*fdhF*) of *Escherichia coli*. *Mol Microbiol* **3**, 187–195.

Birkmann, A., Sawers, R. G. & Böck, A. (1987a). Involvement of the *ntrA* gene product in the anaerobic metabolism of *Escherichia coli*. *Mol Gen Genet* **210**, 535–542.

Birkmann, A., Zinoni, F., Sawers, R. G. & Böck, A. (1987b). Factors affecting transcriptional regulation of the formate-hydrogen-lyase pathway of *Escherichia coli*. *Arch Microbiol* **148**, 44–51.

Blokesch, M. & Böck, A. (2006). Properties of the [NiFe]-hydrogenase maturation protein HypD. *FEBS Lett* **580**, 4065–4068.

Blokesch, M., Albracht, S. P. J., Matzanke, B. F., Drapal, N. M., Jacobi, A. & Böck, A. (2004a). The complex between hydrogenase-maturation proteins HypC and HypD is an intermediate in the supply of cyanide to the active site iron of [NiFe]-hydrogenases. *J Mol Biol* **344**, 155–167.

Blokesch, M., Paschos, A., Bauer, A., Reissmann, S., Drapal, N. & Böck, A. (2004b). Analysis of the transcarbamoylation-dehydration reaction catalyzed by the hydrogenase maturation proteins HypF and HypE. *Eur J Biochem* **271**, 3428–3436.

Bothe, H., Schmitz, O., Yates, M. G. & Newton, W. E. (2010). Nitrogen fixation and hydrogen metabolism in cyanobacteria. *Microbiol Mol Biol Rev* **74**, 529–551.

Boyington, J. C., Gladyshev, V. N., Khangulov, S. V., Stadtman, T. C. & Sun, P. D. (1997). Crystal structure of formate dehydrogenase H: catalysis involving Mo, molybdopterin, selenocysteine, and an Fe_4S_4 cluster. *Science* **275**, 1305–1308.

Boysen, A., Moller-Jensen, J., Kallipolitis, B., Valentin-Hansen, P. & Overgaard, M. (2010). Translational regulation of gene expression by an anaerobically induced small non-coding RNA in *Escherichia coli*. *J Biol Chem* **285**, 10690–10702.

Böck, A., Forchhammer, K., Heider, J., Leinfelder, W., Sawers, R. G., Veprek, B. & Zinoni, F. (1991). Selenocysteine: the 21st amino acid. *Mol Microbiol* **5**, 515–520.

Böck, A., King, P., Blokesch, M. & Posewitz, M. (2006). Maturation of hydrogenases. *Adv Microb Physiol* **51**, 1–71.

Böhm, R., Sauter, M. & Böck, A. (1990). Nucleotide sequence and expression of an operon in *Escherichia coli* coding for formate hydrogenlyase components. *Mol Microbiol* **4**, 231–243.

Brøndsted, L. & Atlung, T. (1994). Anaerobic regulation of the hydrogenase 1 (*hya*) operon of *Escherichia coli*. *J Bacteriol* **176**, 5423–5428.

Bürstel, I., Hummel, P., Siebert, E., Wisitruangsakul, N., Zebger, I., Friedrich, B. & Lenz, O. (2011). Probing the origin of the metabolic precursor of the CO ligand in the catalytic center of [NiFe]-hydrogenase. *J Biol Chem*, doi: 10.1074/jbc.M111.309351, im Druck.

Cammack, R. (1995). Redox enzymes. Splitting molecular hydrogen. *Nature* **373**, 556–557.

Carroll, M. E., Barton, B. E., Gray, D. L., Mack, A. E. & Rauchfuss, T. B. (2011). Active-site models for the nickel-iron hydrogenases: effects of ligands on reactivity and catalytic properties. *Inorganic chemistry* **50**, 9554–9563.

Cartron, M., Maddocks, S., Gillingham, P., Craven, C. & Andrews, S. (2006). Feo - transport of ferrous iron into bacteria. *Biometals* **19**, 143–157.

Castanie-Cornet, M., Penfound, T., Smith, D., Elliott, J. & Foster, J. (1999). Control of acid resistance in *Escherichia coli*. *J Bacteriol* **181**, 3525–3535.

Chan Chung, K. C. & Zamble, D. B. (2011a). Protein interactions and localization of the *Escherichia coli* accessory protein HypA during nickel insertion to [NiFe] hydrogenase. *J Biol Chem*, doi: 10.1074/jbc.M111.290726, im Druck.

Chan Chung, K. C. & Zamble, D. B. (2011b). The *Escherichia coli* metal-binding chaperone SlyD interacts with the large subunit of [NiFe]-hydrogenase 3. *FEBS Lett* **585**, 291–294.

Chippaux, M., Casse, F. & Pascal, M. (1972). Isolation and phenotypes of mutants from *Salmonella typhimurium* defective in formate hydrogenlyase activity. *J Bacteriol* **110**, 766–768.

Cody, G. D., Boctor, N. Z., Filley, T. R., Hazen, R. M., Scott, J. H., Sharma, A. & Yoder, H. S. (2000). Primordial carbonylated iron-sulfur compounds and the synthesis of pyruvate. *Science* **289**, 1337–1340.

Cole, J. (1996). Nitrate reduction to ammonia by enteric bacteria: redundancy, or a strategy for survival during oxygen starvation. *FEMS Microbiology Letters* **136**, 1–11.

Constantinidou, C., Hobman, J. L., Griffiths, L., Patel, M. D., Penn, C. W., Cole, J. A. & Overton, T. W. (2006). A reassessment of the FNR regulon and transcriptomic analysis of the effects of nitrate, nitrite, NarXL, and NarQP as *Escherichia coli* K12 adapts from aerobic to anaerobic growth. *J Biol Chem* **281**, 4802–4815.

Corr, M. J. & Murphy, J. A. (2011). Evolution in the understanding of [Fe]-hydrogenase. *Chemical Society Reviews* **40**, 2279-2292.

Crack, J. C., Jervis, A. J., Gaskell, A. A., White, G. F., Green, J., Thomson, A. J. & Le Brun, N. E. (2008). Signal perception by FNR: the role of the iron-sulfur cluster. *Biochem Soc Trans* **36**, 1144–1148.

Cramm, R. (2009). Genomic view of energy metabolism in *Ralstonia eutropha* H16. *J Mol Microbiol Biotechnol* **16**, 38–52.

Cvetkovic, A., Menon, A. L., Thorgersen, M. P., Scott, J. W., Poole Ii, F. L., Jenney, F. E., Lancaster, W. A., Praissman, J. L., Shanmukh, S., *et al.* (2010). Microbial metalloproteomes are largely uncharacterized. *Nature* **466**, 779–782.

Czech, I., Silakov, A., Lubitz, W. & Happe, T. (2010). The [FeFe]-hydrogenase maturase HydF from *Clostridium acetobutylicum* contains a CO and CN⁻ ligated iron cofactor. *FEBS Lett* **584**, 638–642.

Daegelen, P., Studier, F. W., Lenski, R. E., Cure, S. & Kim, J. F. (2009). Tracing ancestors and relatives of *Escherichia coli* B, and the derivation of B strains REL606 and BL21(DE3). *J Mol Biol* **394**, 634–643.

Davidge, K. S., Sanguinetti, G., Yee, C. H., Cox, A. G., McLeod, C. W., Monk, C. E., Mann, B. E., Motterlini, R. & Poole, R. K. (2009). Carbon monoxide-releasing antibacterial molecules target respiration and global transcriptional regulators. *J Biol Chem* **284**, 4516–4524.

De Pina, K., Navarro, C., Mcwalter, L., Boxer, D. H., Price, N. C., Kelly, S. M., Mandrand-Berthelot, M.-A. & Wu, L.-F. (1995). Purification and characterization of the periplasmic nickel-binding protein NikA of *Escherichia coli* K12. *European Journal of Biochemistry* **227**, 857–865.

Ding, H., Clark, R. J. & Ding, B. (2004). IscA mediates iron delivery for assembly of iron-sulfur clusters in IscU under the limited accessible free iron conditions. *J Biol Chem* **279**, 37499–37504.

Ding, H., Yang, J., Coleman, L. C. & Yeung, S. (2007). Distinct iron binding property of two putative iron donors for the iron-sulfur cluster assembly: IscA and the bacterial frataxin ortholog CyaY under physiological and oxidative stress conditions. *J Biol Chem* **282**, 7997–8004.

Drapal, N. & Böck, A. (1998). Interaction of the hydrogenase accessory protein HypC with HycE, the large subunit of *Escherichia coli* hydrogenase 3 during enzyme maturation. *Biochemistry* **37**, 2941–2948.

Driesener, R. C., Challand, M. R., McGlynn, S. E., Shepard, E. M., Boyd, E. S., Broderick, J. B., Peters, J. W. & Roach, P. L. (2010). [FeFe]-hydrogenase cyanide ligands derived from *S*-adenosylmethionine-dependent cleavage of tyrosine. *Angew Chem Int Ed Engl* **49**, 1687–1690.

Dubini, A. & Sargent, F. (2003). Assembly of Tat-dependent [NiFe] hydrogenases: identification of precursor-binding accessory proteins. *FEBS Lett* **549**, 141–146.

Dubini, A., Pye, R., Jack, R., Palmer, T. & Sargent, F. (2002). How bacteria get energy from hydrogen: a genetic analysis of periplasmic hydrogen oxidation in *Escherichia coli*. *International Journal of Hydrogen Energy* **27**, 1413–1420.

Durand, S. & Storz, G. (2010). Reprogramming of anaerobic metabolism by the FnrS small RNA. *Mol Microbiol* **75**, 1215–1231.

Earhart, C. F. (1996). Uptake and metabolism of iron and molybdenum, Kapitel 71. *EcoSal—Escherichia coli and Salmonella: Cellular and Molecular Biology*, 2nd edn. ASM Press, Washington, DC.

Efremov, R. G., Baradaran, R. & Sazanov, L. A. (2010). The architecture of respiratory complex I. *Nature* **465**, 441–445.

Einsle, O., Tezcan, F. A., Andrade, S. L. A., Schmid, B., Yoshida, M., Howard, J. B. & Rees, D. C. (2002). Nitrogenase MoFe-protein at 1.16 Å resolution: a central ligand in the FeMo-cofactor. *Science* **297**, 1696–1700.

Enoch, H. G. & Lester, R. L. (1975). The purification and properties of formate dehydrogenase and nitrate reductase from *Escherichia coli*. *J Biol Chem* **250**, 6693–6705.

Escolar, L., Perez-Martin, J. & de Lorenzo, V. (1999). Opening the iron box: transcriptional metalloregulation by the Fur protein. *J Bacteriol* **181**, 6223–6229.

Ferenci, T., Zhou, Z., Betteridge, T., Ren, Y., Liu, Y., Feng, L., Reeves, P. R. & Wang, L. (2009). Genomic sequencing reveals regulatory mutations and recombinational events in the widely used MC4100 lineage of *Escherichia coli* K-12. *J Bacteriol* **191**, 4025–4029.

Fontecave, M., Choudens, S. O. de, Py, B. & Barras, F. (2005). Mechanisms of iron-sulfur cluster assembly: the SUF machinery. *J Biol Inorg Chem* **10**, 713–721.

Fontecilla-Camps, J. C., Volbeda, A., Cavazza, C. & Nicolet, Y. (2007). Structure/function relationships of [NiFe]- and [FeFe]-hydrogenases. *Chem Rev* **107**, 4273–4303.

Forzi, L. & Sawers, R. G. (2007). Maturation of [NiFe]-hydrogenases in *Escherichia coli*. *Biometals* **20**, 565–578.

Forzi, L., Hellwig, P., Thauer, R. K. & Sawers, R. G. (2007). The CO and CN^- ligands to the active site Fe in [NiFe]-hydrogenase of *Escherichia coli* have different metabolic origins. *FEBS Lett* **581**, 3317–3321.

Foster, J. W. & Hall, H. K. (1992). Effect of *Salmonella typhimurium* ferric uptake regulator (*fur*) mutations on iron- and pH-regulated protein synthesis. *J Bacteriol* **174**, 4317–4323.

Frey, M. (2002). Hydrogenases: hydrogen-activating enzymes. *Chembiochem* **3**, 153–160.

Friedrich, B., Kortlüke, C., Hogrefe, C., Eberz, G., Silber, B. & Warrelmann, J. (1986). Genetics of hydrogenase from aerobic lithoautotrophic bacteria. *Biochimie* **68**, 133–145.

Fritsch, J., Scheerer, P., Frielingsdorf, S., Kroschinsky, S., Friedrich, B., Lenz, O. & Spahn, C. M. T. (2011a). The crystal structure of an oxygen-tolerant hydrogenase uncovers a novel iron-sulphur centre. *Nature* **479**, 249–252.

Fritsch, J., Loescher, S., Sanganas, O., Siebert, E., Zebger, I., Stein, M., Ludwig, M., De Lacey, A. L., Dau, H., et al. (2011b). [NiFe]- and [FeS]-cofactors in the membrane-bound hydrogenase of *Ralstonia eutropha* investigated by X-ray absorption spectroscopy: insights into O_2-tolerant H_2-cleavage. *Biochemistry* **50**, 5858-5869.

Fritsche, E., Paschos, A., Beisel, H. G., Böck, A. & Huber, R. (1999). Crystal structure of the hydrogenase maturating endopeptidase HYBD from *Escherichia coli J Mol Biol* **288**, 989–998.

Gaffney, J. & Marley, N. (2005). Henry Cavendish (1730-1810): His Contributions and Links to Atmospheric Science. Preprint, Extended Abstract Seventh Conference on Atmospheric Chemistry as part of the 85th *American Meteorological Society (AMS)* Annual Meeting in San Diego, CA, January 9-13, 2005; Paper 1.1, 3pp.

Gasper, R., Scrima, A. & Wittinghofer, A. (2006). Structural insights into HypB, a GTP-binding protein that regulates metal binding. *J Biol Chem* **281**, 27492–27502.

Giel, J. L., Rodionov, D., Liu, M., Blattner, F. R. & Kiley, P. J. (2006). IscR-dependent gene expression links iron-sulphur cluster assembly to the control of O_2-regulated genes in *Escherichia coli. Mol Microbiol* **60**, 1058–1075.

Goldet, G., Brandmayr, C., Stripp, S. T., Happe, T., Cavazza, C., Fontecilla-Camps, J. C. & Armstrong, F. A. (2009). Electrochemical kinetic investigations of the reactions of [FeFe]-hydrogenases with carbon monoxide and oxygen: comparing the importance of gas tunnels and active-site electronic/redox effects. *J Am Chem Soc* **131**, 14979–14989.

Goris, T., Wait, A. F., Saggu, M., Fritsch, J., Heidary, N., Stein, M., Zebger, I., Lendzian, F., Armstrong, F. A., et al. (2011). A unique iron-sulfur cluster is crucial for oxygen tolerance of a [NiFe]-hydrogenase. *Nat Chem Biol* **7**, 310-318.

Graf, E.-G. & Thauer, R. K. (1981). Hydrogenase from *Methanobacterium thermoautotrophicum*, a nickel-containing enzyme. *FEBS letters* **136**, 165-169.

Graham, A., Boxer, D., Haddock, B., Mandrand-Berthelot, A. & Jones, R. (1980). Immunochemical analysis of the membrane-bound hydrogenase of *Escherichia coli. FEBS Lett* **113**, 167–172.

Green, J. & Guest, J. R. (1993a). A role for iron in transcriptional activation by FNR. *FEBS Lett* **329**, 55–58.

Green, J. & Guest, J. R. (1993b). Activation of FNR-dependent transcription by iron: an in vitro switch for FNR. *FEMS Microbiol Lett* **113**, 219–222.

Green, J. & Paget, M. S. (2004). Bacterial redox sensors. *Nat Rev Microbiol* **2**, 954–966.

Green, J., Sharrocks, A. D., Green, B., Geisow, M. & Guest, J. R. (1993). Properties of FNR proteins substituted at each of the five cysteine residues. *Mol Microbiol* **8**, 61–68.

Hantke, K. (1981). Regulation of ferric iron transport in *Escherichia coli* K12: isolation of a constitutive mutant. *Mol Gen Genet* **182**, 288–292.

Hantke, K. (2002). Members of the Fur protein family regulate iron and zinc transport in *E. coli* and characteristics of the Fur-regulated FhuF protein. *J Mol Microbiol Biotechnol* **4**, 217–222.

Hantke, K. (2003). Is the bacterial ferrous iron transporter FeoB a living fossil. *Trends Microbiol* **11**, 192–195.

Happe, R. P., Roseboom, W., Egert, G., Friedrich, C. G., Massanz, C., Friedrich, B. & Albracht, S. P. (2000). Unusual FTIR and EPR properties of the H_2-activating site of the cytoplasmic NAD-reducing hydrogenase from *Ralstonia eutropha. FEBS Lett* **466**, 259–263.

Hasona, A., Self, W. T., Ray, R. M. & Shanmugam, K. T. (1998). Molybdate-dependent transcription of *hyc* and *nar* operons of *Escherichia coli* requires MoeA protein and ModE-molybdate. *FEMS Microbiol Lett* **169**, 111–116.

Hayes, E. T., Wilks, J. C., Sanfilippo, P., Yohannes, E., Tate, D. P., Jones, B. D., Radmacher, M. D., BonDurant, S. S. & Slonczewski, J. L. (2006). Oxygen limitation modulates pH regulation of catabolism and hydrogenases, multidrug transporters, and envelope composition in *Escherichia coli* K-12. *BMC Microbiol* **6**, 89.

Hedderich, R. & Forzi, L. (2005). Energy-converting [NiFe] hydrogenases: more than just H_2 activation. *J Mol Microbiol Biotechnol* **10**, 92–104.

Hopper, S., Babst, M., Schlensog, V., Fischer, H. M., Hennecke, H. & Böck, A. (1994). Regulated expression *in vitro* of genes coding for formate hydrogenlyase components of *Escherichia coli*. *J Biol Chem* **269**, 19597–19604.

Horch, M., Lauterbach, L., Saggu, M., Hildebrandt, P., Lendzian, F., Bittl, R., Lenz, O. & Zebger, I. (2010). Probing the active site of an O_2-tolerant NAD^+-reducing [NiFe]-hydrogenase from *Ralstonia eutropha* H16 by *in situ* EPR and FTIR spectroscopy. *Angew Chem Int Ed Engl* **49**, 8026–8029.

Hu, Y. & Ribbe, M. W. (2011). Biosynthesis of nitrogenase FeMoco. *Coord Chem Rev* **255**, 1218–1224.

Hube, M., Blokesch, M. & Böck, A. (2002). Network of hydrogenase maturation in *Escherichia coli*: role of accessory proteins HypA and HybF. *J Bacteriol* **184**, 3879–3885.

Huber, C. & Wächtershäuser, G. (1997). Activated acetic acid by carbon fixation on (Fe,Ni)S under primordial conditions. *Science* **276**, 245–247.

Huber, C. & Wächtershäuser, G. (1998). Peptides by activation of amino acids with CO on (Ni,Fe)S surfaces: implications for the origin of life. *Science* **281**, 670–672.

Hurley, J. K., Weber-Main, A. M., Hodges, A. E., Stankovich, M. T., Benning, M. M., Holden, H. M., Cheng, H., Xia, B., Markley, J. L., *et al*. (1997). Iron-sulfur cluster cysteine-to-serine mutants of *Anabaena* [2Fe-2S] ferredoxin exhibit unexpected redox properties and are competent in electron transfer to ferredoxin:$NADP^+$ reductase. *Biochemistry* **36**, 15109–15117.

Hussain, H., Grove, J., Griffiths, L., Busby, S. & Cole, J. (1994). A seven-gene operon essential for formate-dependent nitrite reduction to ammonia by enteric bacteria. *Mol Microbiol* **12**, 153–163.

Iuchi, S. & Lin, E. C. (1991). Adaptation of *Escherichia coli* to respiratory conditions: regulation of gene expression. *Cell* **66**, 5–7.

Jacobi, A., Rossmann, R. & Böck, A. (1992). The *hyp* operon gene products are required for the maturation of catalytically active hydrogenase isoenzymes in *Escherichia coli*. *Arch Microbiol* **158**, 444–451.

Jacobson, M. R., Cash, V. L., Weiss, M. C., Laird, N. F., Newton, W. E. & Dean, D. R. (1989). Biochemical and genetic analysis of the *nifUSVWZM* cluster from *Azotobacter vinelandii*. *Mol Gen Genet* **219**, 49–57.

Jeong, H., Barbe, V., Lee, C. H., Vallenet, D., Yu, D. S., Choi, S.-H., Couloux, A., Lee, S.-W., Yoon, S. H., *et al*. (2009). Genome sequences of *Escherichia coli* B strains REL606 and BL21(DE3). *J Mol Biol* **394**, 644–652.

Johnson, M. K. (1998). Iron-sulfur proteins: new roles for old clusters. *Curr Opin Chem Biol* **2**, 173–181.

Jormakka, M. (2002). Molecular basis of proton motive force generation: structure of formate dehydrogenase-N. *Science* **295**, 1863–1868.

Jormakka, M., Richardson, D., Byrne, B. & Iwata, S. (2004). Architecture of NarGH reveals a structural classification of Mo-*bis*MGD enzymes. *Structure* **12**, 95–104.

Kaiser, M. & Sawers, R. G. (1995). Fnr activates transcription from the *P6* promoter of the *pfl* operon *in vitro*. *Mol Microbiol* **18**, 331–342.

Kaluarachchi, H., Chan Chung, K. C. & Zamble, D. B. (2010). Microbial nickel proteins. *Nat Prod Rep* **27**, 681–694.

Kang, Y., Weber, K. D., Qiu, Y., Kiley, P. J. & Blattner, F. R. (2005). Genome-wide expression analysis indicates that FNR of *Escherichia coli* K-12 regulates a large number of genes of unknown function. *J Bacteriol* **187**, 1135–1160.

Kelley, L. A. & Sternberg, M. J. E. (2009). Protein structure prediction on the web: a case study using the Phyre server. *Nat Protoc* **4**, 363–371.

Kerner, M. J., Naylor, D. J., Ishihama, Y., Maier, T., Chang, H.-C., Stines, A. P., Georgopoulos, C., Frishman, D., Hayer-Hartl, M., *et al*. (2005). Proteome-wide analysis of chaperonin-dependent protein folding in *Escherichia coli*. *Cell* **122**, 209–220.

Kiley, P. J. & Beinert, H. (1998). Oxygen sensing by the global regulator, FNR: the role of the iron-sulfur cluster. *FEMS Microbiol Rev* **22**, 341–352.

Kim, D.-H. & Kim, M.-S. (2011). Hydrogenases for biological hydrogen production *Bioresour Technol* **102**, 8357-8367.

Kim, Y. J., Lee, H. S., Kim, E. S., Bae, S. S., Lim, J. K., Matsumi, R., Lebedinsky, A. V., Sokolova, T. G., Kozhevnikova, D. A., *et al*. (2010). Formate-driven growth coupled with H_2 production. *Nature* **467**, 352–355.

Kitagawa, M., Ara, T., Arifuzzaman, M., Ioka-Nakamichi, T., Inamoto, E., Toyonaga, H. & Mori, H. (2005). Complete set of ORF clones of *Escherichia coli* ASKA library (a complete set of *E. coli* K-12 ORF archive): unique resources for biological research. *DNA Res* **12**, 291–299.

Knappe, J. & Sawers, R. G. (1990). A radical-chemical route to acetyl-CoA: the anaerobically induced pyruvate formate-lyase system of *Escherichia coli*. *FEMS Microbiol Rev* **6**, 383–398.

Krasna, A. (1984). Mutants of *Escherichia coli* with altered hydrogenase activity. *J Gen Microbiol* **130**, 779–787.

Kröger, A., Biel, S., Simon, J., Gross, R., Unden, G. & Lancaster, C. R. D. (2002). Fumarate respiration of *Wolinella succinogenes*: enzymology, energetics and coupling mechanism. *Biochim Biophys Acta* **1553**, 23–38.

Kuchenreuther, J. M., Stapleton, J. A. & Swartz, J. R. (2009). Tyrosine, cysteine, and *S*-adenosyl methionine stimulate *in vitro* [FeFe] hydrogenase activation. *PLoS ONE* **4**, e7565.

Kuchenreuther, J. M., George, S. J., Grady-Smith, C. S., Cramer, S. P. & Swartz, J. R. (2011). Cell-free H-cluster synthesis and [FeFe] hydrogenase activation: all five CO and CN⁻ ligands derive from tyrosine. *PLoS ONE* **6**, e20346.

Kumarevel, T., Tanaka, T., Bessho, Y., Shinkai, A. & Yokoyama, S. (2009). Crystal structure of hydrogenase maturating endopeptidase HycI from *Escherichia coli*. *Biochem Biophys Res Commun* **389**, 310–314.

Kurkin, S., Meuer, J., Koch, J., Hedderich, R. & Albracht, S. P. J. (2002). The membrane-bound [NiFe]-hydrogenase (Ech) from *Methanosarcina barkeri*: unusual properties of the iron-sulphur clusters. *Eur J Biochem* **269**, 6101–6111.

Lambertz, C., Leidel, N., Havelius, K. G. V., Noth, J., Chernev, P., Winkler, M., Happe, T. & Haumann, M. (2011). O_2-reactions at the six-iron activesite (H-cluster) in [FeFe]-hydrogenase. *J Biol Chem* **286**, 40614-40623.

Laurinavichene, T. V., Zorin, N. A. & Tsygankov, A. A. (2002). Effect of redox potential on activity of hydrogenase 1 and hydrogenase 2 in *Escherichia coli*. *Arch Microbiol* **178**, 437–442.

Layer, G., Ollagnier-de Choudens, S., Sanakis, Y. & Fontecave, M. (2006). Iron-sulfur cluster biosynthesis: characterization of *Escherichia coli* CyaY as an iron donor for the assembly of [2Fe-2S] clusters in the scaffold IscU. *J Biol Chem* **281**, 16256–16263.

Leach, M. R., Sandal, S., Sun, H. & Zamble, D. B. (2005). Metal binding activity of the *Escherichia coli* hydrogenase maturation factor HypB. *Biochemistry* **44**, 12229–12238.

Lee, J., Patel, P., Sankar, P. & Shanmugam, K. (1985). Isolation and characterization of mutant strains of *Escherichia coli* altered in H_2 metabolism. *J Bacteriol* **162**, 344–352.

Leimkühler, S., Wuebbens, M. M. & Rajagopalan, K. V. (2011). The history of the discovery of the molybdenum cofactor and novel aspects of its biosynthesis in bacteria. *Coord Chem Rev* **255**, 1129–1144.

Lenz, O., Zebger, I., Hamann, J., Hildebrandt, P. & Friedrich, B. (2007). Carbamoylphosphate serves as the source of CN^-, but not of the intrinsic CO in the active site of the regulatory [NiFe]-hydrogenase from *Ralstonia eutropha. FEBS Lett* **581**, 3322–3326.

Liebgott, P.-P., Leroux, F., Burlat, B., Dementin, S., Baffert, C., Lautier, T., Fourmond, V., Ceccaldi, P., Cavazza, C., *et al.* (2010). Relating diffusion along the substrate tunnel and oxygen sensitivity in hydrogenase. *Nat Chem Biol* **6**, 63–70.

Lill, R. (2009). Function and biogenesis of iron-sulphur proteins. *Nature* **460**, 831–838.

Lukey, M. J., Parkin, A., Roessler, M. M., Murphy, B. J., Harmer, J., Palmer, T., Sargent, F. & Armstrong, F. A. (2010). How *Escherichia coli* is equipped to oxidize hydrogen under different redox conditions. *J Biol Chem* **285**, 3928–3938.

Lukey, M. J., Roessler, M. M., Parkin, A., Evans, R. M., Davies, R. A., Lenz, O., Friedrich, B., Sargent, F. & Armstrong, F. A. (2011). Oxygen tolerant [NiFe]-hydrogenases: the individual and collective importance of supernumerary cysteines at the proximal Fe-S cluster. *J Am Chem Soc* **133**, 16881-16892.

Lutz, S., Jacobi, A., Schlensog, V., Böhm, R., Sawers, R. G. & Böck, A. (1991). Molecular characterization of an operon (*hyp*) necessary for the activity of the three hydrogenase isoenzymes in *Escherichia coli. Mol Microbiol* **5**, 123–135.

Lü, W., Du, J., Wacker, T., Gerbig-Smentek, E., Andrade, S. L. A. & Einsle, O. (2011). pH-dependent gating in a FocA formate channel. *Science* **332**, 352–354.

Lüke, I., Butland, G., Moore, K., Buchanan, G., Lyall, V., Fairhurst, S. A., Greenblatt, J. F., Emili, A., Palmer, T. & Sargent, F. (2008). Biosynthesis of the respiratory formate dehydrogenases from *Escherichia coli*: characterization of the FdhE protein. *Arch Microbiol* **190**, 685–696.

Maeda, T., Sanchez-Torres, V. & Wood, T. K. (2008). Protein engineering of hydrogenase 3 to enhance hydrogen production. *Appl Microbiol Biotechnol* **79**, 77–86.

Maier, T. & Böck, A. (1996). Generation of active [NiFe] hydrogenase *in vitro* from a nickel-free precursor form. *Biochemistry* **35**, 10089–10093.

Majdalani, N., Vanderpool, C. K. & Gottesman, S. (2005). Bacterial small RNA regulators. *Crit Rev Biochem Mol Biol* **40**, 93–113.

Manyani, H., Rey, L., Palacios, J. M., Imperial, J. & Ruiz-Argüeso, T. (2005). Gene products of the *hupGHIJ* operon are involved in maturation of the iron-sulfur subunit of the [NiFe] hydrogenase from *Rhizobium leguminosarum* bv. viciae. *J Bacteriol* **187**, 7018–7026.

Martin, W. & Müller, M. (1998). The hydrogen hypothesis for the first eukaryote. *Nature* **392**, 37–41.

Martin, W. & Russell, M. J. (2007). On the origin of biochemistry at an alkaline hydrothermal vent. *Phil Trans R Soc B* **362**, 1887–1925.

McGlynn, S. E., Ruebush, S. S., Naumov, A., Nagy, L. E., Dubini, A., King, P. W., Broderick, J. B., Posewitz, M. C. & Peters, J. W. (2007). *In vitro* activation of [FeFe] hydrogenase: new insights into hydrogenase maturation. *J Biol Inorg Chem* **12**, 443–447.

McGlynn, S. E., Shepard, E. M., Winslow, M. A., Naumov, A. V., Duschene, K. S., Posewitz, M. C., Broderick, W. E., Broderick, J. B. & Peters, J. W. (2008). HydF as a scaffold protein in [FeFe] hydrogenase H-cluster biosynthesis *FEBS Lett* **582**, 2183–2187.

Mellmann, A., Harmsen, D., Cummings, C. A., Zentz, E. B., Leopold, S. R., Rico, A., Prior, K., Szczepanowski, R., Ji, Y., *et al.* (2011). Prospective genomic characterization of the German enterohemorrhagic *Escherichia coli* O104:H4 outbreak by rapid next generation sequencing technology. *PLoS ONE* **6**, e22751.

Menon, A. L. & Robson, R. L. (1994). *In vivo* and in vitro nickel-dependent processing of the [NiFe] hydrogenase in *Azotobacter vinelandii*. *J Bacteriol* **176**, 291–295.

Menon, N. K., Robbins, J., Wendt, J., Shanmugam, K. & Przybyla, A. (1991). Mutational analysis and characterization of the *Escherichia coli hya* operon, which encodes [NiFe] hydrogenase 1. *J Bacteriol* **173**, 4851–4861.

Menon, N. K., Chatelus, C. Y., Dervartanian, M., Wendt, J. C., Shanmugam, K. T., Peck, H. D. & Przybyla, A. E. (1994). Cloning, sequencing, and mutational analysis of the *hyb* operon encoding *Escherichia coli* hydrogenase 2. *J Bacteriol* **176**, 4416–4423.

Messenger, S. & Green, J. (2003). FNR-mediated regulation of *hyp* expression in *Escherichia coli*. *FEMS Microbiol Lett* **228**, 81–86.

Mettert, E. L., Outten, F. W., Wanta, B. & Kiley, P. J. (2008). The impact of O_2 on the Fe-S cluster biogenesis requirements of *Escherichia coli* FNR. *J Mol Biol* **384**, 798–811.

Mnatsakanyan, N., Bagramyan, K. & Trchounian, A. (2004). Hydrogenase 3 but not hydrogenase 4 is major in hydrogen gas production by *Escherichia coli* formate hydrogenlyase at acidic pH and in the presence of external formate. *Cell Biochem Biophys* **41**, 357–366.

Mulder, D. W., Boyd, E. S., Sarma, R., Lange, R. K., Endrizzi, J. A., Broderick, J. B. & Peters, J. W. (2010). Stepwise [FeFe]-hydrogenase H-cluster assembly revealed in the structure of HydA(DeltaEFG). *Nature* **465**, 248–251.

Mulder, D. W., Shepard, E. M., Meuser, J. E., Joshi, N., King, P. W., Posewitz, M. C., Broderick, J. B. & Peters, J. W. (2011). Insights into [FeFe]-hydrogenase structure, mechanism, and maturation. *Structure* **19**, 1038–1052.

Mulrooney, S. B. & Hausinger, R. P. (2003). Nickel uptake and utilization by microorganisms. *FEMS Microbiol Rev* **27**, 239–261.

Murarka, A., Clomburg, J. M., Moran, S., Shanks, J. V. & Gonzalez, R. (2010). Metabolic analysis of wild-type *Escherichia coli* and a pyruvate dehydrogenase complex (PDHC)-deficient derivative reveals the role of PDHC in the fermentative metabolism of glucose. *J Biol Chem* **285**, 31548–31558.

Naas, T., Blot, M., Fitch, W. M. & Arber, W. (1995). Dynamics of IS-related genetic rearrangements in resting *Escherichia coli* K-12. *Mol. Biol. Evol.* **12**, 198–207.

Navarro, C., Wu, L. F. & Mandrand-Berthelot, M. A. (1993). The *nik* operon of *Escherichia coli* encodes a periplasmic binding-protein-dependent transport system for nickel. *Mol Microbiol* **9**, 1181–1191.

Nicolet, Y., Martin, L., Tron, C. & Fontecilla-Camps, J. C. (2010). A glycyl free radical as the precursor in the synthesis of carbon monoxide and cyanide by the [FeFe]-hydrogenase maturase HydG. *FEBS Lett* **584**, 4197-4202.

Niederman, R. A. & Wolin, M. J. (1972). Requirement of succinate for the growth of *Vibrio succinogenes*. *J Bacteriol* **109**, 546–549.

Oh, Y.-K., Raj, S. M., Jung, G. Y. & Park, S. (2011). Current status of the metabolic engineering of microorganisms for biohydrogen production. *Bioresour Technol* **102**, 8357–8367.

Page, C. C., Moser, C. C. & Dutton, P. L. (2003). Mechanism for electron transfer within and between proteins. *Curr Opin Chem Biol* **7**, 551–556.

Palmer, T., Sargent, F. & Berks, B. (2005). Export of complex cofactor-containing proteins by the bacterial Tat pathway. *Trends Microbiol* **13**, 175–180.

Pascal, M., Casse, F., Chippaux, M. & Lepelletier, M. (1975). Genetic analysis of mutants of *Escherichia coli* K12 and *Salmonella typhimurium* LT2 deficient in hydrogenase activity. *Mol Gen Genet* **141**, 173–179.

Paschos, A., Bauer, A., Zimmermann, A., Zehelein, E. & Böck, A. (2002). HypF, a carbamoyl phosphate-converting enzyme involved in [NiFe] hydrogenase maturation. *J Biol Chem* **277**, 49945–49951.

Peters, J. W., Lanzilotta, W. N., Lemon, B. J. & Seefeldt, L. C. (1998). X-ray crystal structure of the Fe-only hydrogenase (CpI) from *Clostridium pasteurianum* to 1.8 angstrom resolution. *Science* **282**, 1853–1858.

Petkun, S., Shi, R., Li, Y., Asinas, A., Munger, C., Zhang, L., Waclawek, M., Soboh, B., Sawers, R.G. & Cygler, M. (2011). Structure of hydrogenase maturation protein HypF with reaction intermediates shows two active sites. *Structure* **19**, 1773-1783.

Podar, M., Anderson, I., Makarova, K. S., Elkins, J. G., Ivanova, N., Wall, M. A., Lykidis, A., Mavromatis, K., Sun, H., *et al.* (2008). A genomic analysis of the archaeal system *Ignicoccus hospitalis-Nanoarchaeum equitans*. *Genome Biol* **9**, R158.

Pohlmann, A., Fricke, W. F., Reinecke, F., Kusian, B., Liesegang, H., Cramm, R., Eitinger, T., Ewering, C., Pötter, M., *et al.* (2006). Genome sequence of the bioplastic-producing "Knallgas" bacterium *Ralstonia eutropha* H16. *Nat Biotechnol* **24**, 1257–1262.

Punginelli, C., Ize, B., Stanley, N. R., Stewart, V., Sawers, R. G., Berks, B. C. & Palmer, T. (2004). mRNA secondary structure modulates translation of Tat-dependent formate dehydrogenase N. *J Bacteriol* **186**, 6311–6315.

Py, B. & Barras, F. (2010). Building Fe-S proteins: bacterial strategies. *Nat Rev Microbiol* **8**, 436–446.

Ramaswamy, S. (2011). Biochemistry. One atom makes all the difference *Science* **334**, 914–915.

Rauchfuss, T. B. (2007). A promising mimic of hydrogenase activity. *Science* **316**, 553–554.

Redwood, M., Mikheenko, I., Sargent, F. & Macaskie, L. (2007). Dissecting the roles of *Escherichia coli* hydrogenases in biohydrogen production. *FEMS Microbiol Lett* **278**, 48–55.

Reissmann, S., Hochleitner, E., Wang, H., Paschos, A., Lottspeich, F., Glass, R. S. & Böck, A. (2003). Taming of a poison: biosynthesis of the NiFe-hydrogenase cyanide ligands. *Science* **299**, 1067–1070.

Richard, D., Sawers, R. G., Sargent, F., McWalter, L. & Boxer, D. (1999). Transcriptional regulation in response to oxygen and nitrate of the operons encoding the [NiFe] hydrogenases 1 and 2 of *Escherichia coli*. *Microbiology* **145**, 2903–2912.

Richardson, D. & Sawers, R. G. (2002). Structural biology. PMF through the redox loop. *Science* **295**, 1842–1843.

Roessler, P. G. & Lien, S. (1984). Purification of hydrogenase from *Chlamydomonas reinhardtii*. *Plant Physiol.* **75**, 705–709.

Rossmann, R., Sawers, R. G. & Böck, A. (1991). Mechanism of regulation of the formate-hydrogenlyase pathway by oxygen, nitrate, and pH: definition of the formate regulon. *Mol Microbiol* **5**, 2807–2814.

Rossmann, R., Sauter, M., Lottspeich, F. & Böck, A. (1994). Maturation of the large subunit (HYCE) of *Escherichia coli* hydrogenase 3 requires nickel incorporation followed by C-terminal processing at Arg537. *Eur J Biochem* **220**, 377–384.

Rossmann, R., Maier, T., Lottspeich, F. & Böck, A. (1995). Characterisation of a protease from *Escherichia coli* involved in hydrogenase maturation. *Eur J Biochem* **227**, 545–550.

Rowe, J. L., Starnes, G. L. & Chivers, P. T. (2005). Complex transcriptional control links NikABCDE-dependent nickel transport with hydrogenase expression in *Escherichia coli*. *J Bacteriol* **187**, 6317–6323.

Römpp, H., Falbe, J. & Regitz, M. (1992). Römpp Chemie Lexikon. Georg Thieme Verlag, Stuttgart.

Rubio, L. M. & Ludden, P. W. (2008). Biosynthesis of the iron-molybdenum cofactor of nitrogenase. *Annu. Rev. Microbiol.* **62**, 93–111.

Ruiz-Herrera, J. & DeMoss, J. A. (1969). Nitrate reductase complex of *Escherichia coli* K-12: participation of specific formate dehydrogenase and cytochrome b_1 components in nitrate reduction. *J Bacteriol* **99**, 720–729.

Sargent, F., Ballantine, S., Rugman, P., Palmer, T. & Boxer, D. (1998). Reassignment of the gene encoding the *Escherichia coli* hydrogenase 2 small subunit-identification of a soluble precursor of the small subunit in a *hypB* mutant. *Eur J Biochem* **255**, 746–754.

Sasahara, K. C., Heinzinger, N. K. & Barrett, E. L. (1997). Hydrogen sulfide production and fermentative gas production by *Salmonella typhimurium* require F_0F_1 ATP synthase activity. *J Bacteriol* **179**, 6736–6740.

Sauter, M., Böhm, R. & Böck, A. (1992). Mutational analysis of the operon (*hyc*) determining hydrogenase 3 formation in *Escherichia coli*. *Mol Microbiol* **6**, 1523–1532.

Sawers, R. G. (1994). The hydrogenases and formate dehydrogenases of *Escherichia coli*. *Antonie Van Leeuwenhoek* **66**, 57–88.

Sawers, R. G. (2005a). Formate and its role in hydrogen production in *Escherichia coli*. *Biochem Soc Trans* **33**, 42–46.

Sawers, R. G. (2005b). Evidence for novel processing of the anaerobically inducible dicistronic *focA-pfl* mRNA transcript in *Escherichia coli*. *Mol Microbiol* **58**, 1441–1453.

Sawers, R. G. (2005c). Expression of *fnr* is constrained by an upstream IS*5* insertion in certain *Escherichia coli* K-12 strains. *J Bacteriol* **187**, 2609–2617.

Sawers, R. G. (2006). Differential turnover of the multiple processed transcripts of the *Escherichia coli focA-pflB* operon. *Microbiology (Reading, Engl)* **152**, 2197–2205.

Sawers, R. G. & Boxer, D. (1986). Purification and properties of membrane-bound hydrogenase isoenzyme 1 from anaerobically grown *Escherichia coli* K12. *Eur J Biochem* **156**, 265–275.

Sawers, R. G. & Clark, D. (2004). Einstelldatum: 27. Juli 2004. Kapitel 3.5.3. Fermentative Pyruvate and Acetyl-Coenzyme A Metabolism, *In* A. Böck, R. Curtiss III, J. B. Kaper, P. D. Karp, F. C. Neidhardt, T. Nyström, J. M. Slauch, C. L. Squires, and D. Ussery (ed.), *EcoSal - Escherichia coli and Salmonella: cellular and molecular biology*. http://www.ecosal.org. ASM Press, Washington, DC.

Sawers, R. G., Ballantine, S. & Boxer, D. (1985). Differential expression of hydrogenase isoenzymes in *Escherichia coli* K-12: evidence for a third isoenzyme. *J Bacteriol* **164**, 1324–1331.

Schwartz, C. J., Giel, J. L., Patschkowski, T., Luther, C., Ruzicka, F. J., Beinert, H. & Kiley, P. J. (2001). IscR, an Fe-S cluster-containing transcription factor, represses expression of *Escherichia coli* genes encoding Fe-S cluster assembly proteins. *Proc Natl Acad Sci USA* **98**, 14895–14900.

Self, W. T., Grunden, A. M., Hasona, A. & Shanmugam, K. T. (1999). Transcriptional regulation of molybdoenzyme synthesis in *Escherichia coli* in response to molybdenum: ModE-molybdate, a repressor of the *modABCD* (molybdate transport) operon is a secondary transcriptional activator for the *hyc* and *nar* operons. *Microbiology (Reading, Engl)* **145**, 41–55.

Shalel-Levanon, S., San, K.-Y. & Bennett, G. N. (2005). Effect of oxygen, and ArcA and FNR regulators on the expression of genes related to the electron transfer chain and the TCA cycle in *Escherichia coli. Metab Eng* **7**, 364–374.

Shepard, E. M., McGlynn, S. E., Bueling, A. L., Grady-Smith, C. S., George, S. J., Winslow, M. A., Cramer, S. P., Peters, J. W. & Broderick, J. B. (2010a). Synthesis of the 2Fe subcluster of the [FeFe]-hydrogenase H cluster on the HydF scaffold. *Proc Natl Acad Sci USA* **107**, 10448–10453.

Shepard, E. M., Duffus, B. R., George, S. J., McGlynn, S. E., Challand, M. R., Swanson, K. D., Roach, P. L., Cramer, S. P., Peters, J. W. & Broderick, J. B. (2010b). [FeFe]-hydrogenase maturation: HydG-catalyzed synthesis of carbon monoxide. *J Am Chem Soc* **132**, 9247–9249.

Shepard, E. M., Boyd, E. S., Broderick, J. B. & Peters, J. W. (2011). Biosynthesis of complex iron-sulfur enzymes. *Curr Opin Chem Biol* **15**, 319–327.

Shima, S., Pilak, O., Vogt, S., Schick, M., Stagni, M. S., Meyer-Klaucke, W., Warkentin, E., Thauer, R. K. & Ermler, U. (2008). The crystal structure of [Fe]-hydrogenase reveals the geometry of the active site. *Science* **321**, 572–575.

Shomura, Y., Yoon, K.-S., Nishihara, H. & Higuchi, Y. (2011). Structural basis for a [4Fe-3S] cluster in the oxygen-tolerant membrane-bound [NiFe]-hydrogenase. *Nature* **479**, 253-256.

Silakov, A., Kamp, C., Reijerse, E., Happe, T. & Lubitz, W. (2009). Spectroelectrochemical characterization of the active site of the [FeFe] hydrogenase HydA1 from *Chlamydomonas reinhardtii. Biochemistry* **48**, 7780–7786.

Soupene, E., van Heeswijk, W. C., Plumbridge, J., Stewart, V., Bertenthal, D., Lee, H., Prasad, G., Paliy, O., Charernnoppakul, P. & Kustu, S. (2003). Physiological studies of *Escherichia coli* strain MG1655: growth defects and apparent cross-regulation of gene expression. *J Bacteriol* **185**, 5611–5626.

Spatzal, T., Aksoyoglu, M., Zhang, L., Andrade, S. L. A., Schleicher, E., Weber, S., Rees, D. C. & Einsle, O. (2011). Evidence for interstitial carbon in nitrogenase FeMo cofactor *Science* **334**, 940.

Spiro, S. & Guest, J. R. (1990). FNR and its role in oxygen-regulated gene expression in *Escherichia coli. FEMS Microbiol Rev* **6**, 399–428.

Spiro, S. & Guest, J. R. (1991). Adaptive responses to oxygen limitation in *Escherichia coli. Trends Biochem Sci* **16**, 310–314.

Spiro, S., Roberts, R. E. & Guest, J. R. (1989). FNR-dependent repression of the *ndh* gene of *Escherichia coli* and metal ion requirement for FNR-regulated gene expression. *Mol Microbiol* **3**, 601–608.

Stephenson, M. & Stickland, L. H. (1931). Hydrogenase: a bacterial enzyme activating molecular hydrogen: The properties of the enzyme. *Biochem J* **25**, 205–214.

Stewart, V. (1988). Nitrate respiration in relation to facultative metabolism in enterobacteria. *Microbiol Rev* **52**, 190–232.

Stripp, S. T., Goldet, G., Brandmayr, C., Sanganas, O., Vincent, K. A., Haumann, M., Armstrong, F. A. & Happe, T. (2009). How oxygen attacks [FeFe] hydrogenases from photosynthetic organisms. *Proc Natl Acad Sci USA* **106**, 17331–17336.

Suppmann, B. & Sawers, R. G. (1994). Isolation and characterization of hypophosphite--resistant mutants of *Escherichia coli*: identification of the FocA protein, encoded by the *pfl* operon, as a putative formate transporter. *Mol Microbiol* **11**, 965–982.

Sydor, A. M., Liu, J. & Zamble, D. B. (2011). Effects of metal on the biochemical properties of *Helicobacter pylori* HypB, a maturation factor of [NiFe]-hydrogenase and urease. *J Bacteriol* **193**, 1359–1368.

Takahashi, Y. & Tokumoto, U. (2002). A third bacterial system for the assembly of iron-sulfur clusters with homologs in archaea and plastids. *J Biol Chem* **277**, 28380–28383.

Tamagnini, P., Axelsson, R., Lindberg, P., Oxelfelt, F., Wünschiers, R. & Lindblad, P. (2002). Hydrogenases and hydrogen metabolism of cyanobacteria. *Microbiol Mol Biol Rev* **66**, 1–20.

Tard, C., Liu, X., Ibrahim, S. K., Bruschi, M., Gioia, L. D., Davies, S. C., Yang, X., Wang, L.-S., Sawers, R. G. & Pickett, C. J. (2005). Synthesis of the H-cluster framework of iron-only hydrogenase. *Nature* **433**, 610–613.

Terpe, K. (2006). Overview of bacterial expression systems for heterologous protein production: from molecular and biochemical fundamentals to commercial systems. *Appl Microbiol Biotechnol* **72**, 211–222.

Thauer, R. K., Jungermann, K. & Decker, K. (1977). Energy conservation in chemotrophic anaerobic bacteria. *Bacteriol Rev* **41**, 100–180.

Thauer, R. K., Kaster, A.-K., Goenrich, M., Schick, M., Hiromoto, T. & Shima, S. (2010). Hydrogenases from methanogenic archaea, nickel, a novel cofactor, and H$_2$ storage. *Annu Rev Biochem* **79**, 507–536.

Theodoratou, E., Paschos, A., Mintz-Weber & Böck, A. (2000). Analysis of the cleavage site specificity of the endopeptidase involved in the maturation of the large subunit of hydrogenase 3 from *Escherichia coli*. *Arch Microbiol* **173**, 110–116.

Theodoratou, E., Huber, R. & Böck, A. (2005). [NiFe]-Hydrogenase maturation endopeptidase: structure and function. *Biochem Soc Trans* **33**, 108–111.

Tokumoto, U. & Takahashi, Y. (2001). Genetic analysis of the *isc* operon in *Escherichia coli* involved in the biogenesis of cellular iron-sulfur proteins. *J Biochem* **130**, 63–71.

Tomory, L. (2009). Let it burn: distinguishing inflammable airs 1766-1790. *Ambix* **56**, 253–272.

Unden, G. & Bongaerts, J. (1997). Alternative respiratory pathways of *Escherichia coli*: energetics and transcriptional regulation in response to electron acceptors. *Biochim Biophys Acta* **1320**, 217–234.

Vignais, P. M. & Billoud, B. (2007). Occurrence, classification, and biological function of hydrogenases: an overview. *Chem Rev* **107**, 4206–4272.

Vignais, P. M., Billoud, B. & Meyer, J. (2001). Classification and phylogeny of hydrogenases. *FEMS Microbiol Rev* **25**, 455–501.

Vinella, D., Brochier-Armanet, C., Loiseau, L., Talla, E. & Barras, F. (2009). Iron-sulfur (Fe/S) protein biogenesis: phylogenomic and genetic studies of A-type carriers. *PLoS Genet* **5**, e1000497.

Vogel, J. & Sharma, C. M. (2005). How to find small non-coding RNAs in bacteria. *Biol Chem* **386**, 1219–1238.

Volbeda, A., Charon, M., Piras, C., Hatchikian, E., Frey, M. & Fontecilla-Camps, J. (1995). Crystal structure of the nickel-iron hydrogenase from *Desulfovibrio gigas*. *Nature* **373**, 580–587.

Volbeda, A., Garcin, E., Piras, C., De Lacey, A. L., Fernandez, V. M., Hatchikian, E. C., Frey, M. & Fontecilla-Camps, J. C. (1996). Structure of the [NiFe] hydrogenase active site: evidence for biologically uncommon Fe ligands. *J Am Chem Soc* **118**, 12989–12996.

Wächtershäuser, G. (2000). Origin of life. Life as we don't know it. *Science* **289**, 1307–1308.

Wächtershäuser, G. (2007). On the chemistry and evolution of the pioneer organism. *Chem. Biodivers.* **4**, 584–602.

Waight, A. B., Love, J. & Wang, D.-N. (2010). Structure and mechanism of a pentameric formate channel. *Nat Struct Mol Biol* **17**, 31–37.

Watanabe, S., Matsumi, R., Arai, T., Atomi, H., Imanaka, T. & Miki, K. (2007). Crystal structures of [NiFe] hydrogenase maturation proteins HypC, HypD, and HypE: insights into cyanation reaction by thiol redox signaling. *Mol. Cell* **27**, 29–40.

Wu, L. & Mandrand-Berthelot, M-A. (1986). Genetic and physiological characterization of new *Escherichia coli* mutants impaired in hydrogenase activity. *Biochimie* **68**, 167–179.

Wu, L., Mandrand-Berthelot, M., Waugh, R., Edmonds, C., Holt, S. & Boxer, D. (1989). Nickel deficiency gives rise to the defective hydrogenase phenotype of *hydC* and *fnr* mutants in *Escherichia coli*. *Mol Microbiol* **3**, 1709–1718.

Wu, L., Navarro, C. & Mandrand-Berthelot, M-A. (1991). The *hydC* region contains a multi-cistronic operon (*nik*) involved in nickel transport in *Escherichia coli*. *Gene* **107**, 37–42.

Wu, L. F. & Mandrand-Berthelot, M-A. (1993). Microbial hydrogenases: primary structure, classification, signatures and phylogeny. *FEMS Microbiol Rev* **10**, 243–269.

Yamamoto, I. & Ishimoto, M. (1978). Hydrogen-dependent growth of *Escherichia coli* in anaerobic respiration and the presence of hydrogenases with different functions. *J Biochem (Tokyo)* **84**, 673–679.

Yan, A. & Kiley, P. J. (2008). Dissecting the role of the N-terminal region of the *Escherichia coli* global transcription factor FNR. *J Bacteriol* **190**, 8230–8233.

Zbell, A. L. & Maier, R. J. (2009). Role of the Hya hydrogenase in recycling of anaerobically produced H_2 in *Salmonella enterica* serovar Typhimurium. *Appl Environ Microbiol* **75**, 1456–1459.

Zhang, A., Altuvia, S., Tiwari, A., Argaman, L., Hengge-Aronis, R. & Storz, G. (1998). The OxyS regulatory RNA represses *rpoS* translation and binds the Hfq (HF-I) protein. *EMBO J* **17**, 6061–6068.

Zhang, J. W., Butland, G., Greenblatt, J. F., Emili, A. & Zamble, D. B. (2005). A role for SlyD in the *Escherichia coli* hydrogenase biosynthetic pathway. *J Biol Chem* **280**, 4360–4366.

Zinoni, F., Birkmann, A., Stadtman, T. & Böck, A. (1986). Nucleotide sequence and expression of the selenocysteine-containing polypeptide of formate dehydrogenase (formate-hydrogen-lyase-linked) from *Escherichia coli*. *Proc Natl Acad Sci U S A* **83**, 4650–4654.

Anhang

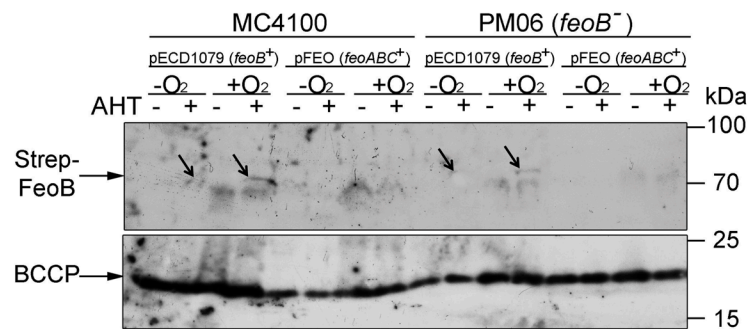## Anhang 1 Zusätzliches Onlinematerial zu Artikel 2.3

Abbildung S1: Plasmidkodierte FeoB Synthese in MC4100 und PM06 (*feoB*::Tn*5*). Weitere Erläuterungen siehe Artikel 2.3.

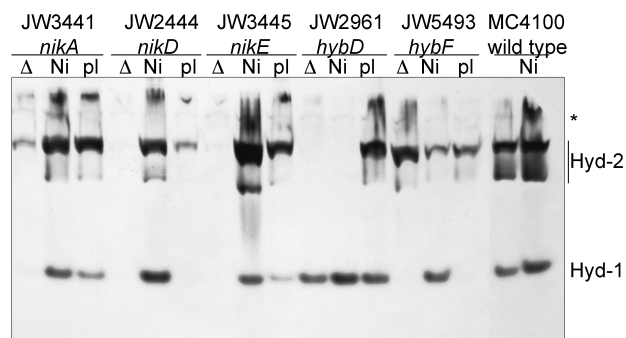## Anhang 2 Zusätzliches Onlinematerial zu Artikel 2.5

Abbildung S1: Partielle Komplementation von Nickel-Transport und Hydrogenase-Reifungs defizienter Mutanten. Weitere Erklärungen siehe Artikel.

Tabelle S1: Aminosäureaustausche von BL21(DE3) Genprodukten mit einer Funktion im Wasserstoff-Metabolismus im Vergleich zu MG1655.

Protein	Amino acid exchanges
AckA, AdhE, ArcA, CarA, ErpA, FhlA, HyaA-F, HybA-E, HybG, HybO, HycE, HycH, HycI, HypA-E, HydN, IhfA, IhfB, IscA, IscR, NarL, NikB, NikC, NikR, PflAB, PTA, SelA, *selC* (tRNA^Sec), FdoGHI	None
CarB (carbamoyl phosphate synthetase)	D434E/D487E
FdhH (*fdhF* – formate dehydrogenase H)	P551L
FNR (transcriptional dual regulator)	Q141Stop
HybD (maturation peptidase for Hyd 2)	A70T
HybF (maturation of Hyd 1 and 2)	L91I
HycA (regulator of the transcriptional regulator FhlA)	T132I
HycB (Fe-S subunit of the FHL complex)	A138T
HycC (membrane subunit of the FHL complex)	V280M
HycD (membrane subunit of the FHL complex)	I46M/I47F
HycF (Fe-S subunit of the FHL complex)	H74R
HycG (small subunit of Hyd-3)	L175Q
HypF (Hyd maturation protein)	R51L/Y62H/K214N/D258E/S565P
NikA (periplasmic binding protein of the nickel ABC transporter)	E191A/S330R
NikD (ATP-binding component of the nickel ABC transporter)	D216Q
NikE (ATP-binding component of the nickel ABC transporter)	I6V/S7C/N19S/A65S/E238D/T265S
SelB (Elongation factor for selenocysteine insertion)	M154I/N232H/A316V/F414S
SelD (Selenophosphate synthase)	E197D
Proteins of hydrogenase 4 operon, usually not synthesized under the conditions tested*	FocB T75A; HyfA D121N/A126V/P127L/T128P; HyfB P66T/I398L/N508D/A512V/Q528R/G571S/ A616V; HyfC frameshift at position 289 within gene; HyfD signal peptide altered; HyfE none; HyfF none; HyfG none; HyfH A45-/C46-/G73R/P126Q/I130V/A134T/I167L/L174P; HyfJ A137T; HyfI R24Q/V69I; HyfR S114P/V177A/C221N/ E225D
Molybdopterin cofactor biosynthesis	MoaA R61S/S111N MoaB R22C MoaC none MoaD M35L MoaE N48K/A102E MobA V1M MobB none MogA E150A MoeA G107V/M120T/A128V/E394D MoeB I36V/T95A/M211L
ModE; ModF; ModA, ModB, ModC (Molybdate transport)	Corresponding genes absent from the genome of BL21(DE3)
FdhD (Formate-dehydrogenase N accessory protein)	D152V
FdhE (Formate dehydrogenase accessory protein)	D259G
Formate dehydrogenase N	FdnG L342F/ S666A FdnH S249A FdnI none
Nitrate reductase	NarG Q1083P NarH D298E NarI P36S/ T52A/ A122S/ L157M
RpoN (sigma 54 factor, subunit of RNA polymerase)	E150D/I165M

**Tabelle S2**: Phänotypische Analyse verschiedener BL21(DE3)-Abkömmlinge in Bezug auf Wasserstoff-Metabolismus.

Strain/Growth condition[1]	Specific hydrogenase activity in U mg protein[-1] ± SD	Qualitative H₂ production[3]	Hyd-1 and Hyd-2 activity after activity staining of native PAGE
Rosetta(DE3) pLysS	< 0.01 (<0.01)	- (-)	- (-)
Rosetta(DE3) pLysS/pCH21	0.07 ± 0.02 (2.51 ± 1.17)	- (+)	+ (+)
C41(DE3)	< 0.01 (< 0.01)	- (-)	- (-)
C41(DE3)/pCH21	0.08 ± 0.03 (3.37 ± 0.44)	- (+)	+ (+)

Anhang 3: Charakterisierung von *fnr*-Gendeletionen

A
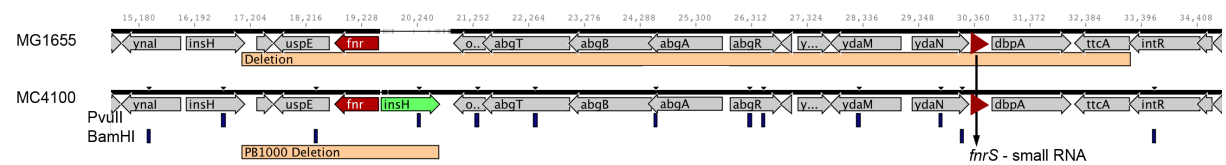
B
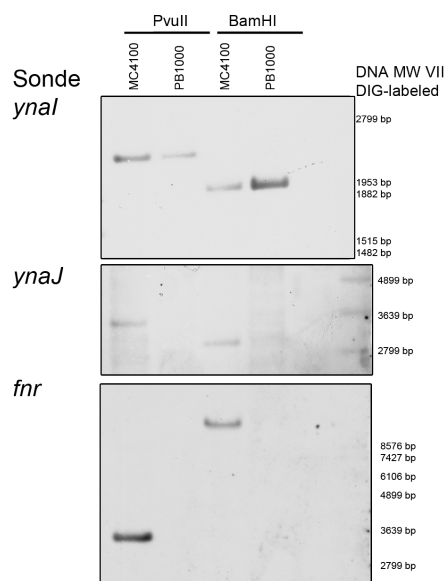
Kartierung der *fnr* Deletionen in MG1655 (oben) und MC4100 (unten) Derivaten. A: MC4100 unterscheidet sich durch ein zusätzliches *insH* Element stromaufwärts von *fnr* (grün), welches beschrieben wurde (Sawers, 2005c). Die Deletionen in MG1655 (Stamm NCM3105) und PB1000 sind durch orange Balken angedeutet. Die Lage der regulatorischen RNA *fnrS* und des *fnr* Gens sind rot gekennzeichnet. Erstellung der Abbildung erfolgte mittels Geneious 3.6.1. **B:** Kartierung der PB1000 Deletion erfolgte mittels Southern Blot mit Sonden u.a. in *ynaI*, *ynaJ*, *uspE*, *fnr* und *ogt*. Dargestellt sind die Autoradiogramme von Sonden, die in den Genen *ynaI* (Ladekontrolle), *ynaJ* und *fnr* binden nach Verdau von 1 µg genomischer DNA von MC4100 und PB1000 mit PvuII und BamHI und Auftrennung in 1 % (w/v) Agarosegel. Die vorhergesagten Schnittstellen sind als blaue Balken in **A** dargestellt. Detektion erfolgte mittels Alkalischer Phosphatase gekoppeltem Anti-Dig Antikörper und den Nachweisreagenz CDP-Star (Roche).

Publikationsliste

Pinske C & Sawers RG (2010). The role of the ferric-uptake regulator Fur and iron homeostasis in controlling levels of the [NiFe]-hydrogenases in *Escherichia coli*. *International Journal of Hydrogen Energy* 35, 8938–8944.

Soboh B, Krüger S, Kuhns M, **Pinske C**, Lehmann A & Sawers RG (2010). Development of a cell-free system reveals an oxygen-labile step in the maturation of [NiFe]-hydrogenase 2 of *Escherichia coli*. *FEBS Lett* 584, 4109–4114.

Pinske C & Sawers RG (2011). Iron restriction induces preferential down-regulation of H_2-consuming over H_2-evolving reactions during fermentative growth of *Escherichia coli*. *BMC Microbiol* 11, 196.

Pinske C, Krüger S, Soboh B, Ihling C, Kuhns M, Braussemann M, Jaroschinsky M, Sauer C, Sargent F, Sinz A & Sawers RG (2011). Efficient electron transfer from hydrogen to benzyl viologen by the [NiFe]-hydrogenases of *Escherichia coli* is dependent on the coexpression of the iron-sulfur cluster-containing small subunit. *Arch Microbiol* 193, 893-903.

Pinske C, Bönn M, Krüger S, Lindenstrauß U & Sawers RG (2011). Metabolic deficiences revealed in the biotechnologically important model bacterium *Escherichia coli* BL21(DE3). *PLoS ONE* 6 (8), e22830.

Soboh B, **Pinske C**, Kuhns M, Waclawek M, Ihling C, Trchounian K, Trchounian A, Sinz A & Sawers RG (2011). The respiratory molybdo-selenoprotein formate dehydrogenases of *Escherichia coli* have hydrogen: benzyl viologen oxidoreductase activity. *BMC Microbiol* 11, 173

Pinske C & Sawers RG (2011). The A-type carrier protein ErpA is essential for formation of an active formate-nitrate respiratory pathway in *Escherichia coli* K-12. *J Bacteriol*, doi:10.1128/JB.06024-11, im Druck.

Trchounian K, **Pinske C**, Sawers RG & Trchounian A (2011). Dependence on the F_0F_1-ATP synthase for the activities of the hydrogen-oxidizing hydrogenases 1 and 2 during glucose and glycerol fermentation at high and low pH in *Escherichia coli*. *J Bioenerg Biomembr*, doi:10.1007/s10863-011-9397-9, im Druck.

Trchounian K, **Pinske C**, Sawers RG & Trchounian A (2011). Characterization of *Escherichia coli* [NiFe]-hydrogenase distribution during fermentative growth at different pHs. *Cell Biochem Biophys,* doi:10.1007/s12013-011-9325-y, im Druck.

Pinske C & Sawers RG (2011). Delivery of iron-sulfur clusters to [NiFe]-hydrogenases in *Escherichia coli* requires the A-type carrier proteins ErpA and IscA. *PLoS ONE*, eingereicht.

Danksagung

Mein innigster Dank gilt Herrn Professor R. Gary Sawers für die Überlassung des überaus interessanten Themas, für seine stetige Diskussionsbereitschaft, für die Freiheiten und das Vertrauen in meine Arbeit. Sehr zu schätzen weiß ich auch seine Unvoreingenommenheit, seine kulturellen Tipps und berufliche Unterstützung und ich frage mich was nun aus dem zweiten Büro in der 206 wird.

Ich danke Herrn Prof. Dr. Dietrich H. Nies für die freundliche Bereitschaft das zweite Gutachten zu übernehmen, sein stetes Interesse am Thema und die angenehme Atmosphäre auf den gemeinsamen Instituts- und VAAM-Feiern.

Für die Bereitschaft das externe Gutachten zu übernehmen, danke ich Herrn Prof. Dr. Thomas Happe vielmals.

Bei den Marburgern Herrn Prof. Johann Heider und Herrn Prof. Rudolf K. Thauer danke ich für die Möglichkeit der Teilnahme an der Summer School und für die wunderschönen Wanderungen zur Schwarzwasserhütte.

Den hiesigen Post-Docs Basem Soboh und Katrin Makdessi-Spinka danke ich für die zahlreichen methodischen Hinweise und die Geduld mit der sie die immer wieder gleichen Fragen beantwortet haben. Außerdem DJ (Herrn Dr. Jöx) für uneingeschränkten Reparaturservice und Ute für ihre Hilfe bei Analytikfragen. Haltet die Ohren steif!

Großer Dank geht an die AG Sinz der Pharmazie Uni Halle, insbesondere Christian Ihling, für die Durchführung der Massenspektrometrie.

Nicht zu vergessen sind die zahllosen Postsendungen von Stämmen und Plasmiden, die mir bereitwillig von Tracy Palmer, der Keio Collection NBRP-*E. coli* am NIG, Oliver Lenz, der AG Nies und von Anderen zur Verfügung gestellt worden sind und ohne die alles viel länger gedauert hätte.

Frau Dr. Anja Hemschemeier und Frau Dr. Camilla Lambertz der AG Photobiotechnologie in Bochum danke ich herzlich für ihre spontane Hilfsbereitschaft, fachliche Kompetenz und ihr kritisches Auge bei Fragen zu *Chlamydomonas* und [FeFe]-Hydrogenasen.

Danke auch an meine Diplomanden Sara, Andor und Sabine für die tolle Zusammenarbeit und die schöne Zeit. Besonderen Dank auch an Mario, der fast genauso lange in der Mibi ‚rumhing' wie ich. Nicht zu vergessen meine Bachelorette Monique, die mit ihrem sprühenden Optimismus ein misslungenes Experiment nur halb so schlecht aussehen ließ. Es hat unendlich Spaß gemacht mit Euch zu arbeiten.

Den Doktoranden Claudi, Marlén, Marco (Fischi), Dörte, Lydia, Hannes und Janine danke ich für den Spaß auf gemeinsamen Feiern, auf den vielen Tagungen und für das gesamte Zwischenmenschliche, was die Arbeit vergessen ließ. Und zusätzlich Dörte für ihr stetes Lächeln über meine Scherze.

Bei den treuen Seelen Claudia H. und Ute Lindenstrauß möchte ich mich herzlichst für ihre stete Hilfsbereitschaft bedanken.

Den restlichen Mitarbeitern, Diplomanden, Praktikanten und Gästen der Mikrobiologie danke ich für die unvergessliche Zeit und die vielen Einflüsse, die meine Arbeit und mein Verständnis stets erweitert haben.

Danke Andy! Für Alles.

Erklärung

Hiermit erkläre ich an Eides statt, dass ich mich mit der vorliegenden Arbeit erstmals um die Erlangung des Doktorgrades bewerbe, die vorliegende Arbeit selbstständig und ohne fremde Hilfe verfasst, andere als die von mir angegebenen Quellen und Hilfsmittel nicht benutzt und die den benutzten Werken wörtlich oder inhaltlich entnommenen Stellen als solche kenntlich gemacht habe.

Halle (Saale), den 13.12.2011

Constanze Pinske

Lebenslauf

Persönliche Daten

Name:	Constanze Pinske
Geburtstag und -ort:	24.12.1983 in Berlin
Staatsangerhörigkeit:	Deutsch
Familienstand:	Ledig
Wohnsitz:	Muldestr. 26; 06122 Halle/Saale

Ausbildung

ab 02/2012	Wissenschaftlicher Mitarbeiter/Postdoc in der Arbeitsgruppe Prof. Sargent, Dundee Schottland
seit 07/2008	Wissenschaftlicher Mitarbeiterin/Doktorandin in der Arbeitsgruppe Prof. Sawers am Institut für Biologie – Mikrobiologie der Martin-Luther-Universität Halle-Wittenberg
	Thema: Reifung und Assemblierung der [NiFe]-Hydrogenasen aus *Escherichia coli*: Eisen und Regulation
10/2003 – 06/2008	Studium Diplom-Biochemie an der Martin-Luther-Universität Halle-Wittenberg und Diplomarbeit zum Thema „Reifung von [NiFe]-Hydrogenasen - Strategie zur Isolierung Hydrogenase-negativer Mutanten von *Escherichia coli*" im Institut für Biologie/ Mikrobiologie in der Arbeitsgruppe von Prof. Sawers
09/1995 – 07/2003	Gymnasiale Ausbildung am Johann-Gottfried Herder Gymnasium in Berlin
08/1999 – 07/2000	High School Exchange Year in Green Run High School, Virginia/USA
09/1990 – 09/1995	Grundschule, Berlin